

LITHUANIAN UNIVERSITY OF HEALTH SCIENCES

Rūta Inčiūraitė

**THE ROLE OF INTESTINAL
EPITHELIAL MICRORNAS
AND GUT MICROBIOTA
IN THE PATHOGENESIS OF
ULCERATIVE COLITIS**

Doctoral Dissertation
Natural Sciences,
Biology (N 010)

Kaunas, 2025

Dissertation has been prepared at the Laboratory of Clinical and Molecular Gastroenterology of the Institute for Digestive Research of the Medical Academy of the Lithuanian University of Health Sciences during the period of 2019–2025.

Scientific Supervisor

Prof. Dr. Jurgita Skiecevičienė (Lithuanian University of Health Sciences, Natural Sciences, Biology – N 010).

Scientific Co-Supervisor

Prof. Dr. Juozas Kupčinskas (Lithuanian University of Health Sciences, Medical and Health Sciences, Medicine – M 001).

The dissertation is defended at the Biology Research Council of the Lithuanian University of Health Sciences.

Chairperson

Prof. Habil. Dr. Vaiva Lesauskaitė (Lithuanian University of Health Sciences, Natural Sciences, Biology – N 010).

Members:

Prof. Dr. Rasa Baniienė (Lithuanian University of Health Sciences, Natural Sciences, Biology – N 010);

Dr. Giedrius Steponaitis (Lithuanian University of Health Sciences, Natural Sciences, Biology – N 010);

Prof. Dr. Tomas Poškus (Vilnius University, Medical and Health Sciences, Medicine – M 001);

Prof. Dr. Konrad Aden (Christian-Albrecht University of Kiel, Natural Sciences, Biology – N 010).

Dissertation will be defended at the open session of the Biology Research Council of the Lithuanian University of Health Sciences at 1 p.m. on the June 3, 2025, in auditorium A-202 of the ‘Santaka’ Valley Centre for Advanced Pharmaceutical and Health Technologies at the Lithuanian University of Health Sciences.

Address: Sukilėlių av. 13, LT-50162 Kaunas, Lithuania.

LIETUVOS SVEIKATOS MOKSLŲ UNIVERSITETAS

Rūta Inčiūraitė

**ŽARNYNO EPITELIO
MIKRORNR IR MIKROBIOTOS
VAIDMUO OPINIO KOLITO
PATOGENEZĖJE**

Daktaro disertacija
Gamtos mokslai,
Biologija (N 010)

Kaunas, 2025

Disertacija rengta 2019–2025 metais Lietuvos sveikatos mokslų universiteto Medicinos akademijos Virškinimo sistemos tyrimų instituto Klinikinės ir molekulinės gastroenterologijos laboratorijoje.

Mokslinė vadovė

prof. dr. Jurgita Skiecevičienė (Lietuvos sveikatos mokslų universitetas, gamtos mokslai, biologija – N 010).

Konsultantas

prof. dr. Juozas Kupčinskas (Lietuvos sveikatos mokslų universitetas, medicinos ir sveikatos mokslai, medicina – M 001).

Disertacija ginama Lietuvos sveikatos mokslų universiteto Biologijos mokslo krypties taryboje:

Pirmininkė

prof. habil. dr. Vaiva Lesauskaitė (Lietuvos sveikatos mokslų universitetas, gamtos mokslai, biologija – N 010).

Nariai:

prof. dr. Rasa Baniienė (Lietuvos sveikatos mokslų universitetas, gamtos mokslai, biologija – N 010);

dr. Giedrius Steponaitis (Lietuvos sveikatos mokslų universitetas, gamtos mokslai, biologija – N 010);

prof. dr. Tomas Poškus (Vilniaus universitetas, medicinos ir sveikatos mokslai, medicina – M 001);

prof. dr. Konrad Aden (Kylio Christiano Albrechto universitetas, gamtos mokslai, biologija – N 010).

Disertacija bus ginama viešajame biologijos mokslo krypties tarybos posėdyje 2025 m. birželio 3 d. 13 val. Lietuvos sveikatos mokslų universiteto „Santakos“ slėnio Naujausių farmacijos ir sveikatos technologijų centro A-202 auditorijoje.

Disertacijos gynimo vietos adresas: Sukilėlių pr. 13, LT-50162 Kaunas, Lietuva.

TABLE OF CONTENTS

ABBREVIATIONS	8
INTRODUCTION	10
Aim and objectives	11
The novelty and relevance of the study	12
1. LITERATURE REVIEW	13
1.1. Ulcerative colitis: overview and key mechanisms	13
1.1.1. Overview of ulcerative colitis	13
1.1.2. Aetiology of UC	14
1.2. Intestinal mucosal barrier and its dysfunction in UC	17
1.2.1. Overview of intestinal mucosa homeostasis	17
1.2.2. Impairment of intestinal epithelium during UC	20
1.3. microRNAs and their role in UC	23
1.3.1. Overview of microRNAs and their mechanism of action	23
1.3.2. miRNA dysregulation in UC	26
1.3.3. Regulatory role of miRNA in colonic mucosa	28
1.4. Gut microbiota and its role in UC	29
1.4.1. Composition and function of gut microbiota	29
1.4.2. Dysbiosis in UC	30
1.4.3. Disruption of host-microbiota interaction in UC	32
1.5. Intestinal organoid models in UC research	33
1.5.1. Overview of intestinal organoid technology	33
1.5.2. Organoid applications and challenges in UC research	35
2. MATERIALS AND METHODS	38
2.1. Ethics statement	38
2.2. Study design and population	38
2.3. Part I. miRNA expression profiling in colonic tissue and epithelial cell populations	40
2.3.1. Collection and disaggregation of colonic biopsies	42
2.3.2. Fluorescence-activated cell sorting (FACS)-based cell enrichment	42
2.3.3. RNA extraction	43
2.3.4. RT-qPCR and data analysis	43
2.3.5. Small RNA library preparation and next-generation sequencing	44
2.3.6. Bioinformatics and statistical analysis of small RNA sequencing data	44
2.3.7. miRNA target gene set enrichment analysis	45
2.3.8. miRNA co-expression network analysis	45

2.4.	Part II. Gut microbiota profiling in faeces	45
2.4.1.	Collection of faecal material and DNA extraction.....	47
2.4.2.	16S rRNA gene library preparation and sequencing	47
2.4.3.	Bioinformatics and statistical analysis of 16S rRNA gene sequencing data	47
2.5.	Part III. Functional analysis of the impact of commensal bacteria on colonic epithelium using intestinal organoid system	48
2.5.1.	Collection of colonic biopsies and establishment of 3D colonic epithelial organoids	50
2.5.2.	Generation of polarised colonic epithelial monolayers.....	51
2.5.3.	Fluorescence microscopy of colonic epithelial organoids and monolayers	52
2.5.4.	DNA extraction	52
2.5.5.	Bisulfite conversion and PCR amplification.....	53
2.5.6.	LINE-1 pyrosequencing.....	53
2.5.7.	Culturing and preparation of bacterial strains.....	53
2.5.8.	Co-culturing of colonic epithelial cell monolayers and bacteria	54
2.5.9.	Isolation of EVs	54
2.5.10.	Characterization of EVs	55
2.5.11.	RNA extraction from cells and EVs	55
2.5.12.	<i>In silico</i> identification of potential host miRNA targets in bacterial genomes	55
2.5.13.	RT-qPCR.....	56
2.5.14.	Statistical analysis	56
3.	RESULTS	57
3.1.	Part I. miRNA expression profiling in colonic tissue and epithelial cell populations	57
3.1.1.	Identification of UC-associated miRNAs in colonic tissue	57
3.1.2.	Involvement of differentially expressed colonic tissue miRNAs in signalling pathways during UC.....	58
3.1.3.	miRNA expression patterns in colonic epithelial cell populations in UC	63
3.1.4.	Comparison of miRNA expression profiles between colonic epithelial cell populations across health states.....	67
3.1.5.	Correlation of miRNA expression in colonic epithelial cell populations with endoscopic activity in UC	69
3.1.6.	miRNA co-expression network in colonic epithelial cell populations across health states	71
3.1.7.	Clinical relevance of miRNA co-expression in UC.....	73
3.2.	Part II. Gut microbiota profiling in faeces	75
3.2.1.	Gut microbiota diversity in UC.....	75
3.2.2.	Identification of UC-associated bacterial abundance signatures	78
3.2.3.	Shared core microbiome between UC patients and non-IBD individuals.....	80

3.3. Part III. Functional analysis of the impact of commensal bacteria on colonic epithelium using intestinal organoid system	82
3.3.1. Morphological evaluation of colonic epithelial organoids and monolayers derived from UC patients and non-IBD individuals	82
3.3.2. Epigenetic dynamics in colonic epithelial organoids.....	86
3.3.3. Selection of commensal bacteria and miRNA candidates for functional testing	88
3.3.4. Impact of commensal bacteria on the homeostasis of the colonic epithelium.....	89
3.3.5. Regulatory potential of commensal bacteria on colonic epithelial miRNA expression and secretion.....	91
4. DISCUSSION	95
4.1. Part I. miRNA expression profiling in colonic tissue and epithelial cell populations	95
4.2. Part II. Gut microbiota profiling in faeces	98
4.3. Part III. Functional analysis of the impact of commensal bacteria on colonic epithelium using intestinal organoid system	100
4.4. Summary	104
CONCLUSIONS.....	107
SANTRAUKA	109
REFERENCES.....	122
PUBLICATIONS.....	143
COPIES OF PUBLICATIONS.....	147
SUPPLEMENTS.....	182
CURRICULUM VITAE	188
ACKNOWLEDGEMENTS.....	191

ABBREVIATIONS

16S rRNA	–	16S ribosomal RNA
2D	–	two-dimensional
3D	–	three-dimensional
AGO	–	Argonaute protein
AhR	–	Aryl-hydrocarbon receptor
AMP	–	antimicrobial peptide
ASV	–	amplicon sequence variant
AUC-ROC	–	area under the receiver operating characteristic curve
BMP	–	Bone morphogenetic protein
CD	–	cluster of differentiation
CgA	–	chromogranin A
CK20	–	cytokeratin 20
DNA	–	deoxyribonucleic acid
DSS	–	dextran sodium sulfate
EGF	–	Epidermal growth factor
EV	–	extracellular vesicle
FACS	–	Fluorescence-activated cell sorting
FC	–	fold change
FDR	–	false discovery rate
GO	–	Gene Ontology
GPR	–	G-coupled receptor
GSEA	–	gene-set enrichment analysis
<i>HSPA1A</i>	–	heat-shock protein 70-coding gene
<i>HSPB1</i>	–	heat-shock protein 27-coding gene
IBD	–	inflammatory bowel disease
IFN- γ	–	Interferon- γ
Ig	–	immunoglobulin
IL	–	interleukin
ILC	–	innate lymphoid cell
Lgr5+	–	Leucine-rich repeat-containing G-protein coupled receptor 5-positive
LINE-1	–	Long interspersed nuclear element-1
M1, M2	–	microRNA co-expression modules 1 and 2
MDS	–	multidimensional scaling
miRNA, miR	–	microribonucleic acid, microRNA
mRNA	–	messenger ribonucleic acid
MUC	–	mucin
NES	–	normalized enrichment score
NF- κ B	–	Nuclear factor-kappa-light-chain-enhancer of activated B cells
P	–	passage
p _{adj.}	–	adjusted p-value
PCR	–	polymerase chain reaction
RNA	–	ribonucleic acid
RNA-seq	–	RNA sequencing
RISC	–	RNA-induced silencing complex
ROCK1	–	Rho-associated coiled-coil containing protein kinase-1
RT-qPCR	–	reverse transcription-quantitative polymerase chain reaction

SCFA	– short-chain fatty acid
STAT	– Signal transducer and activator of transcription
Th	– T-helper cells
<i>TJP1</i>	– zonula occludens-1 coding gene
TLR	– Toll-like receptor
TNF	– Tumor necrosis factor
UC	– ulcerative colitis
UTR	– untranslated region
WGCNA	– weighted gene co-expression network analysis
Wnt	– Wingless/Integrated protein
ZO-1	– zonula occludens-1

INTRODUCTION

Ulcerative colitis (UC) is a chronic inflammatory disorder of the colon, characterised by episodes of relapse and remission, leading to significant morbidity and reduced quality of life [1]. It is already known that UC pathogenesis is driven by a complex interplay between epithelial barrier dysfunction, immune system dysregulation, gut microbiota alterations, genetic susceptibility, and environmental factors [2]. However, despite extensive research, it is still not known, how specific molecular changes in colonic epithelium, gut microbiota, and their interplay functionally contribute to the onset and progression of UC.

The intestinal epithelium acts as a crucial barrier between host immune defenses and luminal microorganisms, playing a central role in maintaining intestinal homeostasis [3]. In UC, this barrier is severely compromised, leading to increased permeability, microbial translocation, and persistent immune activation, which fuels chronic inflammation [4, 5]. Colonic epithelial cells – including colonocytes, goblet cells, and intestinal stem cells – play a pivotal role in barrier maintenance and mucosal defense [4, 6]. Disruptions in epithelial function, such as reduced mucus secretion and impaired tight junction integrity, contribute to sustained inflammation and increased disease severity [7]. Since a major objective in UC management is to induce and maintain long-term remission through mucosal healing and barrier restoration [8], a deeper understanding of the molecular regulators governing epithelial barrier function is essential. Among these regulators, microRNAs (miRNAs) have emerged as critical players in intestinal epithelial homeostasis, modulating gene networks involved in barrier integrity, immune signalling, and epithelial renewal [9].

Recent evidence highlights that miRNAs regulate intestinal permeability [10, 11], however, most existing studies have relied on bulk tissue analyses or immortalised cell lines [12, 13], lacking cell type-specific resolution. This limitation hinders a precise understanding of how miRNA expression varies between different epithelial cell populations in UC. Given that spatially distant intestinal crypt cells have distinct roles in epithelial renewal and barrier function [6, 14], uncovering their miRNA expression signatures may reveal novel regulatory pathways implicated in UC pathogenesis. Furthermore, miRNAs are not solely intracellular regulators – they are secreted into the intestinal lumen [15], where they can influence microbial communities [16, 17]. This raises critical questions regarding the bidirectional relationship between host epithelial miRNAs and gut microbiota and whether these interactions contribute to disease progression or remission.

Beyond epithelial miRNA alterations, gut microbiota composition plays a fundamental role in UC pathophysiology [18, 19]. UC is typically associated with a loss of microbial diversity and an enrichment of pro-inflammatory taxa, yet certain commensal bacterial populations remain stable despite disease progression [20, 21]. The functional relevance of these stable microbial members, particularly their influence on epithelial barrier integrity, remains largely unexplored. While dysbiosis is well-documented, identifying bacteria that persist despite UC-associated microbial shifts may offer new insights into host-microbiota crosstalk. These commensal bacteria play an unknown role in modulating epithelial responses and immune homeostasis, potentially influencing disease course.

Understanding the interplay between colonic epithelial miRNA expression, gut microbiota composition and stability in UC, and their combined effects may provide valuable insights into the disease pathogenesis and potential therapeutic strategies. Given that UC treatments often target immune-mediated inflammation [22], modulating epithelial responses and microbiota dynamics presents a promising avenue for novel interventions. Bridging molecular, microbial, and epithelial perspectives of UC holds a potential to provide a foundation for future biomarker discovery and pave the way for microbiota- and molecularly-informed therapeutic strategies aimed at restoring intestinal barrier integrity and achieving long-term UC remission.

Aim and objectives

The aim of this study was to investigate the role of colonic epithelial microRNAs and gut microbiota in the pathogenesis of ulcerative colitis.

Objectives:

1. To identify ulcerative colitis-specific microRNA expression profiles in colonic tissue and evaluate their role in signalling pathways.
2. To characterise ulcerative colitis-specific microRNA expression patterns in crypt-top and crypt-bottom colonic epithelial cell populations and evaluate their clinical relevance.
3. To determine ulcerative colitis-associated faecal microbiota signatures and identify stably abundant microbiota genera throughout the course of the disease.
4. To evaluate the impact of commensal bacteria on cellular responses in the colonic epithelium of ulcerative colitis patients and non-IBD controls using intestinal organoid model.

The novelty and relevance of the study

This study provides novel evidence on (1) the differential expression of miRNAs in distinct colonic epithelial cell populations of UC patients, as it is the first work to investigate the miRNA profile of crypt-top and crypt-bottom colonic epithelial cells using small RNA sequencing, revealing cell population-specific miRNA expression signatures and uncovering their clinical implications; (2) the composition of commensal gut bacteria and UC-associated features of faecal microbiota, emphasising the potential involvement of the stable bacterial community in the progression of the disease; (3) the interaction between commensal gut microbiota members and colonic epithelial cells of different origins (UC and non-IBD), implying the regulation of the intestinal barrier by stable gut microflora constituents; (4) the application of novel, state-of-the-art *ex vivo/in vitro* experimental system – colonic epithelial organoids – which enabled the generation of disease relevant results; (5) the use of colonic epithelial organoid system, offering further important insights into its stability by investigating the dynamics of global methylation level in intestinal epithelial organoids derived from UC patients and non-IBD individuals during prolonged culturing.

Taken together, this study contributes to a deeper understanding of molecular mechanisms underlying the pathogenesis of UC. The provided results advance knowledge of disease-specific epithelial and microbial processes. Therefore, these findings not only enhance the understanding of UC but also provide a foundation for future biomarker discovery and the development of novel microbiota- or molecular-targeted therapeutic approaches.

1. LITERATURE REVIEW

1.1. Ulcerative colitis: overview and key mechanisms

1.1.1. Overview of ulcerative colitis

Ulcerative colitis (UC) is a chronic inflammatory disorder of the bowel, marked by persistent inflammation of the colon and characterised by a relapsing and remitting course [23, 24]. Disease is usually localised in a continuous fashion, extending from the rectum to the proximal colon [1, 25]. Inflammation in UC is typically characterised by immune cell infiltration into the mucosa, epithelial damage and ulceration, with the inflammation typically limited to the mucosal layer of the colon [26]. Common clinical manifestations include abdominal discomfort, bloody diarrhea with or without mucus, urgency to defecate, and tenesmus [23, 24]. Symptom severity varies from mild to severe and often corresponds to the extent of colonic inflammation [8, 24, 27]. UC is categorized based on the affected region: ulcerative proctitis (limited to the rectum), left-sided colitis (extending up to the splenic flexure), and pancolitis (involving the entire colon) [8, 27].

UC has become a worldwide health concern due to its high incidence in developed nations and the significant rise in cases observed in developing regions (Fig. 1.1.1.1 A) [28–32]. From an epidemiological perspective, UC is more prevalent in industrialised Western countries (Fig. 1.1.1.1 B) [31, 32]. When analysing data from year 2000–2020 in Europe, the annual incidence rate of UC varies significantly, ranging between 3.0 and 23.36 cases per 100,000 person-years among adults [33]. Similarly, prevalence rates also differ across European nations, with estimates spanning from 99.84 to 191.4 cases per 100,000 individuals [32, 33]. Overall, inflammatory bowel diseases (IBD), including UC, affect around 0.3% of the European population, equating to approximately 2.5–3 million people [29, 30]. Northern Europe, particularly Norway, has recorded one of the highest incidence and prevalence in the world, with projections suggesting that IBD could impact 1% of the general population by 2030 [28, 34]. The condition typically emerges between the ages of 15 and 30, with a secondary peak of onset occurring after the age of 60 [23, 35]. Both men and women appear to be equally affected until the age of 45, after which the incidence of UC becomes significantly higher in men compared to women [36, 37].

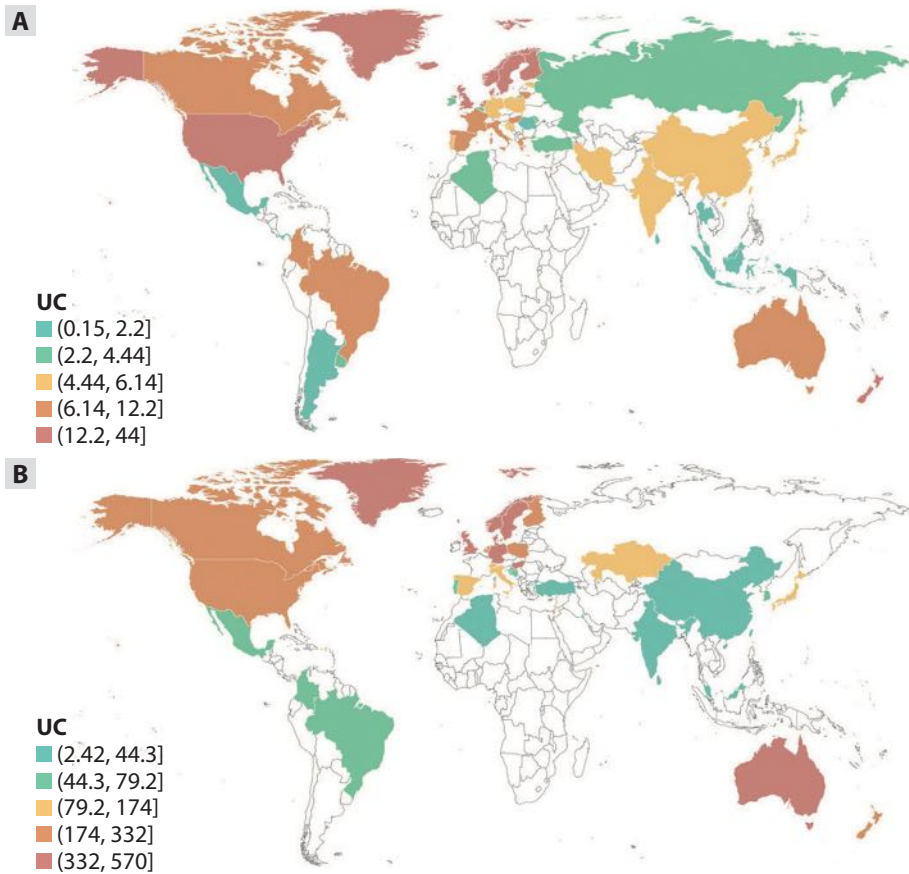


Fig. 1.1.1.1. Global map showing (A) incidence and (B) prevalence of UC in quintiles

Incidence (A) and prevalence (B) rates per 100,000 individuals are displayed and color-coded by quintile. UC – ulcerative colitis. The figure is adapted from Zhang et al. (2024) [32]. Reprinted under a Creative Commons Attribution-Non-Commercial 4.0 International (CC BY-NC 4.0) licence.

1.1.2. Aetiology of UC

The aetiology of UC involves the interactions between multiple factors, including genetic predisposition, epigenetic factors, environmental triggers, immune system dysfunction, gut microbiota alterations, and epithelial barrier defects [23, 24, 38].

Dysregulated immune response. UC is primarily driven by an excessive and dysregulated immune response, which involves both innate and adaptive immune systems [26]. While the exact mechanism remains unclear, diverse immune cells – including T cells, B cells, macrophages, neutrophils, and innate lymphoid cells (ILCs) – play a role in the pathogenesis of UC,

alongside various soluble ligands, including cytokines and chemokines, that modulate immune responses [26, 39]. Immune responses are activated through antigen-presenting cells and T cells, that subsequently trigger an inflammatory cascade also promoting the adaptive immune system action [40, 41]. For instance, in UC, this leads to an exaggerated immune response, particularly involving T helper (Th) 2 and Th17 cells, characterised by increased levels of interleukin (IL)-13, IL-5, IL-17, IL-21, and IL-22 [42]. Dendritic cells play a pivotal role in UC pathogenesis by recognising pathogens via Toll-like receptors (TLRs) and activating transcription factors such as nuclear factor-kappa-light-chain-enhancer of activated B cells (NF- κ B), resulting in the production of proinflammatory cytokines like Tumor necrosis factor (TNF)- α , IL-12, and IL-23 [43]. These cytokines, along with intracellular signalling proteins like Janus kinases (JAKs), contribute to immune cell activation and tissue damage, leading to crypt destruction [26, 43, 44]. Therefore, these molecules are key therapeutic targets, as they mediate chronic inflammation, neutrophil infiltration, and epithelial damage [25, 26, 42, 43]. Activated T cells migrate to the intestinal lamina propria via interactions between α 4 β 7 integrin and mucosal addressin cell adhesion molecule-1, further perpetuating the inflammatory cycle [24, 25]. In UC, an imbalance in ILC subtypes is also evident, with increased ILC1 and ILC2 frequencies and reduced NKp44+ ILC3, which compromises epithelial barrier integrity [45, 46]. Elevated IL-8 levels promote neutrophil accumulation in crypts, exacerbating mucosal injury [26], while IL-9 and IL-17 further contribute to the inflammatory environment [39, 47]. Additionally, UC patients often exhibit increased levels of immunoglobulin (Ig)G autoantibodies against colonic epithelial cells, as well as anti-commensal IgG, which may impair barrier function and enhance Fc region of IgG receptor-triggered signalling, further implicating B cells in disease pathology [48, 49]. These complex interactions highlight the multifactorial nature of UC and underscore the importance of targeted immunotherapy in managing disease progression.

Environmental factors. Numerous studies have shown the impact of various environmental factors on UC onset and progression [38, 50, 51]. Diet, antibiotic use, smoking, and stress are among these environmental factors [50]. Briefly, food choices, as well as food preparation methods are associated with the risk of inflammatory bowel disease (IBD) development [52]. For instance, the adoption of Westernised diet, characterised by high intake of ultra-processed foods and high intake of preservatives and emulsifiers, has been associated with an increased incidence of UC [52–54]. These dietary patterns may disrupt the gut microbiota, alter the protective mucus layers and promote inflammation [52], thus explaining their role in UC. On the other hand, several dietary nutrients, such as omega-3 polyunsaturated fatty acids,

amino acids (tryptophan, glutamine, arginine), histidine, plant polysaccharides, vitamin D, were revealed as potential agents to prevent or treat UC, or regulate gut homeostasis in general [52, 55–58]. Antibiotic exposure, especially during early life, has been associated with an increased risk of developing UC [50]. Antibiotics can alter the gut microbiota, reducing microbial diversity and potentially triggering immune dysregulation [38]. The relationship between tobacco use and UC is complex, as some studies in Western population suggest that non-smokers or individuals who have quit smoking are at a higher risk for UC [59, 60]. Finally, stress has been linked to the exacerbation of UC symptoms by influencing gut motility, permeability, gut microbiota balance, and immune responses, potentially leading to flare-ups [61].

Genetic factors and epigenetic alterations. Around 7.5% of UC variance is explained by genetic factors and 2.8-14% of UC patients report a family history of IBD, with first-degree relatives having a 4-fold increased risk of developing the disease [62]. Thus, UC has a genetic component, with genome-wide association studies identifying over 260 susceptibility loci linked to IBD, of which 67% are shared between UC and Crohn’s disease [63]. These loci involve genes regulating immune detection, cytokine signaling, autophagy, and epithelial barrier integrity [64]. Several UC-specific single nucleotide polymorphisms (SNPs) have been identified in genes such as *ECM1*, *CDH1*, *HNF4 α* , *LAMB1*, and *SLC11A1* which are crucial for mucosal barrier function [65, 66]. Disruptions in these genes may weaken epithelial integrity, increasing susceptibility to microbial invasion and inflammation [67]. Human leukocyte antigen class II genes, particularly *DRB1*01:03*, have been associated with extensive and aggressive UC, while *DR4* appears protective [68]. Additionally, *IL10* SNPs impair IL-10 production, a key immunosuppressive cytokine, contributing to early-onset UC [69]. Other implicated immune-related genes include *IL23R*, *ATG16L1*, and *TLR4*, which regulate innate immune responses [70, 71]. In addition to genetic predisposition, epigenetic changes, such as gene-specific hyper- or hypomethylation as well as dysregulated microRNA (miRNA) expression, have also been associated with the susceptibility to UC or activity status of the disease [72–74]. The more detailed description of the miRNA roles in UC is provided in the literature review section “1.3. microRNAs and their role in UC”.

Intestinal epithelial barrier dysfunction. A compromised epithelial barrier during UC leads to increased intestinal permeability, facilitating microbial translocation and sustained immune activation [7]. Defects in tight junctions, impaired cell regeneration, and excessive apoptosis contribute to the barrier dysfunction in UC and disease severity [5]. The more detailed characterisation of the function of intestinal epithelium and processes related

to its impairment during UC is provided in the literature review section “1.2. *Intestinal mucosal barrier and its dysfunction in UC*”.

Gut microbiota alterations. Dysbiosis, characterised by reduced microbial diversity and an imbalance in beneficial and pathogenic bacteria, has been linked to UC initiation and disease course [21, 75]. Specific microbial metabolites, such as short-chain fatty acids (SCFAs), influence both immune responses and epithelial integrity, thus taking part in epithelial regulation during UC [75, 76]. The more detailed description of the role of gut microbiota in the UC pathogenesis is provided in the literature review section “1.4. *Gut microbiota and its role in UC*”.

1.2. Intestinal mucosal barrier and its dysfunction in UC

1.2.1. Overview of intestinal mucosa homeostasis

The homeostasis of colonic mucosal barrier is maintained by a dynamic interplay between specialised epithelial cells and intercellular junctions [77, 78]. Colonocytes, goblet cells, enteroendocrine cells, tuft cells, and BEST4⁺, each perform unique functions that contribute to epithelial integrity, immune regulation, and microbial defense [79]. Tight junctions, adherens junctions, desmosomes, and tricellular tight junctions work together to maintain barrier integrity and permeability, ensuring that the colon remains protected while allowing controlled interactions with the microbiota [80].

Structural and functional subsets of the colonic mucosal barrier. The intestinal epithelium is a vital barrier that maintains equilibrium between the body and diverse microbial community of the gut [77]. It consists of a single layer of epithelial cells supported by mucus, antimicrobial peptides (AMPs), and immune mediators, forming a multi-layered defense system [81–83]. This barrier prevents harmful substances from entering while allowing essential nutrients to be absorbed, with tight junction proteins regulating permeability [77, 84]. The colonic mucosal barrier consists of physical and chemical components and is organised into four key parts: microbial, mucus, mechanical, and immune barriers (Fig. 1.2.2.1, left) [82, 83]. The mucus layer nourishes beneficial bacteria while blocking pathogens, the epithelial cells form a tight mechanical shield, and immune components, including dendritic cells and cytokines, actively regulate gut homeostasis [4, 77, 82]. The colonic mucosa features a single-layered columnar epithelium, critical for maintaining gut function and immune interactions [4, 7]. Within the epithelium, the crypts house intestinal stem cells that drive continuous renewal, generating transient proliferative cells that differentiate as they migrate toward the surface, where they are eventually shed [3, 6, 78]. These stem cells

can give rise to various specialised cell types, including colonocytes, goblet cells, tuft cells, neuroendocrine cells, and others [6]. Most intestinal cells are absorptive, while crypt cells primarily perform secretory functions, collectively ensuring the integrity and functionality of the epithelial barrier [4].

Key epithelial cell types controlling physical barrier function. The physical barrier in the large intestine is maintained by an epithelium composed of various specialised cell types, each contributing to the maintenance of intestinal homeostasis (Fig. 1.2.2.1, left) [77]. These cells, including colonocytes, goblet cells, enteroendocrine cells, tuft cells, BEST4⁺, stem and transit-amplifying cells, ensure barrier integrity, regulate immune responses, aid in nutrient absorption, and contribute to mucus secretion and antimicrobial defense [4]. Epithelial cells are organised into intestinal crypts, exhibiting spatially specific localization (crypt base-to-top gradient) regulated by the complex distribution of oxygen gradients and numerous niche factors, such as Epidermal growth factor (EGF), Wingless/Integrated proteins (Wnts), Notch, R-spondin, Bone morphogenetic protein (BMP), and others [6, 14, 85, 86]. Colonocytes are the most abundant epithelial cell type in the large intestine and are primarily responsible for water and electrolyte absorption [87]. They facilitate passive diffusion of lipid-soluble molecules and help in maintaining fluid balance by regulating ion transport [78]. In the barrier, colonocytes maintain epithelial integrity through tight junctions, limiting paracellular permeability and preventing microbial translocation [78, 87]. Other highly abundant cells of colonic mucosa are goblet cells – secretory cells that produce and secrete mucins, which form the mucus layer, a critical component of the intestinal barrier [81, 82]. Goblet cells also secrete trefoil peptides and other molecules supporting epithelial repair and defense [81]. By producing mucins, goblet cells create a physical barrier that prevents direct contact between luminal bacteria and the epithelial surface, reducing the risk of inflammation and infection [77, 78, 81, 82]. Although less abundant, enteroendocrine cells play a crucial role in regulating various physiological functions such as gut motility, appetite, glucose homeostasis, and immune responses by secreting peptides like glucagon-like peptide-1 and -2, peptide YY, and vasoactive intestinal peptide [88]. Enteroendocrine cells contribute to mucosal integrity by modulating immune responses and influencing epithelial regeneration [77, 88]. Tuft cells are chemosensory epithelial cells that detect luminal signals and trigger immune responses [89]. They play a key role in recognising intestinal helminths and dietary components [78]. By secreting cytokines such as IL-25, tuft cells promote immune surveillance and help regulate epithelial turnover [4, 90]. BEST4⁺ cells in human colon play a role in innate defense by producing AMPs, regulating mucus hydration and luminal pH, thus promoting host defense and barrier

functionality [91, 92]. Finally, intestinal stem cells (leucine-rich repeat-containing G-protein coupled receptor 5-positive (Lgr5+) cells), located at the base of the crypts, are responsible for the continuous renewal of the epithelial lining ensuring complete turnover of crypt every 3-5 days [6]. These multipotent cells differentiate into all epithelial cell types, ensuring a constant supply of new cells to replace those shed into the lumen [6, 78].

Key junctional complexes maintaining physical barrier integrity and permeability. The integrity of the colonic epithelium depends on specialized intercellular junctions that regulate permeability, maintain structural cohesion, and prevent microbial infiltration (Fig. 1.2.2.1, left) [80]. The first class of such junctions is tight junctions, comprised of transmembrane proteins such as claudins (tightening and pore-forming), occludin, zonula occludens, and tricellular tight junctions [93]. Tight junctions seal the space between adjacent epithelial cells, regulating paracellular permeability and preventing the passage of harmful molecules and microbes [78, 93]. Claudin-1, claudin-3, claudin-4, and claudin-5 contribute to barrier tightening, whereas claudin-2 and claudin-15 allow selective ion transport, helping balance permeability in different regions of intestine [94]. Tricellular tight junctions are formed at the convergence of three epithelial cells and composed of tricellulin and angulin proteins [95]. These junctions seal spaces that bicellular tight junctions cannot completely close, preventing macromolecule leakage [77]. Tricellular tight junctions are crucial for maintaining selective permeability and protecting against bacterial infiltration [77, 95]. Adherens junctions, other junctional complexes, are mainly composed of epithelial cadherins (E-cadherins) linked to β -catenin and the actin cytoskeleton [77]. These junctions provide mechanical stability and mediate intercellular adhesion, playing a critical role in maintaining epithelial integrity and supporting tissue repair [96]. Adherens junctions regulate epithelial cell proliferation and differentiation, ensuring proper renewal of intestinal lining [77, 96]. Third class of junctional structures – desmosomes – are made of desmogleins and desmocollins, which link epithelial cells via interactions with keratin intermediate filaments [97]. Desmosomes reinforce intercellular adhesion, providing resistance to mechanical stress in the colon, which is subject to constant movement and pressure from stool transit [98]. These structures help maintain epithelial cohesion, preventing barrier breakdown and inflammation [97, 98].

Chemical components of intestinal barrier. The colonic barrier in homeostasis relies on a complex chemical defense system composed primarily of mucins (MUC), AMPs, and immunoglobulins, all of which function synergistically to maintain intestinal integrity (Fig. 1.2.2.1, left) [7, 77, 81, 99]. The mucus layer, secreted predominantly by goblet cells, is the first line

of defense, limiting microbial access to the epithelium [81]. This barrier consists of a dense inner mucus layer, almost completely lacking bacteria, and a more porous outer layer that accommodates commensal microbes [4, 100]. In intestinal tract, a total of 21 mucins have been identified and classified into membrane-related mucins, including MUC1, MUC3A/B, MUC4, MUC12, MUC13, MUC15, MUC17, MUC20, and MUC21, and secretory mucins that are further categorised into gel-forming mucins, such as MUC2, MUC5AC, MUC5B, MUC6, MUC19, and nongel-forming mucins, such as MUC7, MUC8, and MUC9 [81, 101]. The principal structural component of colonic mucus is MUC2, a gel-forming mucin that undergoes extensive post-translational modifications, including O-glycosylation and multimerisation, to establish a viscoelastic network that prevents pathogen invasion [81, 82, 102]. Simultaneously, membrane-associated mucins, including MUC1, MUC3A/B, MUC15, MUC20, and others contribute to the formation of glycocalyx in the colon, serving as a protective barrier against microbial adhesion and maintaining epithelial integrity [103]. Additional mucus-associated proteins, including Fc γ -binding protein, Clca1, and Zg16, aid in mucus stability and bacterial aggregation [82]. Moreover, molecules like Ly6/Plaur domain-containing 8 selectively inhibit flagellated bacteria, preventing their translocation through the inner mucus layer [81, 82]. Goblet cells dynamically regulate mucus secretion in response to microbial signals and inflammatory stimuli, such as IL-22 and interferon- γ (IFN- γ), thereby adapting the barrier to environmental changes [4]. In the colon, AMPs – particularly β -defensins – complement the mucus layer by regulating microbial composition, while secretory IgA facilitates immune exclusion by entrapping microbes, preventing epithelial adhesion, and facilitating their clearance within the mucus layer [4, 77].

1.2.2. Impairment of intestinal epithelium during UC

As explained above, the intestinal epithelium serves as a critical barrier that regulates interactions between the host, the gut microbiota, and other luminal contents while maintaining immune homeostasis (Fig. 1.2.2.1, left) [77, 78]. In UC, this barrier is compromised mainly due to increased intestinal permeability, epithelial cell death, and impaired regenerative capacity, leading to chronic inflammation and disease progression (Fig. 1.2.2.1, right) [1, 104–107].

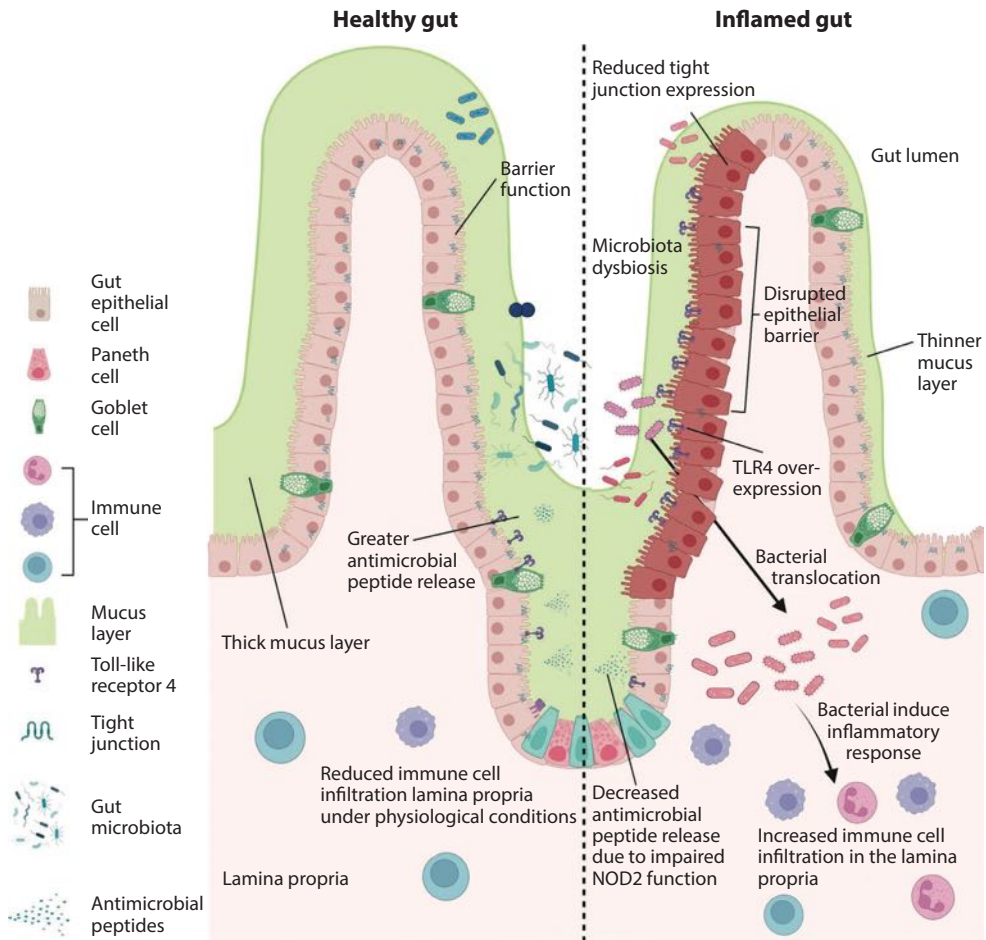


Fig. 1.2.2.1. Key features of a healthy normal (left) and inflamed (right) gut

In homeostatic conditions (**left**), gut has single layer of intact epithelium comprising specialised cell populations and covered in a thick mucus layer. These components limit the access of gut microbiota to the underlying lamina propria. Gut lumen and mucus layer also contain secreted antimicrobial peptides, regulating the growth of commensal pathogenic bacteria. Dysfunction of these components leads to gut inflammation (**right**). It is characterised by thinner mucus layer allowing easier bacterial access to the epithelium. In turn, disruption of epithelial barrier is promoted, which is characterised by impaired expression of tight junctions, allowing luminal bacteria to translocate to the lamina propria. Subsequently, this initiates and sustains the inflammatory responses and increase the infiltration of immune cells from circulation. Inflammation is also characterised by reduced secretion of antimicrobial peptides due to the impaired function of nucleotide-binding oligomerization domain-containing protein 2 (NOD2). This, in turn, causes the overgrowth of bacteria in the lumen. The figure is adapted from Selvakumar et al. (2022) [108]. Reprinted with permission from BMJ Publishing Group Ltd. under licence no. 5998720438266.

Disruption of barrier integrity and increased intestinal permeability.

In UC, intestinal epithelial barrier is severely compromised, leading to increased intestinal permeability and facilitating the translocation of bacterial products into the mucosa, which in turn triggers inflammatory responses (Fig. 1.2.2.1, right) [106]. A common histological change of UC is the disturbed architecture of the crypts, which become shorter and less branched during the disease [71]. Tight junction proteins, responsible for regulating paracellular permeability, are also often dysregulated in UC patients, contributing to the “leaky gut” phenotype [7, 77, 83, 109]. The loss of goblet cells and reduced MUC2 secretion further impair the compromised mucus barrier, increasing susceptibility to microbial invasion [4, 81]. Although it is not yet fully understood whether epithelial barrier dysfunction is a primary driver or a secondary effect of UC, evidence indicate that abnormalities in intestinal permeability persist even in patients during remission, highlighting the fundamental role of barrier defects in disease pathogenesis [7, 110]. Genetic factors, including mutations in tight junction-associated protein coding genes (e.g., *MYO9B*, *MAGI2*, *PARD3*) and mucosal barrier-related genes (e.g., *LYPD8*, *MUC19*), have also been implicated in barrier dysfunction, further supporting the role of genetic predisposition in susceptibility to UC [111, 112]. Oxidative stress has been also shown as a significant primer of colonic inflammation and mucus layer alteration, thus causing integrity and permeability defects of intestinal epithelial barrier [7]. Intestinal permeability associated with oxidative stress is driven by the tyrosine phosphorylation of occludin, leading to altered protein-protein interactions of occludin with ZO-1, β -catenin, and E-cadherin, thereby affecting integrity of intracellular junctions [7, 113]. Additionally, oxidative stress can impair the proper folding of mucins, leading to defective mucus production and increased bacterial adhesion to the epithelial surface, further impairing the integrity of epithelial layer during UC [82, 114].

Excessive epithelial cell death and impaired regeneration. The maintenance of intestinal epithelial integrity depends on the balance between cell proliferation, differentiation, and programmed cell death [3, 115]. In UC, this balance is disrupted due to increased epithelial cell apoptosis and impaired regenerative capacity (Fig. 1.2.2.1, right) [79, 116]. Recombination signal binding protein for immunoglobulin kappa J region (RPB-J) protein is described as a regulator of Notch signalling pathway and its loss or damage leads to impaired intestinal epithelium differentiation and proliferation leading to altered epithelial turnover [117]. Additionally, necroptosis, a proinflammatory form of programmed apoptosis, is also reported to contribute to the epithelial damage seen in UC patients [118]. This process is triggered by inflammatory cytokines, particularly TNF- α , and mediated by kinases such

as RIPK1, RIPK3, and MLKL [119]. The loss of sentinel goblet cells in UC, serving as an early defense mechanism by detecting bacterial invasion, also highlights the compromised regenerative capacity of the colonic epithelium [81, 106]. Inflammatory cytokines, including IL-1 β , IL-18, IFN- γ , and TNF- α , are broadly implicated to modulate epithelial function by enhancing apoptosis and therefore disrupting barrier integrity [120]. Additionally, in UC, elevated levels of IL-22, a cytokine that supports epithelial proliferation and barrier repair, are reported, highlighting the role of ILCs in a compensatory mechanism aimed at restoring intestinal epithelium homeostasis during inflammation in large intestine [121]. Elevated levels of reactive oxygen species indicating oxidative stress in inflamed intestinal mucosa of UC patients have been also associated with increased apoptosis rate, contributing to epithelial cell damage [122].

1.3. microRNAs and their role in UC

1.3.1. Overview of microRNAs and their mechanism of action

Introduction to microRNAs. MicroRNAs (miRNAs) are a conserved class of small, endogenous non-coding RNAs, typically 18-23 nucleotides in length, that function as key post-transcriptional regulators of gene expression [123]. Since their initial discovery in *Caenorhabditis elegans* in 1993, miRNAs have been identified across diverse species, including approximately 2,600 (miRBase v.22) in humans [124, 125]. miRNAs exert their regulatory effects primarily through partial sequence complementarity to target messenger RNAs (mRNAs), most commonly within the 3' untranslated regions (UTRs), leading to mRNA degradation or translational repression [126]. It is estimated that around 60% of human protein-coding genome is regulated by miRNAs [127]. Emerging evidence suggests that under specific physiological conditions, certain miRNAs may also activate translation [125]. miRNAs are implicated in a broad range of biological processes, including development, cell differentiation, and disease pathogenesis, underscoring their fundamental role in maintaining cellular homeostasis and their potential as therapeutic targets [128, 129].

Biogenesis of miRNAs. miRNA biogenesis is a tightly regulated, multistep process that generates mature miRNAs from genomic DNA (with genes located mostly within introns or intergenic regions), enabling their post-transcriptional regulatory functions (Fig. 1.3.1.1) [130]. Briefly, in the canonical pathway, miRNA genes are primarily transcribed by RNA polymerase II into long primary transcripts (pri-miRNAs), which contain characteristic hairpin structures [126, 130]. These pri-miRNAs are processed

in the nucleus by the Microprocessor complex, comprising the RNase III enzyme DROSHA and its cofactor DGCR8, to produce ~55–70 nucleotide precursor miRNAs (pre-miRNAs) with 2-nucleotide 3' overhangs [124, 125]. Pre-miRNAs are then exported to the cytoplasm via Exportin-5 in a RanGTP-dependent manner and further cleaved by Dicer, another RNase III enzyme, often in complex with TRBP, to yield a ~22 nucleotide miRNA duplex [123, 131]. One strand of this duplex, the guide strand, is selectively loaded into an Argonaute (AGO) protein to form the RNA-induced silencing complex (RISC), while the passenger strand is typically degraded [124, 125, 130]. Strand selection is influenced by the thermodynamic stability at the duplex ends and sequence features such as a 5' uracil [131]. Beyond the canonical route, several non-canonical pathways utilise various combinations of canonical processing components to produce functionally mature miRNAs [125]. These non-canonical routes include DROSHA-independent mechanisms like mirtrons (splicing-derived hairpins that bypass nuclear cropping) and Dicer-independent routes where AGO2 directly processes short hairpin RNAs [124, 130, 132].

miRNA-mediated regulation of gene expression. miRNAs regulate gene expression predominantly at the post-transcriptional level by guiding the RISC, which includes AGO proteins, to complementary sequences within target mRNAs (Fig. 1.3.1.1) [124]. The most common binding sites are located in the 3'UTRs of mRNAs, where miRNA-mRNA recognition is largely mediated by the seed region, which is described as nucleotides 2-8 at the 5' end of the miRNA [123, 125]. Canonical miRNA-mRNA interactions, characterised by perfect base pairing within the seed region, are generally sufficient to induce gene silencing [124]. This interaction can be further stabilised by additional base pairing between the 3' region of miRNA and the target mRNA, a mechanism referred to as supplementary binding [123]. In cases where seed region complementarity is suboptimal or disrupted, extensive base pairing at the miRNA 3' end, termed compensatory binding, can restore silencing efficiency [125]. After binding to miRNA response elements, RISC recruits GW182 family proteins [133]. These molecules further serve as scaffolds for downstream effectors such as PAN2-PAN3 and the CCR4-NOT complexes and enable the deadenylation of the polyadenosine tail [124]. Next, mRNA is decapped via DCP2, followed by exonucleolytic degradation by XRN1, effectively reducing mRNA stability and translation [124, 125]. Most miRNA-target interactions in animal cells are only partially complementary and lead to translational repression and mRNA decay, however, a fully complementary interaction can trigger AGO2-mediated endonucleolytic cleavage [123]. Furthermore, miRNA binding is not restricted to the 3'UTR, as the functional sites have been identified in the 5'UTR, coding

regions, and gene promoters [134]. In rare cases, miRNAs can also enhance gene expression, particularly under specific physiological conditions such as cell cycle arrest or nutrient deprivation, where they may interact with AU-rich elements in the 3'UTR and recruit factors like FXR1 in an AGO2-dependent but GW182-independent manner [123, 125, 134].

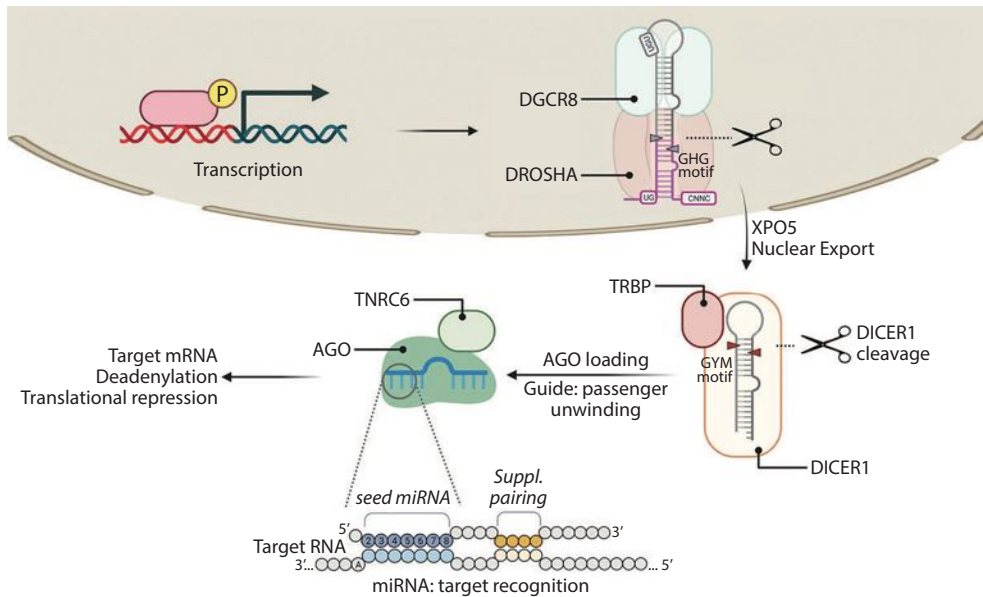


Fig. 1.3.1.1. Canonical miRNA biogenesis pathway and principle of target regulation

Primary transcripts fold into hairpin structures, which are recognized and cleaved by the Microprocessor complex, composed of DROSHA and DGCR8. Cleavage sites (blue arrows) are defined by specific sequence and structural motifs. The resulting precursor is exported to the cytoplasm via XPO5 and further processed by DICER1 (red arrows). The resulting duplex is loaded into an AGO protein, where strand selection occurs, and a mature RISC complex is formed with TNRC6. AGO recognises target RNAs through the seed region (blue circles) and supplemental pairing sites (orange circles). Stable binding leads TNRC6 to recruit deadenylation complexes, resulting in translational repression and mRNA decay. The figure is adapted from Bofill-De Ros et al. (2023) [130]. Reprinted under a Creative Commons Attribution-Non-Commercial 4.0 International (CC BY-NC 4.0) licence.

Intracellular expression, extracellular sorting, and circulation of miRNAs. miRNAs show distinct expression patterns within cells that are influenced by cell type, developmental stage, and physiological state [126, 135, 136]. In many cell types, a small group of miRNAs dominates the total expression, with the five most abundant miRNAs accounting for roughly half of the total miRNA content [135]. While some miRNAs are widely expressed across different tissues, many display cell type-specific expression, suggesting specialised roles in cellular regulation [124, 135]. In addition to their

intracellular functions, miRNAs can be actively secreted into the extracellular space through controlled, energy-dependent mechanisms [137, 138]. miRNAs are commonly released in different types of extracellular vesicles (EVs), including exosomes, microvesicles, and apoptotic bodies [125, 137]. EVs are formed through specific pathways and help protect miRNAs by enclosing them along with proteins and lipids [139]. Extracellular miRNAs can also exist outside EVs, bound to proteins such as AGO2, high-density lipoproteins, and nucleophosmin 1, which contribute to their stability [137, 140]. These mechanisms allow extracellular miRNAs to remain stable in various body fluids, such as plasma, serum, saliva, urine, and faeces, even under conditions that typically degrade RNA, such as changes in pH or repeated freeze-thaw cycles [138, 141, 142]. Secreted miRNAs are reported to serve as signalling molecules, influencing nearby or distant cells by altering gene expression [138]. Circulating miRNAs can enter recipient cells through several pathways, including endocytosis, membrane fusion, or specific receptor-mediated processes [143]. Secretion of miRNAs is considered to be a regulated event, often triggered by external signals, rather than a random release [137–140]. The type and amount of miRNAs carried by EVs can also vary depending on the cell of origin [138, 144].

1.3.2. miRNA dysregulation in UC

Altered miRNA expression in UC pathogenesis. UC is associated with extensive dysregulation of miRNA expression across multiple biological compartments, including colonic tissue, blood, and faeces [145]. As miRNA dysregulation in UC is not restricted to the intestinal mucosa and extends to systemic and luminal compartments, this multi-level alteration highlights their potential involvement in both local and systemic aspects of disease pathophysiology, particularly in modulating inflammation, epithelial integrity, and immune responses [145, 146, 146, 147]. miR-21 is one of the most consistently reported miRNAs in UC, which is upregulated in inflamed colonic mucosa, circulating blood, and faecal samples of UC patients [145, 148–151]. This miRNA is mostly enriched in immune cell populations such as macrophages and T cells within the lamina propria and is reported to contribute to inflammatory cell recruitment and cytokine production [150]. Similarly, the levels of miR-155 are elevated in colonic tissues and faeces [145, 152], and this molecule has been linked to epithelial barrier dysfunction and regulation of tight junction proteins [73]. Despite some contradictory findings, miR-31 is increasingly recognized as a key modulator of the Th17 axis in UC [147, 153, 154]. miR-31 is primarily expressed in epithelial cells, where it regulates cytokine receptor expression and inflammatory signalling

pathways including IL-25, IL-17RA, NF- κ B, and Signal transducer and activator of transcription 3 (STAT3) [147, 153, 154]. Other miRNAs such as miR-16, miR-1246, and miR-223 are also reported to be upregulated in UC and exhibit distinct expression across tissue and faecal samples [15, 145, 148]. Furthermore, the expression of let-7 family members, particularly let-7e and let-7f, are repeatedly reported as altered in colonic tissues depending on disease activity state and have been linked to IL-6 signalling and NF- κ B activation [147, 155, 156]. Large-scale profiling studies have identified numerous differentially expressed miRNAs between active and inactive UC states, in both adult and pediatric populations, further supporting their involvement in the heterogeneity of UC [145, 146, 157–159]. For example, miR-16, miR-28-5p, miR-151-5p, miR-103-2*, miR-199a-5p, miR-340*, miR-362-3p, and miR-532-3p were significantly upregulated in the blood of patients with active UC, while miR-505* was downregulated [148, 157]. In tissue samples, altered expression of miR-7, miR-23a, miR-24, miR-26a, miR-29a/b, miR-126*, miR-127-3p, miR-135b, miR-141, miR-188, miR-195, miR-200b, miR-215, miR-324-3p, and miR 429 during UC has also been reported [160, 161]. These patterns differ not only by disease activity but also across age groups, indicating that miRNA expression signatures may reflect both disease subtype and individual variability in disease progression [147, 155, 161].

Diagnostic and therapeutic potential of miRNAs in UC. In addition to their mechanistic role in disease pathogenesis, miRNAs show potential as diagnostic and therapeutic tools in UC [145, 146]. The stability of these small non-coding RNA molecules in body fluids such as blood and faeces allows for non-invasive detection, with faecal miRNAs demonstrating particularly strong correlations with mucosal inflammation [145, 158, 159]. miR-223, miR-1246, and miR-155 are frequently elevated in the faeces of UC patients and have been associated with disease activity, with miR-223 showing diagnostic accuracy comparable to established inflammatory markers such as calprotectin [148, 159]. From a therapeutic perspective, preclinical models have shown that targeting miRNA expression through mimics or inhibitors can effectively modulate inflammatory responses [148, 161]. Specifically, inhibition of miR-155 or miR-301a in murine colitis models significantly reduced cytokine production and histological damage [162, 163], while administration of miR-141 mimics favored epithelial integrity and reduced inflammation [164].

1.3.3. Regulatory role of miRNA in colonic mucosa

miRNA-mediated disruption of epithelial barrier integrity and intestinal permeability. miRNAs play a crucial role in maintaining the integrity of the intestinal epithelial barrier by regulating tight junction proteins, signalling pathways, and immune interactions [9, 73, 147]. In UC, aberrant expression of several miRNAs has been linked to impaired barrier function and increased intestinal permeability [73]. miR-21, commonly upregulated in UC tissue [149–151], reduces transepithelial electrical resistance and promotes paracellular permeability by targeting *RhoB* and therefore upregulating *ARF4* [165], leading to downregulation of tight junction proteins such as occludin, claudin-1, and claudin-4 [165, 166]. Despite implications of miR-21 to have a context-dependent protective effect via Rho-associated coiled-coil containing protein kinase-1 (ROCK1)-mediated occludin expression [167], the majority of evidence supports a barrier-disruptive role [149–151, 165, 166]. Similarly, miR-155, which is induced by inflammatory cytokines like TNF- α , also compromises barrier function by targeting occludin, claudin-1, claudin-8, and MLCK [73]. miR-223, elevated in serum and faeces of UC patients and derived from mast cell exosomes, was shown to downregulate claudin-8 [168]. Furthermore, inhibition of miR-223 in murine models improves tight junction protein expression and colitis severity [169]. Literature also shows miRNAs such as miR-122a, miR-874, and miR-1290 to have a capacity of reducing the expression of occludin, ZO-1, claudin-1, and MLCK, further contributing to barrier dysfunction [73, 170]. Conversely, certain miRNAs such as miR-320a are associated with enhanced or protective barrier functions, and are reported to promote mucosal repair and enhance barrier integrity [73]. Additionally, miR-93 supports tight junction stability by downregulating *PTK6*, a negative regulator of claudin-3 [171], while miR-34a-5p strengthens barrier integrity by inhibiting *Snail*, a transcriptional repressor of multiple junctional proteins [170]. Furthermore, such miRNAs as miR-16-5p, miR-124, and miR-145 are also implicated in modulating tight junction protein expression and signalling pathways [73, 172].

miRNA control of epithelial injury and repair in UC. miRNAs are also reported to modulate epithelial cell survival, apoptosis, and regenerative capacity [73, 146, 147, 170]. Therefore, dysregulation of miRNAs may disrupt the balance between epithelial injury and repair, taking part in UC pathogenesis as well [146]. For example, miR-150, which is shown to be upregulated in both human and murine colitis, contributes to epithelial injury by interfering with c-Myc, leading to impaired barrier restoration [173]. Additionally, miR-29 family members (miR-29a and miR-29b) appear to

exhibit protective roles in inflammation control, despite their upregulated expression in UC [73, 174]. This is confirmed by the knockout models that showed worsened colitis, indicating the importance of miR-29 family molecules in epithelial maintenance [174]. Furthermore, such miRNAs as miR-23a, miR-26b, and miR-28 have been implicated in reducing pro-inflammatory protein expression, thereby supporting epithelial homeostasis [175].

1.4. Gut microbiota and its role in UC

1.4.1. Composition and function of gut microbiota

The human gut microbiota constitutes a highly dense and taxonomically diverse microbial ecosystem [176, 177]. It is predominantly localised in the colon, where microbial densities reach approximately 10^{11} – 10^{12} microorganisms per gram of luminal content, making it the most densely populated microbial habitat in the human body [176]. Taxonomically, gut microbiota is dominated by four major bacterial phyla – Firmicutes, Bacteroidetes, Proteobacteria, and Actinobacteria – with Firmicutes (particularly *Clostridium* clusters IV and XIVa) forming the majority of mucosa-associated species, and Bacteroidetes dominating the luminal populations [21, 177, 178]. Differences between the mucosal and luminal microbiota are also seen at the bacterial family level, with Lachnospiraceae and Ruminococcaceae enriched in mucosal areas, and Bacteroidaceae and Lactobacillaceae more abundant in the lumen [179, 180]. Gut colonisation begins at birth and changes significantly during early life [181]. Initially, gut is dominated by *Bifidobacterium* spp., then shifting to include *Clostridium*, *Bacteroides*, and diverse Firmicutes (such as *Ruminococcus*, *Faecalibacterium*, and *Veillonella*), reaching a relatively stable adult-like configuration by age three [178, 182]. The microbial composition of the colon varies by region [177, 179, 180, 182]. The right colon contains more *Klebsiella*, *Enterococcus*, and *Lactobacillus*, that support fermentation and the production of SCFAs, while the left colon is richer in *Parabacteroides*, *Bifidobacterium*, and *Dorea*, that are involved in intestinal motility and bile acid metabolism [177, 183]. These bacteria metabolise non-digestible dietary components into functional metabolites, mostly SCFAs such as acetate, propionate, and butyrate, which serve as energy substrates for colonocytes and modulate host lipid metabolism, glucose homeostasis, appetite regulation, and immune responses [184]. The microbiota is also important for the biosynthesis of essential cofactors, vitamins K and B, branched-chain amino acids, polyamines, and various bioactive compounds that influence epithelial cell renewal, immune modula-

tion, and intestinal barrier integrity [185]. Notably, *Akkermansia muciniphila* and *Bacteroides thetaiotaomicron* exhibit specialised mucin-degrading capabilities and therefore contribute to mucus layer maintenance and intestinal epithelial function [186]. Besides that, gut microbiota helps prevent pathogen overgrowth by competing for nutrients and space, producing antimicrobial compounds, and creating an environment that is unfavorable to harmful microorganisms [187]. Although the gut microbiota is highly individual, it remains relatively stable over time [182], and plays a key role in nutrient metabolism, energy regulation, and immune system function, underscoring its importance in sustaining overall host health [177].

1.4.2. Dysbiosis in UC

UC is consistently associated with mucosal and faecal microbial dysbiosis, characterised by reduced microbial diversity and altered composition (Fig. 1.4.2.1) [18, 20, 50]. Numerous studies have shown that patients with UC exhibit a depletion of beneficial commensals, particularly from the phyla Bacteroidetes and Firmicutes, including key butyrate-producing taxa such as *Roseburia hominis* and *Faecalibacterium prausnitzii* [75, 188, 189]. Reduction in butyrate level may impair mucosal healing and contribute to chronic inflammation [190]. Simultaneously, there is an enrichment of potentially pro-inflammatory pathobionts such as Enterobacteriaceae, *Escherichia coli*, *Fusobacterium nucleatum*, and *Enterococcus faecium* [75]. Notably, increased abundance of mucolytic bacteria like *Ruminococcus torques* and decreased levels of *Akkermansia muciniphila* have also been observed, suggesting disruptions in the mucus barrier [186, 191]. Although microbial changes in UC are broadly defined, it is still unclear whether dysbiosis causes the disease or results from it [147, 192]. It is postulated that dysbiosis may trigger inflammation, while inflammation can also promote a dysbiosis by altering the gut's oxidative and metabolic environment [192]. Interestingly, longitudinal studies show that the gut microbiota in UC patients stays relatively stable over time and across disease activity states, but it remains consistently different from that of healthy individuals [19]. Metabolomic alterations are also reported to accompany bacterial compositional shifts, with a decline in SCFAs and other immunoregulators (Fig. 1.4.2.1) [185, 192]. The persistence of dysbiosis in UC suggests it may help sustain the disease and supports the use of microbial-based treatments such as probiotics, dietary interventions, and faecal microbiota transplantation [192]. The latter has shown moderate efficacy, however, further mechanistic insights are required to optimize its application [193]. Overall, dysbiosis in UC is characterised by a reduction in protective anaerobes, expansion of pathobionts, and

disrupted microbial metabolism, which may all contribute to the pathophysiology of this disease [188, 192].

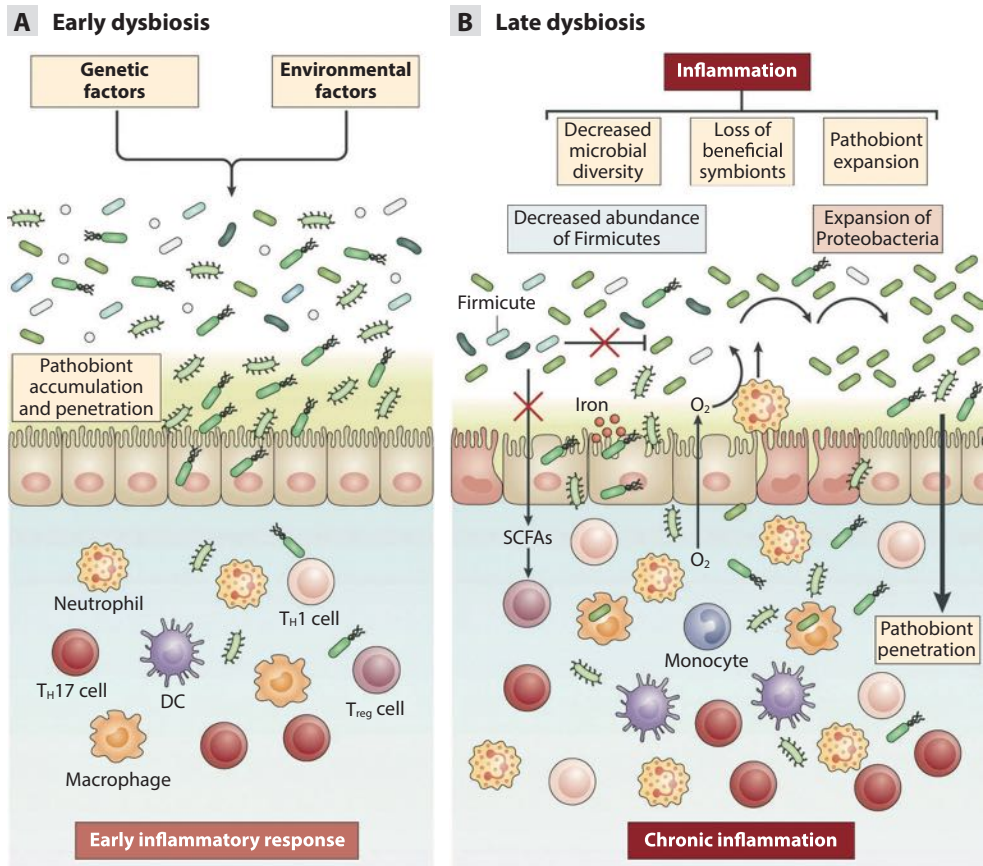


Fig. 1.4.2.1. Early (A) and late (B) dysbiosis in progression of UC

Genetic predispositions associated with IBD, along with environmental influences like diet and antibiotic exposure, can contribute to the build-up and infiltration of harmful pathobionts into the intestinal lamina propria (a process known as early dysbiosis (A)), which may occur before any noticeable clinical symptoms arise. As inflammation progresses, it can lead to more significant shifts in the microbial population, such as an increase in Proteobacteria (a process known as late dysbiosis (B)), driven by factors like elevated oxygen levels, greater nitrate (NO₃⁻) availability, and increased host-derived oxygen acceptors and iron in the gut. This advanced stage of dysbiosis typically involves a reduction in overall microbial diversity and the depletion of beneficial symbiotic bacteria. As a result, there may be increased mucosal adhesion and translocation of normally harmless microbes, which can sustain or intensify chronic inflammation. DC – dendritic cell, T_H cell – T helper cell, T_{reg} cell – regulatory T cell, SCFAs – short-chain fatty acids. The figure is adapted from Caruso et al. (2020) [194]. Reprinted with permission from Springer Nature under licence no. 5998750019851.

1.4.3. Disruption of host-microbiota interaction in UC

The interaction between gut microbiota and colonic epithelium plays a crucial role in maintaining intestinal homeostasis and modulating immune responses [21, 99, 176, 178]. Intestinal epithelial cells, located at the host-microbiota interface, detect microbial signals through pattern recognition receptors such as TLRs and NOD-like receptors [75, 184, 195]. These receptors recognize microbial-associated molecular patterns, including flagellin and lipopolysaccharide, initiating signalling through NF- κ B and phosphoinositide 3-kinase / AKT serine/threonine kinase (PI3K/AKT) that mediate anti-inflammatory and protective responses [184]. In UC, dysregulation of TLR signalling, such as increased TLR4 expression, has been linked to excessive immune activation and impaired barrier integrity [196]. Microbiota-derived metabolites, such as SCFAs, are essential for epithelial energy supply, mucin production, and regulation of gene expression via G-coupled receptor (GPR), such as GPR43, GPR109A, and aryl hydrocarbon receptor (AhR) pathways [184, 197]. As previously mentioned, SCFAs also promote MUC2 secretion by goblet cells, strengthening the mucus barrier that physically separates luminal microorganisms from host tissues [198]. Therefore, in UC, depletion of SCFA-producing bacteria is associated with disrupted mucus layer, increased epithelial permeability, and inflammation [106, 198]. Moreover, altered microbiota can overstimulate ILCs, located near the epithelial cells, resulting in excess secretion of pro-inflammatory cytokines like IL-17 and IFN- γ , further compromising the epithelial barrier [39, 75, 104]. Recent studies also imply the role of host-derived miRNAs, such as miR-124 and miR-1226, in modulation of bacterial gene expression and AMP production, thus as well influencing microbiota composition and inflammation [16, 147]. NF- κ B signalling-induced defensins and other AMPs are reported to be reduced in UC, leading to impaired microbial control [147]. This alteration is as well associated with bacterial products such as bile acid and tryptophan metabolites, influencing epithelial signalling and AMP expression through farnesoid X receptor and AhR pathways [184, 185, 199]. Altogether, the functional crosstalk between host and microbiota is essential for maintaining gut health, and its dysregulation in UC contributes to ongoing inflammation, damage to the epithelium, and worsening of the disease [184, 198, 199].

1.5. Intestinal organoid models in UC research

1.5.1. Overview of intestinal organoid technology

Definition and key features of adult stem cell-derived intestinal organoids. Two main approaches exist to establish intestinal organoids cultures *in vitro*, including adult stem cell-derived organoids or pluripotent stem cell (embryonic or induced)-derived organoids (Fig. 1.5.1.1) [200]. Further review will focus mainly on adult stem cell-derived intestinal epithelial organoids. Intestinal epithelial organoids are three-dimensional (3D) *in vitro* structures derived from adult stem cells (intestinal stem cells), particularly Lgr5⁺ cells isolated from the crypt base [200–203]. Self-organization of these structures is supported by extracellular matrix, such as Matrigel, supplemented for human-derived cells with growth factors including EGF, R-spondin-1, Noggin, nicotinamide, MAPK and ALK small molecule inhibitors, as well as Wnt3a [201, 204, 205]. Morphologically, established organoids are characterised as spheric structures, having apical-basal polarity, a central lumen, and budding crypt-like domains [205]. From a compositional perspective, colonic epithelial organoids consist of a diverse range of specialised intestinal epithelial cells, including colonocytes, goblet cells, and enteroendocrine cells, and may occasionally contain a small number of Paneth cells [203, 205]. This composition closely reflects the cellular heterogeneity of the native colonic epithelium *in vivo* [206]. Colonic epithelial organoids (also known as colonoids) derived from adult patient tissues maintain the phenotypic, genotypic, and epigenetic characteristics of their donor, including disease-specific traits [205, 207, 208]. This enables long-term culture, cryopreservation, and expansion, while preserving region-specific identity and functional relevance [209]. Importantly, organoids are described to recapitulate epithelial physiological activities, such as nutrient absorption, mucus production, hormone secretion, and barrier function [210, 211]. Compared to conventional cancer-derived two-dimensional (2D) cell cultures (e.g., Caco-2, SW-480, or HT-29) and animal models, intestinal organoids provide superior physiological relevance, enhanced experimental reproducibility, and fewer ethical limitations [201]. Their ability to closely mimic the human colonic epithelium *in vitro* / *ex vivo* positions organoids as a powerful platform for investigating human intestinal biology [203, 205–207, 210, 211].

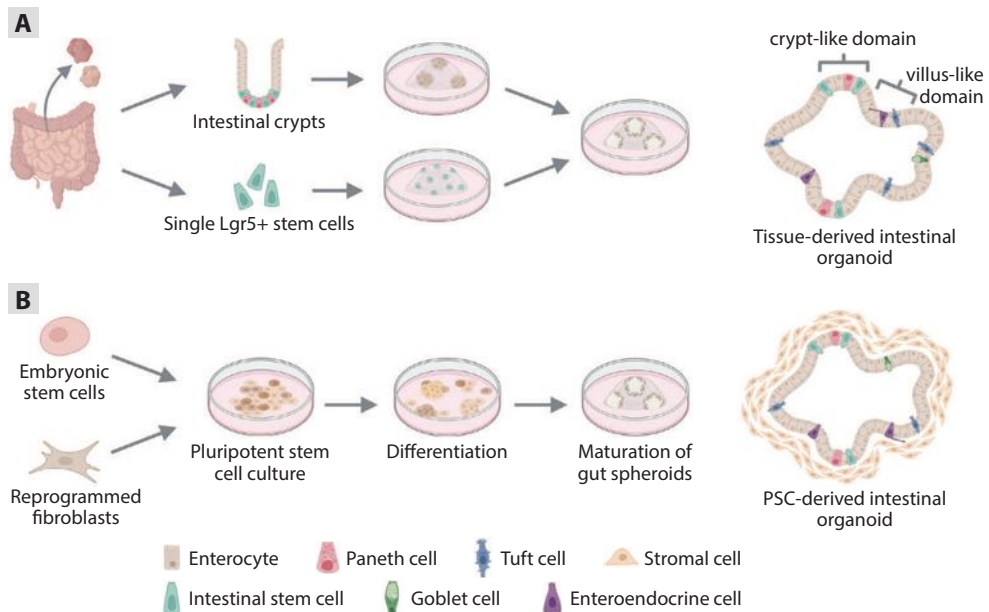


Fig. 1.5.1.1. Establishment of adult stem cell- and pluripotent stem cell-derived intestinal organoids

Two main strategies for generating intestinal organoids are presented. **(A)** One method involves culturing organoids from isolated intestinal crypts or single Lgr5⁺ intestinal stem cells, resulting in epithelial-only structures. **(B)** Alternatively, pluripotent stem cells, including embryonic stem cells and induced pluripotent stem cells, can be guided through a stepwise differentiation process into endoderm and subsequently gut lineages, producing organoids that contain both epithelial and mesenchymal cell types. The figure is adapted from Kromann et al. (2024) [203]. Reprinted under a Creative Commons Attribution 4.0 International (CC BY 4.0) licence.

Adult stem cell-derived epithelial organoids as a platform for modeling intestinal epithelium. The ability of colonic epithelial organoids to simulate epithelial organization, tight junction formation, and polarity enables investigation of epithelial barrier integrity, transport mechanisms, and mucosal interactions [212]. Furthermore, colonoids allow the studies of intestinal stem cell dynamics, epithelial cell turnover, and differentiation, which are critical in regenerative and inflammatory conditions [203, 213]. The ability to generate organoids from biopsies of healthy individuals and patients with various diagnoses allows direct comparison of disease and control phenotypes, including altered methylation patterns and gene expression profiles [205, 210]. Thus, numerous studies have confirmed colonoids as indispensable tool in modeling host-specific epithelial responses, dissecting mechanisms of intestinal diseases, and testing therapeutic interventions with high translational relevance [203, 205, 210–212]. Their capability to be adapted into polarised 2D monolayers or air-liquid interface

cultures improves access to both apical and basolateral compartments, making them well-suited for studying barrier function and host-microbiota interactions [205, 214, 215].

1.5.2. Organoid applications and challenges in UC research

Modeling epithelial barrier dysfunction and regeneration. Organoid models derived from patient colonic stem cells have significantly advanced the study of epithelial barrier disruption and regeneration in UC (Fig. 1.5.2.1) [203, 205, 210–212]. Colonoids enable more accurate modeling of the epithelial responses to pro-inflammatory cytokines such as TNF- α , IL-1 β , and IFN- γ , that are driving the pathogenesis of UC [211, 216]. It has been shown that upon exposure, organoids exhibit hallmark UC characteristics, including disrupted tight junction integrity, redistribution of junctional proteins, impaired epithelial cohesion, and increased apoptotic activity [216]. Studies have also demonstrated altered expression and localisation of tight junction proteins such as occludin, claudin-1, and ZO-1 in UC-derived organoids compared to healthy controls [217–220]. Moreover, organoids facilitate functional studies of epithelial plasticity and regeneration [205, 221]. For instance, IL-22, a cytokine implied in UC pathogenesis, has been shown to enhance epithelial differentiation but impair long-term stem cell maintenance under chronic exposure [222]. In regenerative applications, transplantation of cultured organoids into murine models of DSS-induced colitis has successfully restored epithelial architecture and improved mucosal healing scores, supporting their therapeutic promise [201, 223].

Investigating host-microbiota interactions in UC. Patient-derived colonic epithelial organoids are a controlled system suitable for studying the complex crosstalk between intestinal epithelium and the microbiota in UC (Fig. 1.5.2.1) [205, 211]. Their ability to recapitulate epithelial cell diversity and patient-specific responses are the characteristics that make them an effective platform for exploring microbial adhesion, invasion, and immune modulation [211, 224]. In the literature, co-culture systems combining colonoids with bacteria (such as *Clostridioides difficile*, and *Lactobacillus*) or immune cells (such as T cells, dendritic cells, and ILCs) have uncovered key mechanisms of epithelial cytokine responses and inflammation [203, 225, 226]. What is more, differences in microbial impact between UC and healthy donor-derived microbiota have been shown to affect barrier integrity through impairment of tight junction protein expression and inflammatory gene regulation [227]. Other studies report air-liquid interface models and 2D monolayer formats useful to provide better apical access, enabling studies of mucin production, epithelial permeability, and microbial metabolite effects

[228]. Additionally, recent study demonstrated that the differentiation of specialised epithelial subsets, such as microfold cells, within colonic organoid systems allows the study of antigen sampling and immune activation at the mucosal interface [229]. Therefore, these organoid-based platforms are indispensable in modeling the epithelial-microbial-immune interactions that contribute to UC pathogenesis [203, 205, 207, 210–212, 216].

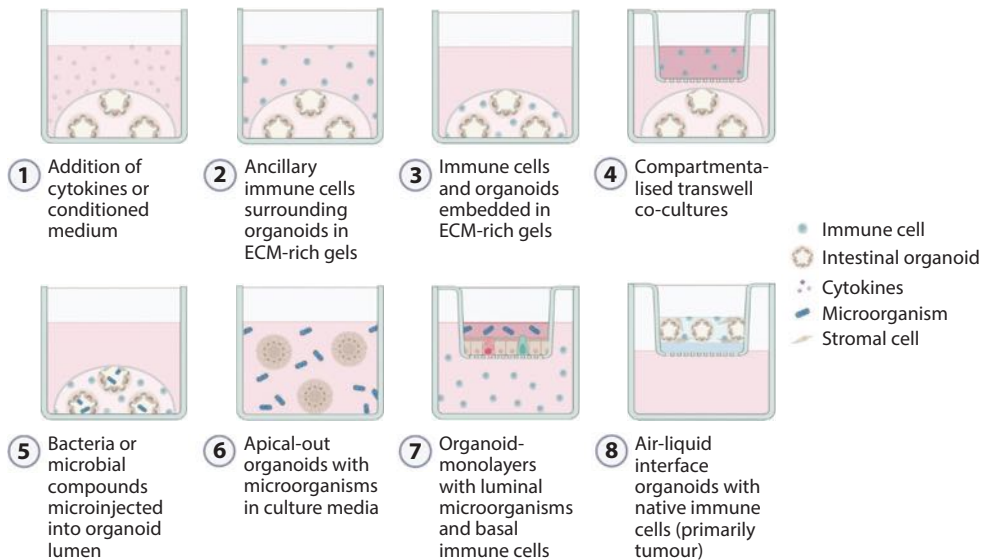


Fig. 1.5.2.1. Applications of adult stem cell-derived intestinal organoids

Intestinal organoids offer broad applications in immunological research. These include exposure to cytokines or media conditioned by immune cells (1), co-culture systems incorporating various immune cell types (2–4), the introduction of microbial elements (5–7), or the use of air-liquid interface organoids, which support the parallel development of resident immune cells (8). The figure is adapted from Kromann et al. (2024) [203]. Reprinted under a Creative Commons Attribution 4.0 International (CC BY 4.0) licence.

Technical limitations and translational challenges. Although useful, current intestinal epithelial organoid models still have important limitations [206, 230, 231]. Specifically, these cultures primarily contain epithelial cells and lack the immune, stromal, and neural components necessary to fully mimic the *in vivo* intestinal environment [203, 209, 212]. This limits their capacity to reflect multicellular interactions that are known to be critical to UC [211]. Additionally, the routine use of these epithelial cell-based platforms is also limited by high costs, technical complexity, and slow expansion rates [205, 232]. Nevertheless, the inflammatory transcriptional profile of UC organoids gradually fades during extended culture unless it is re-induced by inflammatory stimuli [233]. Additional challenges to large-scale application of organoids are also related to ethical considerations regarding human tissue

use, donor variability, and limited biopsy availability [205, 231]. These challenges are being addressed by advancing co-culture systems, standardising protocols and autologous transplantation strategies [210, 234]. Despite limitations, patient-derived organoids are still considered promising precision models for understanding UC and testing personalised therapies [212, 216, 221].

2. MATERIALS AND METHODS

2.1. Ethics statement

The study was approved by the Kaunas Regional Biomedical Research Ethics Committee (Protocol no. BE-2-10, issued on 08/03/2011, and Protocol no. BE-2-31, issued on 22/03/2018). UC patients and non-IBD control individuals were included in the study. Study subject recruitment was conducted in the Department of Gastroenterology at the Hospital of Lithuanian University of Health Sciences (Kaunas, Lithuania) during the periods 2011–2014 and 2017–2023. Study population consisted of individuals of European ancestry. All procedures were performed according to relevant regulations and guidelines. UC patients underwent colonoscopy either due to a disease flare-up or for screening purposes, while non-IBD control participants underwent colonoscopy as part of a colorectal cancer screening program. All patients provided their consent to participate in the study by signing an informed consent form.

2.2. Study design and population

In order to evaluate the role of colonic epithelial miRNAs and gut microbiota in the pathogenesis of UC, the study was divided into three parts (Fig. 2.2.1):

- Part I: miRNA expression profiling in colonic tissue and epithelial cell populations.
- Part II: gut microbiota profiling in faeces.
- Part III: functional analysis of the impact of commensal bacteria on colonic epithelium using intestinal organoid system.

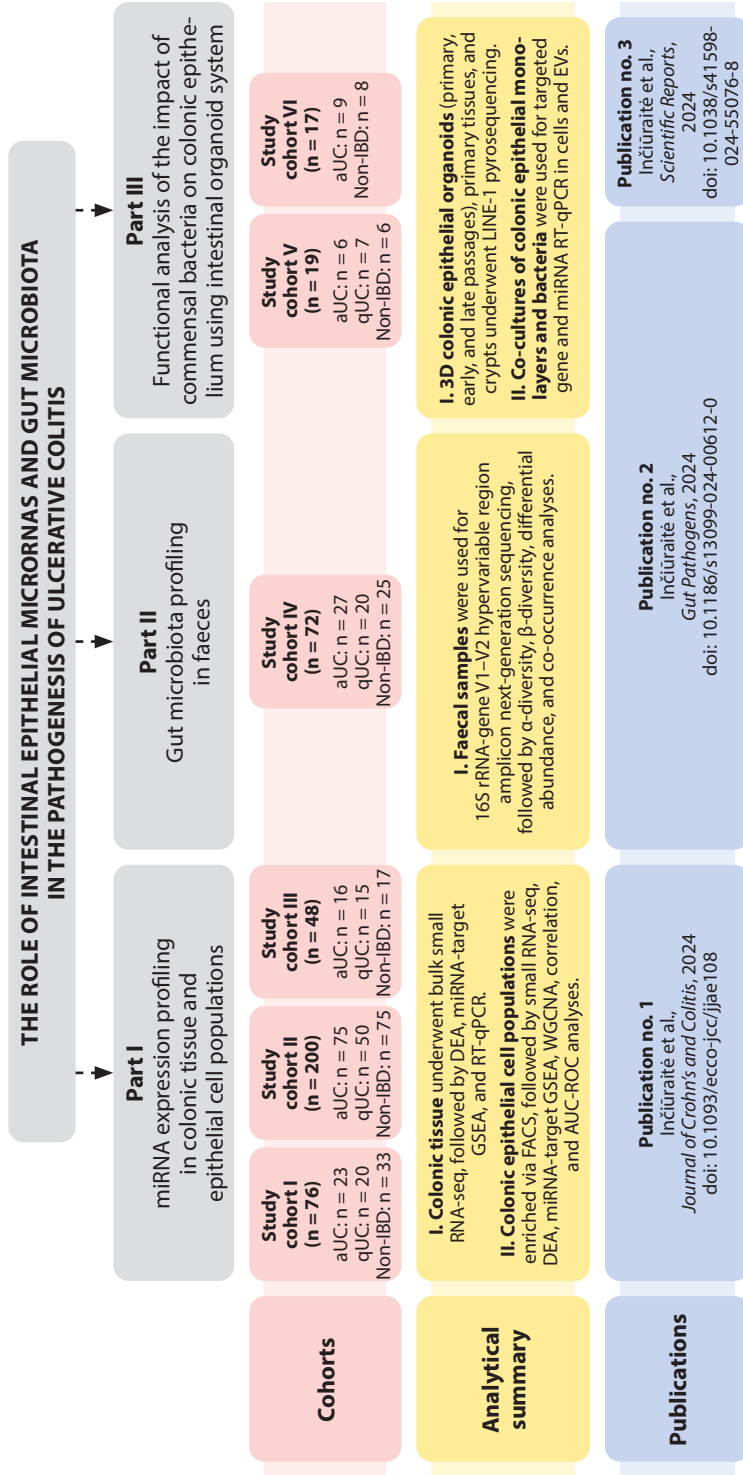


Fig. 2.2.1. Outline of study structure, cohorts, key methods, and resulting publications

aUC – patients with active ulcerative colitis, qUC – patients with quiescent ulcerative colitis, Non-IBD – control individuals without previous history of inflammatory bowel disease, RNA-seq – RNA sequencing, DEA – differential expression analysis, GSEA – gene set enrichment analysis, RT-qPCR – reverse transcription-quantitative polymerase chain reaction, FACS – fluorescence-activated cell sorting, WGCNA – weighted gene co-expression network analysis, AUC-ROC – area under the receiver operating characteristic curve, rRNA – ribosomal RNA, LINE-1 – long interspersed nuclear element-1, EVs – extracellular vesicles. Illustration created with BioRender.com.

Study Parts I–III were conducted using six independent cohorts (study cohorts I–VI) comprising both UC patients and non-IBD individuals. Patients diagnosed with UC, based on standard clinical, endoscopic, and histological criteria [235], were further categorised according to their endoscopic Mayo score: a score of 0–1 was classified as mild disease (healed mucosa), a score of 2 indicated moderate UC, and a score of 3 represented severe UC (characterised by spontaneous bleeding and ulcerations in the colon) [236]. Quiescent UC was confirmed in patients with a stool frequency ≤ 3 /day, absence of rectal bleeding, and healed mucosa.

In Part I, a total 324 colonic biopsy samples were collected from study cohorts I–III. Two of these cohorts ($n = 76$ [study cohort I] and $n = 48$ [study cohort III]) were used for small RNA sequencing at the tissue and epithelial cell population levels, respectively. Biological specimens from study cohort II ($n = 200$) were used for targeted gene expression analysis using reverse transcription-quantitative polymerase chain reaction (RT-qPCR). In Part II, 72 faecal samples from study cohort IV were used for 16S ribosomal RNA (16S rRNA) gene sequencing. In Part III, a total of 36 colonic biopsy samples from study cohorts V and VI were utilised. Study cohort V ($n = 19$) was allocated for pyrosequencing of 3D colonic epithelial organoids, while study cohort VI ($n = 17$) was designated for functional testing of the colonic epithelium using organoid-derived monolayers.

The overview of the study design, cohorts and main outcomes of Parts I–III is summarized in Fig. 2.2.1. A more detailed explanation of the methods used and the characteristics of the study cohorts is provided in subsequent sections and related publications.

2.3. Part I. miRNA expression profiling in colonic tissue and epithelial cell populations

A graphical visualisation of the methods used in the Study Part I and the characteristics of the study cohorts is provided in Fig. 2.3.1.

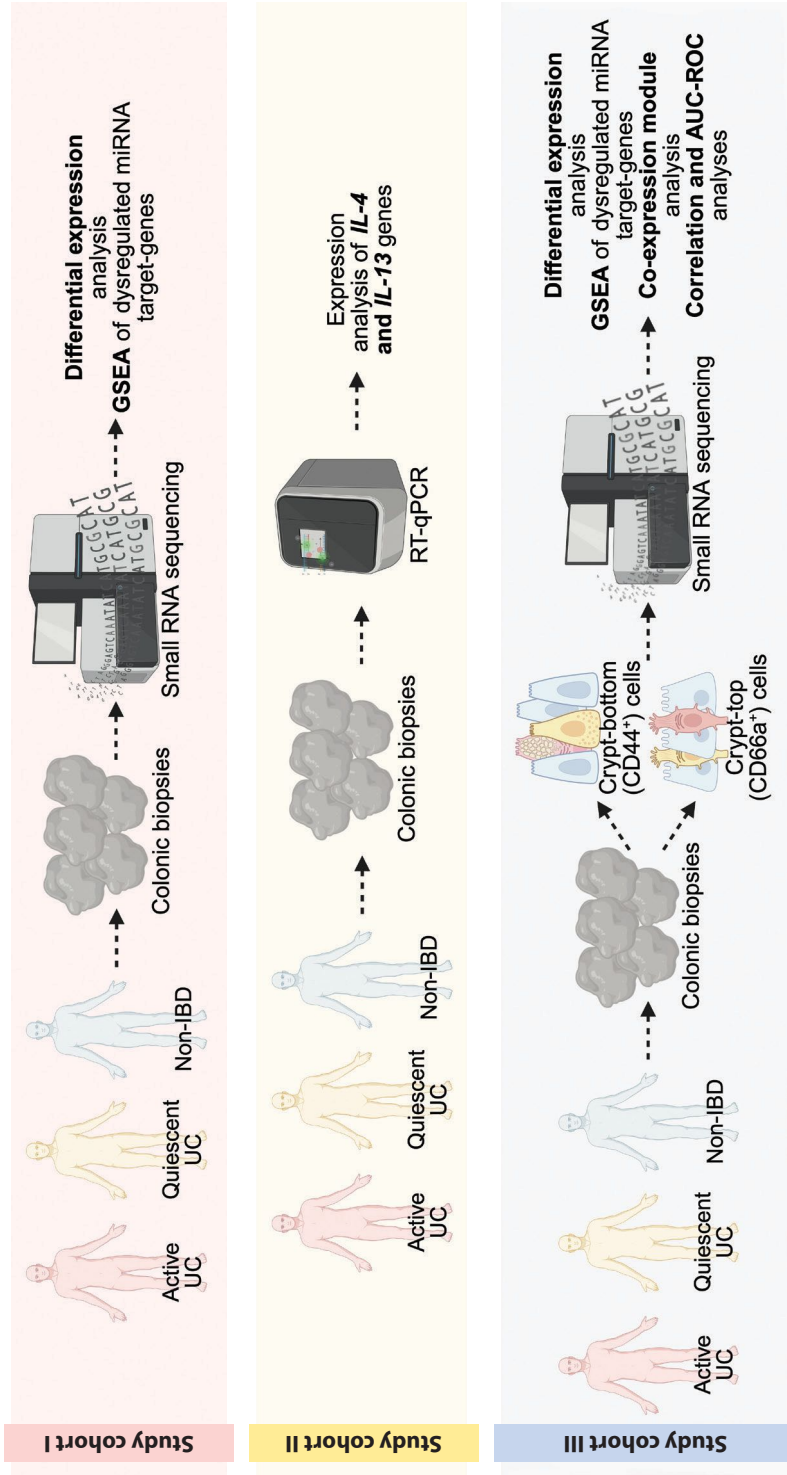


Fig. 2.3.1. Experimental design scheme for Study Part I

UC – ulcerative colitis, Non-IBD – control without previous history of inflammatory bowel disease, GSEA – gene set enrichment analysis, IL – interleukin, PCR – polymerase chain reaction, AUC-ROC – area under the receiver operating characteristic curve. Illustration created with BioRender.com.

2.3.1. Collection and disaggregation of colonic biopsies

Colonic biopsies from study cohorts I and II subjects were collected into sterile cryotubes, snap-frozen and stored at -80°C until further use for tissue miRNA sequencing and targeted gene expression analysis, while biopsies from study cohort III for miRNA sequencing in colonic epithelial cell populations were used fresh and dissociated into single-cell suspensions immediately after collection. The detailed clinicopathological and demographical descriptions of study subjects enrolled in study Part I (study cohorts I–III) are provided in publication “*The microRNA Expression in Crypt-Top and Crypt-Bottom Colonic Epithelial Cell Populations Demonstrates Cell-Type Specificity and Correlates with Endoscopic Activity in Ulcerative Colitis*” [237]. Briefly, when applicable, biopsies were processed mechanically and enzymatically to generate single-cell suspensions. Four to six biopsies were rinsed in $1\times$ Phosphate buffered saline (PBS) containing antibiotics (50 IU/mL penicillin (Gibco, Thermo Fisher Scientific), 50 $\mu\text{g}/\text{mL}$ streptomycin (Gibco, Thermo Fisher Scientific), 0.5 mg/mL gentamicin (Gibco, Thermo Fisher Scientific)). Biopsies were then fragmented into $\sim 1\text{--}2\text{ mm}^3$ sized pieces and incubated in $1\times$ trypsin-ethylenediaminetetraacetic acid (EDTA, Invitrogen, Thermo Fisher Scientific) solution for 40–45 minutes at room temperature with agitation to isolate the intestinal crypts from the surrounding lamina propria. Crypts were then gently transferred into $1\times$ PBS and agitated. The resulting cell suspension was filtered and resuspended in Dulbecco’s Modified Eagle Medium/Nutrient Mixture F-12 (DMEM/F-12) medium (1:1) containing 15 mM 4-(2-hydroxyethyl)-1-piperazineethanesulfonic acid (HEPES) (Gibco, Thermo Fisher Scientific) compatible with flow cytometry analysis.

2.3.2. Fluorescence-activated cell sorting (FACS)-based cell enrichment

Freshly prepared cell suspensions were used for all sorting experiments to ensure cell viability. Antibody staining was performed in $1\times$ PBS with 1% heat-inactivated fetal bovine serum (FBS), and non-specific binding was minimised by pre-incubating cells with Human TruStain FcX (BioLegend) for 10 minutes. Cells were then stained with antibodies at recommended dilutions as previously described by Dalerba et al. [238]. Antibodies included mouse anti-human CD326/EpCAM-FITC (clone VU-1D9, Life Technologies), CD44-APC (clone G44-26, BD Biosciences), CD66a-PE (clone 283340, R&D Systems), CD45-APC-Cy7 (clone 2D1, BioLegend). Excess antibodies were washed off, and cells were resuspended in $1\times$ PBS with 1%

FBS. Flow cytometry and cell sorting were performed using a CyFlow Space cell sorter (Sysmex Partec), data was analysed in FlowJo v10.7 (BD Biosciences). Two colonic epithelial cell populations – CD45⁻/EpCAM⁺/CD44⁺/CD66a⁻ and CD45⁻/EpCAM⁺/CD44⁻/CD66a⁺ – were identified. These populations were described as crypt-bottom cells (including undifferentiated colonic epithelial cells, secretory goblet cells and enteroendocrine cells) and crypt-top cells (comprising absorptive colonocytes and BEST4⁺/OTOP2⁺ cells), respectively. Sorted cells were cryopreserved at -70 °C for total RNA extraction. The detailed gating strategy and single-cell RNA-seq data-derived [91] expression plot of the main markers of cell populations are provided in publication “*The microRNA Expression in Crypt-Top and Crypt-Bottom Colonic Epithelial Cell Populations Demonstrates Cell-Type Specificity and Correlates with Endoscopic Activity in Ulcerative Colitis*” [237].

2.3.3. RNA extraction

Total RNA was extracted from colonic biopsies using miRNeasy Mini Kit (Qiagen) and sorted epithelial cells using Single Cell RNA Purification Kit (Norgen). All procedures were conducted in accordance with the manufacturers’ recommendations, including RNase-Free DNase I (Qiagen) treatment. The concentration of total RNA was quantified using a NanoDrop 2000 spectrophotometer (Thermo Fisher Scientific) and a Qubit 4 fluorometer (Invitrogen, Thermo Fisher Scientific). RNA quality was evaluated with an Agilent 2100 Bioanalyzer (Agilent Biotechnologies).

2.3.4. RT-qPCR and data analysis

The expression of *IL-4* and *IL-13* genes in colonic tissues was quantified by reverse transcribing total RNA with the High-Capacity cDNA Reverse Transcription Kit (Applied Biosystems, Thermo Fisher Scientific) and measuring expression levels using TaqMan Gene Expression Assays (*IL-4*: Hs00174122_m1; *IL-13*: Hs00174379_m1, Applied Biosystems, Thermo Fisher Scientific) on an ABI 7500 Fast Real-Time PCR System (Applied Biosystems, Thermo Fisher Scientific). *IL-4* and *IL-13* cycle of threshold (C_t) values were normalized to the *GAPDH* reference gene (Hs99999905_m1, Applied Biosystems, Thermo Fisher Scientific). All procedures followed the manufacturer’s protocols. The relative gene expression changes were determined using $2^{-\Delta\Delta C_t}$ method [239]. Statistical analyses were conducted in R Studio (v4.0.3), with gene expression differences assessed using the Mann-Whitney *U* test. Significance was set at $p < 0.05$.

2.3.5. Small RNA library preparation and next-generation sequencing

Small RNA libraries were prepared using the TruSeq Small RNA Sample Preparation Kit (Illumina) with 1 µg of total RNA per colonic tissue sample, and the NEXTFLEX Small RNA-seq Kit v.3 (Bioo Scientific) with up to 50 ng of total RNA per sorted cell sample. All procedures followed the manufacturers' protocols. Library yields were evaluated using the Agilent 2200 TapeStation system (Agilent Biotechnologies). TruSeq and NEXTFLEX libraries were pooled (24 and 16 samples per lane, respectively) and sequenced on the HiSeq 4000 platform (Illumina).

2.3.6. Bioinformatics and statistical analysis of small RNA sequencing data

Demultiplexed raw reads (.fastq) were processed using the nf-core/smrnaseq v.1.0.0 pipeline (Nextflow v.20.01.0) with default parameters [240] and 'illumina' or 'nextflex' protocols for tissue or sorted cell libraries, respectively. Reads were aligned to mature and hairpin miRNA sequences from the miRBase v.22.1 database [241]. miRNA annotation was performed with mirTOP (v.0.4.23) [242]. Quality control excluded samples with read counts < 1.5 interquartile range (IQR) and detected miRNAs < 0.5 IQR on a log₂ scale. miRNAs with mean raw counts < 1 or low variability were also excluded. Differential expression analysis was performed on size factor-normalised miRNA counts using DESeq2 [243], incorporating age (scaled and centered) and sex as covariates. Wald test p-values were corrected for false discovery rate (FDR) using the Benjamini-Hochberg method, with significant miRNAs defined by FDR < 0.05 and |log₂FC| > 1. Multidimensional scaling analysis (MDS) was conducted on variance-stabilising transformation (VST) normalized data. Spearman's rank correlation was used to assess associations between sex- and age-adjusted miRNA counts and the endoscopic Mayo subscore with FDR < 0.05 were considered significant. Sex and age effects were removed using the removeBatchEffect function from the limma package [244]. Strength of correlation was defined as follows: 0.00 ≤ |rho| < 0.40 (weak correlation), 0.40 ≤ |rho| < 0.70 (moderate correlation), and 0.70 ≤ |rho| < 1.00 (strong correlation). Statistical analyses and data processing were conducted using R (v4.0.3), with visualisations generated using the ggplot2 package [245].

For more detailed information on small RNA sequencing data processing, please refer to the publication "*The microRNA Expression in Crypt-Top and Crypt-Bottom Colonic Epithelial Cell Populations Demonstrates Cell-*

Type Specificity and Correlates with Endoscopic Activity in Ulcerative Colitis” [237].

2.3.7. miRNA target gene set enrichment analysis

Gene set enrichment analysis (GSEA) was conducted to infer the biological functions of differentially expressed miRNAs, focusing on Reactome pathways [246] and Gene Ontology (GO) categories [247]. Validated miRNA-target interactions (MTIs) were retrieved from miRecords [248], miRTarBase [249], and TarBase [250] using the multiMiR package [251]. MTIs were analysed with hypergeometric tests via the enrichPathway (ReactomePA) [252] and enrichGO (clusterProfiler) [253] functions, using genes expressed in colon crypt-bottom and crypt-top cells as the background reference (from single-cell RNA-seq data, GEO accession GSE116222). Pathways with FDR < 0.05 were considered significantly deregulated. The expression of genes related to IL-4 and IL-13 signalling pathway in colonic cell populations was also analysed using the same dataset (GEO accession: GSE116222).

2.3.8. miRNA co-expression network analysis

Weighted gene co-expression network analysis (WGCNA) was performed to identify co-expressed miRNA modules using the CEMiTool package (v.1.22.0) for R [254]. Variance-filtered, VST-normalised miRNA counts were used to generate co-expression modules, with a minimum of five miRNAs per module and GSEA gene sets. Filtering was applied with a p-value threshold of 0.1. Module eigengene values for co-expressed miRNAs in colonic epithelial cells were also calculated in colon tissue data using WGCNA (v.1.72-1) package for R [255].

Spearman’s rank correlations between module eigengene values and endoscopic Mayo subscore were computed for both colonic epithelial cell populations and tissue, with FDR < 0.05 considered significant. The pROC package (v.1.18.4) [256] was used to calculate the area under the receiver operating characteristic curve (AUC-ROC) to evaluate the ability of module eigengene values to distinguish between active and quiescent UC in both colonic tissue and epithelial cell populations.

2.4. Part II. Gut microbiota profiling in faeces

A graphical visualisation of the methods used in the Study Part II and the characteristics of the study cohort is provided in Fig. 2.4.1.

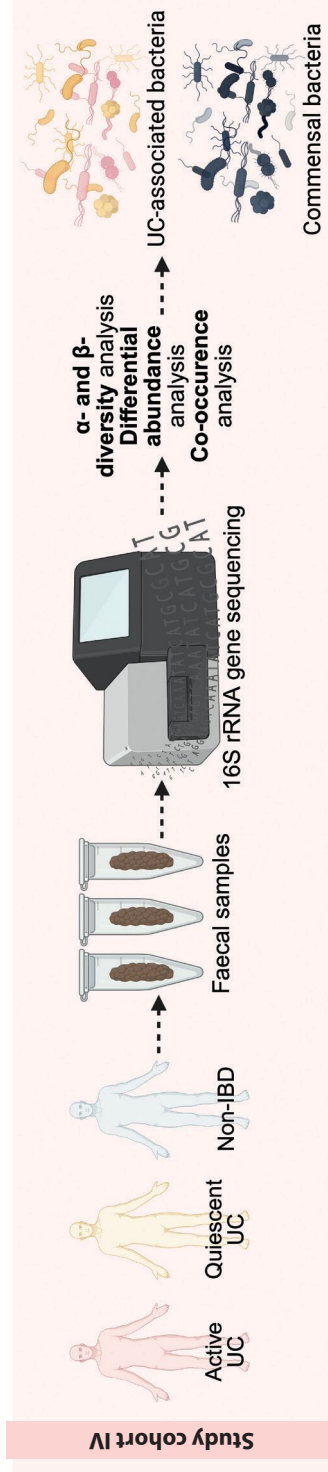


Fig. 2.4.1. Experimental design scheme for Study Part II

UC – ulcerative colitis, Non-IBD – control without previous history of inflammatory bowel disease, rRNA – ribosomal RNA. Illustration created with BioRender.com.

2.4.1. Collection of faecal material and DNA extraction

Up to 200 mg of faecal material per sample was collected and fresh-frozen at -80°C until further use. The detailed clinicopathological and demographical descriptions of study subjects included in study Part II (study cohort IV) are provided in publication “*Constituents of stable commensal microbiota imply diverse colonic epithelial cell reactivity in patients with ulcerative colitis*” [257]. The use of antibiotics within 1 month prior to enrollment in the study was the exclusion criterion for both UC patients and non-IBD controls. Total DNA was extracted using the AllPrep PowerFecal DNA/RNA Kit (Qiagen) in accordance with the manufacturer’s protocol. The purity and concentration of the extracted total DNA were assessed using a Qubit 4 fluorometer (Invitrogen, Thermo Fisher Scientific).

2.4.2. 16S rRNA gene library preparation and sequencing

To generate libraries targeting the V1–V2 hypervariable regions of the bacterial 16S rRNA gene, isolated DNA was amplified using the primer pair 27F (5'-AGAGTTTGATCCTGGCTCAG-3') and 338R (5'-TGCTGCCTCCGTAGGAGT-3') with dual indexing incorporated during the PCR process. The cycling conditions were as follows: initial denaturation at 98°C for 30 seconds, followed by 34 cycles of 98°C for 9 seconds, 50°C for 1 minute, and 72°C for 20 seconds, with a final extension at 72°C for 10 minutes and a hold at 10°C . PCR products were purified and normalised using the SequalPrep Normalization Plate Kit (Invitrogen, Thermo Fisher Scientific). Sequencing of the 16S rRNA gene was performed on the Illumina MiSeq platform using the MiSeq Reagent Kit v3 (2×300 bp; Illumina).

2.4.3. Bioinformatics and statistical analysis of 16S rRNA gene sequencing data

16S rRNA gene sequencing data were processed into amplicon sequence variants (ASVs) and taxonomically annotated using the RDP v18 database [258] with the DADA2 package [259] (v1.10) in R. Reads were truncated to 200 bp (forward) and 150 bp (reverse) and filtered using $\text{maxEE} = 3$, $\text{trimLeft} = 5$, and $\text{truncQ} = 5$ parameters to ensure high-quality data. The rarefaction was applied to normalise the samples and exclude rare ASVs (< 10 counts in $< 10\%$ of samples). α -diversity metrics (Chao1, Simpson, Shannon) and β -diversity (Bray-Curtis dissimilarity) were calculated. PERMANOVA was applied to assess significant changes in β -diversity. Core microbiome analysis included taxa with $\geq 0.1\%$ relative abundance in $\geq 50\%$ of samples. Differential abundance analysis used the Mann-Whitney U test,

focusing on taxa with ≥ 10 counts in $> 20\%$ of samples. p values were adjusted using the Benjamini-Hochberg method, with significance set at $FDR < 0.05$. Compositional plots were generated with the microViz package [260].

For more detailed information on 16S rRNA gene sequencing data processing, please refer to the publication “*Constituents of stable commensal microbiota imply diverse colonic epithelial cell reactivity in patients with ulcerative colitis*” [257].

2.5. Part III. Functional analysis of the impact of commensal bacteria on colonic epithelium using intestinal organoid system

A graphical visualisation of the methods used in the Study Part III and the characteristics of the study cohorts is provided in Fig. 2.5.1.

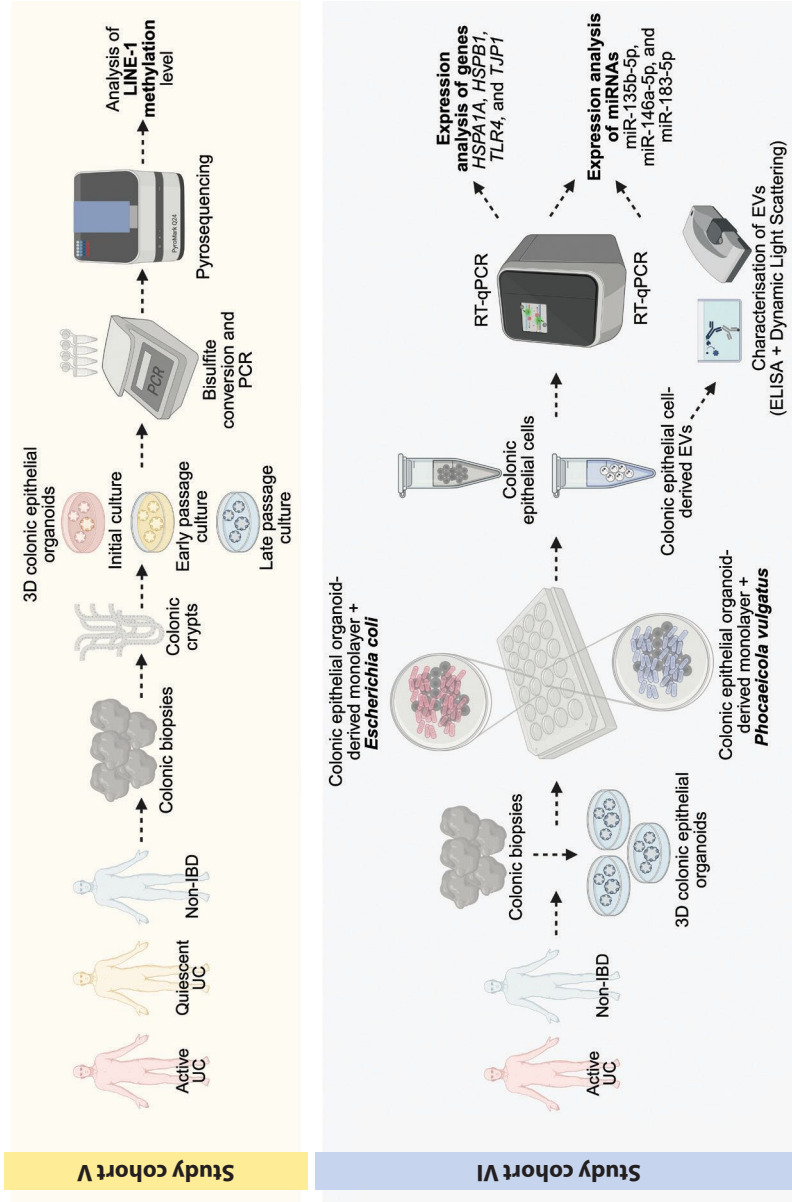


Fig. 2.5.1. Experimental design scheme for Study Part III

UC – ulcerative colitis, Non-IBD – control without previous history of inflammatory bowel disease, 3D – 3-dimensional, LINE-1 – long interspersed nuclear element-1, PCR – polymerase chain reaction, EVs – extracellular vesicles, RT-qPCR – reverse transcription-quantitative polymerase chain reaction, ELISA – enzyme-linked immunosorbent assay. Illustration created with BioRender.com.

2.5.1. Collection of colonic biopsies and establishment of 3D colonic epithelial organoids

Freshly collected colonic biopsies from study cohorts V and VI subjects were processed to establish 3D undifferentiated colonic epithelial organoids from adult intestinal stem cells. The detailed clinicopathological and demographical descriptions of study subjects included in study Part III (study cohorts V and VI) are provided in publications “*Prolonged culturing of colonic epithelial organoids derived from healthy individuals and ulcerative colitis patients results in the decrease of LINE-1 methylation level*” [261] and “*Constituents of stable commensal microbiota imply diverse colonic epithelial cell reactivity in patients with ulcerative colitis*” [257], respectively. Organoid generation procedure was performed following the IntestiCult Organoid Growth Medium (Human) (OGMH, StemCell Technologies) protocol with slight modifications. Biopsies were minced with a sterile scalpel and digested using Gentle Cell Dissociation Reagent (StemCell Technologies). The resulting homogenate was vigorously pipetted in cold DMEM/F-12 medium (supplemented with 1% BSA and 15 mM HEPES), passed through a 70 μm filter, and centrifuged to isolate colonic crypts. The isolated crypts were mixed with Matrigel Matrix (Phenol Red-free, LDEV-Free, Corning), and 50 μL domes of the crypt-Matrigel mixture were plated in 24-well culture plates. Organoids were cultured in OGMH medium supplemented with penicillin/streptomycin (100 $\mu\text{g}/\text{mL}$, Gibco, Thermo Fisher Scientific) and the Rho/ROCK pathway inhibitor Y-27632 (10 μM , StemCell Technologies) during the first two days. Cultures were incubated at 37 $^{\circ}\text{C}$ with 5% CO_2 , and their development was monitored microscopically using the Axio Observer 7 microscope (ZEISS, Carl Zeiss Microscopy) and ZEN 3.1 software (ZEISS, Carl Zeiss Microscopy). Primary splitting was performed 1–2 weeks after establishment, with subsequent passaging every 7–10 days depending on organoid maturity. The first splitting of organoids occurred 7–14 days after establishment, with subsequent passages performed every 7–10 days based on maturity. Organoids from study cohort V were cultured up to the fifth passage, portions of isolated crypts and undifferentiated organoids from passages 0, 1, and 5 were cryopreserved using CryoStor[®] CS10 reagent (StemCell Technologies) and stored at -80°C . Organoid cultures were periodically tested for mycoplasma contamination using MycoSPY Master Mix (Biontexas) following manufacturer’s recommendations.

For more detailed information on 3D colonic epithelial organoid generation, please refer to the publications “*Prolonged culturing of colonic epithelial organoids derived from healthy individuals and ulcerative colitis patients results in the decrease of LINE-1 methylation level*” [261] and “*Constituents of stable commensal microbiota imply diverse colonic epithelial cell reactivity in patients with ulcerative colitis*” [257].

2.5.2. Generation of polarised colonic epithelial monolayers

Human colonic epithelial cell monolayers were derived from 3D colonic epithelial organoids generated from study cohort VI. Briefly, 24-well plates (further used for co-culture establishment) and 8-well chamber slides (Thermo Fisher Scientific) were pre-coated with Collagen I (5 $\mu\text{g}/\text{cm}^2$, Gibco, Thermo Fisher Scientific) for 2 hours at 37 °C. Then, organoids were dissociated into single cells using TrypLE Express (Gibco, Thermo Fisher Scientific) supplemented with Y-27632 (10 μM , StemCell Technologies) at 37 °C for 10 minutes. TrypLE was neutralised with DMEM/F-12 (StemCell Technologies), and the suspension was filtered through a 40 μm cell strainer, centrifuged, and resuspended in IntestiCult OGMH (StemCell Technologies) supplemented with penicillin/streptomycin (100 $\mu\text{g}/\text{mL}$, Gibco, Thermo Fisher Scientific) and Y-27632 (10 μM , StemCell Technologies). 5×10^5 cells per 24-well plate well or 2×10^5 cells per 8-well chamber slide well were seeded onto Collagen I-coated plates and incubated in IntestiCult OGMH (StemCell Technologies) supplemented with penicillin/streptomycin (100 $\mu\text{g}/\text{mL}$, Gibco, Thermo Fisher Scientific) and Y-27632 (10 μM , StemCell Technologies) at 37 °C with 5% CO_2 . Cell growth was monitored daily, and the medium was changed every 2–3 days until 100% confluency was achieved. Culture medium was then switched to IntestiCult Organoid Differentiation Medium (ODMH, StemCell Technologies) supplemented with Notch pathway inhibitor DAPT (5 μM , StemCell Technologies), penicillin/streptomycin (100 $\mu\text{g}/\text{mL}$, Gibco, Thermo Fisher Scientific), and Y-27632 (10 μM , StemCell Technologies) for 5 days. Medium was refreshed every 2 days, and monolayers were evaluated microscopically using the Axio Observer 7 microscope (ZEISS, Carl Zeiss Microscopy) and ZEN 3.1 software (ZEISS, Carl Zeiss Microscopy).

For more detailed information on generation of 3D colonic epithelial organoid-derived monolayers, please refer to the publication “*Constituents of stable commensal microbiota imply diverse colonic epithelial cell reactivity in patients with ulcerative colitis*” [257].

2.5.3. Fluorescence microscopy of colonic epithelial organoids and monolayers

The morphology and cellular composition of 3D colonic epithelial organoids (study cohort V) and derived monolayers (study cohort VI) were assessed using brightfield and immunofluorescence microscopy. Organoid and monolayer growth was monitored daily. For immunofluorescence, both 3D organoids and epithelial monolayers were fixed in 4% paraformaldehyde, permeabilised with 0.5% Triton-X, and blocked with 2% Bovine serum albumin (BSA). Fluorochrome-conjugated monoclonal and polyclonal antibodies were applied at final dilutions ranging from 1:50 to 1:500. Antibodies included mouse anti-human beta-Catenin-Alexa Fluor 488 (clone 15B8, Invitrogen, Thermo Fisher Scientific), ZO-1-Alexa Fluor 555 (clone ZO1-1A12, Invitrogen, Thermo Fisher Scientific), Ki67-Alexa Fluor 488 (clone KI67, Abcam) and rabbit anti-human Mucin-2-Alexa Fluor 555 (Bioss Antibodies), Cytokeratin 20-Alexa Fluor 488 (clone EPR1622Y, Abcam), Chromogranin A-Alexa Fluor 488 (clone EP1030Y, Abcam). Fluorescent probe for F-actin (phalloidin-Alexa Fluor 660, Thermo Fisher Scientific) and stain for cell nuclei (Hoechst 33342, Invitrogen, Thermo Fisher Scientific) were also used in the study. Fluorescence microscopy was performed using Axio Observer 7 microscope (ZEISS, Carl Zeiss Microscopy) and ZEN 3.1 software (ZEISS, Carl Zeiss Microscopy).

For more detailed information on characterization of 3D colonic epithelial organoids and colonic epithelial organoid-derived monolayers, please refer to the publications “*Prolonged culturing of colonic epithelial organoids derived from healthy individuals and ulcerative colitis patients results in the decrease of LINE-1 methylation level*” [261] and “*Constituents of stable commensal microbiota imply diverse colonic epithelial cell reactivity in patients with ulcerative colitis*” [257], respectively.

2.5.4. DNA extraction

DNA was extracted from biopsy samples, cryopreserved crypts, and organoid specimens of study cohort V using the AllPrep DNA/RNA Mini Kit (Qiagen). Briefly, biopsies were lysed on a MagNA Lyser (Roche Diagnostics) at 6000 rpm for 15 seconds twice, with a 15-second break, using Lysing Matrix D tubes (MP Biomedicals) and 350 μ L of Buffer RLT Plus (Qiagen) supplemented with 1% β -mercaptoethanol. Cryopreserved pellets of crypts and organoids were thawed at 4 $^{\circ}$ C, centrifuged at 400 \times g for 5 minutes at 4 $^{\circ}$ C, and resuspended in 350 μ L of Buffer RLT Plus supplemented with 1% β -mercaptoethanol (Qiagen). DNA extraction from the resulting lysates was

completed following the manufacturer's instructions. The concentration of the extracted total DNA was assessed using a Qubit 4 fluorometer (Invitrogen, Thermo Fisher Scientific).

2.5.5. Bisulfite conversion and PCR amplification

A total of 200 ng of genomic DNA underwent bisulfite conversion using the MethylCode™ Bisulfite Conversion Kit (Applied Biosystems, Thermo Fisher Scientific) and amplified via PCR to target a 146 bp LINE-1 region. PCR was performed using custom primers (Forward (F): 5'-TTT TGA GTT AGG TGT GGG ATATA-3'; Reverse (R): 5'-biotin-AAA ATC AAA AAA TTC CCT TTC-3', 0.2 μM each) and the PyroMark® PCR Kit (Qiagen). Thermal cycling conditions were: 95 °C for 15 minutes; 45 cycles of 94 °C for 30 seconds, 56 °C for 30 seconds, and 72 °C for 30 seconds; followed by a final extension at 72 °C for 10 minutes. The specificity of the PCR product was confirmed using 2% agarose gel electrophoresis.

2.5.6. LINE-1 pyrosequencing

Methylation of three CpG sites in the amplified LINE-1 region was analysed using the PyroMark Q24 pyrosequencing system (Qiagen). PCR product was immobilised on Streptavidin Sepharose HP beads (Cytiva), processed with the PyroMark Q24 Vacuum Workstation (Qiagen), and annealed to the sequencing primer (5'-AGT TAG GTG TGG GAT ATA GT-3'). Sequencing was performed with PyroMark Gold Q24 reagents (Qiagen), and all samples were analysed in duplicates. Each run included CpG Methylated Human Genomic DNA (Thermo Fisher Scientific) as a positive control and a PCR-negative control. The pyrograms of the LINE-1 region were analysed using PyroMark Q24 software (v2.0.8, Qiagen). LINE-1 methylation levels $\geq 60\%$ were classified as high, based on prior studies [262–264].

2.5.7. Culturing and preparation of bacterial strains

Reference strains, *Escherichia coli* ATCC 25922 (Thermo Fisher Scientific) and *Phocaeicola vulgatus* ATCC 8482 (American Type Culture Collection), were stored at $-80\text{ }^{\circ}\text{C}$ in Brain Heart Infusion Broth (Thermo Fisher Scientific) with 30% glycerol. Recovery was performed according to the manufacturers' protocols. For cultivation, *E. coli* was grown on Tryptone Soy Agar (TSA, Sigma-Aldrich, Merck KGaA) under aerobic conditions, while *P. vulgatus* was cultured on TSA supplemented with 5% defibrinated sheep blood (Liofilchem) under anaerobic conditions, both for 24 hours at $37\text{ }^{\circ}\text{C}$. Bacterial suspensions for co-culturing experiments were prepared in $1 \times \text{PBS}$.

2.5.8. Co-culturing of colonic epithelial cell monolayers and bacteria

Differentiated patient-derived colonic epithelial cell monolayers from study cohort VI were co-cultured with either *E. coli* or *P. vulgatus*, while monolayers without bacteria served as controls. Briefly, prepared bacterial suspensions were centrifuged at $4000 \times g$ for 5 minutes and resuspended in antibiotic-free IntestiCult ODMH medium (StemCell Technologies) supplemented with DAPT (5 μM , StemCell Technologies) and Y-27632 (10 μM , StemCell Technologies). Co-cultures were assembled by adding 2×10^6 of specific strain per well, fully covered with cells, corresponding to a multiplicity of infection (MOI) of 1 to 2, and incubated for 2 hours at 37 °C with 5% CO₂. After incubation, bacteria-containing medium was removed, monolayers were washed with 1 \times PBS, and fresh IntestiCult ODMH medium with DAPT (5 μM , StemCell Technologies), penicillin/streptomycin (100 $\mu\text{g}/\text{mL}$, Gibco, Thermo Fisher Scientific), and Y-27632 (10 μM , StemCell Technologies) was added. Monolayers were cultured for an additional 24 hours at 37 °C with 5% CO₂. Following incubation, the culture medium from the monolayers was collected into clean tubes, and the monolayers were washed with 1 \times PBS and lysed in Buffer RLT Plus (Qiagen) supplemented with 1% β -mercaptoethanol. Both collected culture medium and cell lysate samples were stored at -80 °C until further use for the isolation and characterization of extracellular vesicles (EVs) and the extraction of nucleic acids from both EVs and cells.

2.5.9. Isolation of EVs

EVs were isolated from co-culture media using the Total Exosome Isolation Reagent (Invitrogen). Briefly, the collected cell culture media were thawed and centrifuged at $3,000 \times g$ for 15 minutes to remove large debris, cells, and cell fragments. The resulting supernatant was mixed with the Total Exosome Isolation Reagent at a ratio of 2:1 (supernatant to reagent) and thoroughly vortexed. Samples were incubated overnight at 4 °C, followed by centrifugation at $10,000 \times g$. The supernatant was discarded, and the EV-containing pellet was resuspended in 1 \times PBS. The isolated EVs were stored at 4 °C for up to one week or at -80 °C for long-term storage until further characterisation and nucleic acid extraction.

2.5.10. Characterization of EVs

The size of isolated EVs was assessed using Dynamic Light Scattering technology with the ZetaSizer Nano ZS system (model ZEN3500, Malvern Panalytical). Precipitated EVs were diluted 1:100 in $1 \times$ PBS, with a final volume of 2 mL prepared in DTS00012 cuvettes. Each sample underwent five measurements, each consisting of 10 runs, with a 1-second pause between runs. The measurement parameters included a refractive index of 1.330, absorption of 0.010, and temperature of 25 °C. Data were recorded using Zetasizer Nano software (v3.30, Malvern Panalytical).

To validate the specificity of the EV isolation method, protein characterisation was performed based on markers from three categories defined in the MISEV2018 guidelines [265]. Three ELISA kits were used, following the manufacturer's protocols: Human CD63 ELISA Kit (Invitrogen, Thermo Fisher Scientific), Human HSP70 ELISA Kit (Invitrogen, Thermo Fisher Scientific), and Human Apo-A1 ELISA Kit (Invitrogen, Thermo Fisher Scientific). Optical density was measured at 450 nm using a Sunrise microplate reader (Tecan Trading AG) and normalized to readings at 620 nm, with data analysed using Magellan software (v7.1, Tecan Trading AG). For each EV sample, two technical replicates were performed, and the average values of the readings were used for subsequent calculations.

2.5.11. RNA extraction from cells and EVs

Total cellular RNA was purified using the AllPrep DNA/RNA Micro Kit (Qiagen) according to the manufacturer's recommendations, including RNase-Free DNase I (Qiagen) treatment. Total EV RNA was purified using Single Cell RNA Purification Kit (Norgen). At the initial stage of the purification protocol, 5.6×10^8 copies of synthetic cel-miR-39-3p were added to each sample as a spike-in control, following the manufacturer's recommendations (Qiagen). The concentration of the extracted total cellular and EV RNA was assessed using a Qubit 4 fluorometer (Invitrogen, Thermo Fisher Scientific).

2.5.12. *In silico* identification of potential host miRNA targets in bacterial genomes

Host miRNAs identified in the expression data in colonic epithelial cell populations (Study Part I, cohort III) were prioritised for analysis in Study Part III based on predefined criteria. Specifically, UC-associated miRNAs from crypt-top cells with a $\log_2FC > 1.5$, $FDR < 0.05$, and theoretical targets in the genomes of *E. coli* and/or *P. vulgatus* were selected for further analysis.

For the identification of host miRNA gene targets in bacterial genomes, the publicly available tool TargetRNA2 (v2.01) [266] was used. This tool identifies potential miRNA binding sites within a specified bacterial replicon based on the user-provided small RNA sequence. The sequences of the investigated miRNAs were obtained from the miRBase database (v22.1) [241]. miRNA and gene target interactions were considered probable when the probability score was $\geq 50\%$, and the p-value was < 0.05 .

2.5.13. RT-qPCR

The expression of selected genes and miRNAs in colonic epithelial monolayers and EVs was analysed using RT-qPCR. For miRNA expression analysis, cDNA was synthesised using TaqMan MicroRNA Reverse Transcription Kit (Applied Biosystems, Thermo Fisher Scientific) and either TaqMan microRNA Assays (hsa-miR-146a-5p: 00468; hsa-miR-183-5p: 002269; hsa-miR-135b-5p: 002261; cel-miR-39-3p: 0002000; Applied Biosystems, Thermo Fisher Scientific) or TaqMan small RNA Assay (RNU48: 001006; Applied Biosystems, Thermo Fisher Scientific). Gene expression analysis was performed using cDNA synthesised with the High-Capacity cDNA Reverse Transcription Kit (Applied Biosystems, Thermo Fisher Scientific) and SYBR Green-based chemistry with specific primers targeting *TLR4*, *HSPA1A*, *HSPB1*, and *TJPI*. For more detailed information on the gene primers used in the study, please refer to the publication “*Constituents of stable commensal microbiota imply diverse colonic epithelial cell reactivity in patients with ulcerative colitis*” [257]. RT-qPCR was performed on a 7500 Fast Real-Time PCR System (Applied Biosystems, Thermo Fisher Scientific), with C_t values normalized to *ACTB* for genes and to RNU48 or cel-miR-39-3p for miRNAs in cells and EVs, respectively. Relative changes in gene and miRNA expression were determined using $2^{-\Delta\Delta C_t}$ method [239].

2.5.14. Statistical analysis

Statistical analyses and data visualisation were performed in R Studio (v4.0.3) using ggplot2 [245], ggsignif [267], and tidyverse [268] packages. The data distribution of study cohorts V and VI was assessed with the Shapiro-Wilk test. Since the data were not normally distributed, the Mann-Whitney *U* test was applied for pairwise comparisons. Results with p-values ≤ 0.05 were considered statistically significant.

3. RESULTS

3.1. Part I. miRNA expression profiling in colonic tissue and epithelial cell populations

3.1.1. Identification of UC-associated miRNAs in colonic tissue

To identify the miRNA expression signatures in active and quiescent UC, small RNA-seq was performed on colonic biopsies from UC patients and non-IBD controls. After normalisation and quality control, 573 unique miRNAs were identified in colon tissue samples. MDS analysis revealed distinct clusters for active UC and non-IBD tissues, while quiescent UC overlapped with both groups, indicating a shift in miRNA expression from a healthy to an inflammatory state (Fig. 3.1.1.1 A).

Differential expression analysis (Fig. 3.1.1.1 B) revealed the greatest miRNA deregulation in active UC compared to non-IBD or quiescent UC, with 93 and 59 miRNAs differentially expressed, respectively ($FDR < 0.05$, $|\log_2FC| > 1$). Quiescent UC also displayed differential expression of 32 miRNAs compared to non-IBD. Notably, 13 miRNAs, including miR-106-5p, miR-125b-1-3p, miR-205-5p, and miR-3182, were consistently deregulated in both active and quiescent UC compared to non-IBD. In contrast, 80 miRNAs, such as miR-190a-5p, miR-223-3p, miR-378i, and miR-3168, were uniquely deregulated in active UC, while 19 miRNAs, including miR-331-3p, miR-409-5p, miR-629-5p, and miR-4497, were specific to quiescent UC. Additionally, miR-1-3p showed a gradual decrease in expression across all pairwise comparisons (quiescent UC vs. non-IBD: $\log_2FC = -1.06$, $FDR = 0.01$; active UC vs. quiescent UC: $\log_2FC = -1.12$, $FDR = 2.8 \times 10^{-3}$; active UC vs. non-IBD: $\log_2FC = -2.18$, $FDR = 3.8 \times 10^{-11}$).

These findings underscore both shared and distinct patterns of miRNA deregulation, suggesting overlapping and unique roles of specific miRNAs in active and quiescent UC tissues.

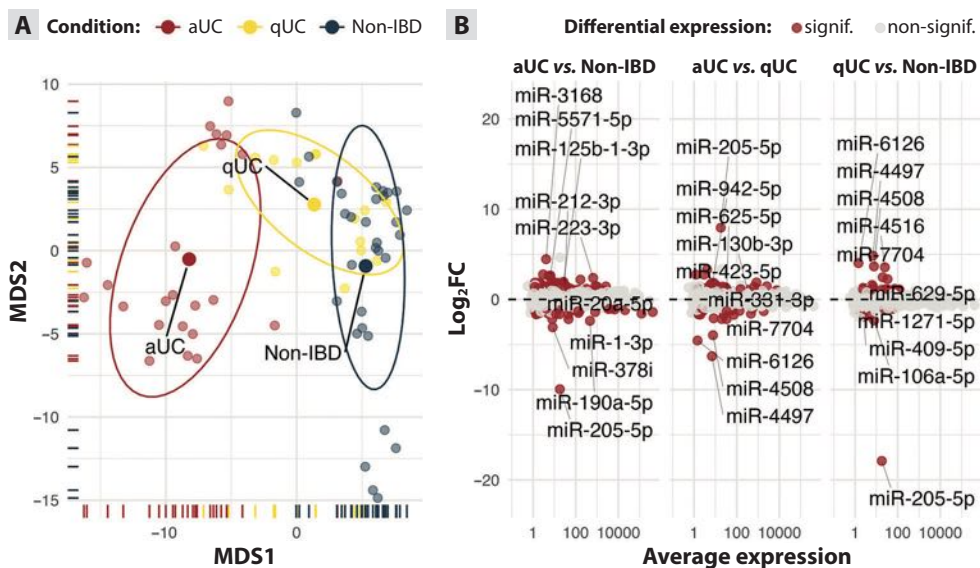


Fig. 3.1.1.1. miRNA expression patterns in colonic tissues of UC patients and non-IBD individuals

(A) MDS plot showing the similarity structure of the normalized miRNA expression profiles in active UC (aUC), quiescent UC (qUC), non-IBD (Non-IBD) colonic tissues. The dots represent distinct samples. The colors represent different conditions. The centers of ellipses represent the group means. The shapes of ellipses are determined by the covariance within each group. (B) Differentially expressed miRNAs in aUC and qUC tissues. Red color indicates significantly differentially expressed miRNAs ($|\log_2FC| > 1$, FDR < 0.05), gray color represents non-differentially expressed miRNAs. The top five up- and down-regulated miRNAs are displayed for each comparison. The horizontal dash line indicates the fold change (FC) threshold for no change in differential expression.

3.1.2. Involvement of differentially expressed colonic tissue miRNAs in signalling pathways during UC

To investigate the biological functions of differentially expressed colonic tissue miRNAs in UC pathogenesis, GSEA was performed for each pairwise comparison (active UC vs. non-IBD, quiescent UC vs. non-IBD, and active UC vs. quiescent UC) using validated target genes of significantly deregulated miRNAs and Reactome pathways. Both active and quiescent UC, compared to non-IBD, showed overrepresentation of interleukin signalling-related pathways among the top significant results, including “Signaling by Interleukins” (R-HSA-449147) and “Interleukin-4 and Interleukin-13 signalling” (R-HSA-6785807), along with additional pathways such as “Intracellular signaling by second messengers” (R-HSA-9006925) and “Diseases of signal transduction by growth factor receptors and second messengers” (R-HSA-5663202) (Fig. 3.1.2.1 A). Target genes of identified pathways were enriched for 20 key miRNAs with the highest number of target genes in

signalling pathways, including miR-1-3p, miR-10b-5p, miR-20a-5p, miR-31-5p, miR-146a-5p, miR-155-5p, miR-205-5p, and miR-223-3p, which are likely to play regulatory roles in these signalling processes (Fig. 3.1.2.1 B).

To further validate the dysregulation of interleukin (IL) pathways in UC tissue, the gene expression patterns of two main cytokines, IL-4 and IL-13, were analysed using RT-qPCR. *IL-13* expression showed a gradual increase across groups (2.19-fold ($p = 0.031$) in quiescent UC vs. non-IBD, 2.91-fold ($p = 7 \times 10^{-4}$) in active UC vs. quiescent UC, and 6.38-fold ($p = 3 \times 10^{-10}$) in active UC vs. non-IBD), while *IL-4* expression remained unchanged (Fig. 3.1.2.1 C). IL-4 and IL-13 signalling-related genes were also explored using GSE116222 [91] dataset to evaluate their expression in epithelial (undifferentiated colonocytes, goblet cells, enteroendocrine cells, crypt-top colonocytes, and colonocytes) and immune (T cells, myeloid cells, mast cells, and B cells) subsets of colonic cell populations in active and quiescent UC and non-IBD. Genes downstream of the IL-4 and IL-13 signalling pathway, including *IL13RA1*, *IL4R*, *JAK1*, *SOCS1*, *STAT3*, and *STAT6*, were expressed in the majority of analysed cells, with potential expression changes observed in active UC compared to non-IBD (Fig. 3.1.2.1 D).

Together, these findings suggest that dysregulated miRNAs in UC tissues contribute to the regulation of inflammation-related pathways, particularly IL-4 and IL-13 signalling, which remain dysregulated in both active and quiescent UC.

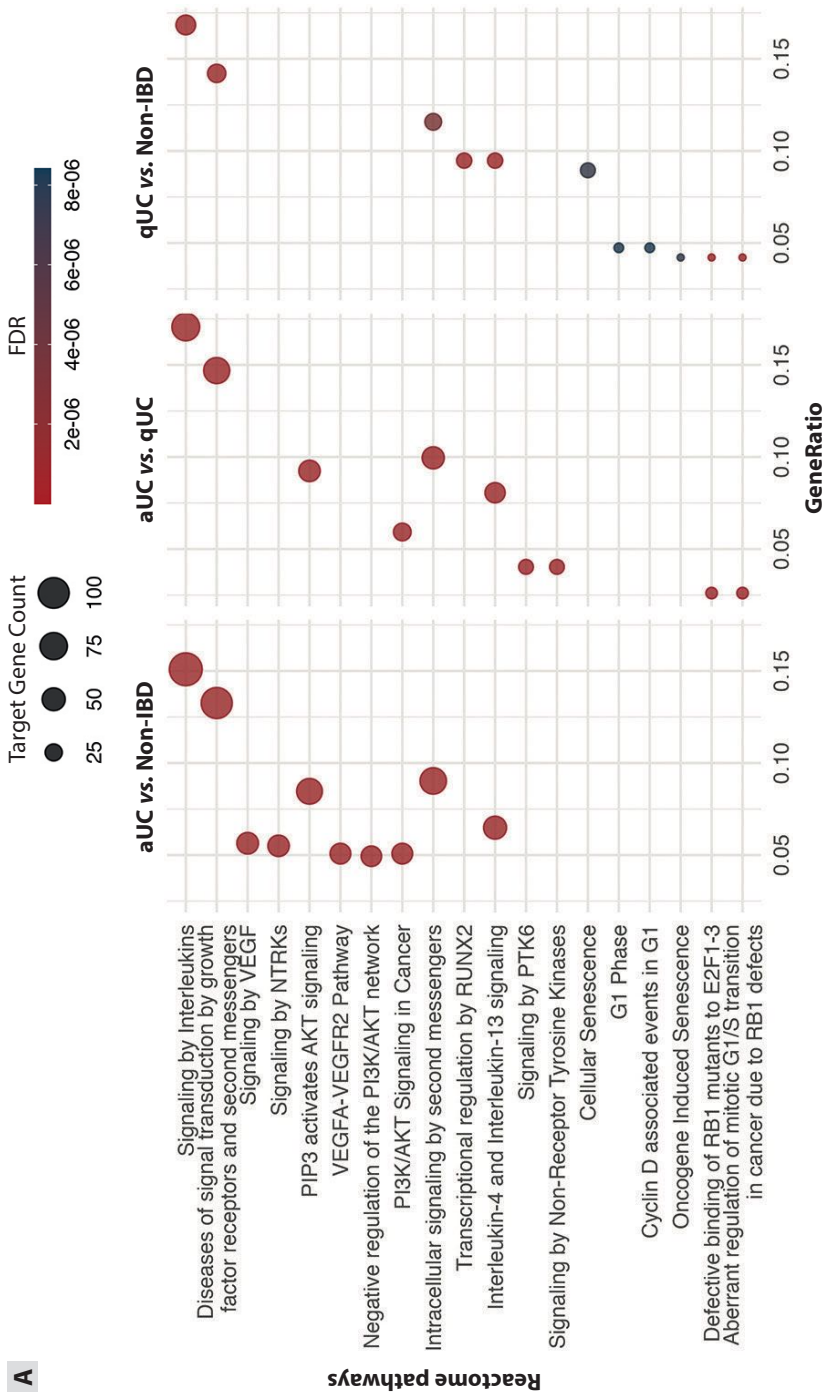


Fig. 3.1.2.1 (A). Association between differentially expressed tissue miRNAs and signalling pathways

(A) A dot plot showing the top 10 overrepresented Reactome pathways in active UC (aUC) and quiescent UC (qUC) colonic tissues, identified through miRNA target-gene set enrichment analysis. Dot size indicates the number of miRNA-target gene interactions within significantly enriched (FDR < 0.05) signalling pathways.

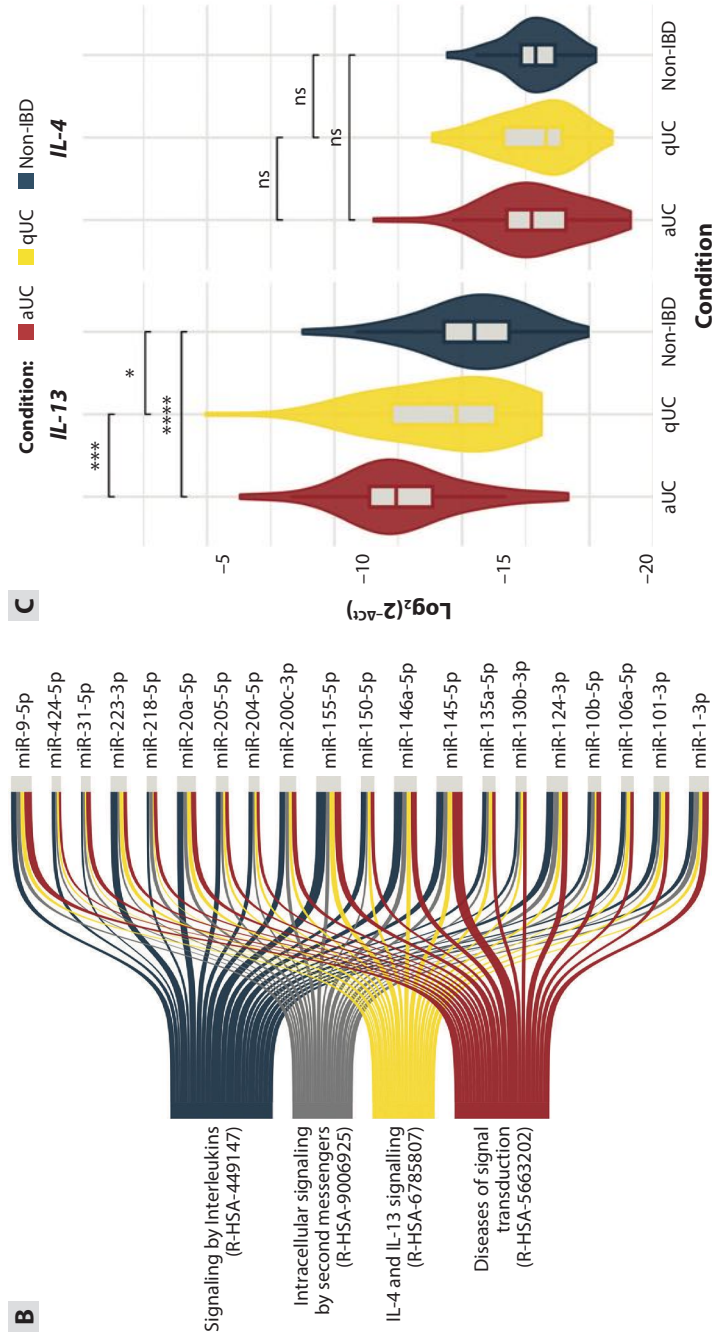


Fig. 3.1.2.1 (B–C). Association between differentially expressed tissue miRNAs and signalling pathways

(B) A Sankey plot illustrating the overlap of significantly enriched (FDR < 0.05) Reactome pathways in pairwise comparisons of aUC and qUC with non-IBD tissues, as identified by miRNA-target GSEA (left panel). The right panel highlights the 20 miRNAs with the highest number of target genes within these pathways. Line width corresponds to the count of miRNA-target gene interactions, while line colors differentiate individual signalling pathways. (C) Violin plots displaying *IL-4* and *IL-13* gene expression levels, measured via RT-qPCR, in colonic tissue samples of patients with aUC and qUC, as well as non-IBD control individuals. The color of each violin represents the corresponding study group. A horizontal line indicates the median expression level, while whiskers represent the quartiles of each group. Gene expression is plotted on a logarithmic scale, with ΔC_T values inverted to reflect the actual expression direction. Statistical significance is denoted as follows: * $p \leq 0.05$, *** $p \leq 0.001$, **** $p \leq 0.0001$, ns – not significant.

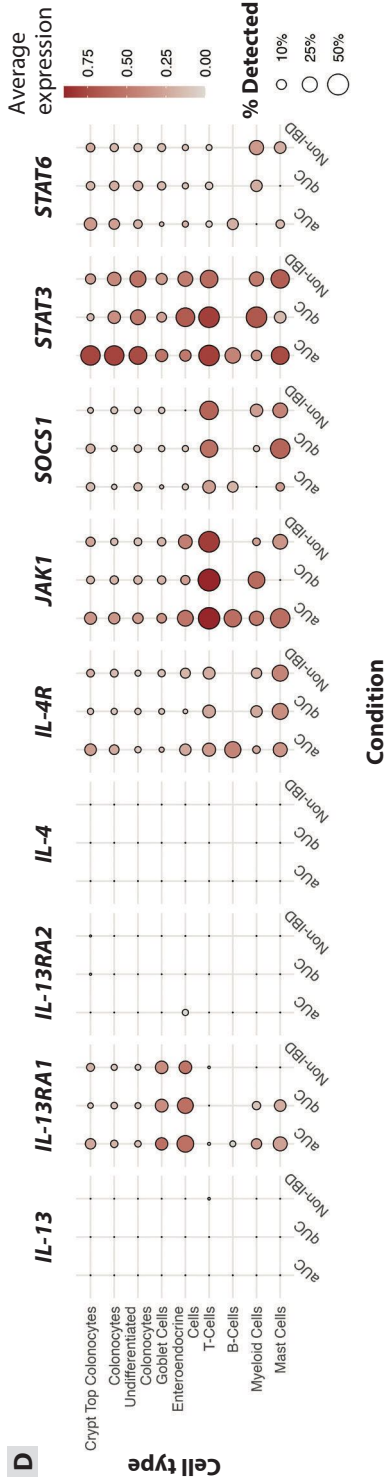


Fig. 3.1.2.1 (D). Association between differentially expressed tissue miRNAs and signalling pathways

(D) A dot plot illustrating the expression of IL-4 and IL-13 signalling pathway-related genes across various epithelial and immune cell populations in human colon tissue (dataset GEO accession number: GSE116222) for aUC, qUC, and non-IBD groups. Dot size represents the percentage of cells expressing each gene within a group, while dot color reflects the average expression level of the gene.

3.1.3. miRNA expression patterns in colonic epithelial cell populations in UC

Flow cytometry analysis revealed a significant increase (FDR < 0.05) in crypt-bottom (CD44⁺) cells in active UC compared to non-IBD (Fig. 3.1.3.1 A). Normalised RNA sequencing data identified 436 unique miRNAs expressed in crypt-bottom (CD44⁺) and crypt-top (CD66a⁺) colonic epithelial cells. While the overall miRNA transcriptomes of these cell types were largely similar, as indicated by MDS analysis, significant differences in miRNA expression were observed within these populations in different UC states (Fig. 3.1.3.1 B).

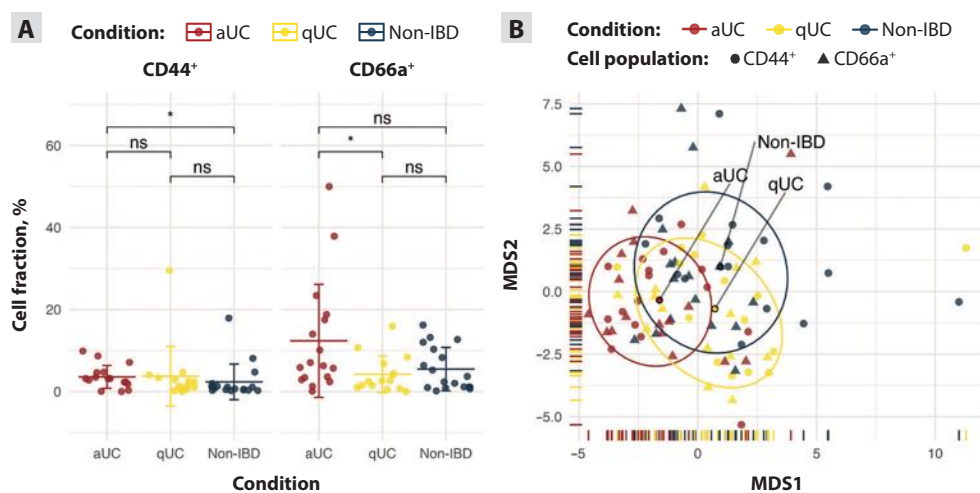


Fig. 3.1.3.1. miRNA expression signatures in distinct colonic epithelial cell populations of UC patients and non-IBD controls

(A) Plot showing the distribution of crypt-top (CD66a⁺) and crypt-bottom (CD44⁺) epithelial cell populations in active UC (aUC), quiescent UC (qUC), and non-IBD control colonic tissues. Each dot represents an individual patient sample. Vertical lines indicate the mean \pm SD for each group. A non-parametric Mann–Whitney *U* test was used for group comparisons, with **p* < 0.05 considered significant. (B) MDS plot visualising the similarity structure of normalised miRNA expression in crypt-top (CD66a⁺) and crypt-bottom (CD44⁺) colonic epithelial cells across aUC, qUC, and non-IBD. Each dot represents an individual sample, with shape indicating the epithelial cell population and color denoting the condition. Ellipses represent group covariance, with their centroids corresponding to the group mean.

Pairwise comparisons within the same colonic epithelial cell population identified miRNAs associated with UC inflammation. Consistent with tissue-level analyses, the number of differentially expressed miRNAs ($FDR < 0.05$, $|\log_2FC| > 1$) in both cell populations increased with disease activity (Fig. 3.1.3.2 A). Specifically, in crypt-bottom ($CD44^+$) cells, 15 miRNAs were dysregulated in quiescent UC compared to non-IBD, 28 miRNAs in active UC compared to quiescent UC, and 38 miRNAs in active UC compared to non-IBD. Similarly, in crypt-top ($CD66a^+$) cells, 11 miRNAs were differentially expressed between active UC and quiescent UC, 15 miRNAs between quiescent UC and non-IBD, and 29 miRNAs – between active UC and non-IBD. Notably, no miRNAs were commonly differentially expressed across all three pairwise comparisons (active UC vs. non-IBD, quiescent UC vs. non-IBD, and active UC vs. quiescent UC) in both crypt-bottom ($CD44^+$) and crypt-top ($CD66a^+$) cells. However, six miRNAs (miR-15b-5p, miR-194-3p, miR-222-3p, miR-223-3p, miR-574-3p, and miR-3195) were commonly deregulated in crypt-bottom ($CD44^+$) cells, while eight miRNAs (let-7c-5p, miR-1-3p, miR-106b-3p, miR-125b-5p, miR-194-3p, miR-335-5p, miR-552-3p, and miR-1290) were identified in crypt-top ($CD66a^+$) cells in active and quiescent UC compared to non-IBD (Fig. 3.1.3.2 B–C).

GSEA analysis performed using validated target genes of significantly deregulated miRNAs revealed significant overlap in dysregulated pathways across epithelial cell populations in both UC states (Fig. 3.1.3.2 D), with overrepresented pathways from Reactome database including “Signaling by Interleukins” (R-HSA-449147), “Interleukin-4 and Interleukin-13 signaling” (R-HSA-6785807), and “Signaling by Receptor Tyrosine Kinases” (R-HSA-9006934). Noteworthy, the most overrepresented Reactome pathways in crypt-bottom ($CD44^+$) cells from the quiescent UC group (compared to non-IBD) differed from those in the active UC group and uniquely featured “Signaling by Nuclear Receptors” (R-HSA-9006931) and “Extra-nuclear Estrogen Signaling” (R-HSA-9009391).

To conclude, changes in miRNA expression in crypt-bottom ($CD44^+$) and crypt-top ($CD66a^+$) epithelial cells during UC potentially contribute to the shared regulatory signalling pathways, indicating that colonic epithelial cells are potentially the key drivers of the observations made in the bulk colonic tissue samples.

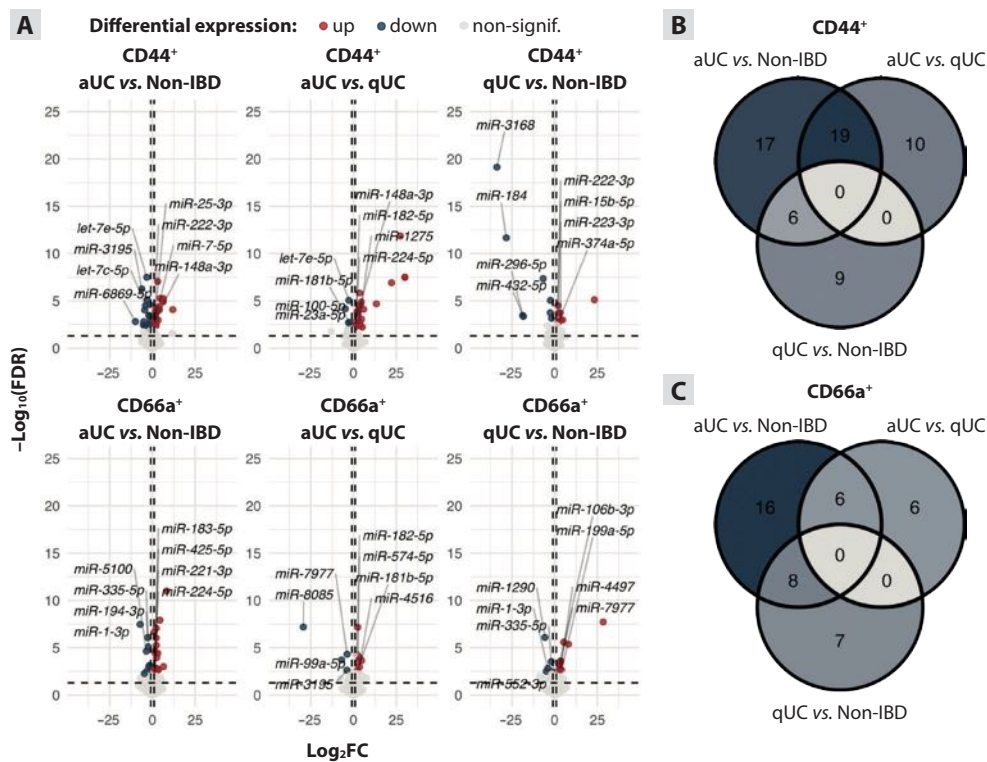


Fig. 3.1.3.2 (A–C). Differential miRNA expression in colonic epithelial cell populations of UC patients and non-IBD controls

(A) Volcano plots showing differentially expressed miRNAs in crypt-top (CD66a⁺) and crypt-bottom (CD44⁺) colonic epithelial cells from active UC (aUC), quiescent UC (qUC), and non-IBD controls. Colored points indicate significantly differentially expressed miRNAs (FDR < 0.05, |log₂FC| > 1) between the compared groups. Vertical dashed lines marks |log₂FC| > 1, horizontal dashed line marks FDR < 0.05 in logarithmic scale. (B–C) Venn diagrams illustrating the number of shared and unique differentially expressed miRNAs in: (B) crypt-bottom (CD44⁺) colonic epithelial cells across UC activity states, and (C) crypt-top (CD66a⁺) colonic epithelial cells across UC activity states.

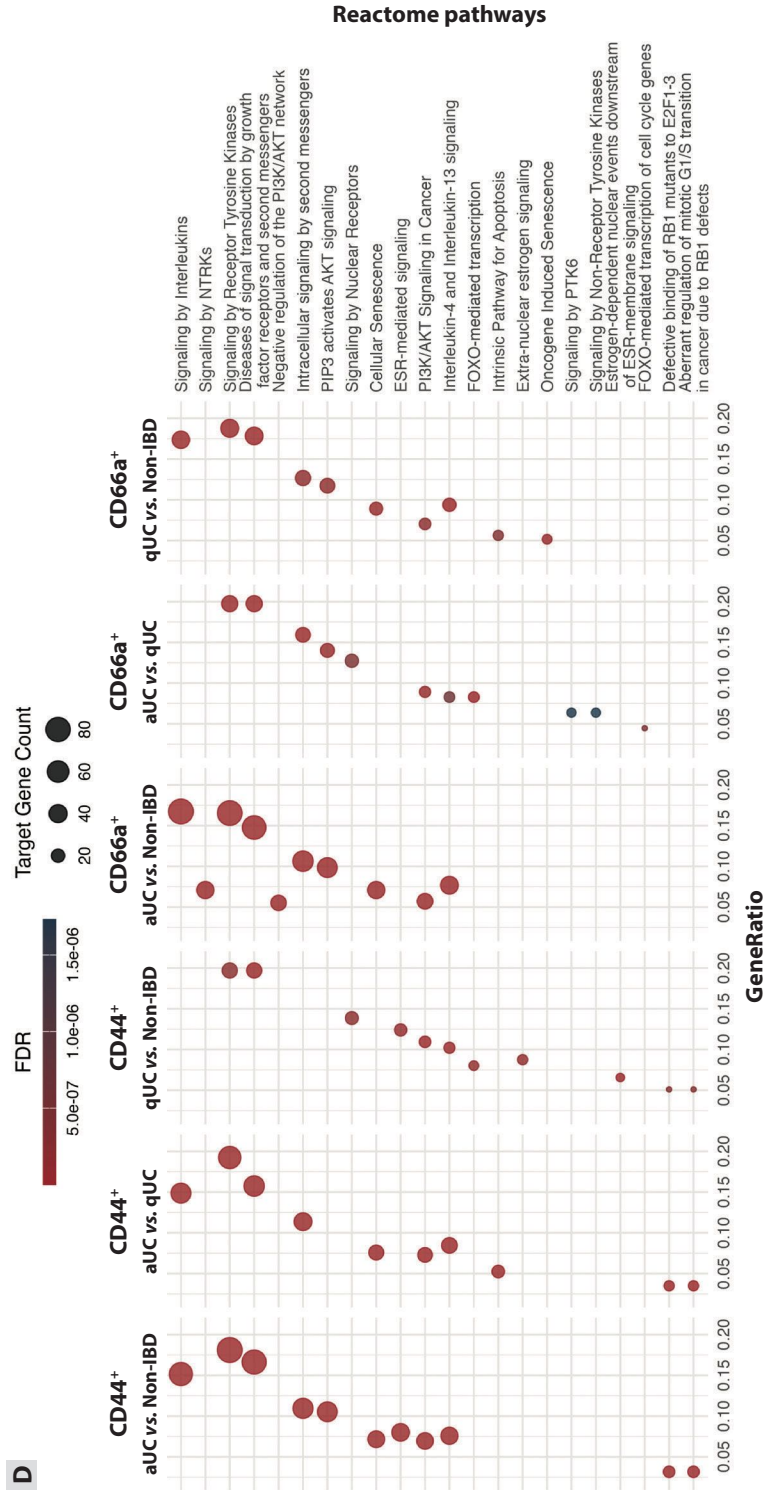


Fig. 3.1.3.2 (D). *Differential miRNA expression in colonic epithelial cell populations of UC patients and non-IBD controls*

(D) Enriched Reactome pathways identified through miRNA-target GSEA, displaying the top five FDR-ranked pathways in crypt-bottom (CD44⁺) and crypt-top (CD66a⁺) colonic epithelial cell populations in aUC, qUC, and non-IBD. Dot size represents the proportion of miRNA gene targets within significantly enriched (FDR < 0.05) signalling pathways.

3.1.4. Comparison of miRNA expression profiles between colonic epithelial cell populations across health states

To further investigate miRNA expression signatures between colonic epithelial cell populations among different health states (active UC, quiescent UC, and non-IBD), pairwise comparisons were conducted between crypt-bottom (CD44⁺) and crypt-top (CD66a⁺) epithelial cells. This analysis identified 24 differentially expressed miRNAs (FDR < 0.05, $|\log_2FC| > 1$) in active UC, nine in quiescent UC, and 22 in non-IBD (Fig. 3.1.4.1 A). Notably, most of these miRNAs were uniquely dysregulated in each comparison, with only two miRNAs, miR-106b-3p and miR-1290, differentially expressed in both active UC (CD44⁺ vs. CD66a⁺) and quiescent UC (CD44⁺ vs. CD66a⁺), and two miRNAs, miR-296-5p and miR-432-5p, shared between active UC and non-IBD (CD44⁺ vs. CD66a⁺) (Fig. 3.1.4.1 B).

GSEA of miRNA target-genes differentially expressed in colon crypt-bottom (CD44⁺) and crypt-top (CD66a⁺) cells revealed that overrepresented biological processes (GO terms) in active UC and non-IBD were predominantly related to cell differentiation and motility (Fig. 3.1.4.1 C). Interestingly, biological processes such as “epithelium migration” (GO:0090132) and “epithelial cell migration” (GO:0010631) were uniquely enriched in active UC. In contrast, in quiescent UC, target genes of differentially expressed miRNAs between epithelial cell populations were primarily associated with cell migration-related pathways and exhibited the lowest level of enrichment.

In summary, these findings suggest that miRNA expression responses are specific to colonic epithelial cell populations and vary with inflammatory activity. Furthermore, the distinct involvement of aberrantly expressed miRNAs between crypt-bottom (CD44⁺) and crypt-top (CD66a⁺) cells underscores their role in regulation of intestinal barrier integrity.

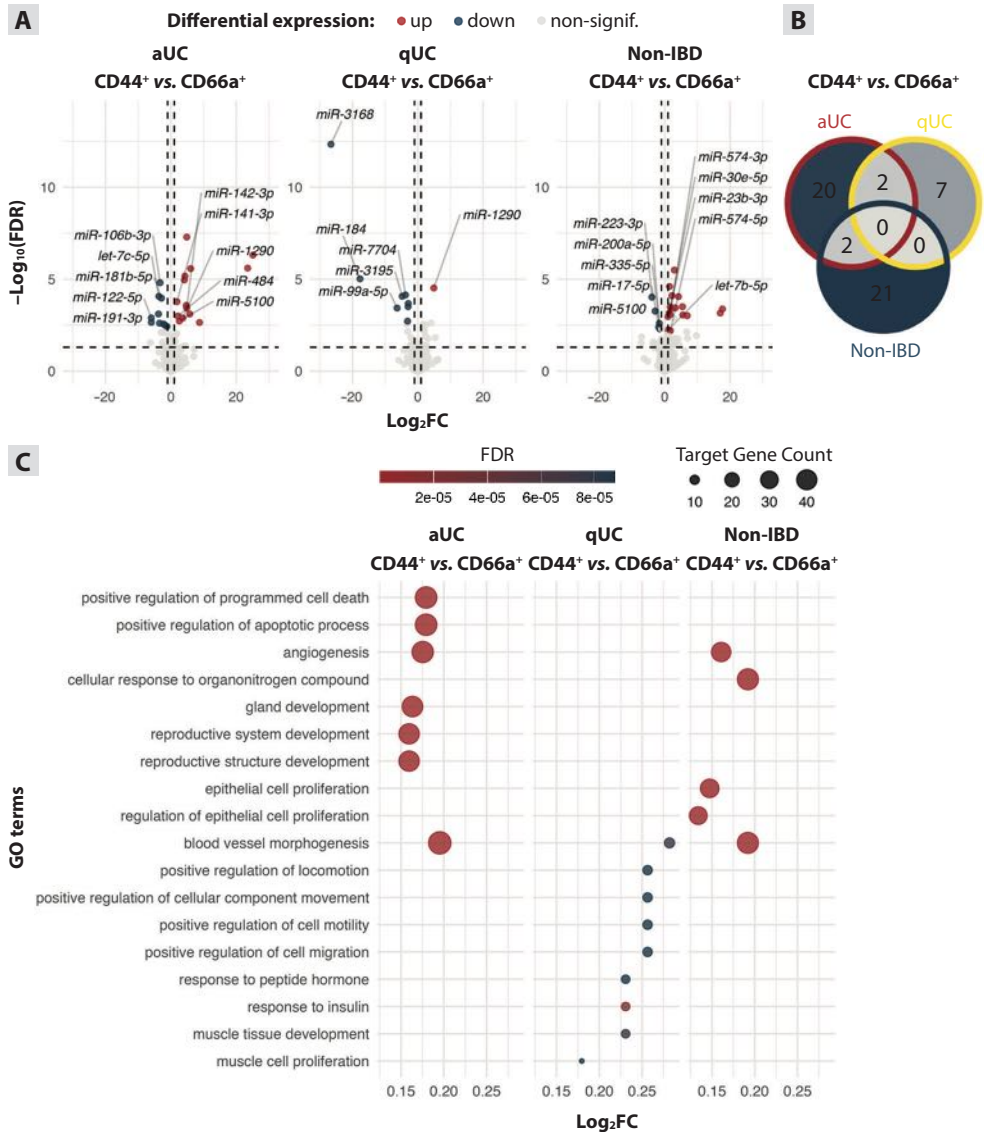


Fig. 3.1.4.1. miRNA expression patterns in distinct colonic epithelial cell populations across different health states

(A) Volcano plots illustrating differentially expressed miRNAs between colonic epithelial cell populations in active UC (aUC), quiescent UC (qUC), and non-IBD control. Colored points indicate significantly differentially expressed miRNAs ($FDR < 0.05$, $|\log_2FC| > 1$) between the compared groups. Vertical dashed lines marks $|\log_2FC| > 1$, horizontal dashed line marks $FDR < 0.05$ in logarithmic scale. (B) Venn diagram illustrating the number of shared and unique differentially expressed miRNAs between crypt-bottom ($CD44^+$) and crypt-top ($CD66a^+$) colonic epithelial cells under the same conditions. (C) Overrepresented Gene Ontologies (GO) with the five lowest FDR values between crypt-bottom ($CD44^+$) and crypt-top ($CD66a^+$) colonic epithelial cell populations in aUC, qUC, and non-IBD, identified via miRNA-target GSEA. The size of each dot corresponds to the number of miRNA gene targets within significantly enriched ($FDR < 0.05$) GO categories.

3.1.5. Correlation of miRNA expression in colonic epithelial cell populations with endoscopic activity in UC

To investigate the relationship between miRNA expression levels and endoscopic Mayo subscore in crypt-top (CD66a⁺) and crypt-bottom (CD44⁺) colonic epithelial cells, Spearman's correlation analysis was conducted. In crypt-bottom (CD44⁺) cells, the analysis identified 34 miRNAs with moderate positive correlations and six miRNAs with moderate negative to endoscopic Mayo subscore. Similarly, in crypt-top (CD66a⁺) cells, 23 miRNAs showed moderate positive correlations, while seven miRNAs demonstrated moderate negative correlations with endoscopic Mayo subscore (Fig. 3.1.5.1). The results revealed substantial overlap in disease activity-associated miRNAs between the two epithelial cell populations, with 29 miRNAs showing moderate correlations in both crypt-top (CD66a⁺) and crypt-bottom (CD44⁺) cells. However, population-specific correlations were also identified. Specifically, 21 miRNA (including let-7b-5p, let-7e-5p, and miR-141-5p) exhibited moderate correlations with endoscopic Mayo subscore exclusively in crypt-bottom (CD44⁺) cells, while 15 miRNAs were unique to crypt-top (CD66a⁺) cells (including miR-127-3p, miR-146a-5p, and miR-193b-5p).

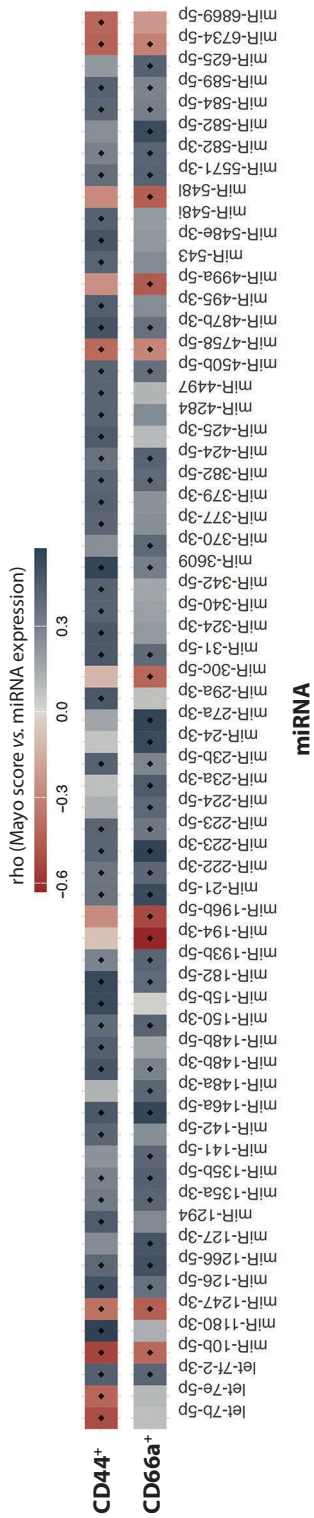


Fig. 3.1.5.1. Association of colonic epithelial cell miRNA expression with endoscopic activity of UC

Heatmap illustrating the correlation between normalized miRNA expression and the endoscopic Mayo subscore in colonic epithelial cell populations: crypt-bottom (CD44⁺) (upper panel) and crypt-top (CD66a⁺) (lower panel). Box colors indicate Spearman's correlation coefficient (ρ), while diamonds highlight significant correlations (FDR < 0.05) within each cell population.

Additionally, among these cell population-specific miRNAs, eight miRNAs (e.g., let-7b-5p, let-7e-5p, miR-10b-5p, miR-15b-5p, miR-31-5p, miR-182-5p, miR-223-3p, and miR-6869-5p) were identified as differentially expressed in crypt-bottom (CD44⁺) cells, while ten miRNAs (e.g., miR-10b-5p, miR-21-5p, miR-24-3p, miR-27a, miR-135b-5p, miR-146a-5p, miR-194-3p, miR-196b-5p, miR-224-5p, miR-222-3p) were differentially expressed in crypt-top (CD66a⁺) cells across varying stages of UC activity.

Overall, the findings highlight both shared and colonic epithelial cell population-specific correlations between miRNA expression levels and endoscopic UC disease activity, shedding light on the potential role of miRNAs in UC pathogenesis and progression.

3.1.6. miRNA co-expression network in colonic epithelial cell populations across health states

To further explore miRNA dynamics, we conducted a more detailed analysis to assess whether specific miRNAs in colonic epithelial cell populations are co-expressed. Using WGCNA, we detected a miRNA co-expression network for both colonic epithelial cell populations (Fig. 3.1.6.1 A) and identified two distinct co-expression modules, designated as modules one (M1) and two (M2). Module M1 included 13 miRNAs (miR-10b-5p, miR-27a-3p, miR-31-5p, miR-135b-5p, miR-146a-5p, miR-182-5p, miR-183-5p, miR-194-3p, miR-196b-5p, miR-221-3p, miR-222-3p, miR-223-3p, and miR-574-5p), while module M2 contained 11 miRNAs (let-7b-5p, let-7e-5p, miR-1-3p, miR-15b-5p, miR-100-5p, miR-125a-5p, miR-125b-5p, miR-143-3p, miR-181b-5p, miR-195-5p, and miR-5100). Notably, several miRNAs in module M1, such as miR-10b-5p, miR-31-5p, and miR-223-3p, were previously recognised as key regulators of genes involved in interleukin signalling pathways (Fig. 3.1.3.2 D).

Subsequent enrichment analysis of the modules, assessed through normalised enrichment score (NES) (Fig. 3.1.6.1 B), demonstrated that module M1 was highly enriched in both crypt-top (CD66a⁺) and crypt-bottom (CD44⁺) colonic epithelial cells of patients with active UC, with NES values of 1.71 ($p_{\text{adj.}} = 9.7 \times 10^{-3}$) and 1.67 ($p_{\text{adj.}} = 0.029$), respectively. In contrast, module M1 showed significant reduction in enrichment within both colonic epithelial cell populations of non-IBD controls, reflected by NES values of -1.79 ($p_{\text{adj.}} = 7.7 \times 10^{-3}$) and -1.74 ($p_{\text{adj.}} = 0.05$), respectively. Interestingly, module M2 displayed an opposite enrichment pattern to module M1. In crypt-top (CD66a⁺) and crypt-bottom (CD44⁺) colonic epithelial cells of patients with active UC, module M2 was significantly decreased, with NES values of -1.84 ($p_{\text{adj.}} = 9.7 \times 10^{-3}$) and -1.80 ($p_{\text{adj.}} = 0.029$), respectively. However, in

patients with quiescent UC, module M2 was significantly enriched, but exclusively in crypt-bottom (CD44⁺) cells, with an NES value of 2.08 ($p_{adj.} = 3.3 \times 10^{-4}$).

Overall, the findings revealed potential miRNA co-expression patterns in UC, that are distinctive to both crypt-top (CD66a⁺) and crypt-bottom (CD44⁺) colonic epithelial cell populations.

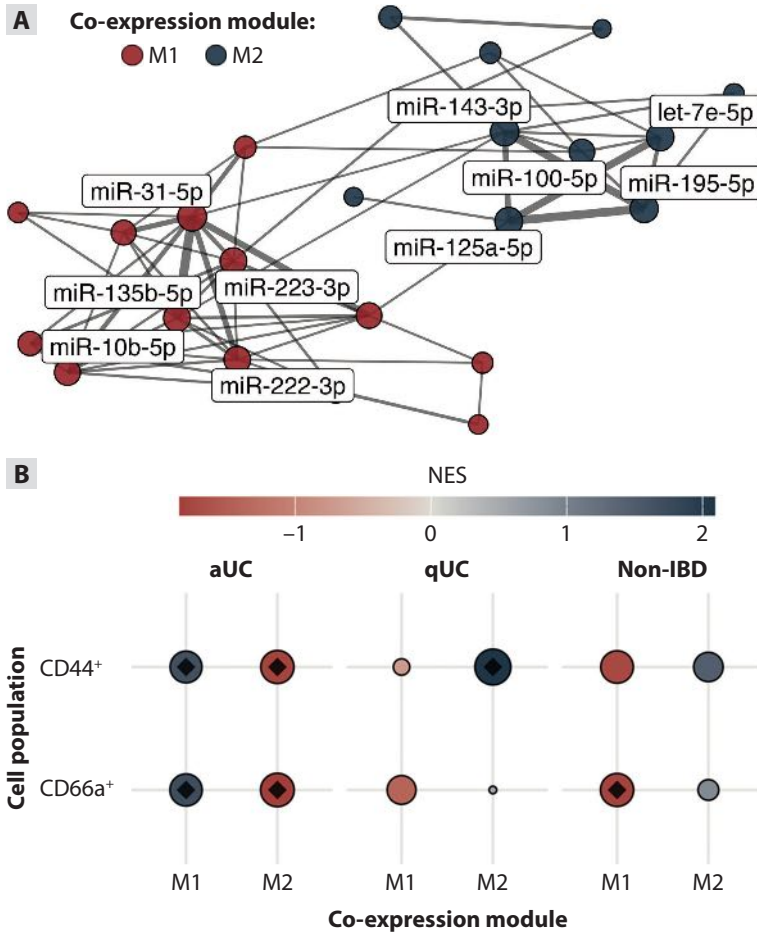


Fig. 3.1.6.1. miRNA co-expression network and enrichment in colonic epithelial cell populations of UC patients and non-IBD controls

(A) Network representation of detected co-expression modules (M1 and M2) in crypt-top (CD66a⁺) and crypt-bottom (CD44⁺) colonic epithelial cells from individuals with active UC (aUC), quiescent UC (qUC), and non-IBD controls. Node color indicates module identity, while node size reflects the strength of connectivity. (B) Dot plot illustrating the normalised enrichment score (NES) of modules M1 and M2 across crypt-top (CD66a⁺) and crypt-bottom (CD44⁺) colonic epithelial cells from patients with aUC, qUC, and non-IBD controls. Dot color and size correspond to the NES value and its absolute magnitude, respectively. Diamond highlight significant values ($p_{adj.} < 0.05$).

3.1.7. Clinical relevance of miRNA co-expression in UC

Further, the analysis focused on module M1, which we hypothesised to have a pro-inflammatory role, to investigate its association with clinical characteristics of UC in distinct colonic epithelial cell populations. To evaluate this, we examined the relationship between the module M1 eigengene value, representing the summarised module expression, and the endoscopic Mayo subscore using Spearman's correlation. The analysis identified a significant moderate positive correlation for both crypt-top (CD66a⁺) and crypt-bottom (CD44⁺) epithelial cells, with rho values of 0.68 (FDR = 1.08×10^{-7}) and 0.60 (FDR = 1.07×10^{-5}), respectively (Fig. 3.1.7.1 A).

To additionally assess the utility of module M1 eigengene expression in distinguishing between active and quiescent UC, AUC-ROC analysis was performed. In crypt-bottom (CD44⁺) cells, this approach yielded an AUC of 80.0% (confidence interval [CI]: 63.6–96.4%), while in crypt-top (CD66a⁺) cells, module M1 expression demonstrated even greater discriminative ability, with an AUC of 87.9% (CI: 74.0–100.0%) when differentiating quiescent UC from active UC (Fig. 3.1.7.1 B).

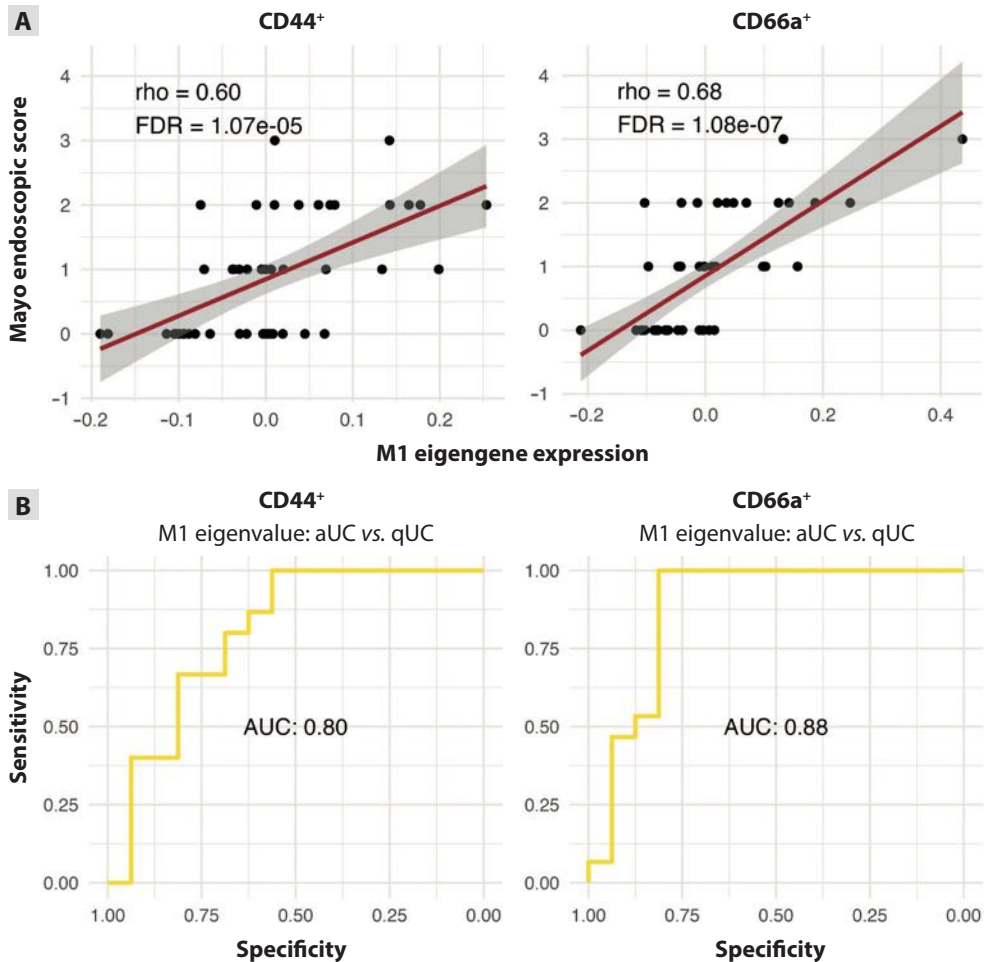


Fig. 3.1.7.1. Association of miRNA co-expression module M1 with clinical metrics in colonic epithelial cell populations

(A) Plots illustrate the correlation between the M1 module eigengene value and Mayo endoscopic score in crypt-top (CD66a⁺) and crypt-bottom (CD44⁺) colonic epithelial cells. Each dot is corresponding to an individual sample. (B) Plots display AUC-ROC curves assessing the ability of the M1 module eigengene value to differentiate between active UC (aUC) and quiescent UC (qUC) in crypt-top (CD66a⁺) and crypt-bottom (CD44⁺) colonic epithelial cells. rho – Spearman’s correlation coefficient, FDR – false discovery rate, AUC – area under the receiver operating characteristic curve.

To determine whether these findings align with observations in colonic tissue, module M1 eigengene values were calculated for biopsy samples, and the same analyses were conducted. The eigengene value in colonic tissue exhibited a strong positive correlation with the endoscopic Mayo subscore (rho = 0.703, FDR = 1.22×10^{-11}) (Fig. 3.1.7.2 A), while the AUC for distinguishing active from quiescent UC was 85.0% (CI: 72.2–97.1%)

(Fig. 3.1.7.2 B). These results suggest a high degree of similarity between the expression patterns in colonic tissue and crypt-top (CD66a⁺) colonic epithelial cells.

In summary, these findings indicate that miRNA co-expression module M1 is a promising biomarker for endoscopic UC activity, exhibiting robust predictive performance across crypt-top (CD66a⁺) and crypt-bottom (CD44⁺) colonic epithelial cells, as well as in whole colonic tissue.

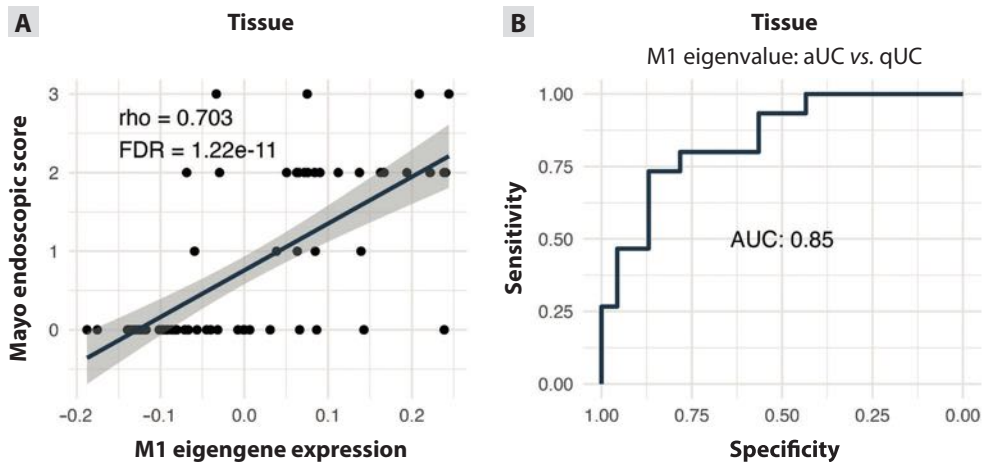


Fig. 3.1.7.2. Association of miRNA co-expression module M1 with clinical metrics in colonic tissue

(A) Plot illustrates the correlation between the M1 module eigengene value and Mayo endoscopic score in colonic tissue. Each dot is corresponding to an individual sample. (B) Plot displays AUC-ROC curve assessing the ability of the M1 module eigengene value to differentiate between active UC (aUC) and quiescent UC (qUC) in colonic tissue. rho – Spearman’s correlation coefficient, FDR – false discovery rate, AUC – area under the receiver operating characteristic curve.

3.2. Part II. Gut microbiota profiling in faeces

3.2.1. Gut microbiota diversity in UC

To investigate the composition of the gut microbiota, 16S rRNA gene sequencing was conducted on faecal samples from individuals with active and quiescent UC, as well as non-IBD controls. Prior to analysis, sequencing reads underwent thorough preprocessing with strict quality control measures. Initially, a total of 7,430,623 paired-end reads across all samples were obtained. After further filtering, 6,696,006 reads were retained, which constituted 90.1% of the initial count. Denoising preserved 6,489,333 reads (97.1% of filtered), ensuring high-quality sequences. Subsequently, merging of forward and reverse reads maintained 5,717,237 reads (89.4% of denoised). After the chimeric sequence removal step, a total of 4,824,962 reads were retained,

which constituted 84.39% of the reads after merging, amounting to an average of 67,013 reads per sample. These non-chimeric reads underwent taxonomic annotation. Consequently, the minimum number of reads per sample was established at 22,032, which was then applied as the threshold for rarefaction across all samples.

Chao1, Shannon, and Simpson indices were calculated to assess bacterial α -diversity (Fig. 3.2.1.1 A), revealing that patients with either active or quiescent UC exhibited significantly lower species richness and diversity compared to non-IBD controls (Chao1: $p = 5.7 \times 10^{-4}$ and $p = 1.8 \times 10^{-3}$, Shannon: $p = 5.0 \times 10^{-3}$ and $p = 1.8 \times 10^{-3}$, respectively). However, Simpson index only demonstrated a trend toward reduced species evenness and did not reach statistical significance between active or quiescent UC patients and non-IBD controls ($p = 0.064$ and $p = 0.059$, respectively). Notably, no significant differences were observed between UC patients with different disease activity status, indicating that even during disease remission, UC patients exhibit reduced microbial α -diversity compared to non-IBD individuals.

The Bray-Curtis dissimilarity index was calculated to evaluate the microbial community composition (β -diversity). These results supported the changes and trends observed in α -diversity. Specifically, β -diversity differed significantly between either active or quiescent UC patients and non-IBD subjects ($p = 8.0 \times 10^{-3}$, $R^2 = 0.047$; $p = 0.01$, $R^2 = 0.052$, respectively). However, the magnitude of variation in microbial composition had a weak effect on health status, as further reflected by clustering analysis, where no significant grouping was detected among different UC activity states ($p = 0.49$) (Fig. 3.2.1.1 B). The Bray-Curtis index was also calculated to assess the in-between sample dissimilarity within each group (Fig. 3.2.1.1 C). Consistent with the β -diversity trend, Bray-Curtis distances (μ) within samples of the same group showed that, compared to non-IBD controls ($\mu = 0.548 \pm 0.118$), samples from patients with active UC ($\mu = 0.640 \pm 0.168$, $p = 2.3 \times 10^{-12}$) or quiescent UC ($\mu = 0.607 \pm 0.148$, $p = 1.3 \times 10^{-5}$) exhibited greater pairwise dissimilarity. Furthermore, quiescent UC patients demonstrated significantly higher within-group similarity compared to those with active UC ($p = 0.044$).

Collectively, these findings demonstrate reduced diversity and an altered gut microbiota composition in UC patients, regardless of disease activity status, when compared to non-IBD individuals.

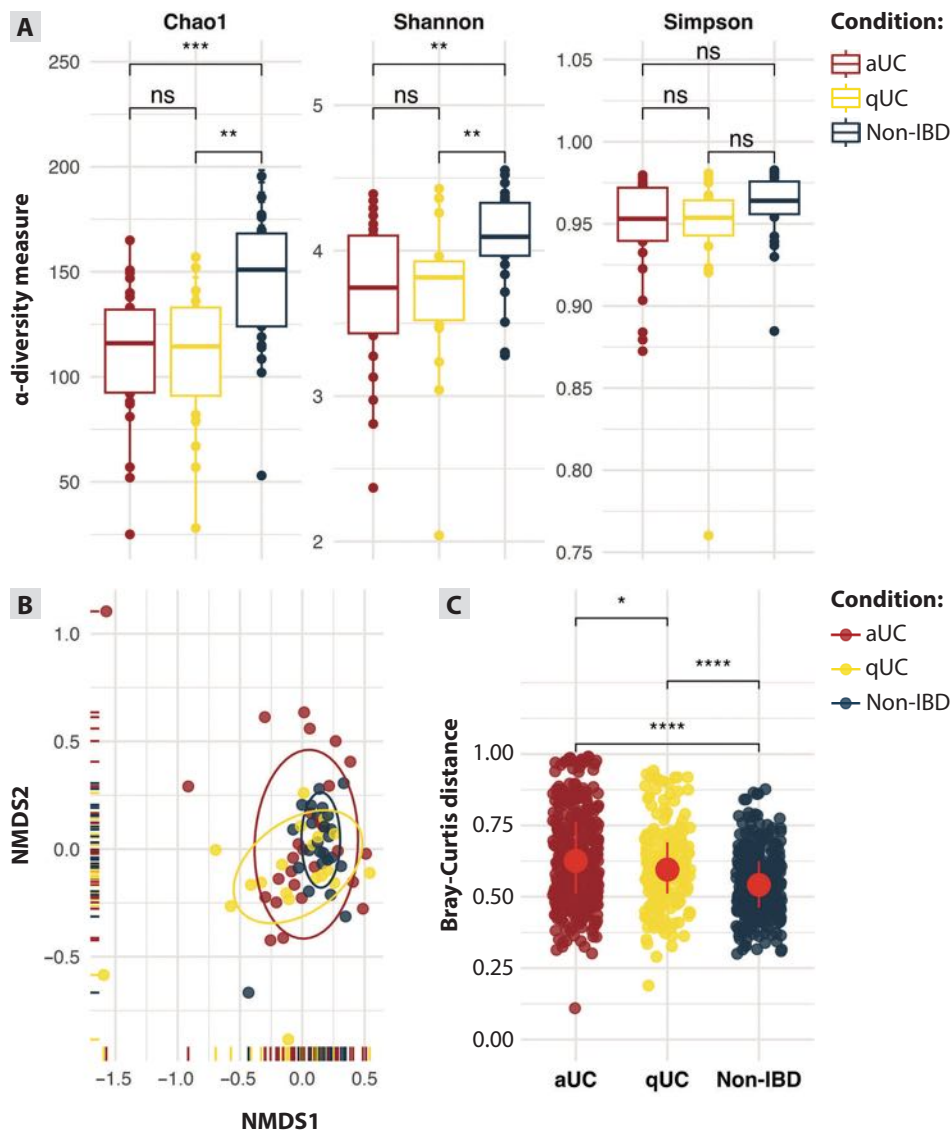


Fig. 3.2.1.1. Faecal microbiota diversity in UC patients and non-IBD individuals

(A) Boxplots displaying α -diversity metrics, with median and interquartile range (Q1–Q3). Asterisks represent p-values from Wilcoxon rank-sum tests comparing groups; ** $p < 0.01$, *** $p < 0.001$. Colors represent different conditions – active UC (aUC), quiescent UC (qUC), and non-IBD. (B) Non-metric multidimensional scaling (NMDS) plot based on Bray-Curtis distances, depicting microbial composition differences among groups. Colors and ellipses represent different conditions. (C) Scatter plot illustrating within-group sample similarity, assessed using the Bray-Curtis dissimilarity index. Asterisks represent p-values comparing groups; * $p < 0.05$, **** $p < 0.0001$.

3.2.2. Identification of UC-associated bacterial abundance signatures

Next, a global bacteria composition analysis across health states indicated that the faecal microbiome of UC patients (both active and quiescent) is dominated by bacteria from the *Phocaeicola* and *Faecalibacterium* genera, while in non-IBD individuals, it is primarily dominated by *Phocaeicola* and *Prevotella* (Fig. 3.2.2.1 A). To further explore the altered bacterial taxa in UC, co-occurrence and differential abundance analyses were conducted. Among the 40 identified genera, five showed statistically significant differences ($|\log_2\text{FC}| > 0$ and $\text{FDR} < 0.05$) in relative abundance between UC patients (both active and quiescent) and non-IBD controls (Fig. 3.2.2.1 B). Specifically, when compared to non-IBD individuals, the relative abundance of the genera *Alistipes* ($|\log_2\text{FC}| = 1.39$, $\text{FDR} = 0.019$), *Paraprevotella* ($|\log_2\text{FC}| = 0.91$, $\text{FDR} = 4.2 \times 10^{-3}$), *Mediterraneibacter* ($|\log_2\text{FC}| = 1.53$, $\text{FDR} = 1.2 \times 10^{-3}$), *Coprococcus* ($|\log_2\text{FC}| = 1.12$, $\text{FDR} = 0.033$), *Cuneatibacter* ($|\log_2\text{FC}| = 2.29$, $\text{FDR} = 4.2 \times 10^{-3}$) was decreased in faecal samples of UC patients.

Taken together, differential abundance analysis uncovers UC bacterial signatures and, along with diversity analyses, highlights key bacterial shifts associated with disease pathogenesis.

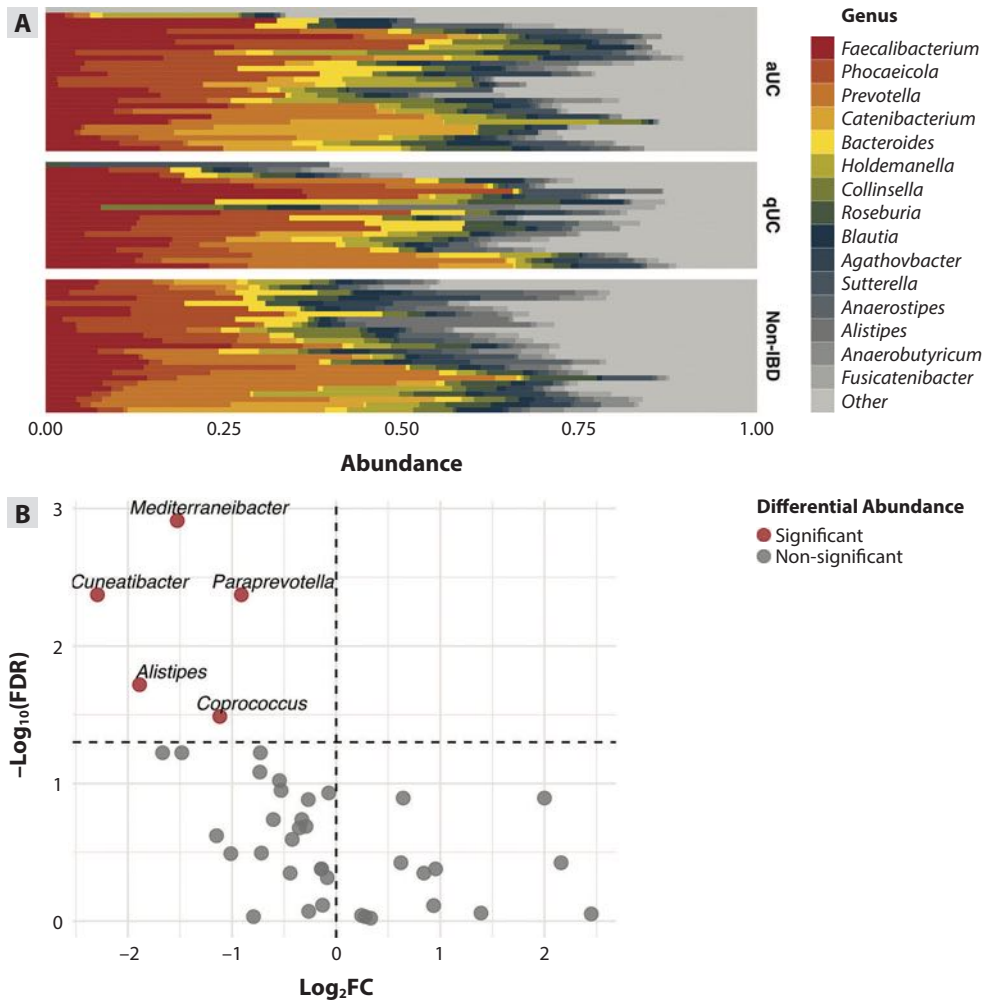


Fig. 3.2.2.1. Bacterial genera composition in the faeces of UC patients non-IBD controls

(A) Bar charts illustrating the relative abundance of the 15 most abundant genera in the study cohort (active UC (aUC), quiescent UC (qUC), and non-IBD). Less abundant genera grouped as “Other”. (B) Differentially abundant bacterial genera in aUC faecal samples compared to non-IBD. Horizontal dash line indicates the statistical significance threshold (FDR = 0.05) in logarithmic scale, vertical dash line indicates the threshold for no change in differential abundance. FC – fold change, FDR – false discovery rate (corrected p values resulted from Wilcoxon rank-sum test).

3.2.3. Shared core microbiome between UC patients and non-IBD individuals

As UC is associated not only with gut dysbiosis but also with altered bacterial recognition and defense mechanisms [198, 269], commensal microbiota may play an important role in influencing the intestinal epithelium during UC. Therefore, a shared core microbiome was identified across patients with different stages of UC and non-IBD individuals. First, the number of core taxa was determined for different study groups (i.e., those with $\geq 0.1\%$ relative abundance in $\geq 50\%$ of samples). This analysis resulted in 31, 31, and 38 core bacterial ASVs in the active UC, quiescent UC, and non-IBD groups, respectively. After differential abundance analysis, a total of 27 genera were identified as shared and consistently present in the faeces of patients with both active and quiescent UC, as well as non-IBD controls (Fig. 3.2.3.1 A). Among them, the top 10 most abundant were *Phocaeicola* (relative abundance in UC: $14.63\% \pm 13.50$; relative abundance in non-IBD: $12.06\% \pm 9.56$), *Faecalibacterium* (UC: $14.37\% \pm 10.76$; non-IBD: $9.20\% \pm 5.74$), *Prevotella* (UC: $7.31\% \pm 12.11$; non-IBD: $10.66\% \pm 12.04$), *Collinsella* (UC: $4.93\% \pm 5.55$; non-IBD: $3.92\% \pm 3.26$), *Holdemanella* (UC: $4.19\% \pm 6.20$; non-IBD: $4.58\% \pm 6.49$), *Sutterella* (UC: $3.95\% \pm 5.91$; non-IBD: $2.20\% \pm 3.53$), *Roseburia* (UC: $3.81\% \pm 4.24$; non-IBD: $4.20\% \pm 3.22$), *Bacteroides* (UC: $3.55\% \pm 4.93$; non-IBD: $3.77\% \pm 4.09$), *Escherichia/Shigella* (UC: $3.37\% \pm 8.77$; non-IBD: $0.62\% \pm 1.25$), and *Blautia* (UC: $3.09\% \pm 3.00$; non-IBD: $3.42\% \pm 2.38$) (Fig. 3.2.3.1 B).

Taken together, the findings suggest that a significant portion of the gut microbiota remains stable and unchanged during the course of UC pathogenesis. These microbiota constituents may be relevant to mechanisms underlying the onset and progression of UC.

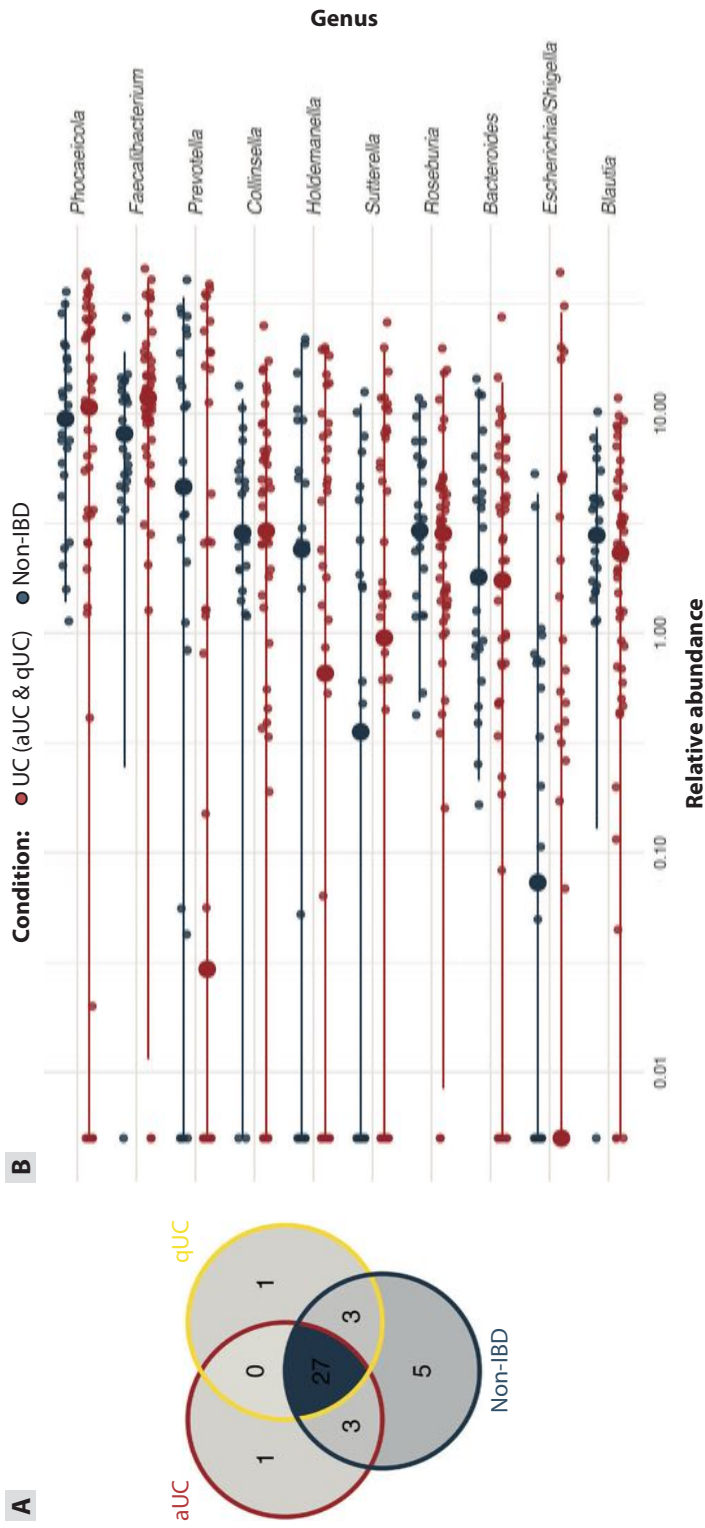


Fig. 3.2.3.1. Core faecal microbiome in UC patients and non-IBD individuals

(A) Venn diagram illustrating shared and unique core taxa at the genus level, defined by a minimum abundance of 0.1% in at least 20% of samples within each group (active UC (aUC), quiescent UC (qUC), and non-IBD (Non-IBD)). Outline colors represent different groups. (B) The 10 most consistently abundant genera in UC (both aUC and qUC) and non-IBD (Non-IBD) groups. Colors of the dots represent different groups. Smaller dots represent individual samples, while bigger dots represent the medians.

3.3. Part III. Functional analysis of the impact of commensal bacteria on colonic epithelium using intestinal organoid system

3.3.1. Morphological evaluation of colonic epithelial organoids and monolayers derived from UC patients and non-IBD individuals

To investigate the stable core gut microbiota and the differential responses of colonic epithelial cells from non-IBD individuals and UC patients, co-culturing experiments were performed using advanced patient-derived colonic epithelial organoid technology. This approach allowed for the development of organoid-derived epithelial monolayers. Before the co-cultivation experiments, the experimental system was evaluated on both morphological and molecular levels.

First, undifferentiated 3D colonic epithelial organoids were qualitatively evaluated using both light and fluorescence microscopy, confirming that organoids derived from both non-IBD individuals and UC patients in active or quiescent phases exhibited stable morphological phenotypes during long-term culturing (up to two months). The organoids were grown in primary culture (passage 0 (P0)) for one to two weeks before passaging, with growth dynamics closely monitored. The progression from freshly isolated crypts (at day 0) to small structures (at days 5–8) and eventually large cystic organoids (at days 8–14) was consistently observed across all groups. Importantly, neither the clinical diagnosis nor the duration of cultivation affected cellular behavior or the microscopic appearance of the organoids, as they maintained the characteristic cystic morphology even at high passage numbers (up to passage 5 (P5)) (Fig. 3.3.1.1 A). Immunofluorescence analysis further validated the proper polarity of the epithelial cells forming the organoids. This polarity was indicated by basolateral expression of β -catenin and apical expression of F-actin, establishing a central lumen (Fig. 3.3.1.1 B). The patient-derived 3D organoids (both UC and non-IBD) also closely resembled the cellular architecture of human colonic epithelium, displaying high expression of the proliferation marker Antigen Ki-67 (Ki-67) and tight junction protein zonula occludens-1 (ZO-1). Conversely, markers of specialized colonic cell types – including colonocytes (Cytokeratin 20, CK20), goblet cells (Mucin 2, MUC2), and enteroendocrine cells (Chromogranin A, CgA) – were expressed at comparatively lower levels (Fig. 3.3.1.1 C–G), as expected in undifferentiated structures.

The analogous microscopic evaluation of differentiated colonic epithelial monolayers derived from 3D organoids of UC patients with active disease and non-IBD controls yielded similar results. Specifically, colonic epithelial monolayers from both UC and non-IBD groups exhibited pronounced expression of markers for the main specialized cell populations of the large intestine – colonocytes, goblet cells, and enteroendocrine cells – as well as proliferative cells and intercellular tight junctions (Fig. 3.3.1.1 H–K).

These observations, encompassing the timing of organoid formation, epithelial polarisation, and cellular composition, highlight the utility of colonic organoids in studies of epithelial barrier regulation in both UC patients and non-IBD controls.

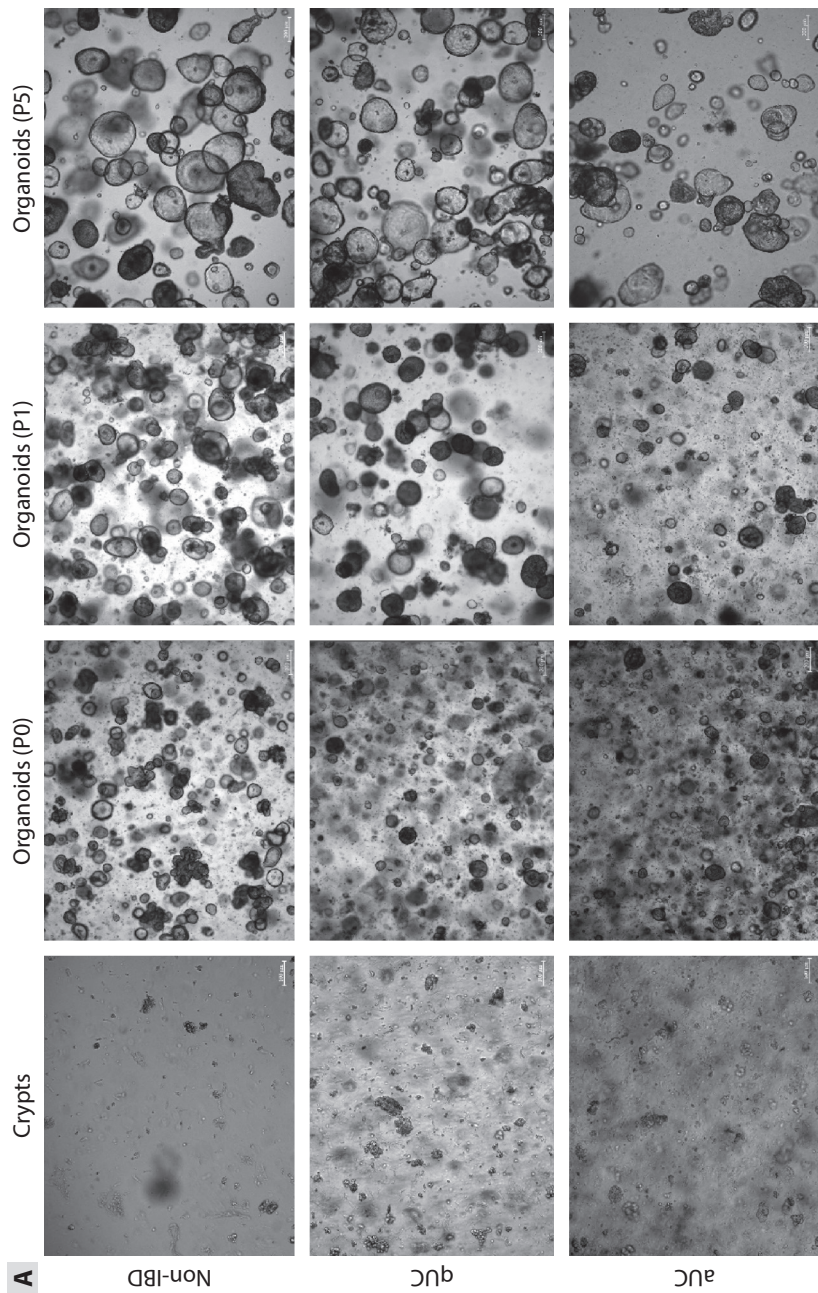


Fig. 3.3.1.1 (A). Morphology and cellular composition of representative 3D colonic epithelial organoids and 2D colonic epithelial monolayers

(A) Brightfield microscopy images showing dynamics of crypt-to-late passage growth of colonic epithelial organoids in non-IBD, quiescent UC (qUC), and active UC (aUC) groups. Scale bar is 100 μm for crypts and 200 μm for organoids. P – passage.

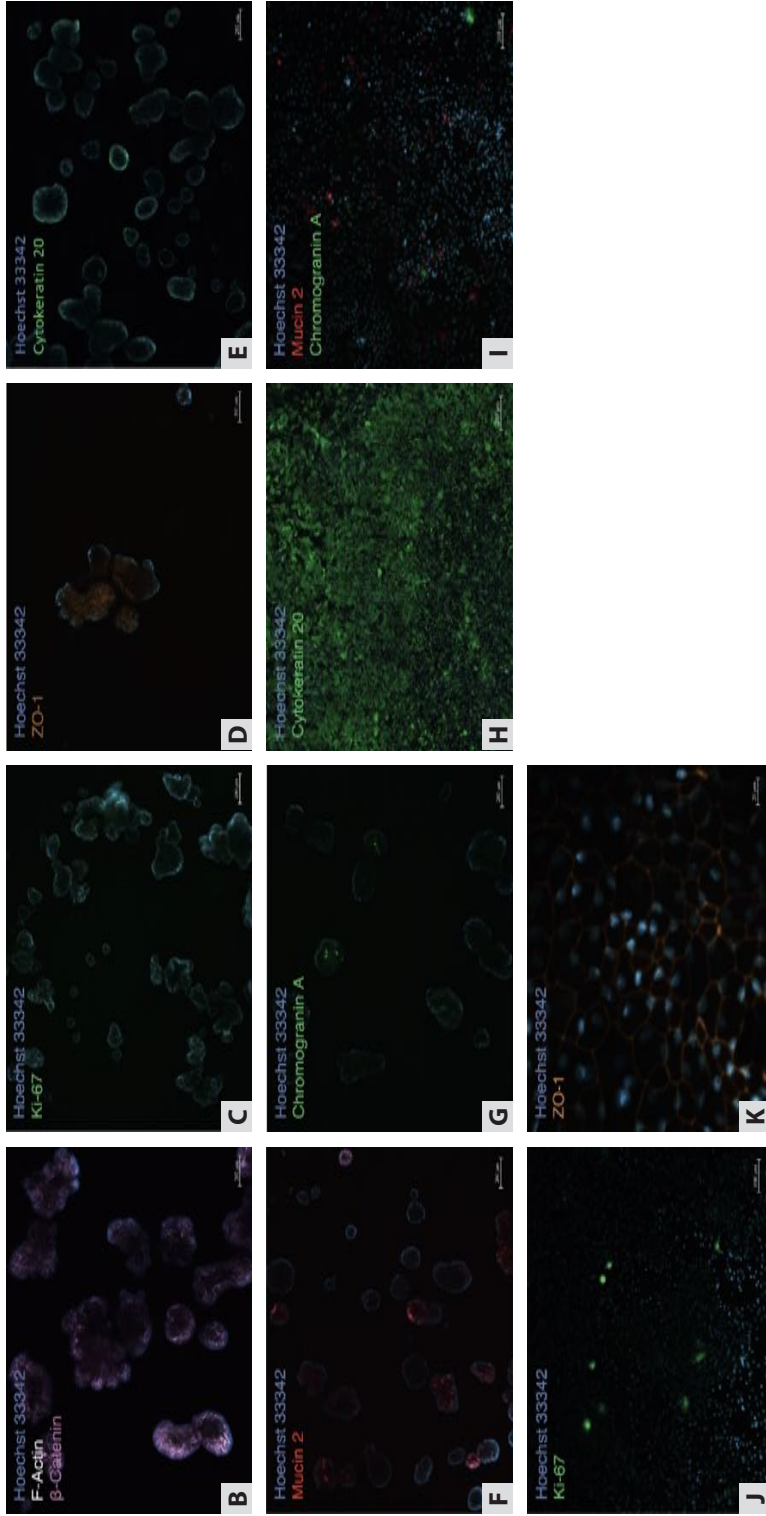


Fig. 3.3.1.1 (B-K). Morphology and cellular composition of representative 3D colonic epithelial organoids and 2D colonic epithelial monolayers

(B-G) Fluorescence microscopy images showing expression of cellular and structural markers in 3D colonic epithelial organoids. Scale bar is 200 μ m. (H-K) Fluorescence microscopy images showing the expression of cellular and structural markers in 2D colonic epithelial monolayers derived from 3D organoids. Scale bar is 200 μ m (H), 100 μ m (I, J), and 20 μ m (K).

3.3.2. Epigenetic dynamics in colonic epithelial organoids

To expand the evaluation of the selected experimental system on the molecular level, epigenetic dynamics were assessed by performing pyrosequencing and quantitatively comparing global methylation in colonic tissues and organoids derived from non-IBD controls, as well as from patients with active and quiescent UC. Methylation levels of LINE-1 were assessed at multiple points, including colonic biopsies, isolated colonic crypts, and organoid cultures at different passages (primary – P0, early – P1, and late – P5).

Across all biological samples, the LINE-1 region was found to be highly methylated (above 60%), with slight variations depending on the health condition and sample type (Fig. 3.3.2.1). Specifically, LINE-1 methylation values across the entire cohort ranged from $69.4\% \pm 2.9\%$ in quiescent UC biopsies to $61.8\% \pm 3.8\%$ in active UC P1 organoids. In the primary organoid cultures, non-IBD and quiescent UC groups exhibited nearly identical global methylation levels. In P0 organoids, methylation levels for non-IBD and quiescent UC were $66.9\% \pm 4.1\%$ and $66.0\% \pm 3.9\%$ ($p_{\text{adj.}} = 0.1$), while the active UC group exhibited a further tendency of decrease ($65.6\% \pm 4.2\%$, $p_{\text{adj.}} = 0.841$ and $p_{\text{adj.}} = 0.1$ compared to non-IBD and quiescent UC, respectively).

A notable decrease in LINE-1 methylation was observed during long-term culturing (Fig. 3.3.2.1). In late-passage (P5) organoids, LINE-1 methylation dropped significantly compared to initial biopsy samples in all study subject groups. Specifically, in the non-IBD group, P5 organoids a significant reduction in LINE-1 methylation compared to biopsies (by 8.1%, $p_{\text{adj.}} = 1.04 \times 10^{-4}$), crypts (by 8.0%, $p_{\text{adj.}} = 2.48 \times 10^{-4}$), and early-passage organoids (P0: by 6.3%, $p_{\text{adj.}} = 2.00 \times 10^{-3}$; P1: by 5.9%, $p_{\text{adj.}} = 0.019$). Similarly, in the quiescent UC group, a notable reduction in LINE-1 methylation was observed between colonic biopsies and early and late-passage organoids with methylation level drop by 4.0% in P1 organoids ($p_{\text{adj.}} = 6.0 \times 10^{-3}$) and 5.0% in P5 organoids ($p_{\text{adj.}} = 1.0 \times 10^{-3}$). The active UC group followed the same trend, with LINE-1 methylation decreasing significantly by 4.9% in P1 organoids compared to biopsy samples ($p_{\text{adj.}} = 0.012$) and by 4.6% when compared to crypt samples ($p_{\text{adj.}} = 0.019$). Although the reduction in LINE-1 methylation was also observed in late-passage active UC organoids by 4.0%, the difference did not reach statistical significance ($p_{\text{adj.}} = 0.102$).

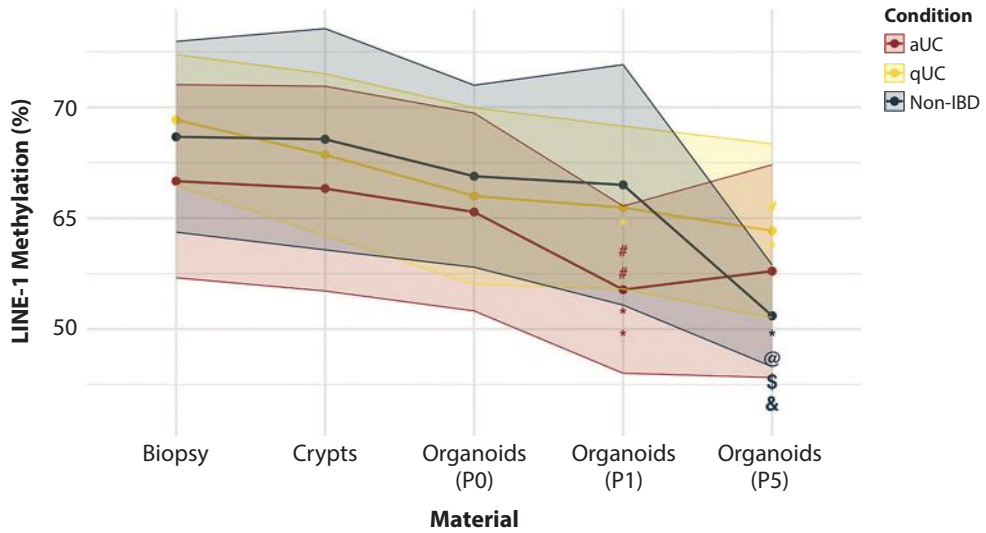


Fig. 3.3.2.1. Dynamics of LINE-1 methylation levels in colonic tissues and colonic epithelial organoids derived from UC patients and non-IBD controls

Colors represent the study subject groups, dots indicate the mean LINE-1 methylation values, and the transparent area along the lines represent the standard deviation. *, @, \$, and & mark statistically significant differences ($p_{adj.} < 0.05$) when comparing different materials within the same condition: * indicates differences compared to biopsy, @ indicates differences compared to crypts, \$ indicates differences compared to organoids (P0), & indicates differences compared to organoids (P1). # marks statistically significant differences ($p_{adj.} < 0.05$) when comparing active UC (aUC) or quiescent UC (qUC) to non-IBD. P – passage.

Furthermore, analysis of sub-cultured colonic epithelial organoid LINE-1 methylation dynamics highlighted that the pace of methylation reduction differed between health conditions (Fig. 3.3.2.1). In early-passage organoids, LINE-1 methylation in active UC samples was 4.7% ($p_{adj.} = 0.018$) and 3.7% ($p_{adj.} = 0.01$) lower than in non-IBD and quiescent UC groups, respectively. Interestingly, late-passage non-IBD organoids also experienced substantial methylation decline, reaching levels comparable to active UC organoids. By P5, the non-IBD group showed a significant difference of 3.8% compared to quiescent UC organoids ($p_{adj.} = 0.024$), indicating that long-term culturing influences epigenetic changes even in non-IBD samples.

Overall, these findings suggest that long-term cultivation of colonic epithelial organoids is associated with LINE-1 hypomethylation, with the pace of decline varying based on the initial health condition. This provides valuable insights for further use of this system in co-culturing experiments involving both non-IBD and active UC colonic epithelial monolayers.

3.3.3. Selection of commensal bacteria and miRNA candidates for functional testing

Prior to functional testing of the commensal microbiota members and their impact on the expression of colonic epithelial cell genes and miRNAs, selection and prioritisation were performed for both miRNAs and bacteria.

First, based on the results of Part II of this thesis, combined with literature data, two commensal bacterial genera exhibiting high and low relative abundance (*Phocaeicola* and *Escherichia/Shigella*, respectively) in both UC and non-IBD groups were selected for functional testing. Specifically, *Phocaeicola vulgatus* ATCC 8482 (referred to as *P. vulgatus*) and *Escherichia coli* ATCC 25922 (referred to as *E. coli*) were chosen as representative strains from these shared core microbiota genera.

Subsequently, selection was performed for colonic epithelial miRNAs. The 10 miRNAs from the Study Part I, identified as up-regulated ($\log_2FC > 1.5$, $FDR < 0.05$) in crypt-top (CD66a⁺) cells during active UC compared to non-IBD, were chosen for further analysis (Fig. 3.3.3.1): miR-31-5p ($\log_2FC = 8.33$, $FDR = 1.03 \times 10^{-11}$), miR-191-3p ($\log_2FC = 6.52$, $FDR = 1.00 \times 10^{-3}$), miR-135b-5p ($\log_2FC = 4.47$, $FDR = 1.30 \times 10^{-6}$), miR-27a-3p ($\log_2FC = 2.27$, $FDR = 4.84 \times 10^{-6}$), miR-146a-5p ($\log_2FC = 2.27$, $FDR = 1.50 \times 10^{-4}$), miR-182-5p ($\log_2FC = 2.27$, $FDR = 9.14 \times 10^{-7}$), miR-222-3p ($\log_2FC = 1.76$, $FDR = 6.42 \times 10^{-4}$), miR-183-5p ($\log_2FC = 1.75$, $FDR = 0.194$), miR-221-3p ($\log_2FC = 1.51$, $FDR = 0.0345$), and miR-24-3p ($\log_2FC = 1.50$, $FDR = 4.61 \times 10^{-4}$).

Finally, all selected miRNAs were tested *in silico* for potential targets in the genomes of *P. vulgatus* and *E. coli*. The results revealed that miR-31-5p, miR-191-3p, and miR-221-3p did not have any theoretical target genes in either bacterial strain. Six miRNAs were identified to potentially target one or two genes exclusively in *E. coli*: miR-27a-3p (*pyrB*: probability = 54%, $p = 2.2 \times 10^{-6}$), miR-222-3p (*cysI*: 51%, $p = 8.6 \times 10^{-5}$), miR-182-5p (*mukB*: 59%, $p = 7.8 \times 10^{-7}$), miR-135b-5p (*mukB*: 59%, $p = 1.4 \times 10^{-5}$; *cysI*: 52%, $p = 3.4 \times 10^{-5}$), miR-24-3p (*pyrB*: 54%, $p = 2.5 \times 10^{-5}$; *cysI*: 51%, $p = 3.6 \times 10^{-5}$), and miR-146a-5p (*mukB*: 59%, $p = 2.0 \times 10^{-5}$; *cysI*: 51%, $p = 5.0 \times 10^{-5}$). One miRNA, miR-183-5p, showed potential targets in both *E. coli* (*mukB*: 59%, $p = 5.3 \times 10^{-7}$) and *P. vulgatus* (*BVU_RS05340*: 51%, $p = 1.2 \times 10^{-7}$).

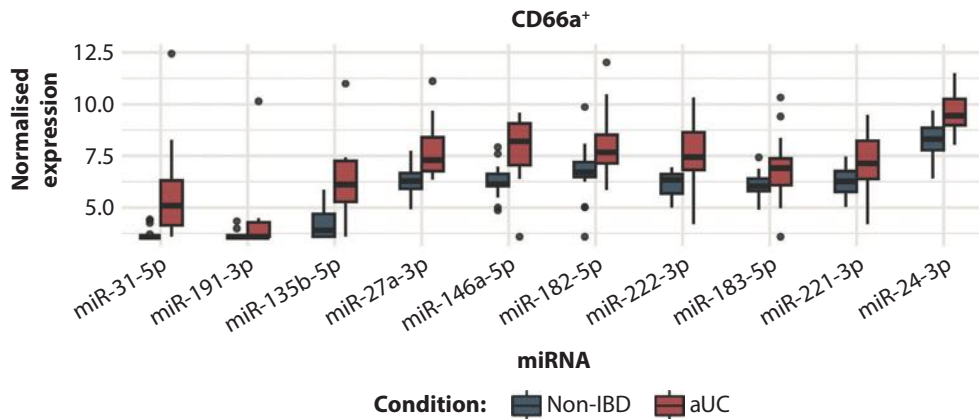


Fig. 3.3.3.1. Expression of selected crypt-top ($CD66a^+$) colonic epithelial cell miRNAs in patients with active UC and non-IBD controls

Box colors indicate sample groups: active UC (aUC) and non-IBD control individuals. The individual dots represent outliers. The y-axis represents normalised expression values obtained via variance stabilising transformation. miRNAs on x-axis are ordered from left to right by decreasing expression difference between the two groups.

To conclude, two commensal bacteria strains – *E. coli* and *P. vulgatus* – and three miRNA candidates with the strongest probabilities and highest number of target genes in these bacteria – miR-135b-5p, miR-146a-5p, and miR-183-5p – were prioritised for functional testing in colonic epithelial organoid-based systems.

3.3.4. Impact of commensal bacteria on the homeostasis of the colonic epithelium

Functional analysis of commensal bacteria was performed at the level of colonic epithelial cell gene expression, using epithelial monolayers established from both individuals with active UC and those without IBD (non-IBD). Colonic epithelial monolayers were co-cultured with *E. coli* and *P. vulgatus* (Fig. 3.3.4.1 A). Host response to the bacteria was assessed through targeted gene expression analysis, focusing on markers related to pathogen recognition (the gene coding for Toll-like receptor 4: *TLR4*), cellular stress signalling (the genes coding for Heat-shock proteins 70 and 27: *HSPA1A* and *HSPB1*), and tight junction maintenance (the gene coding for zonula occludens-1: *TJPI*).

Analysis of the cellular marker gene expression did not show significant changes; however, it revealed some important patterns (Fig. 3.3.4.1 B). Even though not significant, the most pronounced and distinct effects were observed on *TJPI* expression in relation to bacterial exposure in epithelial mono-

layers from UC patients and non-IBD controls (Fig. 3.3.4.1 B, right and left panels, respectively). Specifically, in monolayers derived from UC patients, the expression of *TJPI* demonstrated a tendency to decrease after incubation with both species (*E. coli*: FC = 0.42, $p = 0.796$; *P. vulgatus*: FC = 0.72, $p = 1.0$). In contrast, the expression of *TJPI* in the non-IBD epithelial monolayers changed in the opposite direction and showed a trend toward an increase after exposure to commensal bacteria (*E. coli*: FC = 3.52 and $p = 0.328$; *P. vulgatus*: FC = 1.86 and $p = 0.397$). Additionally, neither of the tested bacteria had a significant impact on the expression of *TLR4* in epithelial cells from both UC patients and non-IBD controls when compared to unstimulated cells (*E. coli*: FC = 0.54, $p = 1.0$ [UC] and FC = 0.82, $p = 0.463$ [non-IBD]; *P. vulgatus*: FC = 0.89, $p = 0.73$ [UC] and FC = 2.05, $p = 1.0$ [non-IBD]). The expression of *HSPA1A* also did not change significantly following exposure to both bacteria (*E. coli*: FC = 0.73, $p = 0.73$ [UC] and FC = 1.41, $p = 0.959$ [non-IBD]; *P. vulgatus*: FC = 1.24, $p = 0.863$ [UC] and FC = 1.23, $p = 0.878$ [non-IBD]). Similar results were observed when assessing the expression of *HSPB1* between cell cultures exposed to bacteria and those mock-treated (*E. coli*: FC = 0.72, $p = 0.489$ [UC] and FC = 1.18, $p = 0.878$ [non-IBD]; *P. vulgatus*: FC = 1.27, $p = 0.436$ [UC] and FC = 0.80, $p = 0.574$ [non-IBD]).

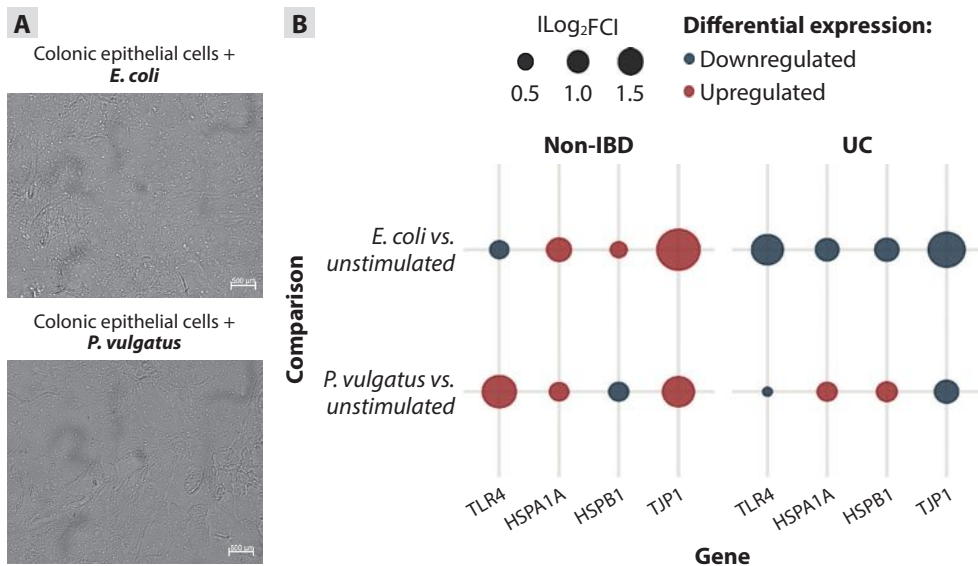


Fig. 3.3.4.1. Commensal bacteria-induced gene expression changes in colonic epithelial cells of UC patients and non-IBD controls

(A) Representative images of colonic epithelial cell co-cultures with *E. coli* and *P. vulgatus*. (B) Dot plot showing relative gene expression changes in UC and non-IBD groups. The color of the dots represents the direction of gene expression changes. The size of the dots represents absolute values of gene expression fold changes on a logarithmic scale. FC – fold change.

What is more, as patient-derived experimental systems were used for testing and no statistically significant differences were identified, the variance in normalised gene expression was also evaluated, which could at least partially explain the observations. As assessed from coefficient of variance (CV), the expression values of all four genes across all three culturing conditions and two diagnoses showed high variance, with CV ranging from 0.24 for *HSPB1* gene in mock-treated UC epithelial cells to 18.84 for *TJP1* gene in *E. coli*-exposed epithelial monolayers.

In summary, these findings indicate a trend toward a differential response to *E. coli* and *P. vulgatus* regarding tight junction regulation between colonic epithelial cell monolayers derived from UC patients and non-IBD individuals. The results also highlight the highly patient-specific variability of host responses to intestinal bacteria, with colonic epithelial cells from different individuals reacting variably to the same bacterial species.

3.3.5. Regulatory potential of commensal bacteria on colonic epithelial miRNA expression and secretion

To further explore whether commensal bacteria can influence the expression of colonic epithelial miRNA and their secretion in EVs, targeted miRNA expression analysis was performed in both epithelial cell and EV compartments.

Prior to miRNA expression analysis, EVs collected from colonic epithelial cell cultures were evaluated for their characteristic features, including size and the expression of surface and internal (both specific and non-specific) markers. The analysis confirmed the specificity of the EV isolation method for these structures, with 88.8% of detected vesicles having average size of 36.63 nm (± 18.64) and the expected presence of EV markers or the absence of non-specific proteins. Specifically, the average concentration of CD63 in the EVs of non-IBD controls was 26.12 pg/mL (± 0.85) in unstimulated samples, 29.03 pg/mL (± 7.23) in samples stimulated with *E. coli*, and 31.73 pg/mL (± 6.23) in samples stimulated with *P. vulgatus*. Similarly, in the EVs of the colonic epithelial cells of UC patients, the concentration of CD63 was 25.61 pg/mL (± 18.37) in unstimulated samples, 25.50 pg/mL (± 20.41) in samples stimulated with *E. coli*, and 25.63 pg/mL (± 17.69) in samples stimulated with *P. vulgatus*. Meanwhile, the average concentration of another exosome marker, HSP70, in the EVs of non-IBD controls was 2064.93 pg/mL (± 2181.35) in unstimulated samples, 528.99 pg/mL (± 403.63) in samples stimulated with *E. coli*, and 484.82 pg/mL (± 430.60) in samples stimulated with *P. vulgatus*. In the EVs of cells of UC patients, the concentration of HSP70 was 574.52 pg/mL (± 521.84) in unstimulated samples,

385.66 pg/mL (\pm 301.59) in samples stimulated with *E. coli*, and 875.64 pg/mL (\pm 301.59) in samples stimulated with *P. vulgatus*. In contrast, the Apo-A1 protein was undetectable in all samples from both study groups, indicating good specimen purity and the absence of contamination.

Finally, miRNA expression was evaluated. First, the baseline expression of selected miRNAs was compared between UC and non-IBD cultures. No significant differences were observed between the groups (FC = 0.77, p = 0.165 [miR-183-5p]; FC = 1.00, p = 0.710 [miR-135b-5p]; and FC = 1.08, p = 1.00 [miR-146a-5p]). Next, similar to the evaluation of bacterial effects at the gene expression level, targeted miRNA expression analysis was conducted comparing samples exposed to bacteria with those that were mock-treated, revealing trends in miRNA expression changes associated with inflammation activity of the material organoids originated from (Fig. 3.3.5.1). However, the observed changes did not reach statistical significance. In the non-IBD group, miR-183-5p and miR-135b-5p expression in epithelial cells tended to decrease after exposure to *E. coli*, compared to non-exposed cells (FC = 0.84, p = 0.574, and FC = 0.87, p = 0.798, respectively), while miR-146a-5p expression showed an increasing trend (FC = 1.37, p = 0.798) (Fig. 3.3.5.1, upper-left panel). Similar miRNA expression trends were observed in the EVs derived from the epithelial cells of non-IBD controls: after bacterial exposure, there was a decrease in miR-183-5p and miR-135b-5p expression and an increase in miR-146a-5p expression compared to control conditions (FC = 0.80, p = 0.574; FC = 0.72, p = 0.798; and FC = 1.21, p = 0.798, respectively) (Fig. 3.3.5.1, upper-right panel). Interestingly, the expression trends in the UC patient group differed from those observed in non-IBD controls after exposure to *E. coli*. In the UC group, the expression of all three examined miRNAs, miR-183-5p, miR-135b-5p, and miR-146a-5p, showed a tendency to increase in colonic epithelial cells after bacterial exposure (FC = 1.53, p = 0.730; FC = 1.71, p = 0.666; and FC = 2.39, p = 0.258, respectively) (Fig. 3.3.5.1, lower-left panel). Similar expression trends were recorded in the EVs from the epithelial cells of UC patients, where miR-183-5p, miR-135b-5p, and miR-146a-5p showed a tendency to increase compared to the unstimulated control (FC = 1.32, p = 0.730; FC = 1.32, p = 0.666; and FC = 2.07, p = 0.258, respectively) (Fig. 3.3.5.1, lower-right panel). After cultivation of colonic epithelial cells with another commensal bacterium, *P. vulgatus*, the expression of all analysed miRNAs showed almost no change compared to non-stimulated cells in either the control individuals (FC = 1.04, p = 0.382 [miR-183-5p]; FC = 0.99, p = 0.234 [miR-135b-5p]; and FC = 1.16, p = 0.161 [miR-146a-5p]) (Fig. 3.3.5.1, upper-left panel) or in the epithelial monolayers of UC patients (FC = 0.99, p = 0.605 [miR-183-5p]; FC = 0.95, p = 0.489 [miR-135b-5p]; and FC = 0.99, p = 1.00

[miR-146a-5p]) (Fig. 3.3.5.1, lower-left panel). Meanwhile, in the EVs of both the non-IBD and UC groups, contact with *P. vulgatus* resulted in a decrease in the expression of miR-183-5p and miR-135b-5p compared to control conditions (Fig. 3.3.5.1, upper- and lower-right panels). In the non-IBD group, the expression levels were FC = 0.59 (p = 0.382) and FC = 0.51 (p = 0.234), respectively, while in the UC group, they were FC = 0.70 (p = 0.605) and FC = 0.73 (p = 0.489), respectively. In contrast, miR-146a expression showed a decreasing trend only in the EVs of non-IBD group (FC = 0.53, p = 0.161) compared to unstimulated cells (Fig. 3.3.5.1, upper-right panel), while in the UC group, it remained unchanged (FC = 1.05, p = 1.00) (Fig. 3.3.5.1, lower-right panel).

To conclude, these observations imply potential differential regulatory properties of commensal microbiota constituents, specifically *E. coli* and *P. vulgatus*, on miRNA expression in colonic epithelial cell monolayers derived from UC patients and non-IBD individuals, as well as their secreted EVs. Together, these findings suggest that *E. coli* may contribute to inflammation-associated miRNA changes in UC, whereas *P. vulgatus* may play a regulatory role in extracellular signalling.

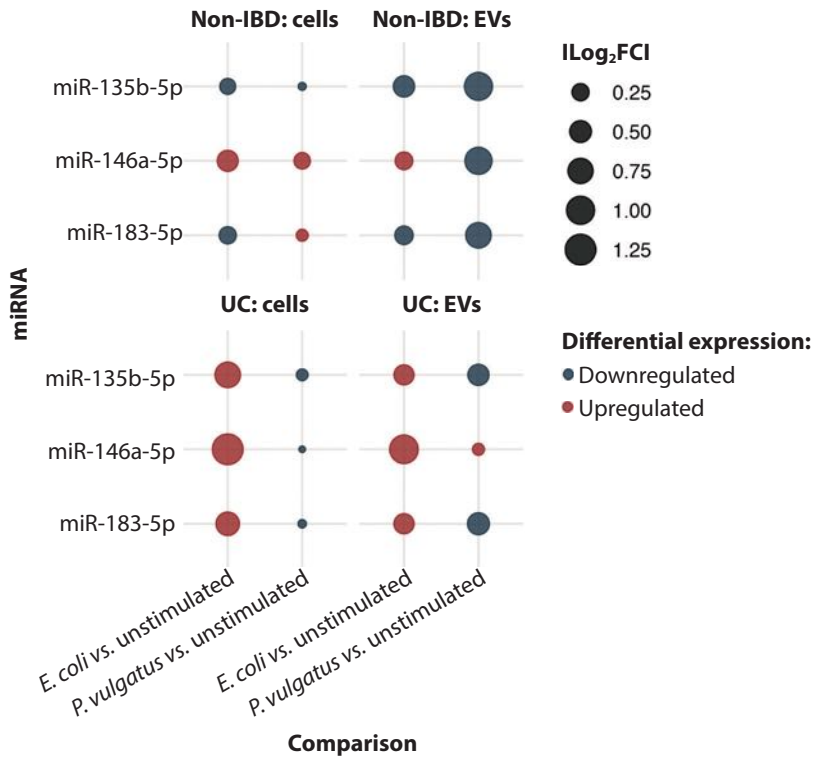


Fig. 3.3.5.1. Commensal bacteria-induced miRNA expression changes in colonic epithelial cells and extracellular vesicles of UC patients and non-IBD controls

The color of the dots represents the direction of gene expression changes. The size of the dots represents absolute values of gene expression fold changes on a logarithmic scale. EVs – extracellular vesicles, FC – fold change.

4. DISCUSSION

4.1. Part I. miRNA expression profiling in colonic tissue and epithelial cell populations

Despite extensive research efforts and significant advancements in understanding UC, its underlying molecular mechanisms remain largely elusive. In particular, there is a considerable gap in knowledge regarding the expression patterns of regulatory non-coding miRNAs in UC within specific cell populations. To address this, the first part of this thesis provided an overview of miRNA expression in complex colonic mucosa samples from UC patients, along with detailed profiles of spatially distinct colonic epithelial cell population-specific miRNA expression in both active and quiescent UC. Additionally, this work highlighted differences in miRNA expression between two colonic epithelial cell populations – crypt-bottom (CD44⁺) and crypt-top (CD66a⁺) cells, explored potential biological pathways influenced by dysregulated miRNAs in colonic epithelial cells during UC, identified miRNA co-expression network, and examined its clinical relevance.

A key finding of this study was the distinct miRNA expression responses in different colonic epithelial cell populations during UC. Inflammation influenced the expression of several miRNAs in crypt-bottom (CD44⁺) cells compared to crypt-top (CD66a⁺) cells, potentially impacting cell proliferation, differentiation, and intestinal barrier integrity. Notably, let-7c-5p was significantly downregulated, while miR-501-3p was upregulated in crypt-bottom (CD44⁺) cells during active UC. Given previous findings that let-7c-5p overexpression and miR-501-3p inhibition reduce colorectal cancer cell proliferation [270, 271], their deregulation may contribute to the increased presence of crypt-bottom (CD44⁺) cells observed in the flow cytometry experiments. Additionally, during active UC, increased miR-1-3p and decreased miR-125b-5p expression was identified in crypt-bottom (CD44⁺) colonic epithelial cells relative to crypt-top (CD66a⁺) cells. Since miR-1-3p upregulation and miR-125b-5p downregulation have been linked to epithelial barrier dysfunction [172, 272], this suggests that barrier impairment is already present in crypt-bottom (CD44⁺) cells during active UC. However, it remains unclear whether this is a UC-specific phenomenon or a general inflammatory response in the gut, warranting further investigation through functional studies.

Next, this study also showed that some differentially expressed miRNAs in crypt-bottom (CD44⁺) and/or crypt-top (CD66a⁺) cells were linked to the endoscopic Mayo subscore. Among these, well-known anti-inflammatory

miRNAs [273] such as miR-223-3p, miR-146a-5p, miR-21-5p, and miR-31-5p stood out. Notably, miR-223-3p and miR-146a-5p are induced via the TLR-NF- κ B pathway [274], a key regulator of inflammation [275], explaining their association with disease activity. Additionally, miR-141-5p expression in crypt-bottom (CD44⁺) cells correlated with UC activity, aligning with its known role in UC pathogenesis through CXCL5 targeting [276]. Some negative correlations were also observed in this study. Specifically, the expression of let-7b-5p and let-7e-5p in crypt-bottom (CD44⁺) cells negatively correlated with the Mayo subscore, a pattern absent in crypt-top (CD66a⁺) cells. let-7b was among the most highly expressed miRNAs in the intestinal epithelium, and let-7e has been previously linked to cell differentiation [277]. These findings suggest that let-7 miRNAs influence intestinal inflammation by maintaining the stemness of crypt-bottom (CD44⁺) cells, explaining their exclusive correlation with disease activity in colonic epithelial cells that reside closer to crypt base.

Notably, correlation and weighted co-expression network analyses revealed that certain miRNAs not only associate with the endoscopic Mayo subscore but also form an inflammation-related expression network linked to the clinical disease activity. Among two identified miRNA co-expression modules in crypt-bottom (CD44⁺) and/or crypt-top (CD66a⁺) cells, module M1 was significantly enriched in both colonic epithelial cell populations of active UC patients. This module included miRNAs such as miR-31-5p, miR-135b-5p, miR-27a-3p, miR-222-3p, and miR-223-3p, which have been previously reported to be upregulated in inflamed, noninflamed, and precancerous colon tissues, as well as in UC patient faeces [148, 278–281]. These miRNAs are reported to be involved in inflammatory response regulation [169, 282], such as role of miR-222-3p in *SOCS1* inhibition and subsequent *STAT3* activation [283]. The results of the module M1 miRNAs analysis revealed that they also participate in interleukin signalling pathways by targeting genes like *CCND1*, *FOXO3*, *IGF1R*, *ICAM1*, *STAT6*, *STAT1*, and *STAT5A*. Interestingly, module M1 in colonic tissue resembled the pattern observed in crypt-top (CD66a⁺) cells, likely due to the abundance of absorptive colonocytes in the mucosal layer [91, 99]. In contrast, module M2 showed an inverse correlation with the Mayo subscore and was enriched exclusively in crypt-bottom (CD44⁺) cells of quiescent UC patients and included let-7e-5p (also discussed above), suggesting anti-inflammatory properties.

Finally, the Part I of this thesis also explored the role of differentially expressed miRNAs in key biological pathways. Initial small RNA-seq analysis of colonic mucosa biopsies from active and quiescent UC patients, compared to non-IBD controls, identified multiple deregulated miRNAs

significantly enriched in pathways related to inflammation and epithelial barrier function. Notably, miRNAs associated with IL-4 and IL-13 signalling were altered not only in active UC but also in quiescent cases, suggesting persistent dysregulation of this pathway. IL-4 and IL-13 are known to affect epithelial chloride secretion and barrier integrity [284, 285]. IL-13, in particular, is overproduced in UC mucosa, leading to apoptosis, tight junction disruption, and impaired restitution [286, 287]. While some studies report decreased IL-13 levels in pediatric active UC [288], clinical trials and pre-clinical studies on inhibition of IL-13 (e.g., tralokinumab and anrukinzumab [289], as well as anti-IL-R α 2 [290]) continue to explore its therapeutic potential. Further analysis in crypt-bottom (CD44⁺) and crypt-top (CD66a⁺) colonic epithelial cells revealed miRNA deregulation in UC, with targets again enriched in the IL-4 and IL-13 pathways. Since these cytokines are primarily produced by immune cells [291], miRNA regulation likely occurs at the level of downstream targets such as *FOXO3*, *SOCS1*, and *STAT3*, that were observed in this study as overrepresented genes in certain regulatory pathways. During active UC, crypt-bottom (CD44⁺) and crypt-top (CD66a⁺) cells showed upregulation of miR-31-5p, miR-182-6p, miR-221-3p, and miR-222-3p, all known to target *FOXO3* [251]. This suggests a potential reduction in *FOXO3* expression, which has already been observed in UC mucosa [292] and may contribute to more severe inflammation. Additionally, miR-21-5p and miR-221-3p, that target *SOCS1* [251] – a key regulator of IL-4 signalling [293] – were elevated in both studied colonic epithelial cell populations. *SOCS1* downregulation has been shown to enhance IL-13 signalling in human epithelial cells [294, 295], further implicating miRNA-mediated regulation in UC progression. Beyond interleukin signalling, this study identified epithelial barrier-related miRNA functions varying by health state and cell population. For example, in quiescent UC, miRNAs such as miR-15b-5p, miR-222-3p, and miR-223-3p in crypt-bottom (CD44⁺) cells may regulate nuclear receptors and extra-nuclear estrogen signalling, aligning with previous findings on nuclear receptor involvement in intestinal barrier functions such as expression of tight junctions and secretion of mucus [296]. Additionally, distinct miRNA expression patterns between crypt-bottom (CD44⁺) and crypt-top (CD66a⁺) cells in active UC suggest a role in epithelial cell migration, a process known to occur along the crypt-villus axis [297] and to be heightened in IBD [298]. While these findings highlight potential miRNA-driven regulatory mechanisms, caution is needed in interpreting GSEA results due to the limitations in miRNA target prediction, which remain unresolved challenge in the field [299].

In summary, Part I of this thesis identified miRNA deregulation in crypt-bottom (CD44⁺) and crypt-top (CD66a⁺) colonic epithelial cells in UC, revealing cell population- and health state-dependent expression patterns. It also uncovered distinct miRNA networks and their associations with endoscopic disease activity. Furthermore, the putative functional roles of differentially expressed miRNAs were explored, highlighting their potential involvement in biological pathways critical for maintaining intestinal barrier function in both active and quiescent UC. These findings underscore the regulatory significance of miRNAs in specific colonic epithelial cell populations during UC pathogenesis and suggest potential miRNA candidates for further functional evaluation in broader context of intestinal inflammation.

4.2. Part II. Gut microbiota profiling in faeces

Alterations in the gut microbiome are widely recognised as functionally significant, often overshadowing the potential roles of unaltered microbial taxa. Research has largely focused on microbiome shifts and their potential roles in UC pathogenesis, disease activity monitoring, and treatments like faecal microbiota transplantation. However, the contribution of the core microbiome – microbial groups that remain unchanged despite overall diversity loss in UC – remains unclear. Understanding both altered and unaltered microbial counterparts may provide deeper insights into their respective roles in disease progression and relapse. To address this, the second part of this thesis analysed the faecal microbiota composition in UC, assessing both its dysbiotic and preserved components to better understand their contributions to the disease environment.

The Part II of this thesis described UC-associated microbial characteristics. Initial analysis showed that significant reduction in faecal microbiota richness and diversity was a key feature of UC. This aligns with multiple recent studies that also repeatedly reported the impaired microbial balance in UC patients' stool and mucosa samples compared to healthy controls [191, 300, 301]. These independent studies associated reduced bacterial diversity with disease triggering and worsening dysbiosis in IBD patients, suggesting that diminished microbial diversity contributes to both the onset and progression of UC [108, 191, 300–302]. What is more, the results of the thesis Part II indicated that this microbial imbalance persists even in quiescent UC, indicating that microbial alterations continue despite clinical remission. This finding is concordant with other studies, that demonstrated that the gut microbiota in UC patients remains consistently stable, regardless of disease activity state or treatment adjustments [19, 303]. Reduced bacterial diversity in the gut microbiota has been mechanistically linked to intestinal inflam-

mation through several pathways, namely, loss of beneficial metabolites, expansion of pathobionts, and impaired gut barrier function [304, 305]. Subsequent differential abundance analysis in the study Part II uncovered additional layer of gut microbiota alterations in UC. Five bacterial genera such – *Alistipes*, *Paraprevotella*, *Mediterraneibacter*, *Coprococcus*, and *Cuneatibacter* – were identified to be less abundant in the faecal samples of UC patients compared to non-IBD individuals. The majority of these genera have also been reported by other studies as altered in IBD [306–309]. Although studies on these bacteria are limited and further research is needed to fully understand their roles in both human health and IBD, from the functional perspective, identified bacterial genera are known to contribute significantly to gut homeostasis mainly through SCFA production, such as butyrate and acetate [310, 311]. Multiple studies have reported that SCFAs, particularly butyrate, support intestinal barrier integrity by stabilising tight junction gene expression via hypoxia-inducible factor, inhibiting inflammatory pathways (TNF- α , IL-6, NF- κ B, Akt), and suppressing Th17 responses, thereby reducing inflammation and delaying disease progression [190, 312–314]. Therefore, reduced abundance of SCFA-producing bacteria can disrupt intestinal barrier function and immune regulation, potentially affecting the onset, progression and/or relapse of UC [76, 315, 316].

Since UC involves gut dysbiosis and impaired bacterial defence [198, 269], commensal microbiota may also influence the intestinal epithelium. Therefore, the research of this thesis extended to the analysis of shared core microbiome across UC patients and non-IBD individuals. Usually, the term commensal microbiota refers to the community of microorganisms residing within a host organism without causing harm and also playing essential roles in physiological processes [317]. Results of Part II of this thesis highlighted genera such as *Bacteroides*, *Collinsella*, *Faecalibacterium*, *Phocaeicola*, *Roseburia*, and *Sutterella*, as consistent bacterial genera in faeces. While *Bacteroides*, *Faecalibacterium*, *Phocaeicola*, and *Roseburia* were classified as core genera, previous studies have reported variations in their abundance in UC [189, 318, 319]. On the other hand, some studies suggested *Bacteroides* and *Roseburia* to persist across individuals with UC and non-IBD despite the inflammatory environment in UC and offer resilience against disease progression [320]. These discrepancies may stem from factors like demographics and dietary habits, as environmental influences largely shape the microbiome [321]. Overall, comparing our findings with other studies remains challenging since most focus on microbiome alterations rather than commonalities. Nevertheless, interest in the core unaltered microbiota subset and its potential role in UC is growing, as reflected in studies analysing the mecha-

nisms of action of commensal microbiota and its produced and/or secreted molecules [322, 323].

To conclude, Part II this thesis provided a comprehensive analysis of faecal microbiota composition in the context of UC. The findings not only identified disease-specific shifts in bacterial diversity, richness and genus abundance but also revealed microbial taxa that remain consistently abundant during disease progression. Despite their stability, these bacterial genera may contribute to UC pathogenesis through yet unexplored pathways.

4.3. Part III. Functional analysis of the impact of commensal bacteria on colonic epithelium using intestinal organoid system

In the third part of this thesis, functional studies assessing the potential effect of previously identified commensal microbiota on the colonic epithelium in both health and UC was conducted using state-of-the-art system – colonic epithelial organoid models. These experimental platforms enable a more physiological exploration of processes happening at the interface between the intestinal epithelium and gut microbiota [324].

Prior to functional testing, several technical aspects were addressed to gain a broader understanding of the characteristics of colonic epithelial organoid-based experimental system, specifically, its cellular composition and methylation dynamics. Intestinal organoids are considered a physiologically relevant system in terms of variety colonic epithelial cells, including absorptive cells (colonocytes or enterocytes, in large and small intestinal organoids, respectively), secretory goblet cells, Paneth cells (mostly in small intestinal organoids), enteroendocrine cells, proliferative cells being present and functionally active in the culture [200–202]. However, cell differentiation of stem cells into specific populations depends on culturing conditions and the availability of factors [202]. This highlights the need to characterise the cultures for major epithelial cell subpopulations to assess how well the established experimental system mimics the *in vivo* colonic epithelium. Thus, in the initial stage of Part III of this thesis, a qualitative characterization of cellular composition in organoids and their monolayers was performed. Resulting findings regarding the timing of colonic epithelial organoid formation, epithelial polarisation, and cellular composition align with previous studies that have also characterised *ex vivo* experimental models derived from adult human stem cells for investigating the intestinal system [220, 325]. Additionally, *in vitro* environment lacks key *in vivo* factors like gut microbiota and cellular signals [326], which may lead to molecular alterations during prolonged culturing. While genetic stability has been established [327], little is known about epigenetic regulation, particularly in IBD. There-

fore, LINE-1 methylation fluctuations in non-IBD organoids and tracked epigenetic changes in cultures from tissues of active and quiescent UC patients was performed as a second part of experimental system characterisation. LINE-1 was selected as a marker reflecting global methylation level due to its proportion in human genome which reaches up to 20% [328]. LINE-1 methylation across different colon sample types, from whole biopsies to crypt-derived epithelial organoids cultured over time was assessed. Consistently high methylation in colon tissue, isolated crypts, and early- and late-passage organoids from both non-IBD individuals and UC patients was found in this study. Notably, methylation was highest in non-IBD cultures, while active UC showed hypomethylation, aligning with previous findings on DNA methylation changes in UC [262, 329, 330]. Importantly, our analysis identified that prolonged colonic epithelial organoid culturing led to a decline in LINE-1 methylation, with a more pronounced reduction in non-IBD-derived organoids compared to UC samples. This highlights the importance of considering passage number when analysing epigenetic changes. While prior studies have examined genome-wide methylation in intestinal organoids – including both IBD and non-IBD cases, as well as adult and pediatric samples – there remains a lack of consensus in the literature on the methylation dynamics of these systems [208, 331, 332]. While some studies propose intestinal epithelial organoids as stable system maintaining intestinal site-specific profile [331, 332], others report significant culturing duration-related methylation profile shifts [208]. Our study uniquely tracked LINE-1 methylation as a surrogate for global DNA methylation throughout extended culture periods. Resulting findings suggested that LINE-1 methylation patterns differed between primary tissue and established organoids, with a diagnosis-dependent rate of decline. Given its consistency with global methylation trends [262, 329, 330], LINE-1 could serve as a useful biomarker for assessing epigenetic changes in colonic epithelial organoids.

After comprehensive evaluation of selected experimental system, representative unaltered commensal bacterial species were selected for functional testing, combining findings from Part II of this thesis with data reported in the literature. As a result, *E. coli* and *P. vulgatus* were chosen to investigate their interactions with colonic epithelial cells of both UC patients and non-IBD individuals. The selection of these species was based on two key factors, namely, the feasibility of culturing them using well-established protocols, including their compatibility with intestinal epithelial cell co-cultures, and their recognised roles as stable and abundant members of the human gut microbiota, with documented functional relevance in intestinal homeostasis and disease. From a technical standpoint, the ability to maintain and co-culture bacteria with epithelial cells was a decisive criterion. Many core gut

microbiota genera identified in the Part II of this thesis, such as *Roseburia*, *Romboutsia*, and *Anaerotignum*, are strict anaerobes [333–335], making their growth and handling in co-culture systems challenging. Furthermore, we opted for commercially available strains rather than patient-derived isolates, which further limited our selection. While both *E. coli* (non-pathogenic strain ATCC 252922) and *P. vulgatus* (ATCC 8482) require anaerobic conditions for optimal growth [336, 337], they can also adapt to conditions suitable for mammalian epithelial cells [224, 338], making them practical choices for co-culture experiments. Their ability to grow efficiently under controlled conditions allowed the systematic investigation of their impact on colonic epithelial function. Nevertheless, beyond technical considerations, both species are known to play important roles in the gut ecosystem. *E. coli*, in its non-pathogenic form, contributes to essential physiological functions such as vitamin K and B₁₂ synthesis and serves as a defense against pathogenic colonization [339]. However, its role in UC remains controversial [340]. Some studies suggest that specific probiotic strains, such as *E. coli* Nissle 1917, can effectively maintain UC remission [341], while others implicate *E. coli* in the disease process by promoting inflammation and epithelial dysfunction [342, 343]. Similarly, *P. vulgatus* has been reported to have both protective and detrimental effects in the context of UC. On the one hand, studies have shown that *P. vulgatus* proteases may contribute to epithelial barrier dysfunction [319], a key feature of UC pathogenesis [344]. Conversely, some experimental models have demonstrated that *P. vulgatus* can attenuate DSS-induced colitis symptoms in mice [345], indicating a potentially beneficial role under certain conditions.

Finally, to explore how specific core microbiota constituents influence the homeostasis of colonic epithelium in UC patients and non-IBD individuals, co-culturing experiments were performed using bacteria and intestinal organoid monolayers. Initially, cellular gene expression analysis uncovered response differences between UC patients and non-IBD individuals. Assessment of gene expression changes in epithelial cell markers related to bacterial interaction and effects – *TLR4* (pathogen recognition) [346], *TJPI* (tight junction integrity) [347], and *HSPA1A/HSPB1* (cellular stress response) [348] – uncovered differential epithelial responses in UC and non-IBD colonic epithelial cells. Notably, *TJPI* expression showed a tendency to differ between UC- and non-IBD-derived monolayers exposed to *E. coli* and *P. vulgatus*, suggesting inverse trends in tight junction regulation, though these differences did not reach statistical significance. We hypothesise that this variability may be attributed to patient-specific responses, as the experimental system was derived from individual patient samples [349]. This was also followed by non-significant cellular stress and pathogen recognition

responses in either culture. These findings may be linked to previously reported mechanisms, such as *P. vulgatus*-mediated epithelial barrier disruption via proteolytic activity [319]. Additionally, studies suggest that mucosa-associated *E. coli* expansion in UC allows interaction with surface epithelial cells without direct invasion, potentially triggering inflammatory responses that compromise the epithelial barrier [350]. Conversely, other studies highlight the beneficial role of commensal *E. coli* in colonic epithelial cell recovery, associating it with the expression of G-protein-coupled chemo-attractant family receptor FRP2 in epithelial cells [351]. Moreover, the gene expression fluctuations detected in Part III of this thesis further emphasise the potential importance of IBD-related genetic predisposition in shaping cellular responses to bacterial interactions [184], such as polymorphisms or variants of genes coding receptors involved in the recognition of microbe/ pathogen-associated molecular patterns such as *TLR2*, *TLR4*, *TLR5*, *TLR9*, or *NOD1*, *NOD2* (with the last two genes more relevant in the context of Crohn's disease) [352–357]. Overall, given the conflicting literature on *P. vulgatus* and *E. coli* in UC, these observations highlight the complexity of host-microbiota interactions and suggest that the functional impact of these bacteria may depend on disease status, environmental factors, or microbial strain-specific properties.

Colonic epithelial cell responses to commensal bacteria strains were also evaluated in terms of miRNA expression and EV-mediated secretion to gain deeper insights into potential mechanisms underlying UC. The discovery that miRNAs can stimulate rather than repress mitochondrial genome-encoded transcripts provided a theoretical framework for a potential interplay between miRNAs and commensal gut bacteria [358]. This connection arises from the fact that miRNAs are secreted via faecal exosomes from intestinal epithelial cells, and widely accepted theory that mitochondria evolved from bacteria [359]. Also, recent studies have demonstrated correlations between faecal miRNA levels and gut microbiota composition [360, 361], while *in vitro* experiments indicated that certain host-derived miRNAs can enter bacterial cells and selectively promote the growth of specific strains, further supporting the hypothesis that miRNAs may play a role in shaping gut microbiota composition [16]. Building on this context, the third part of this thesis focused on evaluating three UC-associated miRNAs in the cellular and EVs compartments of colonic epithelial monolayers following incubation with *E. coli* or *P. vulgatus*. The selection of these miRNAs was based on their potential to interact with bacteria by targeting bacterial genes. However, no significant alterations miRNA expression or their secretion via EVs were observed in co-cultures. Notably, *P. vulgatus* induced only minimal miRNA expression shifts in both cells and EVs across UC and non-IBD-derived cultures, sug-

gesting a limited impact of this bacterium on intestinal homeostasis at the miRNA level. This observation aligns with previous findings suggesting that *P. vulgatus*, while a stable gut microbiota constituent, may not be a primary driver of UC-associated inflammatory responses [362]. In contrast, *E. coli* exhibited a distinct influence, particularly in UC-derived epithelial cells. Specifically, *E. coli* showed a tendency to upregulate UC-associated miRNAs – miR-183-5p, miR-135b-5p, and miR-146a-5p – in both colonic epithelial cells and EVs of UC patient cultures, whereas miRNA expression changes in non-IBD cultures were less consistent. These miRNAs have been implicated in inflammation and epithelial barrier regulation [363, 364], suggesting that *E. coli* may play a role in exacerbating UC-related epithelial responses. While further studies are needed to determine whether this miRNA modulation contributes to barrier dysfunction or immune signalling alterations, our findings support a complex regulatory network in which host-derived miRNAs contribute to host-microbiota interactions, with potential implications for gut homeostasis and disease pathogenesis. Overall, the Part III of this thesis underscores the importance of considering both bacterial strain-specific effects and host conditions when evaluating gut microbiota interactions with the intestinal epithelium.

To summarize, Part III of this thesis characterised colonic epithelial organoid models, assessing their cellular composition and methylation dynamics while highlighting the impact of prolonged culturing on DNA methylation in UC and non-IBD samples. *E. coli* and *P. vulgatus* were then selected for functional testing based on their stability and suitability for co-culture. Co-culture experiments revealed their differential effects on tight junction maintenance and miRNA expression, with *E. coli* more strongly influencing UC-associated miRNAs in colonic epithelial cells and EVs. These findings highlight the complex interplay between host miRNAs and gut microbiota, warranting further investigation into their role in UC pathogenesis.

4.4. Summary

This thesis explored the intricate relationship between colonic epithelial miRNAs, gut microbiota, and the intestinal epithelium in UC, aiming to better understand their roles in disease manifestation. By integrating miRNA expression profiling, gut microbiota characterization, and functional studies using colonic epithelial organoids, this work provides new insights into how epithelial regulatory mechanisms and microbial interactions contribute to UC pathogenesis.

In Part I, miRNA expression analysis revealed cell-type-specific regulatory patterns in crypt-bottom (CD44⁺) and crypt-top (CD66a⁺) colonic epithelial cells during UC, highlighting key inflammatory and barrier-related miRNAs. Several dysregulated miRNAs, including miR-31-5p, miR-135b-5p, miR-223-3p, and miR-146a-5p, correlated with endoscopic disease activity and were enriched in pathways involved in intestinal barrier integrity, immune signalling, and epithelial differentiation. Notably, miR-135b-5p and miR-146a-5p, which were later explored in thesis Part III, were also previously identified as regulators of epithelial inflammation and host-microbiota interactions [365–368], supporting the hypothesis that their dysregulation may contribute to barrier dysfunction and chronic inflammation in UC. Additionally, let-7c-5p downregulation and miR-501-3p upregulation in crypt-bottom (CD44⁺) cells suggest a role in proliferation and impaired differentiation [270, 271, 277], which may exacerbate epithelial damage in UC. Given that miRNAs such as miR-135b-5p, and miR-146a-5p, miR-183-5p were later implied to be modulated by commensal bacteria in thesis Part III, these findings suggest a potential regulatory network linking epithelial miRNAs and microbial interactions.

Part II focused on the gut microbiota composition in UC, emphasising not only microbial diversity loss and dysbiosis but also the persistence of core bacterial genera despite inflammation. While previous research has primarily focused on microbial shifts, this study highlights that unaltered commensal bacteria may still play critical roles in intestinal homeostasis and immune regulation [369]. Not only the genera found to be depleted in UC, but also many of the identified core genera, including *Faecalibacterium*, *Roseburia*, and *Bacteroides*, are known SCFA producers, crucial for intestinal epithelial health, tight junction maintenance, and anti-inflammatory signalling [310, 311, 316]. These findings align with emerging research suggesting that specific microbial species may either worsen or alleviate UC symptoms by influencing epithelial function [370]. Given that association between gut bacteria and host miRNAs exists [16, 360, 361], the study Part III further aimed to check the functional impact of *E. coli* and *P. vulgatus* – stable members of the microbiota regardless the UC – on intestinal epithelium and its miRNA levels.

To investigate direct host-microbiota interactions, Part III employed colonic epithelial organoid models to functionally assess the impact of *E. coli* and *P. vulgatus* on epithelial regulation. These models confirmed that epithelial cells remain functionally active *in vitro*, though prolonged culture induced slight epigenetic modifications, such as LINE-1 methylation changes, which should be considered in experimental designs. Co-culture experiments implied that *E. coli* exhibited a stronger effect on epithelial gene

expression and tight junction regulation, as well as UC-associated miRNA expression and secretion, particularly affecting miR-183-5p, miR-135b-5p, and miR-146a-5p. The observed upregulation tendency of miR-135b-5p and miR-146a-5p in UC epithelial cells suggests that *E. coli* may compromise barrier function and potentiate immune activation, consistent with its previously reported effects on epithelial integrity [367, 368, 371]. In contrast, *P. vulgatus* showed minimal effects on miRNA expression, supporting previous observations that its role in UC remains ambiguous, potentially strain- or environment-dependent [362, 372]. These results reinforce the idea that host-derived miRNAs may not only be markers of UC [368] but also active regulators of microbial-epithelial interactions [373], potentially influencing disease progression and therapeutic outcomes.

Together, Part I–III of this thesis underscore the potential role of miRNAs and gut microbiota in regulating the colonic epithelium and their collective impact on UC pathogenesis. The findings demonstrate that epithelial miRNAs play a key role in barrier maintenance and immune signaling, while commensal bacteria taxa can modulate these regulatory networks, further shaping epithelial responses. Importantly, the functional interplay between miRNAs and stable gut microbiota suggests a multilayered mechanism in UC pathogenesis, where host and microbial factors dynamically interact. Future research should further explore these host-microbiota regulatory networks, as targeting miRNA-mediated microbial interactions may open novel therapeutic and diagnostic strategies for UC.

CONCLUSIONS

- 1.1. The number of differentially expressed microRNAs in colonic tissue increased progressively with the activity of ulcerative colitis, with 19 microRNAs being specific to quiescent ulcerative colitis and 80 microRNAs uniquely dysregulated in active ulcerative colitis. miR-1-3p showed a gradual decrease in expression from non-IBD to quiescent ulcerative colitis and further to active disease.
- 1.2. Ulcerative colitis-associated tissue microRNAs were involved in interleukin pathways, particularly interleukin-4 and interleukin-13 signalling. A gradual increase in *IL-13* expression across ulcerative colitis states has been confirmed, while *IL-4* levels remained unchanged. *IL-4* and *IL-13* signalling-related genes were broadly expressed across epithelial and immune cell populations, with potential expression changes in active ulcerative colitis.
- 2.1. The extent of microRNA dysregulation correlated with ulcerative colitis activity in both crypt-top and crypt-bottom colonic epithelial cells, with 15 microRNAs being specific to crypt-top and 15 microRNAs to crypt-bottom cells in quiescent ulcerative colitis, whereas 29 microRNAs being dysregulated in crypt-top and 38 microRNAs in crypt-bottom cells in active ulcerative colitis. These microRNAs in both cell populations likely contributed to interleukin signalling and other signal transduction pathways involved in ulcerative colitis pathogenesis.
- 2.2. Differentially expressed microRNAs between crypt-top and crypt-bottom colonic epithelial cells were specific to health status, with 24 identified in active ulcerative colitis, 9 in quiescent ulcerative colitis, and 22 in non-IBD. Regardless of ulcerative colitis activity, these microRNAs were associated with inflammatory processes and the maintenance of intestinal epithelial barrier integrity through their target-genes.
- 2.3. Two distinct microRNA co-expression modules were identified in colonic epithelial cells. The M1 module, consisting of 13 microRNAs, was associated with active ulcerative colitis and was enriched in both crypt-top and crypt-bottom cells. The M2 module, comprising 11 microRNAs, was linked to quiescent ulcerative colitis and was predo-

minantly expressed in crypt-bottom cells. The expression of M1 module correlated with endoscopic disease activity and effectively distinguished patients with quiescent disease from those with active ulcerative colitis.

3. Ulcerative colitis patients had a decreased faecal bacteria α - and β -diversity, along with a significant depletion of genera *Alistipes*, *Coprococcus*, *Cuneatibacter*, *Mediterraneibacter*, *Paraprevotella*. A core group of 27 bacterial genera remained unchanged across all three study groups (active ulcerative colitis, quiescent ulcerative colitis, and non-IBD), with *Phocaeicola* and *Escherichia/Shigella* consistently abundant in all participants.
- 4.1. The commensal core bacteria *Escherichia coli* and *Phocaeicola vulgatus* did not induce significant changes in the expression of colonic epithelial cell gene markers associated with bacterial recognition, cellular stress, or tight junction integrity (*TLR4*, *HSPA1A*, *HSPB1*, and *TJPI*). However, both bacteria showed a trend toward increasing *TJPI* expression in colonic epithelial cells from non-IBD individuals, whereas in cells of ulcerative colitis patients, they tended to decrease *TJPI* expression.
- 4.2. *Escherichia coli* and *Phocaeicola vulgatus* did not significantly alter candidate microRNA expression. However, *Escherichia coli* tended to increase miR-183-5p, miR-135b-5p, and miR-146a-5p expression in colonic epithelial cells and extracellular vesicles of ulcerative colitis patients, while in non-IBD controls, it increased miR-146a-5p but decreased miR-183-5p and miR-135b-5p expression. *Phocaeicola vulgatus* tended to reduce miR-183-5p and miR-135b-5p levels only in extracellular vesicles of both groups.

SANTRAUKA

Įvadas

Opinis kolitas (OpK) – tai lėtinė uždegiminė storosios žarnos liga (UŽL), pasižyminti augančiu sergamumo dažniu bei paūmėjimų ir remisijų epizodais, dėl kurių mažėja ir sergančiųjų gyvenimo kokybė [1]. Yra žinoma, kad OpK patogenezę lemia sudėtinga sąveika tarp epitelinio barjero disfunkcijos, imuninės sistemos reguliacijos sutrikimų, žarnyno mikrobiotos pokyčių, genetinio polinkio ir aplinkos veiksnių [2]. Vis dėlto, nepaisant intensyvių mokslinių tyrimų, vis dar nėra aišku, kaip konkretūs molekuliniai storosios žarnos epitelio ir žarnyno mikrobiotos pokyčiai bei jų tarpusavio sąveika funkciškai prisideda prie OpK pasireiškimo ir progresavimo.

Žarnyno epitelis veikia kaip esminis barjeras tarp šeimininko imuninės gynybos ir žarnyno spindyje esančių mikroorganizmų, ir atlieka pagrindinį vaidmenį palaikant žarnyno homeostazę [3]. Sergant OpK, šis barjeras yra stipriai sutrikdomas, dėl ko padidėja pralaidumas, vyksta mikroorganizmų translokacija ir nuolatinis imuninės sistemos aktyvinimas, palaikantis lėtinį uždegimą [4, 5]. Tokios storosios žarnos epitelinės ląstelės kaip kolonocitai, taurinės (goblet) ląstelės ir žarnyno kamieninės ląstelės atlieka esminį vaidmenį palaikant barjerinę funkciją ir užtikrinant gleivinės apsaugą [4, 6]. Epitelio funkcijos sutrikimai, tokie kaip sumažėjusi gleivių sekrecija ar sutrikusi tarpląstelių glaudžiųjų jungčių struktūra, prisideda prie užsitęsusio uždegimo ir sunkesnės ligos eigos [7]. Kadangi vienas svarbiausių OpK gydymo tikslų yra pasiekti ilgalaikę remisiją ir ją palaikyti, atkuriant gleivinės barjerą [8], būtina giliau suprasti molekulinis reguliatorius, kontroliuojančius epitelinio barjero funkciją. Tarp šių reguliatorių mikroRNR (miRNR) tyrinėjamos kaip esminiai žarnyno epitelio homeostazės dalyviai – jos reguliuoja genų tinklus, susijusius su žarnyno barjero vientisumu, imuniniais signalais ir epitelio atsinaujinimu [9].

Naujausi duomenys rodo, kad miRNR reguliuoja žarnyno pralaidumą [10, 11], tačiau dauguma tyrimų buvo atlikti naudojant bendros audinių masės (angl. *bulk*) analizę ar immortalizuotas ląstelių linijas [12, 13], todėl vis dar trūksta informacijos apie ląstelių tipui specifines miRNR. Iki šiol atliktų tyrimų pobūdis riboja galimybę tiksliai suprasti, kaip miRNR raiška skiriasi tarp skirtingų epitelinių ląstelių populiacijų OpK metu. Atsižvelgiant į tai, kad anatomiškai skirtingose žarnos kriptų vietose esančios epitelinės ląstelės atlieka skirtingas funkcijas barjero palaikyme ir atsinaujinime [6, 14], jų miRNR raiškos ypatumų nustatymas gali atskleisti naujus reguliacinius kelius, susijusius su OpK patogenezė. Be to, miRNR nėra tik viduląsteliniai

regulatoriai – jos išskiriamos į žarnyno spindį [15], kur gali daryti poveikį ir mikrobiotai [16, 17]. Tai kelia esminių klausimų apie dvikryptę sąveiką tarp epitelinių miRNR ir žarnyno mikrobiotos bei galimą jų įtaką ligos progresavimui ar remisijai.

Be epitelinių miRNR pokyčių, žarnyno mikrobiotos sudėtis taip pat atlieka svarbų vaidmenį OpK patofiziologijoje [18, 19]. OpK dažnai siejamas su sumažėjusia mikrobiotos įvairove ir uždegimą skatinančių bakterijų gausėjimu, tačiau tam tikros komensalinės bakterijų grupės išlieka stabilios nepaisant ligos eigos [20, 21]. Šių stabiliai egzistuojančių mikroorganizmų funkcinė reikšmė, ypač jų įtaka epitelio barjero vientisumui, iki šiol išlieka mažai ištirta. Nors disbiozė yra gerai dokumentuota, tų bakterijų, kurios išlieka nepaisant ligai būdingų mikrobiotos pokyčių, identifikavimas gali suteikti naujų įžvalgų apie šeimininko ir mikrobiotos sąveiką. Šios komensalinės bakterijos gali turėti dar neatskleistą vaidmenį reguliuojant epitelio atsakus ir imuninę homeostazę, galbūt kontroliuodamos ligos eigą.

Storosios žarnos epitelio miRNR raiškos, žarnyno mikrobiotos sudėties ir stabilumo sąveikos supratimas bei jų bendras poveikis gali suteikti vertingų įžvalgų apie OpK patogenezę ir galimas terapines strategijas. Kadangi OpK gydymas dažniausiai nukreiptas į imuninę sistemą [22], epitelio atsakų ir mikrobiotos dinamikos moduliavimas tampa perspektyvia naujų intervencijų kryptimi. Molekulinių, mikrobiologinių ir epitelinių OpK aspektų sujungimas gali pasitarnauti būsimam biožymenų atradimui bei atverti kelią mikrobiota ar molekuliniiais mechanizmais paremtų gydymo strategijų, skirtų atkurti žarnyno barjero vientisumą ir pasiekti ilgalaikę OpK remisiją, kūrimui.

Darbo tikslas ir uždaviniai

Šio darbo tikslas – ištirti storosios žarnos epitelio mikroRNR ir žarnyno mikrobiotos vaidmenį opinio kolito patogenezėje.

Uždaviniai:

1. Nustatyti su opiniu kolitu susijusius mikroRNR raiškos profilius storosios žarnos audiniuose ir įvertinti šių molekulių vaidmenį signaliniuose keliuose.
2. Charakterizuoti opiniam kolitui būdingus mikroRNR raiškos profilius storosios žarnos kriptų viršuje ir dugne esančių epitelinių ląstelių populiacijose bei įvertinti jų klinikinę reikšmę.
3. Nustatyti su opiniu kolitu susijusius išmatų mikrobiotos pokyčius ir identifikuoti bakterijų gentis, kurių gausumas ligos eigoje nesikeičia.

4. Naudojant žarnyno organoidų modelį, įvertinti komensaliųjų bakterijų poveikį storosios žarnos epitelinėms ląstelėms opinio kolito pacientų ir kontrolinėje nesergančiųjų uždegimine žarnyno liga grupėse.

Darbo naujumas ir aktualumas

Šis darbas pateikia naujus įrodymus apie (1) miRNR raiškos pakitimus skirtingose storosios žarnos epitelinių ląstelių populiacijose sergant OpK – tai pirmasis darbas, kuriame tiriami kriptų viršutinės ir dugno dalies ląstelių miRNR profiliai, taikant mažųjų RNR sekoskaitą, identifikuojant ląstelėms specifinę molekulių raišką ir atskleidžiant jų ryšį su klinikinėmis charakteristikomis; (2) komensaliųjų bakterijų ir su OpK susijusios išmatų mikrobiotos sudėtį, išryškinant stabilios bakterijų bendruomenės galimą vaidmenį ligos progresavime; (3) komensaliųjų mikroorganizmų sąveiką su skirtingos kilmės epitelinėmis ląstelėmis (OpK ir nesergančių UŽL (ne-UŽL)), atskleidžiančius reguliacinę stabilios mikrofloros komponentų įtaką žarnyno barjerui; (4) šiuolaikinės, pažangios *ex vivo/in vitro* tyrimų sistemos – storosios žarnos epitelinių organoidų – taikymą, leidusį generuoti ligai reikšmingus rezultatus; (5) organoidų sistemos epigenetinio stabilumo analizę – tiriant bendro metilinimo lygio dinamiką ilgalaikėse OpK pacientų ir ne-UŽL asmenų epitelinių organoidų kultūrose.

Apibendrinant, šis darbas prisideda prie gilesnio molekulinio mechanizmo, slypinčių už OpK patogenezės, supratimo. Gauti rezultatai suteikia naujų žinių apie ligai specifinius epitelinius ir mikrobiologinius procesus. Todėl šie duomenys ne tik praturtina supratimą apie OpK, bet ir sudaro pagrindą būsimiems biožymenų paieškos tyrimams bei mikrobiotos ar molekulinio pagrindu grįstų terapijų kūrimui.

Medžiagos ir metodai

Siekiant įvertinti storosios žarnos epitelio miRNR ir žarnyno mikrobiotos vaidmenį opinio kolito patogenezėje, buvo išskirtos trys tyrimo dalys:

- **I dalis:** miRNR raiškos profiliavimas storosios žarnos audinyje ir epitelinių ląstelių populiacijose.
- **II dalis:** žarnyno mikrobiotos profiliavimas išmatose.
- **III dalis:** funkcinė komensaliųjų bakterijų poveikio storosios žarnos epiteliumi analizė, naudojant žarnyno organoidų sistemą.

Tyrimas atliktas vadovaujantis Kauno regioninio biomedicininų tyrimų etikos komiteto suteiktais leidimais (protokolo Nr. BE-2-10, išduotas 2011-03-08, ir protokolo Nr. BE-2-31, išduotas 2018-03-22). Tyrimo I–III dalys buvo vykdomos su šešiomis nepriklausomomis kohortomis (tyrimo kohortos I–VI), į kurias įtraukti tiek OpK pacientai, tiek kontroliniai (ne-UŽL) asmenys. Visi asmenys pasirašė informuoto sutikimo formą, patvirtinančią jų dalyvavimą tyrime. I dalyje iš tyrimo I–III kohortų buvo surinkti 324 storosios žarnos biopsijų mėginiai. Dvi iš šių kohortų ($n = 76$ [kohorta I] ir $n = 48$ [kohorta III]) buvo naudojamos mažųjų RNR sekoskaitai audinių ir epitelinių ląstelių populiacijų lygmenyse. Biologiniai mėginiai iš kohortos II ($n = 200$) buvo naudojami taikininei genų raiškos analizei taikant atvirkštinės transkripcijos kiekybinę polimerazės grandininę reakciją (AT-kPGR). II dalyje 72 išmatų mėginiai iš tyrimo kohortos IV buvo naudojami bakterijų 16S ribosominės RNR (16S rRNR) geno sekoskaitai. III dalyje iš viso buvo panaudoti 36 storosios žarnos biopsijų mėginiai iš kohortų V ir VI. Tyrimo kohorta V ($n = 19$) buvo skirta trimačių (3D) storosios žarnos epitelinių organoidų pirosekoskaitai, o kohorta VI ($n = 17$) – funkciniam storosios žarnos epitelio ir bakterijų testavimui naudojant iš 3D organoidų iškultivuotus epitelinius monosluoksnius.

I dalis. Siekiant ištirti žarnyno žarnos miRNR ir žarnyno mikrobiotos vaidmenį OpK patogenezėje, buvo atliktas miRNR raiškos profiliavimas storosios žarnos audiniuose ir epitelinių ląstelių populiacijose. Biopsijos iš tiriamųjų kohortų I–II buvo užšaldytos arba (kohorta III) disocijuotos į pavienių ląstelių suspensijas. Epitelinės ląstelės buvo rūšiuotos fluorescencija-aktyvuotų ląstelių rūšiavimo (FACS) metodu pagal paviršinius žymenis, identifikuojant dvi populiacijas: kriptų dugne ($CD45^-/EpCAM^+/CD44^+/CD66a^-$) ir kriptų viršuje esančias ($CD45^-/EpCAM^+/CD44^+/CD66a^+$) ląsteles, naudojant *CyFlow Space (Sysmex Partec)* ląstelių rūšiuotuvą. Iš gautų mėginių buvo išskirta visuminė RNR, jos kokybė įvertinta spektrofotometriškai (*NanoDrop 2000, Thermo Fisher Scientific*) arba fluorimetriškai (*Qubit 4, Invitrogen, Thermo Fisher Scientific*) bei bioanalizatoriumi *Agilent 2100 (Agilent Biotechnologies)*. *IL-4* ir *IL-13* genų raiška audiniuose analizuota AT-kPGR metodu, naudojant komercinius *TaqMan* pradmenis ir zondus bei *7500 Fast Real-Time PCR System (Applied Biosystems)* analizatorių. Kopijinės DNR sintezė PGR reakcijai atlikta naudojant *High-Capacity cDNA Reverse Transcription Kit (Thermo Fisher Scientific)* rinkinį. Raiškos duomenys normalizuoti pagal *GAPDH* geno raišką ir tarp grupių palyginti taikant $2^{-\Delta\Delta Ct}$ metodą. Statistinė analizė atlikta R (v4.0.3) aplinkoje, skirtumai tarp grupių laikyti reikšmingais, kai $p < 0,05$ (*Mann–Whitney U* testas). Audinių ir ląstelių populiacijų mažųjų RNR sekoskaitos bibliotekos paruoštos atitinkamai su *TruSeq Small RNR Sample Preparation Kit (Illumina)* ir

NEXTFLEX Small RNA-seq Kit v.3 (Bioo Scientific) rinkiniais bei sekvenuotos *HiSeq 4000 (Illumina)* platformoje. Pirminė sekoskaitos duomenų analizė (nuskaitymų matricos sugeneravimas) atlikta naudojant *nf-core/smrnaseq v1.0.0* analizės eigos algoritmą. Antrinė analizė vykdyta R (v4.0.3) aplinkoje. Analizė atlikta su duomenimis, kuriems pirmiausia pritaikyta variaciją stabilizuojančia transformacija pagrįsta miRNR nuskaitymų normalizacija. Diferencinės raiškos analizė atlikta su *DESeq2* paketu, taikant korekciją pagal amžių ir lytį, miRNR raiška laikyta reikšmingai pakitusia, kai Benjamini-Hochberg metodu koreguota p vertė (FDR) < 0,05 ir absoliutus raiškos pokytis kartais logaritminėje skalėje ($|\log_2PK|$) > 1. miRNR genų taikinių rinkinio praturtinimo analizė (angl. *Gene set enrichment analysis*, GSEA) atlikta su validuotų miRNR genų taikinių, ekspresuojamų storosios žarnos audiniuose arba epitelinių ląstelių populiacijose, sąrašu (sugeneruotu, remiantis viešai prijamu RNR sekoskaitos duomenų rinkiniu; GEO kodas: GSE116222) bei *Reactome* duomenų baze ir *Gene Ontology* (GO) kategorijomis. Taip pat atlikta daugiamačių skalių analizė (angl. *Multidimensional scaling analysis*, MDS), Spirmeno koreliacinė analizė tarp miRNR raiškos ir endoskopinio Mayo balo, svertinė genų ko-ekspresijos tinklo analizė (angl. *Weighted gene co-expression network analysis*, WGCNA) atlikta su *CEMiTool* paketu, AUC-ROC įverčiai apskaičiuoti su *pROC* paketu. Su interleukino (IL)-4 ir IL-13 signaliniu keliu susijusių genų raiška storosios žarnos ląstelių populiacijose buvo analizuota naudojant jau minėtą viešai prieinamą sekoskaitos duomenų rinkinį (GEO kodas: GSE116222).

II dalis. Žarnyno mikrobiotos analizė atlikta su IV kohortos išmatų mėginiais, surinktais ir užšaldytais –80 °C temperatūroje. Dalyviai, vartoję antibiotikus per 30 dienų iki tyrimo, į tyrimą buvo neįtraukti. Visuminė DNR išgryninta naudojant *AllPrep PowerFecal DNA/RNA (Qiagen)* rinkinį, koncentracija įvertinta *Qubit 4 (Invitrogen, Thermo Fisher Scientific)* fluorimetru. Bakterijų 16S rRNR geno V1–V2 sritis pagausinta naudojant universalius 27F/338R pradmenis, bibliotekos sekvenuotos *MiSeq (Illumina)* platformoje (2 × 300 bp). Duomenys analizuoti R (v4.0.3) aplinkoje su *DADA2* (v1.10) paketu, taikant kokybės filtravimą ir ampliconų sekų variantų (angl. *Amplicon sequence variant*, ASV) anotaciją pagal RDP (v18) duomenų bazę. Mėginiai suvienodinti taikant išretinimą (angl. *rarefaction*), pašalinant retus ASV. α -įvairovė įvertinta naudojant *Chao1*, *Simpson* ir *Shannon* rodiklius, o β -įvairovė – *Bray–Curtis* rodiklį, taikant *PERMANOVA* testą. Šerdine mikrobiota laikytos taksonų grupės, sudarančios $\geq 0,1$ proc. gausumo ≥ 50 proc. mėginių. Diferencinė gausumo analizė atlikta *Mann–Whitney U* testu, taikant *Benjamini–Hochberg* korekciją (FDR < 0,05). Vizualizacijos atliktos naudojant *microViz* paketą.

III dalis. Iš storosios žarnos biopsijų (kohortos V ir VI) buvo išauginti 3D epiteliniai organoidai, naudojant *Matrigel* (*Corning*) ekstraląstelinį matriksą ir *IntestiCult* žmogaus organoidų augimo terpę (*StemCell Technologies*). Diferencijuoti epiteliniai monosluoksniai buvo gauti organoidus disocijavus į pavienes ląsteles ir užsėjus 5×10^5 ląstelių ant I tipo kolagenu (*Gibco, Thermo Fisher Scientific*) dengtų ląstelių kultūrų plokštelių dugno ir jas kultivuojant su *IntestiCult* žmogaus organoidų diferenciacijos terpę (*StemCell Technologies*). Pirmiausia, morfologija ir žymenų raiška įvertinta naudojant šviesinę ir (imuno)fluorescencinę mikroskopiją (*Axio Observer 7, ZEISS*), pasitelkiant fluorochromais žymėtus antikūnus, nukreiptus prieš β -kateniną, F-aktiną, ZO-1, Citokeratiną 20, Muciną 2, Ki67, Chromograni- ną A, bei *Hoechst 33342* (*Invitrogen, Thermo Fisher Scientific*) dažą. Tolesniame charakterizavimo etape bendro DNR metilinimo lygis 3D organoi- duose tirtas pirosekoskaitos metodu, taikant bisulfitinę konversiją (*Methyl- Code, Thermo Fisher Scientific*), LINE-1 fragmento amplifikaciją (*PyroMark PCR Kit, Qiagen*) ir analizę *PyroMark Q24* (v2.0.8, *Qiagen*) programa. Vertintos trijų CpG vietų metilinimo reikšmės. Statistinė analizė atlikta R (v4.0.3) aplinkoje, skirtumai tarp grupių laikyti reikšmingais, kai $p < 0,05$ (*Mann–Whitney U* testas). Bakterijos ir miRNR funkciniais eksperimentams buvo pasirinktos pagal iš anksto nustatytus kriterijus. Kriterijus atitiko *Escherichia coli* (*E. coli*) ir *Phocaeicola vulgatus* (*P. vulgatus*) bei aktyvaus OpK metu kriptų viršuje esančiose epitelinėse ląstelėse padidėjusios raiškos miRNR ($\log_2PK > 1,5$, $FDR < 0,05$), turinčios teorinių taikinių pasirinktų bakterijų genomuose. Taikiniai *in silico* buvo identifikuoti naudojantis *TargetRNA2* (v2.01) atviros prieigos įrankiu. Storosios žarnos epitelinių monosluoksninių kultūrose su pasirinktais bakterijų štamais – *E. coli* ATCC 25922 ir *P. vulgatus* ATCC 8482 – buvo naudojami 100 proc. padengimo, 5 dienas diferencijuoti monosluoksniai. Paruoštos bakterijų suspensijos (2×10^6 /šulinėlyje, siekiant užtikrinti infekcijos santykį, lygų 1–2) inkubuotos su ląstelėmis 2 val. diferenciacijos terpėje be antibiotikų. Po inkubacijos ląstelės nuplautos, terpė pakeista į diferenciacijos terpę su penicilinu/streptomycinu (*Gibco, Thermo Fisher Scientific*), inkubuota 24 val. Po inkubacijos buvo surinktos ląstelių terpės ir lizatai. Ekstraląstelinės pūslelės (angl. *extracellular vesicles*, EV) iš ląstelių terpių izoliuotos naudojant *Total Exosome Isolation* reagentą (*Invitrogen*), jų dydis įvertintas *ZetaSizer Nano ZS* (mode- lis ZEN3500, *Malvern Panalytical*) sistema, EV žymenys (CD63, HSP70, ApoA1) baltymo lygmeniu – *ELISA* metodu, naudojant komercinius *Invitro- gen* (*Thermo Fisher Scientific*) rinkinius pagal gamintojo rekomendacijas. Visuminė RNR iš ląstelių išgryninta *AllPrep DNA/RNA Micro Kit* (*Qiagen*), iš EV – *Single Cell RNA Purification Kit I* (*Norgen*) rinkiniais, kiekybinis RNR įvertinimas atliktas *Qubit 4* (*Invitrogen, Thermo Fisher Scientific*)

fluorimetru. miRNR raiškos analizei kopijinės DNR sintezė atlikta naudojant *TaqMan MicroRNA Reverse Transcription Kit* (*Applied Biosystems, Thermo Fisher Scientific*) ir specifinius *TaqMan* (*Applied Biosystems, Thermo Fisher Scientific*) pradmenis ir zondus. Genų raiškos analizei kopijinės DNR sintezė atlikta naudojant *High-Capacity cDNA Reverse Transcription Kit* (*Thermo Fisher Scientific*) rinkinį. miRNR raiška įvertinta tikrojo-laiko PGR metodu, naudojant komercinius *TaqMan* pradmenis ir zondus bei *7500 Fast Real-Time PCR System* (*Applied Biosystems*) analizatorių. Genų raiška įvertinta tikrojo-laiko PGR metodu, naudojant *SYBR Green* chemiją (*Applied Biosystems, Thermo Fisher Scientific*) ir specifinius *TLR4, HSPA1A, HSPB1* ir *TJPI* genų pradmenis. Genų raiškos duomenys normalizuoti pagal *ACTB* raišką, ląstelių miRNR – pagal RNU48 raišką, o EV miRNR – pagal cel-miR-39-3p raišką. Raiškos pokyčiai tarp grupių nustatyti taikant $2^{-\Delta\Delta Ct}$ metodą. Statistinė analizė atlikta R (v4.0.3) aplinkoje, skirtumai tarp grupių laikyti reikšmingais, kai $p < 0,05$ (*Mann–Whitney U* testas).

Pagrindiniai rezultatai

I dalis. Iš viso storosios žarnos audiniuose identifikuotos 573 unikalios miRNR. MDS analizė parodė aiškų aktyvaus OpK ir ne-UŽL grupių atskyrimą pagal miRNR raiškos profilius, tuo tarpu OpK remisijos grupė dėtėsi tarp šių dviejų būklių. Diferencinės raiškos analizė atskleidė, kad aktyvaus OpK metu, lyginant su ne-UŽL, storosios žarnos audiniuose reikšmingai skyrėsi (FDR < 0,05, $|\log_2 PK| > 1$) 93 miRNR, o lyginant su OpK remisijos grupe – 59 miRNR. OpK remisijos grupę palyginus su ne-UŽL, nustatytas reikšmingas 32 miRNR raiškos pokytis. 13 pakitusios raiškos miRNR (tarp jų, miR-106-5p, miR-125b-1-3p, miR-205-5p, miR-3182) buvo nustatytos abiejose OpK pacientų grupėse, palyginti su ne-UŽL. miR-1-3p buvo vienintelė miRNR, kurios raiška reikšmingai skyrėsi visose porinėse lyginamosiose grupėse ($\log_2 PK$ nuo $-1,06$ iki $-2,18$, FDR nuo $0,01$ iki $3,8 \times 10^{-11}$). Storosios žarnos audinyje pakitusios raiškos miRNR genų taikinių GSEA analizė atskleidė reikšmingą kelių, susijusių su signalo perdavimu per interleukinus, dominavimą. Tarp labiausiai reikšmingai praturtintų *Reactome* kelių nustatyti „Interleukinų signaliniai keliai“ (R-HSA-449147), „Interleukino-4 ir interleukino-13 signalinis kelias“ (R-HSA-6785807), „Viduląstelinis signalo perdavimas per antrines molekules“ (R-HSA-9006925), „Signalų perdavimo sutrikimai, susiję su augimo veiksnių receptoriais ir antrinėmis molekulėmis“ (R-HSA-5663202). Šiuose signaliniuose keliuose dominavo 20 miRNR su didžiausiu taikinių skaičiumi, tarp jų: miR-1-3p, miR-10b-5p, miR-20a-5p, miR-31-5p, miR-146a-5p, miR-155-5p, miR-205-

5p, miR-223-3p. *IL-13* raiška audiniuose laipsniškai didėjo: 2,19 karto ($p = 0,031$) OpK remisija vs. ne-UŽL, 2,91 karto ($p = 7 \times 10^{-4}$) aktyvus OpK vs. OpK remisija, ir 6,38 karto ($p = 3 \times 10^{-10}$) aktyvus OpK vs. ne-UŽL, tuo tarpu *IL-4* raiška išliko nepakitusi. Naudojant GSE116222 rinkinį, *IL-4/IL-13* kelio genų (*IL13RA1*, *IL4R*, *JAK1*, *SOCS1*, *STAT3*, *STAT6*) raiška buvo nustatyta daugumoje epitelinių ir imuninių ląstelių populiacijų.

Storosios žarnos epitelinėse ląstelėse (kriptų dugno (CD44⁺) ir kriptų viršuje esančiose (CD66a⁺)) identifikuotos 436 unikalios miRNR. MDS analizė parodė bendrą transkriptomų panašumą, tačiau reikšmingai besiskiriančios raiškos miRNR skaičius didėjo kartu su OpK aktyvumu. Kriptų dugno (CD44⁺) ląstelėse OpK remisijos metu buvo reikšmingai pakitusi 15 miRNR raiška, aktyvaus OpK – 38 miRNR; kriptų viršuje esančiose (CD66a⁺) ląstelėse atitinkamai – 15 ir 29 miRNR raiška. Palyginus aktyvų OpK ir OpK remisiją su ne-UŽL, pakitusi miR-15b-5p, miR-194-3p, miR-222-3p, miR-223-3p, miR-574-3p raiška nustatyta kriptų dugno (CD44⁺) ląstelėse. Tuo tarpu kriptų viršuje esančiose (CD66a⁺) ląstelėse OpK grupėse buvo disreguluotos let-7c-5p, miR-1-3p, miR-106b-3p, miR-125b-5p, miR-194-3p, miR-335-5p, miR-552-3p ir miR-1290. GSEA analizė atskleidė bendrus disreguluotus kelius: „Interleukinų signaliniai keliai“ (R-HSA-449147), „Interleukino-4 ir interleukino-13 signalinis kelias“ (R-HSA-6785807), „Signalų perdavimas per tirozino kinazių receptorius“ (R-HSA-9006934). Lyginant kriptų dugno (CD44⁺) ir kriptų viršuje esančias (CD66a⁺) ląsteles skirtingų sveikatos būklių metu, aktyvaus OpK metu nustatyta pakitusi 24 miRNR raiška, OpK remisijos metu – 9 miRNR, ne-UŽL – 22 miRNR. Aktyvaus OpK metu dominavo *GO* biologiniai procesai, susiję su ląstelių judėjimu, pavyzdžiui, „Epitelio migracija“ (GO:0090132) ir „Epitelinių ląstelių migracija“ (GO:0010631), tuo tarpu OpK remisijos metu praturtinimas buvo silpnėjęs.

Galiausiai, WGCNA analizė storosios žarnos epitelinėse ląstelėse identifikavo du miRNR ko-ekspresijos modulius – M1 (sudarytą iš 13 miRNR: miR-10b-5p, miR-27a-3p, miR-31-5p, miR-135b-5p, miR-146a-5p, miR-182-5p, miR-183-5p, miR-194-3p, miR-196b-5p, miR-221-3p, miR-222-3p, miR-223-3p ir miR-574-5p) ir M2 (sudarytą iš 11 miRNR: let-7b-5p, let-7e-5p, miR-1-3p, miR-15b-5p, miR-100-5p, miR-125a-5p, miR-125b-5p, miR-143-3p, miR-181b-5p, miR-195-5p ir miR-5100). M1 modulis buvo reikšmingai praturtintas aktyvaus OpK metu kriptų viršuje esančiose (CD66a⁺) ląstelėse (normalizuotas praturtinimo balas (NES) = 1,71, $p_{kor.} = 9,7 \times 10^{-3}$) ir kriptų dugno (CD44⁺) ląstelėse (NES = 1,67, $p_{kor.} = 0,029$), o ne-UŽL ląstelėse – reikšmingai sumažėjęs (atitinkamai NES = -1,79 ir -1,74, $p_{kor.} = 7,7 \times 10^{-3}$ ir 0,05). M1 eigengeno (apibendrintos modulio raiškos) koreliacija su endoskopiniu Mayo balu siekė $\rho = 0,68$ (CD66a⁺, FDR = $1,08 \times 10^{-7}$) ir

$\rho = 0,60$ ($CD44^+$, $FDR = 1,07 \times 10^{-5}$). AUC-ROC analizėje M1 modulio eigengeno vertė atskiriant aktyvų OpK nuo OpK remisijos siekė 87,9 proc. ($CD66a^+$, pasikliautinis intervalas (PI): 74,0–100,0 proc.), 80,0 proc. ($CD44^+$, PI: 63,6–96,4 proc.), o audinio lygmenyje – 85,0 proc. (PI: 72,2–97,1 proc.), koreliacija su endoskopiniu Mayo balu – $\rho = 0,703$, $FDR = 1,22 \times 10^{-11}$.

II dalis. Žarnyno mikrobiotos sudėtis buvo vertinama 16S rRNR geno sekoskaitos metodu, naudojant aktyvaus OpK ir OpK remisijos pacientų bei ne-UŽL asmenų išmatų mėginius. Po kokybės kontrolės nustatytas minimalus skaitymų skaičius mėginyje – 22 032, kuris taikytas išretinimui. Bakterijų α -įvairovė, palyginti su ne-UŽL, buvo reikšmingai sumažėjusi tiek aktyvaus OpK, tiek OpK remisijos grupėse pagal du indeksus (atitinkamai *Chao1*: $p = 5,7 \times 10^{-4}$ ir $1,8 \times 10^{-3}$, *Shannon*: $p = 5,0 \times 10^{-3}$ ir $1,8 \times 10^{-3}$). Tuo tarpu *Simpson* indeksas nepasiekė statistinio reikšmingumo (atitinkamai $p = 0,064$ ir $0,059$). Bakterijų α -įvairovės skirtumų tarp aktyvaus OpK ir OpK remisijos grupių nenustatyta. Mikrobiotos β -įvairovė, vertinta pagal *Bray–Curtis* nepanašumo indeksą, reikšmingai skyrėsi tarp abiejų OpK grupių ir ne-UŽL asmenų (aktyvus OpK: $p = 8,0 \times 10^{-3}$, $R^2 = 0,047$; OpK remisija: $p = 0,01$, $R^2 = 0,052$). Vis dėlto, šie skirtumai turėjo silpną efektą, o klasterizacijos analizė neparodė reikšmingo susigrupavimo pagal ligos aktyvumą ($p = 0,49$).

Mikrobiotos sudėties analizė parodė, kad tiek aktyvaus OpK, tiek OpK remisijos pacientų išmatų mikrobiomuose dominavo *Phocaeicola* ir *Faecalibacterium* gentys, o ne-UŽL grupėje – *Phocaeicola* ir *Prevotella*. Iš 40 identifikuotų genčių penkios pasižymėjo reikšmingai mažesniu gausumu OpK pacientų mėginiuose, palyginti su ne-UŽL: *Alistipes* ($|\log_2PK| = 1,39$, $FDR = 0,019$), *Paraprevotella* ($|\log_2PK| = 0,91$, $FDR = 4,2 \times 10^{-3}$), *Mediterraneibacter* ($|\log_2PK| = 1,53$, $FDR = 1,2 \times 10^{-3}$), *Coprococcus* ($|\log_2PK| = 1,12$, $FDR = 0,033$) ir *Cuneatibacter* ($|\log_2PK| = 2,29$, $FDR = 4,2 \times 10^{-3}$).

Galiausiai apibūdintas ir šerdinis mikrobiomas – tai taksonai su $\geq 0,1$ proc. santykinio gausumu ≥ 50 proc. mėginių. Grupėse identifikuotų šerdinių ASV skaičius: 31 (aktyvus OpK), 31 (OpK remisija) ir 38 (ne-UŽL). Tarp jų identifikuotos 27 bendros gentys, stabiliai nustatytos visose tiriamosiose grupėse. Iš jų, 10 gausiausių genčių buvo: *Phocaeicola* (santykinis gausumas OpK mėginiuose: $14,63 \text{ proc.} \pm 13,50$; santykinis gausumas ne-UŽL mėginiuose: $12,06 \text{ proc.} \pm 9,56$), *Faecalibacterium* (OpK: $14,37 \text{ proc.} \pm 10,76$; ne-UŽL: $9,20 \text{ proc.} \pm 5,74$), *Prevotella* (OpK: $7,31 \text{ proc.} \pm 12,11$; ne-UŽL: $10,66 \text{ proc.} \pm 12,04$), *Collinsella* (OpK: $4,93 \text{ proc.} \pm 5,55$; ne-UŽL: $3,92 \text{ proc.} \pm 3,26$), *Holdemanella* (OpK: $4,19 \text{ proc.} \pm 6,20$; ne-UŽL: $4,58 \text{ proc.} \pm 6,49$), *Sutterella* (OpK: $3,95 \text{ proc.} \pm 5,91$; ne-UŽL: $2,20 \text{ proc.} \pm 3,53$), *Roseburia* (OpK: $3,81 \text{ proc.} \pm 4,24$; ne-UŽL: $4,20 \text{ proc.} \pm 3,22$), *Bacteroides* (OpK: $3,55 \text{ proc.} \pm 4,93$; ne-UŽL: $3,77 \text{ proc.} \pm 4,09$),

Escherichia/Shigella (OpK: 3,37 proc. \pm 8,77; ne-UŽL: 0,62 proc. \pm 1,25) ir *Blautia* (OpK: 3,09 proc. \pm 3,00; ne-UŽL: 3,42 proc. \pm 2,38).

III dalis. Prieš atliekant storosios žarnos epitelinių ląstelių ir bakterijų funkcinę analizę, eksperimentinė sistema buvo įvertinta morfologiniu ir molekulinio lygmenimis. Šviesinės ir (imuno)fluorescencinės mikroskopijos pagalba kokybiškai įvertinus, nustatyta, kad nediferencijuoti 3D storosios žarnos epiteliniai organoidai, suformuoti iš ne-UŽL ir OpK pacientų biopsijų, ilgalaikio kultivavimo metu išlaiko stabilią morfologiją. Epitelio poliškumas 3D organoiduose buvo patvirtintas stebint bazolateralinę β -katenino ir apikalinę F-aktino raišką. Tiek 3D organoiduose, tiek iš jų sugeneruotuose epiteliniuose monoslukuksniuose taip pat nustatyta proliferuojančių ląstelių (Ki67), glaudžiųjų jungčių (ZO-1) bei specializuotų ląstelių – kolonocitų (Citokeratinas 20), taurinių (gobletų; Mucinas 2) ir enteroendokrinių (Chromograninas A) ląstelių – žymenų raiška. Tuo tarpu LINE-1 metilinimo lygis buvo tirtas trijų pacientų grupių storosios žarnos biopsijose, kriptose ir iš jų sugeneruotuose organoiduose skirtingais persėjimais (P0, P1, P5). LINE-1 regionas visuose mėginiuose buvo stipriai metilintas (> 60 proc.), tačiau 3D organoidų kultivavimo metu metilinimo lygis reikšmingai mažėjo. Specifiškai, vėlyvo persėjimo (P5) organoiduose LINE-1 metilinimo lygis visose trijose grupėse (aktyvus OpK, OpK remisija, ne-UŽL) reikšmingai sumažėjo, palyginti su biopsijomis. Be to, persėtų storosios žarnos epitelinių organoidų LINE-1 metilinimo dinamikos analizė parodė, kad metilinimo mažėjimo greitis skyrėsi tarp skirtingų pacientų grupių. Aktyvaus OpK P1 organoiduose LINE-1 metilinimo lygis buvo 4,7 proc. mažesnis nei ne-UŽL ($p_{kor.} = 0,018$) ir 3,7 proc. mažesnis nei OpK remisijos grupėje ($p_{kor.} = 0,01$). P5 persėjimo taške ne-UŽL organoiduose bendras metilinimo lygis buvo reikšmingai 3,8 proc. mažesnis nei OpK remisijos grupėje ($p_{kor.} = 0,024$).

In silico analizėje buvo įvertinti pasirinktų miRNR taikiniai *E. coli* ir *P. vulgatus* genomuose. Atitinkamai tolimesnei analizei pasirinktos trys miRNR. Dvi iš jų turėjo teorinių taikinių *E. coli* genome: miR-135b-5p (*mukB*: 59 proc., $p = 1,4 \times 10^{-5}$; *cysI*: 52 proc., $p = 3,4 \times 10^{-5}$) ir miR-146a-5p (*mukB*: 59 proc., $p = 2,0 \times 10^{-5}$; *cysI*: 51 proc., $p = 5,0 \times 10^{-5}$). Viena miRNR – miR-183-5p – turėjo po vieną geną taikinį *E. coli* ir *P. vulgatus* genomuose (atitinkamai *mukB*: 59 proc., $p = 5,3 \times 10^{-7}$ ir *BVU_RS05340*: 51 proc., $p = 1,2 \times 10^{-7}$).

Funkcinė analizė, atlikta su storosios žarnos epitelinių ląstelių ir bakterijų kultūromis neparodė reikšmingų *TJPI*, *TLR4*, *HSPA1A* ar *HSPB1* genų raiškos pokyčių, tačiau atskleidė keletą įdomių tendencijų. Buvo pastebėta, kad nors skirtumai nepasiekė statistinio reikšmingumo, *E. coli* ir *P. vulgatus* skirtingai veikė *TJPI* raišką OpK ir ne-UŽL epitelinėse ląstelėse. OpK pacientų epiteliniuose monoslukuksniuose *TJPI* raiška po inkubacijos su

bakterijomis mažėjo (*E. coli*: PK = 0,42, p = 0,796; *P. vulgatus*: PK = 0,72, p = 1,0), o ne-UŽL monosluoksniuose – didėjo (*E. coli*: PK = 3,52, p = 0,328; *P. vulgatus*: PK = 1,86, p = 0,397). Prieš vertinant miRNR raišką, iš ląstelių kultivavimo terpės izoliuotos EV buvo apibūdintos pagal dydį (vidurkis – 36,63 nm ± 18,64) ir žymenų raišką. Patvirtinta aptinkama specifinių EV žymenų – CD63 ir HSP70 – raiška, o nespecifinio žymens ApoA1 – nedetektuota. Galiausiai, lyginant bazinę miR-183-5p, miR-135b-5p ir miR-146a-5p raišką neveiktose ląstelėse tarp OpK ir ne-UŽL grupių, reikšmingų skirtumų nenustatyta (atitinkamai, PK = 0,77, 1,00 ir 1,08, p > 0,05). Abiejų tiriamųjų grupių storosios žarnos epitelinių ląstelių stimuliacijos bakterijomis metu, kaip ir genų raiškos analizės atveju, užfiksuoti skirtumai nepasiekė statistinio reikšmingumo, bet atskleidė keletą tendencijų. Po inkubacijos su *E. coli*, ne-UŽL grupės ląstelėse ir EV miR-183-5p ir miR-135b-5p raiška buvo linkusi mažėti, o miR-146a-5p – didėti. Tuo tarpu OpK grupėje visų trijų miRNR raiška po inkubacijos su *E. coli* demonstravo tendenciją didėti. *P. vulgatus* poveikis buvo silpnesnis: miR-183-5p ir miR-135b-5p raiška EV struktūrose buvo linkusi mažėti abiejose tiriamųjų grupėse, o sumažėjusi miR-146a-5p raiška užfiksuota tik ne-UŽL EV mėginiuose.

Išvados

- 1.1. Pakitusios raiškos mikroRNR skaičius storosios žarnos audinyje didėjo laipsniškai, priklausomai nuo opinio kolito aktyvumo: 19 mikroRNR raiška buvo pakitusi neaktyvaus opinio kolito audiniuose, o 80 mikroRNR – aktyvaus. miR-1-3p raiška storosios žarnos audiniuose nuosekliai mažėjo nuo kontrolinių nesergančiųjų uždegimine žarnyno liga iki esančiųjų opinio kolito remisijoje ir esančiųjų aktyvioje ligos fazėje.
- 1.2. Su opinio kolitu susijusios audinio mikroRNR dalyvavo interleukinų signaliniuose keliuose, ypač interleukino-4 ir interleukino-13 kaskadoje. Patvirtintas laipsniškas, su opinio kolitu aktyvumu susijęs *IL-13* geno raiškos didėjimas, o *IL-4* geno raiška nesikeitė. Su interleukino-4 ir interleukino-13 signaliniu keliu susijusių genų raiška buvo nustatyta epitelinėse ir imuninėse storosios žarnos ląstelių populiacijose bei turėjo su opinio kolitu sietiną raiškos tendenciją.

- 2.1. mikroRNR raiškos pokyčių mastas koreliavo su opinio kolito aktyvumu storosios žarnos kriptų viršuje ir dugne esančių epitelinių ląstelių populiacijose. Opinio kolito remisijos metu 15 mikroRNR raiška buvo pakitusi kriptų viršuje ir kitų 15 mikroRNR – kriptų dugne esančiose epitelinėse ląstelėse, o aktyvios ligos fazės metu kriptų viršuje ir dugne esančiose ląstelėse buvo disreguluotos atitinkamai 29 ir 38 mikroRNR. Šios mikroRNR abiejose ląstelių populiacijose dalyvavo interleukinų bei kituose signalų perdavimo keliuose, susijusiuose su opinio kolito patogeneze.
- 2.2. mikroRNR, kurių raiška skyrėsi tarp kriptų viršuje ir dugne esančių epitelinių ląstelių, buvo specifinės diagnozei: 24 mikroRNR raiška tarp ląstelių populiacijų skyrėsi aktyvaus opinio kolito, 9 – ligos remisijos ir 22 – kontrolinėje nesergančiųjų uždegimine žarnyno liga grupėje. Nepriklausomai nuo opinio kolito aktyvumo, šios mikroRNR per savo genus taikinius buvo susijusios su uždegiminiais procesais ir žarnyno epitelio barjero vientisumo palaikymu.
- 2.3. Storosios žarnos epitelinėse ląstelėse buvo identifikuoti du mikroRNR raiškos moduliai. M1 modulis, sudarytas iš 13 mikroRNR, buvo susijęs su aktyviu opinio kolitu ir buvo gausiai ekspresuojamas tiek kriptų viršuje, tiek kriptų dugne esančiose epitelinėse ląstelėse. M2 modulis apėmė 11 mikroRNR, buvo susijęs su opinio kolito remisija ir dominavo kriptų dugno epitelinėse ląstelėse. M1 modulio raiška koreliavo su endoskopiniu ligos aktyvumu ir efektyviai atskyrė pacientus ligos remisijoje nuo sergančių aktyviu opinio kolitu.
3. Opinio kolito pacientų išmatose buvo nustatytas sumažėjęs bakterijų α - ir β -įvairovės lygis bei reikšmingas *Alistipes*, *Coprococcus*, *Cuneatebacter*, *Mediterraneibacter* ir *Paraprevotella* genčių sumažėjimas. Visose trijose tyrimo grupėse (pacientai, esantys aktyvioje opinio kolito fazėje ar remisijoje, ir kontroliniai asmenys, nesergantys uždegimine žarnyno liga) 27 bakterijų gentys išliko nepakitusios. Tarp jų identifikuotos *Phocaeicola* ir *Escherichia/Shigella* gentys, kurios buvo stabiliai gausiai aptinkamos visų tiriamųjų mėginiuose.
- 4.1. Komensalinės bakterijos *Escherichia coli* ir *Phocaeicola vulgatus* nesukėlė reikšmingų storosios žarnos epitelinių ląstelių genų, susijusių su bakterijų atpažinimu, ląstelių stresu ar glaudžiujų jungčių vientisumu (*TLR4*, *HSPA1A*, *HSPB1* ir *TJPI*), raiškos pokyčių. Tačiau abiejų bakterijų poveikis kontrolinės nesergančiųjų uždegimine žarnyno liga grupės epitelinėse ląstelėse buvo linkęs didinti *TJPI* raišką, o opinio kolito pacientų ląstelėse – ją mažinti.

4.2. *Escherichia coli* ir *Phocaeicola vulgatus* reikšmingai nepakeitė tirtų mikroRNR raiškos. Vis dėlto, *Escherichia coli* buvo linkusi didinti miR-183-5p, miR-135b-5p ir miR-146a-5p raišką tiek epitelinėse ląstelėse, tiek ekstraląstelinėse pūslelėse sergančiųjų opiniiu kolitu grupėje, o kontrolinėje nesergančiųjų uždegimine žarnyno liga grupėje didino miR-146a-5p, bet mažino miR-183-5p ir miR-135b-5p raišką. *Phocaeicola vulgatus* buvo linkusi mažinti miR-183-5p ir miR-135b-5p lygį tik ekstraląstelinėse pūslelėse abiejose grupėse.

REFERENCES

1. Kobayashi T, Siegmund B, Le Berre C, Wei SC, Ferrante M, Shen B, et al. Ulcerative colitis. *Nat Rev Dis Primers*. 2020;6(1):74.
2. Guan Q. A Comprehensive review and update on the pathogenesis of inflammatory bowel disease. *J Immunol Res*. 2019;2019(1):7247238.
3. Bao L, Shi B, Shi YB. Intestinal homeostasis: a communication between life and death. *Cell Biosci*. 2020;10(1):66.
4. Okumura R, Takeda K. Roles of intestinal epithelial cells in the maintenance of gut homeostasis. *Exp Mol Med*. 2017;49(5):e338.
5. Iacucci M, Santacroce G, Majumder S, Morael J, Zammarchi I, Maeda Y, et al. Opening the doors of precision medicine: novel tools to assess intestinal barrier in inflammatory bowel disease and colitis-associated neoplasia. *Gut*. 2024;73(10):1749–62.
6. Choi J, Augenlicht LH. Intestinal stem cells: guardians of homeostasis in health and aging amid environmental challenges. *Exp Mol Med*. 2024;56(3):495–500.
7. Chelakkot C, Ghim J, Ryu SH. Mechanisms regulating intestinal barrier integrity and its pathological implications. *Exp Mol Med*. 2018;50(8):1–9.
8. Harbord M, Eliakim R, Bettenworth D, Karmiris K, Katsanos K, Kopylov U, et al. Third European evidence-based consensus on diagnosis and management of ulcerative colitis. Part 2: Current management. *J Crohns Colitis*. 2017;11(7):769–84.
9. McKenna LB, Schug J, Vourekas A, McKenna JB, Bramswig NC, Friedman JR, et al. MicroRNAs control intestinal epithelial differentiation, architecture, and barrier function. *Gastroenterology*. 2010;139(5):1654–64.e1.
10. Cichon C, Sabharwal H, Rüter C, Schmidt MA. MicroRNAs regulate tight junction proteins and modulate epithelial/endothelial barrier functions. *Tissue Barriers*. 2014;2(4):e944446.
11. Ye D, Guo S, Alsadi R, Ma TY. MicroRNA regulation of intestinal epithelial tight junction permeability. *Gastroenterology*. 2011;141(4):1323–33.
12. Rishik S, Hirsch P, Grandke F, Fehlmann T, Keller A. miRNATissueAtlas 2025: an update to the uniformly processed and annotated human and mouse non-coding RNA tissue atlas. *Nucleic Acids Res*. 2025;53(D1):D129–37.
13. Patil AH, Baran A, Brehm ZP, McCall MN, Halushka MK. A curated human cellular microRNAome based on 196 primary cell types. *GigaScience*. 2022;11:giac083.
14. Shahriyari L, Komarova NL, Jilkin A. The role of cell location and spatial gradients in the evolutionary dynamics of colon and intestinal crypts. *Biol Direct*. 2016;11(1):42.
15. Ji Y, Li X, Zhu Y, Li N, Zhang N, Niu M. Faecal microRNA as a biomarker of the activity and prognosis of inflammatory bowel diseases. *Biochem Biophys Res Commun*. 2018;503(4):2443–50.
16. Liu S, da Cunha AP, Rezende RM, Cialic R, Wei Z, Bry L, et al. The Host Shapes the Gut Microbiota via Fecal MicroRNA. *Cell Host Microbe*. 2016;19(1):32–43.
17. Liu S, Rezende RM, Moreira TG, Tankou SK, Cox LM, Wu M, et al. Oral Administration of miR-30d from feces of MS patients suppresses MS-like symptoms in mice by expanding Akkermansia muciniphila. *Cell Host Microbe*. 2019;26(6):779–794.e8.
18. Ryan FJ, Ahern AM, Fitzgerald RS, Laserna-Mendieta EJ, Power EM, Clooney AG, et al. Colonic microbiota is associated with inflammation and host epigenomic alterations in inflammatory bowel disease. *Nat Commun*. 2020;11(1):1512.

19. Öhman L, Lasso A, Strömbeck A, Isaksson S, Hesselmar M, Simrén M, et al. Fecal microbiota dynamics during disease activity and remission in newly diagnosed and established ulcerative colitis. *Sci Rep*. 2021;11(1):8641.
20. Akiyama S, Nishijima S, Kojima Y, Kimura M, Ohsugi M, Ueki K, et al. Multi-biome analysis identifies distinct gut microbial signatures and their crosstalk in ulcerative colitis and Crohn's disease. *Nat Commun*. 2024;15(1):10291.
21. Sartor RB. Microbial Influences in Inflammatory Bowel Diseases. *Gastroenterology*. 2008;134(2):577–94.
22. Das R, Steinhart AH. Choosing Therapies in Ulcerative Colitis. *J Can Assoc Gastroenterol*. 2024;7(1):9–21.
23. Gajendran M, Loganathan P, Jimenez G, Catinella AP, Ng N, Umapathy C, et al. A comprehensive review and update on ulcerative colitis. *Disease-a-Month*. 2019;65(12):100851.
24. Segal JP, LeBlanc JF, Hart AL. Ulcerative colitis: an update. *Clinical Medicine*. 2021;21(2):135–9.
25. Aslam Nasar, Lo Sheng Wei, Sikafi Rafid, Barnes Tom, Segal Jonathan, Smith Philip J, et al. A review of the therapeutic management of ulcerative colitis. *Therap Adv Gastroenterol*. 2022;15:17562848221138160.
26. Liang Y, Li Y, Lee C, Yu Z, Chen C, Liang C. Ulcerative colitis: molecular insights and intervention therapy. *Molecular Biomedicine*. 2024;5:42.
27. Pabla BS, Schwartz DA. Assessing severity of disease in patients with ulcerative colitis. *Gastroenterol Clin North Am*. 2020;49(4):671–88.
28. Lirhus SS, Høivik ML, Moum B, Anisdahl K, Melberg HO. Incidence and prevalence of inflammatory bowel disease in Norway and the impact of different case definitions: A nationwide registry study. *Clin Epidemiol*. 2021;13:287–94.
29. Mak WY, Zhao M, Ng SC, Burisch J. The epidemiology of inflammatory bowel disease: East meets West. *J Gastroenterol Hepatol*. 2020;35(3):380–9.
30. Burisch J, Jess T, Martinato M, Lakatos PL, ECCO-EpiCom. The burden of inflammatory bowel disease in Europe. *J Crohns Colitis*. 2013;7(4):322–37.
31. Lin D, Jin Y, Shao X, Xu Y, Ma G, Jiang Y, et al. Global, regional, and national burden of inflammatory bowel disease, 1990–2021: Insights from the global burden of disease 2021. *Int J Colorectal Dis*. 2024;39(1):139.
32. Zhang Y, Chu X, Wang L, Yang H. Global patterns in the epidemiology, cancer risk, and surgical implications of inflammatory bowel disease. *Gastroenterol Rep*. 2024;12:goae053.
33. Caron B, Honap S, Peyrin-Biroulet L. Epidemiology of inflammatory bowel disease across the ages in the era of advanced therapies. *J Crohns Colitis*. 2024;18(Suppl 2):ii3–ii15.
34. Ng SC, Shi HY, Hamidi N, Underwood FE, Tang W, Benchimol EI, et al. Worldwide incidence and prevalence of inflammatory bowel disease in the 21st century: a systematic review of population-based studies. *The Lancet*. 2017;390(10114):2769–78.
35. Lewis JD, Parlett LE, Jonsson Funk ML, Brensinger C, Pate V, Wu Q, et al. Incidence, prevalence, and racial and ethnic distribution of inflammatory bowel disease in the United States. *Gastroenterology*. 2023;165(5):1197–205.e2.
36. Greuter T, Manser C, Pittet V, Vavricka SR, Biedermann L, on behalf of Swiss IBDnet, an official working group of the Swiss Society of Gastroenterology. Gender differences in inflammatory bowel disease. *Digestion*. 2020;101(Suppl 1):98–104.

37. Shah SC, Khalili H, Gower-Rousseau C, Olen O, Benchimol EI, Lyngé E, et al. Sex-based differences in incidence of inflammatory bowel diseases—pooled analysis of population-based studies from Western countries. *Gastroenterology*. 2018;155(4):1079-89.e3.
38. Singh N, Bernstein CN. Environmental risk factors for inflammatory bowel disease. *United Eur Gastroenterol J*. 2022;10(9):1047–53.
39. Nakase H, Sato N, Mizuno N, Ikawa Y. The influence of cytokines on the complex pathology of ulcerative colitis. *Autoimmun Rev*. 2022;21(3):103017.
40. Sands BE, Kaplan GG. The role of TNF α in ulcerative colitis. *J Clin Pharmacol*. 2007;47(8):930–41.
41. Ordás I, Eckmann L, Talamini M, Baumgart DC, Sandborn WJ. Ulcerative colitis. *The Lancet*. 2012;380(9853):1606–19.
42. Neurath MF. Targeting immune cell circuits and trafficking in inflammatory bowel disease. *Nat Immunol*. 2019;20(8):970–9.
43. Nakase H. Treatment of inflammatory bowel disease from the immunological perspective. *Immunol Med*. 2020;43(2):79–86.
44. Danese S, D’Amico F, Bonovas S, Peyrin-Biroulet L. Positioning tofacitinib in the treatment algorithm of moderate to severe ulcerative colitis. *Inflamm Bowel Dis*. 2018;24(10):2106–12.
45. Luo W, Tian L, Tan B, Shen Z, Xiao M, Wu S, et al. Update: Innate lymphoid cells in inflammatory bowel disease. *Dig Dis Sci*. 2022;67(1):56–66.
46. Schulz-Kuhnt A, Neurath MF, Wirtz S, Atreya I. Innate lymphoid cells as regulators of epithelial integrity: therapeutic implications for inflammatory bowel diseases. *Front Med*. 2021;8:656745.
47. Baraldo S, Faffe DS, Moore PE, Whitehead T, McKenna M, Silverman ES, et al. Interleukin-9 influences chemokine release in airway smooth muscle: role of ERK. *Am J Physiol Lung Cell Mol Physiol*. 2003;284(6):L1093–102.
48. Kuwada T, Shiokawa M, Kodama Y, Ota S, Kakiuchi N, Nannya Y, et al. Identification of an anti-integrin $\alpha\beta 6$ autoantibody in patients with ulcerative colitis. *Gastroenterology*. 2021;160(7):2383-2394.e21.
49. Castro-Dopico T, Dennison TW, Ferdinand JR, Mathews RJ, Fleming A, Clift D, et al. Anti-commensal IgG drives intestinal inflammation and type 17 immunity in ulcerative colitis. *Immunity*. 2019;50(4):1099-1114.e10.
50. Ananthakrishnan AN, Bernstein CN, Iliopoulos D, Macpherson A, Neurath MF, Ali RAR, et al. Environmental triggers in IBD: A review of progress and evidence. *Nat Rev Gastroenterol Hepatol*. 2018;15:39–49.
51. Burke KE, Boumitri C, Ananthakrishnan AN. Modifiable environmental factors in inflammatory bowel disease. *Curr Gastroenterol Rep*. 2017;19(5):21.
52. Manski S, Noverati N, Policarpo T, Rubin E, Shivashankar R. Diet and nutrition in inflammatory bowel disease: A review of the literature. *Crohns Colitis* 360. 2024;6(1):otad077.
53. Naimi S, Viennois E, Gewirtz AT, Chassaing B. Direct impact of commonly used dietary emulsifiers on human gut microbiota. *Microbiome*. 2021;9:66.
54. Chassaing B, Koren O, Goodrich JK, Poole AC, Srinivasan S, Ley RE, et al. Dietary emulsifiers impact the mouse gut microbiota promoting colitis and metabolic syndrome. *Nature*. 2015;519(7541):92–6.
55. Meeker S, Seamons A, Maggio-Price L, Paik J. Protective links between vitamin D, inflammatory bowel disease and colon cancer. *World J Gastroenterol*. 2016;22(3):933–48.

56. Sugihara K, Morhardt TL, Kamada N. The role of dietary nutrients in inflammatory bowel disease. *Front Immunol.* 2019;10:945.
57. Fletcher J, Cooper SC, Ghosh S, Hewison M. The role of vitamin D in inflammatory bowel disease: Mechanism to management. *Nutrients.* 2019;11(5):1019.
58. Barbalho SM, De R, Goulart A, Quesada K, Dib Bechara M. Inflammatory bowel disease: can omega-3 fatty acids really help? *Ann Gastroenterol.* 2016;29(1):37-43.
59. Chen BC, Weng MT, Chang CH, Huang LY, Wei SC. Effect of smoking on the development and outcomes of inflammatory bowel disease in Taiwan: a hospital-based cohort study. *Sci Rep.* 2022;12(1):7665.
60. Mahid SS, Minor KS, Soto RE, Hornung CA, Galandiuk S. Smoking and inflammatory bowel disease: A meta-analysis. *Mayo Clin Proc.* 2006;81(11):1462–71.
61. Araki M, Shinzaki S, Yamada T, Arimitsu S, Komori M, Shibukawa N, et al. Psychologic stress and disease activity in patients with inflammatory bowel disease: A multicenter cross-sectional study. *PLoS One.* 2020;15(5):e0233365.
62. Moller FT, Andersen V, Wohlfahrt J, Jess T. Familial risk of inflammatory bowel disease: A population-based cohort study 1977–2011. *AM J Gastroenterol.* 2015; 110(4):564-71.
63. Caliendo G, D’Elia G, Makker J, Passariello L, Albanese L, Molinari AM, et al. Biological, genetic and epigenetic markers in ulcerative colitis. *Adv Med Sci.* 2023; 68(2):386–95.
64. El Hadad J, Schreiner P, Vavricka SR, Greuter T. The genetics of inflammatory bowel disease. *Mol Diagn Ther.* 2024;28(1):27–35.
65. van Sommeren S, Visschedijk MC, Festen EAM, de Jong DJ, Ponsioen CY, Wijmenga C, et al. HNF4 α and CDH1 are associated with ulcerative colitis in a Dutch cohort. *Inflamm Bowel Dis.* 2011;17(8):1714–8.
66. Fisher SA, Tremelling M, Anderson CA, Gwilliam R, Bumpstead S, Prescott NJ, et al. Genetic determinants of ulcerative colitis include the ECM1 locus and five loci implicated in Crohn’s disease. *Nat Genet.* 2008;40(6):710–2.
67. Prager M, Buettner J, Buening C. Genes involved in the regulation of intestinal permeability and their role in ulcerative colitis. *J Dig Dis.* 2015;16(12):713–22.
68. Cleynen I, Boucher G, Jostins L, Schumm LP, Zeissig S, Ahmad T, et al. Inherited determinants of Crohn’s disease and ulcerative colitis phenotypes: a genetic association study. *The Lancet.* 2016;387(10014):156–67.
69. Franke A, Balschun T, Karlsen TH, Sventoraityte J, Nikolaus S, Mayr G, et al. Sequence variants in IL10, ARPC2 and multiple other loci contribute to ulcerative colitis susceptibility. *Nat Genet.* 2008;40(11):1319–23.
70. Lauro R, Mannino F, Irrera N, Squadrito F, Altavilla D, Squadrito G, et al. Pharmacogenetics of biological agents used in inflammatory bowel disease: A systematic review. *Biomedicines.* 2021;9(4):344.
71. Kaur A, Goggolidou P. Ulcerative colitis: understanding its cellular pathology could provide insights into novel therapies. *J Inflamm.* 2020;17(1):15.
72. Cooke J, Zhang H, Greger L, Silva AL, Massey D, Dawson C, et al. Mucosal genome-wide methylation changes in inflammatory bowel disease. *Inflamm Bowel Dis.* 2012;18(11):2128–37.
73. Al-Sadi R, Engers J, Abdulqadir R. Talk about micromanaging! Role of microRNAs in intestinal barrier function. *AM J Physiol Gastrointest Liver Physiol.* 2020;319(2): G170–4.

74. Gould NJ, Davidson KL, Nwokolo CU, Arasaradnam RP. A systematic review of the role of DNA methylation on inflammatory genes in ulcerative colitis. *Epigenomics*. 2016;8(5):667–84.
75. Nascimento R de P do, Machado AP da F, Galvez J, Cazarin CBB, Maróstica Junior MR. Ulcerative colitis: Gut microbiota, immunopathogenesis and application of natural products in animal models. *Life Sci*. 2020;258:118129.
76. Zhang Z, Zhang H, Chen T, Shi L, Wang D, Tang D. Regulatory role of short-chain fatty acids in inflammatory bowel disease. *Cell Commun Signal*. 2022;20(1):64.
77. Neurath MF, Artis D, Becker C. The intestinal barrier: a pivotal role in health, inflammation, and cancer. *Lancet Gastroenterol Hepatol*. 2025. In press.
78. Allaire JM, Crowley SM, Law HT, Chang SY, Ko HJ, Vallance BA. The intestinal epithelium: central coordinator of mucosal immunity. *Trends Immunol*. 2018;39(9):677–96.
79. Turner JR. Intestinal mucosal barrier function in health and disease. *Nat Rev Immunol*. 2009;9(11):799–809.
80. Raya-Sandino A, Luissint AC, Kusters DHM, Narayanan V, Flemming S, Garcia-Hernandez V, et al. Regulation of intestinal epithelial intercellular adhesion and barrier function by desmosomal cadherin desmocollin-2. *Mol Biol Cell*. 2021;32(8):753–68.
81. Gustafsson JK, Johansson ME V. The role of goblet cells and mucus in intestinal homeostasis. *Nat Rev Gastroenterol Hepatol*. 2022;19(12):785–803.
82. Song C, Chai Z, Chen S, Zhang H, Zhang X, Zhou Y. Intestinal mucus components and secretion mechanisms: what we do and do not know. *Exp Mol Med*. 2023;55(4):681–91.
83. Suzuki T. Regulation of the intestinal barrier by nutrients: The role of tight junctions. *Anim Sci J*. 2020;91(1):e13357.
84. Cardoso-Silva D, Delbue D, Itzlinger A, Moerkens R, Withoff S, Branchi F, et al. Intestinal barrier function in gluten-related disorders. *Nutrients*. 2019;11(10):2325.
85. Sumigray KD, Terwilliger M, Lechler T. Morphogenesis and compartmentalization of the intestinal crypt. *Dev Cell*. 2018;45(2):183-197.e5.
86. Kosinski C, Li VSW, Chan ASY, Zhang J, Ho C, Tsui WY, et al. Gene expression patterns of human colon tops and basal crypts and BMP antagonists as intestinal stem cell niche factors. *Proc Natl Acad Sci U S A*. 2007;104(39):15418–23.
87. Blachier F, de Sá Resende A, da Silva Fogaça Leite G, Vasques da Costa A, Lancha Junior AH. Colon epithelial cells luminal environment and physiopathological consequences: impact of nutrition and exercise. *Nutrire*. 2018;43(1):2.
88. Gribble FM, Reimann F. Enteroendocrine Cells: Chemosensors in the intestinal epithelium. *Annu Rev Physiol*. 2016;78:277–99.
89. Schneider C, O’Leary CE, Locksley RM. Regulation of immune responses by tuft cells. *Nat Rev Immunol*. 2019;19(9):584–93.
90. Coutry N, Nguyen J, Soualhi S, Gerbe F, Meslier V, Dardalhon V, et al. Cross talk between Paneth and tuft cells drives dysbiosis and inflammation in the gut mucosa. *Proc Natl Acad Sci*. 2023;120(25):e2219431120.
91. Parikh K, Antanaviciute A, Fawcner-Corbett D, Jagielowicz M, Aulicino A, Lagerholm C, et al. Colonic epithelial cell diversity in health and inflammatory bowel disease. *Nature*. 2019;567(7746):49–55.
92. Malonga T, Vialaneix N, Beaumont M. BEST41 cells in the intestinal epithelium. *Am J Physiol Cell Physiol*. 2024;326(6):C1345–52.
93. Otani T, Furuse M. Tight junction structure and function revisited. *Trends Cell Biol*. 2020;30(10):805–17.

94. Garcia-Hernandez V, Quiros M, Nusrat A. Intestinal epithelial claudins: expression and regulation in homeostasis and inflammation. *Ann N Y Acad Sci.* 2017;1397(1):66–79.
95. Higashi T, Chiba H. Molecular organization, regulation and function of tricellular junctions. *Biochim Biophys Acta Biomembr.* 2020;1862(2):183143.
96. Lessey LR, Robinson SC, Chaudhary R, Daniel JM. Adherens junction proteins on the move – from the membrane to the nucleus in intestinal diseases. *Front Cell Dev Biol.* 2022;5(10):998373.
97. Schlegel N, Boerner K, Waschke J. Targeting desmosomal adhesion and signalling for intestinal barrier stabilization in inflammatory bowel diseases – lessons from experimental models and patients. *Acta Physiol (Oxford).* 2021;231(1):e13492.
98. Sikora M, Ermel UH, Seybold A, Kunz M, Calloni G, Reitz J, et al. Desmosome architecture derived from molecular dynamics simulations and cryo-electron tomography. *Proc Natl Acad Sci U S A.* 2020;117(44):27132–40.
99. Allaire JM, Crowley SM, Law HT, Chang SY, Ko HJ, Vallance BA. The intestinal epithelium: central coordinator of mucosal immunity. *Trends Immunol.* 2018;39(9):677–96.
100. Johansson ME V, Phillipson M, Petersson J, Velcich A, Holm L, Hansson GC, et al. The inner of the two Muc2 mucin-dependent mucus layers in colon is devoid of bacteria. *Proc Natl Acad Sci U S A.* 2008;105(39):15064–9.
101. Corfield AP. The interaction of the gut microbiota with the mucus barrier in health and disease in human. *Microorganisms.* 2018;6(3):78.
102. Javitt G, Khmelnitsky L, Albert L, Bigman LS, Elad N, Morgenstern D, et al. Assembly mechanism of mucin and von Willebrand factor polymers. *Cell.* 2020;183(3):717-729.e16.
103. Grondin JA, Kwon YH, Far PM, Haq S, Khan WI. Mucins in intestinal mucosal defense and inflammation: Learning from clinical and experimental studies. *Front Immunol.* 2020;11:2054.
104. Neurath MF. Cytokines in inflammatory bowel disease. *Nat Rev Immunol.* 2014;14(5):329–42.
105. Kang Y, Park H, Choe BH, Kang B. The role and function of mucins and its relationship to inflammatory bowel disease. *Front Med.* 2022;9:848344.
106. van der Post S, Jabbar KS, Birchenough G, Arike L, Akhtar N, Sjøvall H, et al. Structural weakening of the colonic mucus barrier is an early event in ulcerative colitis pathogenesis. *Gut.* 2019;68(12):2142–51.
107. Krug SM, Bojarski C, Fromm A, Lee IM, Dames P, Richter JF, et al. Tricellulin is regulated via interleukin-13-receptor α_2 , affects macromolecule uptake, and is decreased in ulcerative colitis. *Mucosal Immunol.* 2018;11(2):345–56.
108. Selvakumar D, Evans D, Coyte KZ, McLaughlin J, Brass A, Hancock L, et al. Understanding the development and function of the gut microbiota in health and inflammation. *Frontline Gastroenterol.* 2022;13(e1):e13-e21.
109. Jin XY, Li DD, Quan W, Chao Y, Zhang B. Leaky gut, circulating immune complexes, arthralgia, and arthritis in IBD: coincidence or inevitability? *Front Immunol.* 2024;15:1347901.
110. Katinios G, Casado-Bedmar M, Walter SA, Vicario M, González-Castro AM, Bednarska O, et al. Increased colonic epithelial permeability and mucosal eosinophilia in ulcerative colitis in remission compared with irritable bowel syndrome and health. *Inflamm Bowel Dis.* 2020;26(7):974–84.

111. Annese V. Genetics and epigenetics of IBD. *Pharmacol Res.* 2020;159:104892.
112. McGovern DPB, Kugathasan S, Cho JH. Genetics of inflammatory bowel diseases. *Gastroenterology.* 2015;149(5):1163–76.e2.
113. Kale G, Naren AP, Sheth P, Rao RK. Tyrosine phosphorylation of occludin attenuates its interactions with ZO-1, ZO-2, and ZO-3. *Biochem Biophys Res Commun.* 2003;302(2):324–9.
114. Wlodarska M, Thaiss CA, Nowarski R, Henao-Mejia J, Zhang JP, Brown EM, et al. NLRP6 inflammasome orchestrates the colonic host-microbial interface by regulating goblet cell mucus secretion. *Cell.* 2014;156(5):1045–59.
115. Liu CY, Cham CM, Chang EB. Epithelial wound healing in inflammatory bowel diseases: the next therapeutic frontier. *Transl Res.* 2021;236:35–51.
116. Ungaro R, Mehandru S, Allen PB, Peyrin-Biroulet L, Colombel JF. Ulcerative colitis. *Lancet.* 2017;389(10080):1756–70.
117. Pastorelli L, Salvo C De, Mercado JR, Vecchi M, Pizarro TT. Central role of the gut epithelial barrier in the pathogenesis of chronic intestinal inflammation: Lessons learned from animal models and human genetics. *Front Immunol.* 2013;4:280.
118. Liu C, Wang H, Han L, Zhu Y, Ni S, Zhi J, et al. Targeting P2Y14R protects against necroptosis of intestinal epithelial cells through PKA/CREB/RIPK1 axis in ulcerative colitis. *Nat Commun.* 2024;15(1):2083.
119. Patankar J V, Becker C. Cell death in the gut epithelium and implications for chronic inflammation. *Nat Rev Gastroenterol Hepatol.* 2020;17(9):543–56.
120. Place DE, Kanneganti TD. Cell death-mediated cytokine release and its therapeutic implications. *J Exp Med.* 2019;216(7):1474–86.
121. Yamamoto-Furusho JK, Miranda-Pérez E, Fonseca-Camarillo G, Sánchez-Muñoz F, Dominguez-Lopez A, Barreto-Zuñiga R. Colonic epithelial upregulation of interleukin 22 (IL-22) in patients with ulcerative colitis. *Inflamm Bowel Dis.* 2010;16(11):1823.
122. Wan Y, Yang L, Jiang S, Qian D, Duan J. Excessive apoptosis in ulcerative colitis: crosstalk between apoptosis, ROS, ER stress, and intestinal Homeostasis. *Inflamm Bowel Dis.* 2022;28(4):639–48.
123. Diener C, Keller A, Meese E. The miRNA–target interactions: An underestimated intricacy. *Nucleic Acids Res.* 2024;52(4):1544–57.
124. Shang R, Lee S, Senavirathne G, Lai EC. microRNAs in action: biogenesis, function and regulation. *Nat Rev Genet.* 2023;24(12):816–33.
125. O’Brien J, Hayder H, Zayed Y, Peng C. Overview of microRNA biogenesis, mechanisms of actions, and circulation. *Front Endocrinol.* 2018;9:402.
126. Tian H, Cheng L, Liang Y, Lei H, Qin M, Li X, et al. MicroRNA therapeutic delivery strategies: A review. *J Drug Deliv Sci Technol.* 2024;93:105430.
127. Friedman RC, Farh KKH, Burge CB, Bartel DP. Most mammalian mRNAs are conserved targets of microRNAs. *Genome Res.* 2009;19(1):92–105.
128. Fehlmann T, Lehallier B, Schaum N, Hahn O, Kahraman M, Li Y, et al. Common diseases alter the physiological age-related blood microRNA profile. *Nat Commun.* 2020;11:5958.
129. Diener C, Keller A, Meese E. Emerging concepts of miRNA therapeutics: from cells to clinic. *Trends Genet.* 2022;38(6):613–26.
130. Bofill-De Ros X, Vang Ørom UA. Recent progress in miRNA biogenesis and decay. *RNA Biol.* 2024;21(1):1–8.
131. Medley JC, Panzade G, Zinovyeva AY. microRNA strand selection: Unwinding the rules. *Wiley Interdiscip Rev RNA.* 2021;12(3):e1627.

132. Havens MA, Reich AA, Duelli DM, Hastings ML. Biogenesis of mammalian microRNAs by a non-canonical processing pathway. *Nucleic Acids Res.* 2012;40(10):4626–40.
133. Matsuura-Suzuki E, Kiyokawa K, Iwasaki S, Tomari Y. The requirement of GW182 in miRNA-mediated gene silencing in Drosophila larval development. *bioRxiv* [preprint]. 2024.
134. de Mello AS, Ferguson BS, Shebs-Maurine EL, Giotto FM. MicroRNA biogenesis, gene regulation mechanisms, and availability in foods. *Non-coding RNA.* 2024;10(5):52.
135. de Rie D, Abugessaisa I, Alam T, Arner E, Arner P, Ashoor H, et al. An integrated expression atlas of miRNAs and their promoters in human and mouse. *Nat Biotechnol.* 2017;35(9):872–8.
136. Paul P, Chakraborty A, Sarkar D, Langthasa M, Rahman M, Bari M, et al. Interplay between miRNAs and human diseases. *J Cell Physiol.* 2018;233(3):2007–18.
137. Xu D, Di K, Fan B, Wu J, Gu X, Sun Y, et al. MicroRNAs in extracellular vesicles: Sorting mechanisms, diagnostic value, isolation, and detection technology. *Front Bioeng Biotechnol.* 2022;10:948959.
138. Sohel MH. Extracellular/Circulating microRNAs: Release mechanisms, functions and challenges. *Achiev Life Sci.* 2016;10(2):175–86.
139. Lee YJ, Shin KJ, Chae YC. Regulation of cargo selection in exosome biogenesis and its biomedical applications in cancer. *Exp Mol Med.* 2024;56(4):877–89.
140. Groot M, Lee H. Sorting mechanisms for microRNAs into extracellular vesicles and their associated diseases. *Cells.* 2020;9(4):1044.
141. Mitchell PS, Parkin RK, Kroh EM, Fritz BR, Wyman SK, Pogosova-Agadjanyan EL, et al. Circulating microRNAs as stable blood-based markers for cancer detection. *Proc Natl Acad Sci U S A.* 2008;105(30):10513–8.
142. Parashar D, Mukherjee T, Gupta S, Kumar U, Das K. MicroRNAs in extracellular vesicles: A potential role in cancer progression. *Cell Signal.* 2024;121:111263.
143. Wu Q, Li L, Jia Y, Xu T, Zhou X. Advances in studies of circulating microRNAs: origination, transportation, and distal target regulation. *J Cell Commun Signal.* 2023;17(3):445–55.
144. Bär C, Thomas T, and de Gonzalo-Calvo D. Circulating miRNAs as mediators in cell-to-cell communication. *Epigenomics.* 2019;11(2):111–3.
145. Schönauen K, Le N, von Arnim U, Schulz C, Malfertheiner P, Link A. Circulating and fecal microRNAs as biomarkers for inflammatory bowel diseases. *Inflamm Bowel Dis.* 2018;24(7):1547–57.
146. Malham M, James J, Jakobsen C, Høgdall E, Holmstroem K, Wewer V, et al. The mucosal microRNA profile relates to age and severity of disease in patients with ulcerative colitis. *Inflamm Bowel Dis.* 2021;27(Suppl 1):S11.
147. Casado-Bedmar M, Viennois E. MicroRNA and gut microbiota: Tiny but mighty – novel insights into their cross-talk in inflammatory bowel disease pathogenesis and therapeutics. *J Crohns Colitis.* 2022;16(6):992–1005.
148. Masi L, Capobianco I, Magri C, Marafini I, Petito V, Scaldaferri F. MicroRNAs as innovative biomarkers for inflammatory bowel disease and prediction of colorectal cancer. *Int J Mol Sci.* 2022;23(14):7991.
149. Onisor D, Brusnic O, Banescu C, Carstea C, Sasaran M, Stoian M, et al. miR-155 and miR-21 as diagnostic and therapeutic biomarkers for ulcerative colitis: There is still a long way to go. *Biomedicines.* 2024;12(6):1315.

150. Thorlacius-Ussing G, Schnack Nielsen B, Andersen V, Holmstrøm K, Pedersen AE. Expression and localization of miR-21 and miR-126 in mucosal tissue from patients with inflammatory bowel disease. *Inflamm Bowel Dis*. 2017;23(5):739–52.
151. Yan H, Zhang X, Xu Y. Aberrant expression of miR-21 in patients with inflammatory bowel disease: A protocol for systematic review and meta analysis. *Medicine*. 2020;99(17):e19693.
152. Kalla R, Ventham NT, Kennedy NA, Quintana JF, Nimmo ER, Buck AH, et al. MicroRNAs: New players in IBD. *Gut*. 2015;64(3):504–17.
153. Shi T, Xie Y, Fu Y, Zhou Q, Ma Z, Ma J, et al. The signaling axis of microRNA-31/interleukin-25 regulates Th1/Th17-mediated inflammation response in colitis. *Mucosal Immunol*. 2017;10(4):983–95.
154. Tian Y, Xu J, Li Y, Zhao R, Du S, Lv C, et al. MicroRNA-31 reduces inflammatory signaling and promotes regeneration in colon epithelium, and delivery of mimics in microspheres reduces colitis in mice. *Gastroenterology*. 2019;156(8):2281-96.e6.
155. Wu F, Zikusoka M, Trindade A, Dassopoulos T, Harris ML, Bayless TM, et al. MicroRNAs are differentially expressed in ulcerative colitis and alter expression of macrophage inflammatory peptide-2 α . *Gastroenterology*. 2008;135(5):1624-35.e24.
156. Iliopoulos D, Hirsch HA, Struhl K. An epigenetic switch involving NF- κ B, lin28, let-7 microRNA, and IL6 links inflammation to cell transformation. *Cell*. 2009;139(4):693–706.
157. Paraskevi A, Theodoropoulos G, Papaconstantinou I, Mantzaris G, Nikiteas N, Gazouli M. Circulating microRNA in inflammatory bowel disease. *J Crohns Colitis*. 2012; 6(9):900–4.
158. Rashid H, Hossain B, Siddiqua T, Kabir M, Noor Z, Ahmed M, et al. Fecal microRNAs as potential biomarkers for screening and diagnosis of intestinal diseases. *Front Mol Biosci*. 2020;7:181.
159. Verdier J, Breunig IR, Ohse MC, Roubrocks S, Kleinfeld S, Roy S, et al. Faecal microRNAs in inflammatory bowel diseases. *J Crohns Colitis*. 2020;14(1):110–7.
160. Wu F, Zikusoka M, Trindade A, Dassopoulos T, Harris ML, Bayless TM, et al. MicroRNAs are differentially expressed in ulcerative colitis and alter expression of macrophage inflammatory peptide-2 α . *Gastroenterology*. 2008;135(5):1624-35.e24.
161. James JP, Riis LB, Malham M, Høgdall E, Langholz E, Nielsen BS. MicroRNA biomarkers in IBD-differential diagnosis and prediction of colitis-associated cancer. Vol. 21, *Int J Mol Sci*. 2020;21(21):1–19.
162. Zhu F, Li H, Liu Y, Tan C, Liu X, Fan H, et al. miR-155 antagomir protect against DSS-induced colitis in mice through regulating Th17/Treg cell balance by Jarid2/Wnt/ β -catenin. *Biomed Pharmacother*. 2020;126:109909.
163. He C, Shi Y, Wu R, Sun M, Fang L, Wu W, et al. miR-301a promotes intestinal mucosal inflammation through induction of IL-17A and TNF- α in IBD. *Gut*. 2016;65(12):1938-50.
164. Yan R, Liang X, Hu J. miR-141-3p alleviates ulcerative colitis by targeting SUGT1 to inhibit colonic epithelial cell pyroptosis. *Autoimmunity*. 2023;56(1):2220988.
165. Yang Y, Ma Y, Shi C, Chen H, Zhang H, Chen N, et al. Overexpression of miR-21 in patients with ulcerative colitis impairs intestinal epithelial barrier function through targeting the Rho GTPase RhoB. *Biochem Biophys Res Commun*. 2013;434(4):746–52.
166. Nakata K, Sugi Y, Narabayashi H, Kobayakawa T, Nakanishi Y, Tsuda M, et al. Commensal microbiota-induced microRNA modulates intestinal epithelial permeability through the small GTPase ARF4. *J Biol Chem*. 2017;292(37):15426–33.

167. Liu Z, Li C, Chen S, Lin H, Zhao H, Liu M, et al. MicroRNA-21 increases the expression level of occludin through regulating ROCK1 in prevention of intestinal barrier dysfunction. *J Cell Biochem.* 2019;120(3):4545–54.
168. Li M, Zhao J, Cao M, Liu R, Chen G, Li S, et al. Mast cells-derived miR-223 destroys intestinal barrier function by inhibition of CLDN8 expression in intestinal epithelial cells. *Biol Res.* 2020;53:12.
169. Wang H, Chao K, Ng SC, Bai AH, Yu Q, Yu J, et al. Pro-inflammatory miR-223 mediates the cross-talk between the IL23 pathway and the intestinal barrier in inflammatory bowel disease. *Genome Biol.* 2016;17:58.
170. Tili E, Michaille JJ, Piurowski V, Rigot B, Croce CM. MicroRNAs in intestinal barrier function, inflammatory bowel disease and related cancers – their effects and therapeutic potentials. *Curr Opin Pharmacol.* 2017;37:142–50.
171. Haines RJ, Beard RS, Eitner RA, Chen L, Wu MH. TNF α /IFN γ mediated intestinal epithelial barrier dysfunction is attenuated by microRNA-93 downregulation of PTK6 in mouse colonic epithelial cells. *PLoS One.* 2016;11(4):e0154351.
172. Martínez C, Rodiño-Janeiro BK, Lobo B, Stanifer ML, Klaus B, Granzow M, et al. miR-16 and miR-125b are involved in barrier function dysregulation through the modulation of claudin-2 and cingulin expression in the jejunum in IBS with diarrhoea. *Gut.* 2017;66(9):1537–8.
173. Fukata T, Mizushima T, Nishimura J, Okuzaki D, Wu X, Hirose H, et al. The supercarbonate apatite-microRNA complex inhibits dextran sodium sulfate-induced colitis. *Mol Ther Nucleic Acids.* 2018;12:658–71.
174. Brain O, Owens BMJ, Pichulik T, Allan P, Khatamzas E, Leslie A, et al. The intracellular sensor NOD2 induces microrna-29 expression in human dendritic cells to limit IL-23 release. *Immunity.* 2013;39(3):521–36.
175. Monaghan TM, Seekatz AM, Markham NO, Yau TO, Hatziapostolou M, Jilani T, et al. Fecal microbiota transplantation for recurrent clostridioides difficile infection associates with functional alterations in circulating microRNAs. *Gastroenterology.* 2021; 161(1):255-70.e4.
176. Martens EC, Neumann M, Desai MS. Interactions of commensal and pathogenic microorganisms with the intestinal mucosal barrier. *Nat Rev Microbiol.* 2018;16(8): 457–70.
177. Ma Z, Zuo T, Frey N, Rangrez AY. A systematic framework for understanding the microbiome in human health and disease: from basic principles to clinical translation. *Signal Transduct Target Ther.* 2024;9(1):237.
178. Daniel N, Lécuyer E, Chassaing B. Host/microbiota interactions in health and diseases – time for mucosal microbiology! *Mucosal Immunol.* 2021;14(5):1006–16.
179. Vollger MR, Guitart X, Dishuck PC, Mercuri L, Harvey WT, Gershman A, et al. Segmental duplications and their variation in a complete human genome. *Science.* 2025;376(6588):eabj6965.
180. Nava GM, Friedrichsen HJ, Stappenbeck TS. Spatial organization of intestinal microbiota in the mouse ascending colon. *ISME J.* 2011;5(4):627–38.
181. Christian M, Sabrina D, Francesca B, Eoghan C, Francesca T, Jennifer M, et al. The first microbial colonizers of the human gut: Composition, activities, and health implications of the infant gut microbiota. *Microbiol Mol Biol Rev.* 2017;81(4):10-1128.
182. Huttenhower C, Gevers D, Knight R, Abubucker S, Badger JH, Chinwalla AT, et al. Structure, function and diversity of the healthy human microbiome. *Nature.* 2012; 486(7402):207–14.

183. She JJ, Liu WX, Ding XM, Guo G, Han J, Shi FY, et al. Defining the biogeographical map and potential bacterial translocation of microbiome in human 'surface organs'. *Nat Commun.* 2024;15:427.
184. Eshleman EM, Alenghat T. Epithelial sensing of microbiota-derived signals. *Genes Immun.* 2021;22(5):237–46.
185. Krautkramer KA, Fan J, Bäckhed F. Gut microbial metabolites as multi-kingdom intermediates. *Nat Rev Microbiol.* 2021;19(2):77–94.
186. Glover JS, Ticer TD, Engevik MA. Characterizing the mucin-degrading capacity of the human gut microbiota. *Sci Rep.* 2022;12:8456.
187. Caballero-Flores G, Pickard JM, Núñez G. Microbiota-mediated colonization resistance: mechanisms and regulation. *Nat Rev Microbiol.* 2023;21(6):347–60.
188. Le Berre C, Honap S, Peyrin-Biroulet L. Ulcerative colitis. *Lancet.* 2023;402(10401):571–84.
189. Machiels K, Joossens M, Sabino J, De Preter V, Arijis I, Eeckhaut V, et al. A decrease of the butyrate-producing species *Roseburia hominis* and *Faecalibacterium prausnitzii* defines dysbiosis in patients with ulcerative colitis. *Gut.* 2014;63(8):1275–83.
190. Zou X, Ji J, Qu H, Wang J, Shu DM, Wang Y, et al. Effects of sodium butyrate on intestinal health and gut microbiota composition during intestinal inflammation progression in broilers. *Poult Sci.* 2019;98(10):4449–56.
191. Nishihara Y, Ogino H, Tanaka M, Ihara E, Fukaura K, Nishioka K, et al. Mucosa-associated gut microbiota reflects clinical course of ulcerative colitis. *Sci Rep.* 2021;11:13743.
192. Ni J, Wu GD, Albenberg L, Tomov VT. Gut microbiota and IBD: Causation or correlation? *Nat Rev Gastroenterol Hepatol.* 2017;14(10):573–84.
193. Paramsothy S, Paramsothy R, Rubin DT, Kamm MA, Kaakoush NO, Mitchell HM, et al. Faecal microbiota transplantation for inflammatory bowel disease: A systematic review and meta-analysis. *J Crohns Colitis.* 2017;11(10):1180–99.
194. Caruso R, Lo BC, Núñez G. Host–microbiota interactions in inflammatory bowel disease. *Nat Rev Immunol.* 2020;20(7):411–26.
195. Caruso R, Warner N, Inohara N, Núñez G. NOD1 and NOD2: Signaling, host defense, and inflammatory disease. *Immunity.* 2014;41(6):898–908.
196. Dai W, Long L, Wang X, Li S, Xu H. Phytochemicals targeting Toll-like receptors 4 (TLR4) in inflammatory bowel disease. *Chin Med.* 2022;17(1):53.
197. Macia L, Tan J, Vieira AT, Leach K, Stanley D, Luong S, et al. Metabolite-sensing receptors GPR43 and GPR109A facilitate dietary fibre-induced gut homeostasis through regulation of the inflammasome. *Nat Commun.* 2015;6:6734.
198. Fang J, Wang H, Zhou Y, Zhang H, Zhou H, Zhang X. Slimy partners: the mucus barrier and gut microbiome in ulcerative colitis. *Exp Mol Med.* 2021;53(5):772–87.
199. Lavelle A, Sokol H. Gut microbiota-derived metabolites as key actors in inflammatory bowel disease. *Nat Rev Gastroenterol Hepatol.* 2020;17(4):223–37.
200. Taelman J, Diaz M, Guiu J. Human intestinal organoids: Promise and challenge. *Front Cell Dev Biol.* 2022;10:903292.
201. Tian C mei, Yang M feng, Xu H ming, Zhu M zheng, Yue NN, Zhang Y, et al. Stem cell-derived intestinal organoids: a novel modality for IBD. *Cell Death Discov.* 2023;9(1):255.
202. Gómez DP, Boudreau F. Organoids and their use in modeling gut epithelial cell lineage differentiation and barrier properties during intestinal diseases. *Front Cell Dev Biol.* 2021;9:745409.

203. Kromann EH, Cearra AP, Neves JF. Organoids as a tool to study homeostatic and pathological immune–epithelial interactions in the gut. *Clin Exp Immunol.* 2024; 218(1):28–39.
204. Sato T, Vries RG, Snippert HJ, van de Wetering M, Barker N, Stange DE, et al. Single Lgr5 stem cells build crypt-villus structures in vitro without a mesenchymal niche. *Nature.* 2009;459(7244):262–5.
205. Parente IA, Chiara L, Bertoni S. Exploring the potential of human intestinal organoids: Applications, challenges, and future directions. *Life Sci.* 2024;352:122875.
206. Zhao Z, Chen X, Dowbaj AM, Sljukic A, Bratlie K, Lin L, et al. Organoids. *Nat Rev Methods Primers.* 2022;2:94.
207. Ylostalo JH. 3D Stem Cell Culture. *Cells.* 2020;9(10):2178.
208. Edgar RD, Perrone F, Foster AR, Payne F, Lewis S, Nayak KM, et al. Culture-associated DNA methylation changes impact on cellular function of human intestinal organoids. *Cell Mol Gastroenterol Hepatol.* 2022;14(6):1295–310.
209. Clinton J, McWilliams-Koeppen P. Initiation, expansion, and cryopreservation of human primary tissue-derived normal and diseased organoids in embedded three-dimensional culture. *Curr Protoc Cell Biol.* 2019;82:e66.
210. Ghorbaninejad M, Asadzadeh-Aghdai H, Baharvand H, Meyfour A. Intestinal organoids: A versatile platform for modeling gastrointestinal diseases and monitoring epigenetic alterations. *Life Sci.* 2023;319:121506.
211. Xiang T, Wang J, Li H. Current applications of intestinal organoids: a review. *Stem Cell Res Ther.* 2024;15(1):155.
212. Pleguezuelos-Manzano C, Puschhof J, van den Brink S, Geurts V, Beumer J, Clevers H. Establishment and culture of human intestinal organoids derived from adult stem cells. *Curr Protoc Immunol.* 2020;130:e106.
213. Rahman S, Ghiboub M, Donkers JM, van de Steeg E, van Tol EAF, Hakvoort TBM, et al. The progress of intestinal epithelial models from cell lines to gut-on-chip. *Int J Mol Sci.* 2021;22(24):13472.
214. Lock JY, Carlson TL, Carrier RL. Mucus models to evaluate the diffusion of drugs and particles. *Adv Drug Deliv Rev.* 2018;124:34–49.
215. Wang Y, Kim R, Sims CE, Allbritton NL. Building a thick mucus hydrogel layer to improve the physiological relevance of in vitro primary colonic epithelial models. *Cell Mol Gastroenterol Hepatol.* 2019;8(4):653-55.e5.
216. Kollmann C, Buerkert H, Meir M, Richter K, Kretschmar K, Flemming S, et al. Human organoids are superior to cell culture models for intestinal barrier research. *Front Cell Dev Biol.* 2023;11:1223032.
217. Kelsen JR, Dawany N, Conrad MA, Karakasheva TA, Maurer K, Wei JM, et al. Colonoids from patients with pediatric inflammatory bowel disease exhibit decreased growth associated with inflammation severity and durable upregulation of antigen presentation genes. *Inflamm Bowel Dis.* 2021;27(2):256–67.
218. Singh V, Johnson K, Yin J, Lee S, Lin R, Yu H, et al. Chronic inflammation in ulcerative colitis causes long-term changes in goblet cell function. *Cell Mol Gastroenterol Hepatol.* 2022;13(1):219–32.
219. Meir M, Salm J, Fey C, Schweinlin M, Kollmann C, Kannapin F, et al. Enteroids generated from patients with severe inflammation in Crohn’s disease maintain alterations of junctional proteins. *J Crohns Colitis.* 2020;14(10):1473–87.
220. d’Aldebert E, Quaranta M, Sébert M, Bonnet D, Kirzin S, Portier G, et al. Characterization of human colon organoids from inflammatory bowel disease patients. *Front Cell Dev Biol.* 2020;8:363.

221. Rutherford D, Ho GT. Therapeutic potential of human intestinal organoids in tissue repair approaches in inflammatory bowel diseases. *Inflamm Bowel Dis.* 2023;29(9):1488–98.
222. Pavlidis P, Tsakmaki A, Pantazi E, Li K, Cozzetto D, Digby- Bell J, et al. Interleukin-22 regulates neutrophil recruitment in ulcerative colitis and is associated with resistance to ustekinumab therapy. *Nat Commun.* 2022;13:5820.
223. Sugimoto S, Ohta Y, Fujii M, Matano M, Shimokawa M, Nanki K, et al. Reconstruction of the human colon epithelium in vivo. *Cell Stem Cell.* 2018;22(2):171–6.e5.
224. Puschhof J, Pleguezuelos-Manzano C, Martinez-Silgado A, Akkerman N, Saftien A, Boot C, et al. Intestinal organoid cocultures with microbes. *Nat Protoc.* 2021;16(10):4633–49.
225. Engevik MA, Engevik KA, Yacyshyn MB, Wang J, Hassett DJ, Darien B, et al. Human *Clostridium difficile* infection: Inhibition of NHE3 and microbiota profile. *Am J Physiol Gastrointest Liver Physiol.* 2014;308(6):G497–509.
226. Hou Q, Ye L, Liu H, Huang L, Yang Q, Turner JR, et al. *Lactobacillus* accelerates ISCs regeneration to protect the integrity of intestinal mucosa through activation of STAT3 signaling pathway induced by LPLs secretion of IL-22. *Cell Death Differ.* 2018;25(9):1657–70.
227. Arnauts K, Sudhakar P, Verstockt S, Lapierre C, Potche S, Caenepeel C, et al. Microbiota, not host origin drives ex vivo intestinal epithelial responses. *Gut Microbes.* 2022;14(1):2089003.
228. Rees WD, Telkar N, Lin DTS, Wong MQ, Poloni C, Fathi A, et al. An in vitro chronic damage model impairs inflammatory and regenerative responses in human colonoid monolayers. *Cell Rep.* 2022;38(3):110283.
229. Rouch JD, Scott A, Lei NY, Solorzano-Vargas RS, Wang J, Hanson EM, et al. Development of functional Microfold (M) cells from intestinal stem cells in primary human enteroids. *PLoS One.* 2016;11(1):e0148216.
230. Mollaki V. Ethical challenges in organoid use. *BioTech.* 2021;10(3):12.
231. de Jongh D, Massey EK, Berishvili E, Fonseca LM, Lebreton F, Bellofatto K, et al. Organoids: a systematic review of ethical issues. *Stem Cell Res Ther.* 2022;13(1):337.
232. Hirokawa Y, Clarke J, Palmieri M, Tan T, Mouradov D, Li S, et al. Low-viscosity matrix suspension culture enables scalable analysis of patient-derived organoids and tumoroids from the large intestine. *Commun Biol.* 2021;4(1):1067.
233. Arnauts K, Verstockt B, Ramalho AS, Vermeire S, Verfaillie C, Ferrante M. Ex vivo mimicking of inflammation in organoids derived from patients with ulcerative colitis. *Gastroenterology.* 2020;159(4):1564–7.
234. Noel G, Baetz NW, Staab JF, Donowitz M, Kovbasnjuk O, Pasetti MF, et al. A primary human macrophage-enteroid co-culture model to investigate mucosal gut physiology and host-pathogen interactions. *Sci Rep.* 2017;7:45270.
235. Magro F, Gionchetti P, Eliakim R, Ardizzone S, Armuzzi A, Barreiro-de Acosta M, et al. Third European evidence-based consensus on diagnosis and management of ulcerative colitis. Part 1: Definitions, diagnosis, extra-intestinal manifestations, pregnancy, cancer surveillance, surgery, and ileo-anal pouch disorders. *J Crohns Colitis.* 2017;11(6):649–70.
236. Schroeder KW, Tremaine WJ, Ilstrup DM. Coated oral 5-aminosalicylic acid therapy for mildly to moderately active ulcerative colitis. A randomized study. *N Engl J Med.* 1987;317(26):1625–9.
237. Inciuraite R, Ramonaite R, Kupcinskas J, Dalgiediene I, Kulokiene U, Kiudelis V, et al. The microRNA expression in crypt-top and crypt-bottom colonic epithelial cell

- populations demonstrates cell-type specificity and correlates with endoscopic activity in ulcerative colitis. *J Crohns Colitis*. 2024;18(12):2033–44.
238. Dalerba P, Kalisky T, Sahoo D, Rajendran PS, Rothenberg ME, Leyrat AA, et al. Single-cell dissection of transcriptional heterogeneity in human colon tumors. *Nat Biotechnol*. 2011;29(12):1120–7.
 239. Livak KJ, Schmittgen TD. Analysis of relative gene expression data using real-time quantitative PCR and the 2- $\Delta\Delta$ CT method. *Methods*. 2001;25(4):402–8.
 240. Ewels PA, Peltzer A, Fillinger S, Patel H, Alneberg J, Wilm A, et al. The nf-core framework for community-curated bioinformatics pipelines. *Nat Biotechnol*. 2020;38(3):276–8.
 241. Kozomara A, Birgaoanu M, Griffiths-Jones S. miRBase: from microRNA sequences to function. *Nucleic Acids Res*. 2019;47(D1):D155–62.
 242. Desvignes T, Loher P, Eilbeck K, Ma J, Urgese G, Fromm B, et al. Unification of miRNA and isomiR research: the mirGFF3 format and the mirtop API. *Bioinformatics*. 2020;36(3):698–703.
 243. Love MI, Huber W, Anders S. Moderated estimation of fold change and dispersion for RNA-seq data with DESeq2. *Genome Biol*. 2014;15(12):1–21.
 244. Ritchie ME, Phipson B, Wu D, Hu Y, Law CW, Shi W, et al. limma powers differential expression analyses for RNA-sequencing and microarray studies. *Nucleic Acids Res*. 2015;43(7):e47.
 245. Wickham H. *ggplot2: Elegant Graphics for Data Analysis*. 2nd ed. Cham: Springer; 2016.
 246. Jassal B, Matthews L, Viteri G, Gong C, Lorente P, Fabregat A, et al. The reactome pathway knowledgebase. *Nucleic Acids Res*. 2020;48(D1):D498–503.
 247. Thomas PD, Ebert D, Muruganujan A, Mushayahama T, Albou LP, Mi H. PANTHER: Making genome-scale phylogenetics accessible to all. *Protein Sci*. 2022;31(1):8–22.
 248. Xiao F, Zuo Z, Cai G, Kang S, Gao X, Li T. miRecords: an integrated resource for microRNA-target interactions. *Nucleic Acids Res*. 2009;37(Database issue):D105–10.
 249. Hsu SD, Lin FM, Wu WY, Liang C, Huang WC, Chan WL, et al. miRTarBase: a database curates experimentally validated microRNA-target interactions. *Nucleic Acids Res*. 2011;39(Database issue):D163–9.
 250. Karagkouni D, Paraskevopoulou MD, Chatzopoulos S, Vlachos IS, Tastsoglou S, Kanellos I, et al. DIANA-TarBase v8: a decade-long collection of experimentally supported miRNA-gene interactions. *Nucleic Acids Res*. 2018;46(D1):D239–45.
 251. Ru Y, Kechris KJ, Tabakoff B, Hoffman P, Radcliffe RA, Bowler R, et al. The multiMiR R package and database: integration of microRNA-target interactions along with their disease and drug associations. *Nucleic Acids Res*. 2014;42(17):e133.
 252. Yu G, He QY. ReactomePA: an R/Bioconductor package for reactome pathway analysis and visualization. *Mol Biosyst*. 2016;12(2):477–9.
 253. Wu T, Hu E, Xu S, Chen M, Guo P, Dai Z, et al. clusterProfiler 4.0: A universal enrichment tool for interpreting omics data. *Innovation (Camb)*. 2021;2(3):100141.
 254. Russo PST, Ferreira GR, Cardozo LE, Bürger MC, Arias-Carrasco R, Maruyama SR, et al. CEMiTool: a Bioconductor package for performing comprehensive modular co-expression analyses. *BMC Bioinformatics*. 2018;19(1):56.
 255. Langfelder P, Horvath S. WGCNA: an R package for weighted correlation network analysis. *BMC Bioinformatics*. 2008;9(1):559.
 256. Robin X, Turck N, Hainard A, Tiberti N, Lisacek F, Sanchez JC, et al. pROC: an open-source package for R and S+ to analyze and compare ROC curves. *BMC Bioinformatics*. 2011;12(1):77.

257. Inciuraitė R, Gedgaudas R, Lukosevicius R, Tilinde D, Ramonaite R, Link A, et al. Constituents of stable commensal microbiota imply diverse colonic epithelial cell reactivity in patients with ulcerative colitis. *Gut Pathog.* 2024;16(1):16.
258. Maidak BL, Olsen GJ, Larsen N, Overbeek R, McCaughey MJ, Woese CR. The RDP (Ribosomal Database Project). *Nucleic Acids Res.* 1997;25(1):109–11.
259. Callahan BJ, McMurdie PJ, Rosen MJ, Han AW, Johnson AJA, Holmes SP. DADA2: High-resolution sample inference from Illumina amplicon data. *Nat Methods.* 2016;13(7):581–3.
260. Barnett D, Arts I, Penders J. microViz: an R package for microbiome data visualization and statistics. *J Open Source Softw.* 2021;6(63):3201.
261. Inciuraitė R, Steponaitienė R, Raudze O, Kulokiene U, Kiudelis V, Lukosevicius R, et al. Prolonged culturing of colonic epithelial organoids derived from healthy individuals and ulcerative colitis patients results in the decrease of LINE-1 methylation level. *Sci Rep.* 2024;14(1):4456.
262. Kupcinskis J, Steponaitienė R, Langner C, Smailyte G, Skieceviciene J, Kupcinskis L, et al. LINE-1 hypomethylation is not a common event in preneoplastic stages of gastric carcinogenesis. *Sci Rep.* 2017;7(1):4828.
263. Schernhammer ES, Giovannucci E, Kawasaki T, Rosner B, Fuchs CS, Ogino S. Dietary folate, alcohol and B vitamins in relation to LINE-1 hypomethylation in colon cancer. *Gut.* 2010;59(6):794–9.
264. Ogino S, Nishihara R, Lochhead P, Imamura Y, Kuchiba A, Morikawa T, et al. Prospective study of family history and colorectal cancer risk by tumor LINE-1 methylation level. *J Natl Cancer Inst.* 2013;105(2):130–40.
265. Théry C, Witwer KW, Aikawa E, Jose Alcaraz M, Anderson JD, Andriantsitohaina R, et al. Minimal information for studies of extracellular vesicles 2018 (MISEV2018): a position statement of the International Society for Extracellular Vesicles and update of the MISEV2014 guidelines. *J Extracell Vesicles.* 2018;7(1):1535750.
266. Kery MB, Feldman M, Livny J, Tjaden B. TargetRNA2: Identifying targets of small regulatory RNAs in bacteria. *Nucleic Acids Res.* 2014;42(Web Server issue):W124–9.
267. Ahlmann-Eltze C, Patil I. ggsignif: R Package for Displaying Significance Brackets for 'ggplot2'. [preprint]. 2021. Available from: <https://osf.io/7awm6>.
268. Wickham H, Averick M, Bryan J, Chang W, McGowan L, François R, et al. Welcome to the Tidyverse. *J Open Source Softw.* 2019;4(43):1686.
269. Zheng D, Liwinski T, Elinav E. Interaction between microbiota and immunity in health and disease. *Cell Res.* 2020;30(6):492–506.
270. Wu F, Xing T, Gao X, Liu F. miR 501 3p promotes colorectal cancer progression via activation of Wnt/ β catenin signaling. *Int J Oncol.* 2019;55(3):671–83.
271. Akao Y, Nakagawa Y, Naoe T. let-7 microRNA functions as a potential growth suppressor in human colon cancer cells. *Biol Pharm Bull.* 2006;29(5):903–6.
272. Sun TY, Li YQ, Zhao FQ, Sun HM, Gao Y, Wu B, et al. MiR-1-3p and miR-124-3p synergistically damage the intestinal barrier in the ageing colon. *J Crohns Colitis.* 2022;16(4):656–67.
273. Tahamant A, Teymoori-Rad M, Nakstad B, Salimi V. Anti-Inflammatory microRNAs and their potential for inflammatory diseases treatment. *Front Immunol.* 2018;9:1377.
274. Hübenthal M, Franke A, Lipinski S, Juzenas S. MicroRNAs and inflammatory bowel disease. In: Hedin C, Rioux JD, D'Amato M, editors. *Molecular Genetics of Inflammatory Bowel Disease.* Springer, Cham. 2019;203–30.
275. Pasparakis M. IKK/NF-kappaB signaling in intestinal epithelial cells controls immune homeostasis in the gut. *Mucosal Immunol.* 2008;1(Suppl 1):S54–7.

276. Cai M, Chen S, Hu W. MicroRNA-141 is involved in ulcerative colitis pathogenesis via aiming at CXCL5. *J Interferon Cytokine Res.* 2017;37(9):415–20.
277. Chirshhev E, Oberg KC, Ioffe YJ, Unternaehrer JJ. Let-7 as biomarker, prognostic indicator, and therapy for precision medicine in cancer. *Clin Transl Med.* 2019;8(1):24.
278. Tian Y, Xu J, Li Y, Zhao R, Du S, Lv C, et al. MicroRNA-31 reduces inflammatory signaling and promotes regeneration in colon epithelium, and delivery of mimics in microspheres reduces colitis in mice. *Gastroenterology.* 2019;156(8):2281-96.e6.
279. Su C, Huang DP, Liu JW, Liu WY, Cao YO. miR-27a-3p regulates proliferation and apoptosis of colon cancer cells by potentially targeting BTG1. *Oncol Lett.* 2019; 18(3):2825–34.
280. Zhou J, Liu J, Gao Y, Shen L, Li S, Chen S. miRNA-based potential biomarkers and new molecular insights in ulcerative colitis. *Front Pharmacol.* 2021;12:707776.
281. Béres NJ, Szabó D, Kocsis D, Szűcs D, Kiss Z, Müller KE, et al. Role of altered expression of miR-146a, miR-155, and miR-122 in pediatric patients with inflammatory bowel disease. *Inflamm Bowel Dis.* 2016;22(2):327–35.
282. Gwiggner M, Martinez-Nunez RT, Whiteoak SR, Bondanese VP, Claridge A, Collins JE, et al. MicroRNA-31 and microRNA-155 are overexpressed in ulcerative colitis and regulate IL-13 signaling by targeting interleukin 13 receptor α -1. *Genes.* 2018;9(2):85.
283. Xia F, Bo W, Ding J, Yu Y, Wang J. MiR-222-3p aggravates the inflammatory response by targeting SOCS1 to activate STAT3 signaling in ulcerative colitis. *Turk J Gastroenterol.* 2022;33(11):934–44.
284. Saatian B, Rezaee F, Desando S, Emo J, Chapman T, Knowlden S, et al. Interleukin-4 and interleukin-13 cause barrier dysfunction in human airway epithelial cells. *Tissue Barriers.* 2013;1(2):e24333.
285. Hertati A, Hayashi S, Ogawa Y, Yamamoto T, Kadowaki M. Interleukin-4 receptor α subunit deficiency alleviates murine intestinal inflammation in vivo through the enhancement of intestinal mucosal barrier function. *Front Pharmacol.* 2020 Oct 28; 11:573470.
286. Heller F, Florian P, Bojarski C, Richter J, Christ M, Hillenbrand B, et al. Interleukin-13 is the key effector Th2 cytokine in ulcerative colitis that affects epithelial tight junctions, apoptosis, and cell restitution. *Gastroenterology.* 2005;129(2):550–64.
287. Rosen MJ, Frey MR, Washington MK, Chaturvedi R, Kuhnhein LA, Matta P, et al. STAT6 activation in ulcerative colitis: a new target for prevention of IL-13-induced colon epithelial cell dysfunction. *Inflamm Bowel Dis.* 2011;17(11):2224–34.
288. Kadivar K, Ruchelli ED, Markowitz JE, Defelice ML, Strogatz ML, Kanzaria MM, et al. Intestinal interleukin-13 in pediatric inflammatory bowel disease patients. *Inflamm Bowel Dis.* 2004;10(5):593–8.
289. Giuffrida P, Caprioli F, Facciotti F, Di Sabatino A. The role of interleukin-13 in chronic inflammatory intestinal disorders. *Autoimmun Rev.* 2019;18(5):549–55.
290. Karnele EP, Pasricha TS, Ramalingam TR, Thompson RW, Gieseck RL 3rd, Knilans KJ, et al. Anti-IL-13R α 2 therapy promotes recovery in a murine model of inflammatory bowel disease. *Mucosal Immunol.* 2019;12(5):1174–86.
291. Heeb LEM, Egholm C, Boyman O. Evolution and function of interleukin-4 receptor signaling in adaptive immunity and neutrophils. *Genes Immun.* 2020;21(3):143–9.
292. Min M, Yang J, Yang YS, Liu Y, Liu LM, Xu Y. Expression of transcription factor FOXO3a is decreased in patients with ulcerative colitis. *Chin Med J.* 2015;128(20): 2759–63.

293. Bidgood GM, Keating N, Doggett K, Nicholson SE. SOCS1 is a critical checkpoint in immune homeostasis, inflammation and tumor immunity. *Front Immunol.* 2024; 15:1419951.
294. Doran E, Choy DF, Shikotra A, Butler CA, O'Rourke DM, Johnston JA, et al. Reduced epithelial suppressor of cytokine signalling 1 in severe eosinophilic asthma. *Eur Respir J.* 2016;48(3):715–25.
295. Wang H, Hu DQ, Xiao Q, Liu YB, Song J, Liang Y, et al. Defective STING expression potentiates IL-13 signaling in epithelial cells in eosinophilic chronic rhinosinusitis with nasal polyps. *J Allergy Clin Immunol.* 2021;147(5):1692–703.
296. Jacenik D, Zielińska M, Mokrowiecka A, Michlewska S, Małecka-Panas E, Kordek R, et al. G protein-coupled estrogen receptor mediates anti-inflammatory action in Crohn's disease. *Sci Rep.* 2019;9(1):6749.
297. Krndija D, El Marjou F, Guirao B, Richon S, Leroy O, Bellaiche Y, et al. Active cell migration is critical for steady-state epithelial turnover in the gut. *Science.* 2019; 365(6454):705–10.
298. Martini E, Krug SM, Siegmund B, Neurath MF, Becker C. Mend your fences: The epithelial barrier and its relationship with mucosal immunity in inflammatory bowel disease. *Cell Mol Gastroenterol Hepatol.* 2017;4(1):33–46.
299. Godard P, van Eyll J. Pathway analysis from lists of microRNAs: common pitfalls and alternative strategy. *Nucleic Acids Res.* 2015;43(7):3490–7.
300. Malham M, Vestergaard M V, Bataillon T, Villesen P, Dempfle A, Bang C, et al. The composition of the fecal and mucosa-adherent microbiota varies based on age and disease activity in ulcerative colitis. *Inflamm Bowel Dis.* 2025;31(2):501–13.
301. Alam MT, Amos GCA, Murphy ARJ, Murch S, Wellington EMH, Arasaradnam RP. Microbial imbalance in inflammatory bowel disease patients at different taxonomic levels. *Gut Pathog.* 2020;12:1.
302. Gong D, Gong X, Wang L, Yu X, Dong Q. Involvement of reduced microbial diversity in inflammatory bowel disease. *Gastroenterol Res Pract.* 2016;2016(1):6951091.
303. Zhu R, Tang J, Xing C, Nan Q, Liang G, Luo J, et al. The distinguishing bacterial features from active and remission stages of ulcerative colitis revealed by paired fecal metagenomes. *Front Microbiol.* 2022;13:883495.
304. Cipelli M, da Silva EM, Câmara NOS. Gut microbiota resilience mechanisms against pathogen infection and its role in inflammatory bowel disease. *Curr Clin Microbiol Rep.* 2023;10(4):187–97.
305. Di Vincenzo F, Del Gaudio A, Petito V, Lopetuso LR, Scaldaferri F. Gut microbiota, intestinal permeability, and systemic inflammation: a narrative review. *Intern Emerg Med.* 2024;19(2):275–93.
306. de Meij TGJ, de Groot EFJ, Peeters CFW, de Boer NKH, Kneepkens CMF, Eck A, et al. Variability of core microbiota in newly diagnosed treatment-naïve paediatric inflammatory bowel disease patients. *PLoS One.* 2018;13(8):e0197649.
307. Elmassry MM, Sugihara K, Chankhamjon P, Kim Y, Camacho FR, Wang S, et al. A meta-analysis of the gut microbiome in inflammatory bowel disease patients identifies disease-associated small molecules. *Cell Host Microbe.* 2025;33(2):218–34.e12.
308. Zakerska-Banaszak O, Tomczak H, Gabryel M, Batur A, Wolko L, Michalak M, et al. Dysbiosis of gut microbiota in Polish patients with ulcerative colitis: a pilot study. *Sci Rep.* 2021;11(1):2166.
309. Herrera-deGuise C, Varela E, Sarrabayrouse G, Pozuelo del Río M, Alonso VR, Sainz NB, et al. Gut microbiota composition in long-remission ulcerative colitis is close to a healthy gut microbiota. *Inflamm Bowel Dis.* 2023;29(9):1362–9.

310. Xiaoying L, Mingchao X, Ruiting L, Dalong H, Suping Z, Shuwei Z, et al. Gut commensal *Alistipes shahii* improves experimental colitis in mice with reduced intestinal epithelial damage and cytokine secretion. *mSystems*. 2025;10(3):e01607–24.
311. Notting F, Pirovano W, Sybesma W, Kort R. The butyrate-producing and spore-forming bacterial genus *Coprococcus* as a potential biomarker for neurological disorders. *Gut Microbiome (Camb)*. 2023;4:e16.
312. Zhang M, Zhou Q, Dorfman RG, Huang X, Fan T, Zhang H, et al. Butyrate inhibits interleukin-17 and generates Tregs to ameliorate colorectal colitis in rats. *BMC Gastroenterol*. 2016;16(1):84.
313. Chen G, Ran X, Li B, Li Y, He D, Huang B, et al. Sodium butyrate inhibits inflammation and maintains epithelium barrier integrity in a TNBS-induced inflammatory bowel disease mice model. *EBioMedicine*. 2018;30:317–25.
314. Kelly CJ, Zheng L, Campbell EL, Saeedi B, Scholz CC, Bayless AJ, et al. Crosstalk between microbiota-derived short-chain fatty acids and intestinal epithelial HIF augments tissue barrier function. *Cell Host Microbe*. 2015;17(5):662–71.
315. Liu W, Luo X, Tang J, Mo Q, Zhong H, Zhang H, et al. A bridge for short-chain fatty acids to affect inflammatory bowel disease, type 1 diabetes, and non-alcoholic fatty liver disease positively: by changing gut barrier. *Eur J Nutr*. 2021;60(5):2317–30.
316. Zhang D, Jian YP, Zhang YN, Li Y, Gu LT, Sun HH, et al. Short-chain fatty acids in diseases. *Cell Commun Signal*. 2023;21(1):212.
317. Hayes CL, Dong J, Galipeau HJ, Jury J, McCarville J, Huang X, et al. Commensal microbiota induces colonic barrier structure and functions that contribute to homeostasis. *Sci Rep*. 2018;8(1):14184.
318. Zhou Y, Zhi F. Lower level of *Bacteroides* in the gut microbiota is associated with inflammatory bowel disease: A meta-analysis. *Biomed Res Int*. 2016;2016:5828959.
319. Mills RH, Dulai PS, Vázquez-Baeza Y, Saucedo C, Daniel N, Gerner RR, et al. Multi-omics analyses of the ulcerative colitis gut microbiome link *Bacteroides vulgatus* proteases with disease severity. *Nat Microbiol*. 2022;7(2):262–76.
320. Shi Y, Mu L. An expanding stage for commensal microbes in host immune regulation. *Cell Mol Immunol*. 2017;14(4):339–48.
321. Spor A, Koren O, Ley R. Unravelling the effects of the environment and host genotype on the gut microbiome. *Nat Rev Microbiol*. 2011;9(4):279–90.
322. Liang L, Yang C, Liu L, Mai G, Li H, Wu L, et al. Commensal bacteria-derived extracellular vesicles suppress ulcerative colitis through regulating the macrophages polarization and remodeling the gut microbiota. *Microb Cell Fact*. 2022;21(1):88.
323. Schreiber F, Villemain C, Sharpington T, Lawley TD, Robinson MJ, Bakdash G. Mechanistic understanding of MB310: a consortium of gut commensal bacteria for the treatment of ulcerative colitis. *J Crohns Colitis*. 2025;19(Suppl 1):i418–i418.
324. Kromann EH, Cearra AP, Neves JF. Organoids as a tool to study homeostatic and pathological immune–epithelial interactions in the gut. *Clin Exp Immunol*. 2024;218(1):28–39.
325. Co JY, Margalef-Català M, Li X, Mah AT, Kuo CJ, Monack DM, et al. Controlling epithelial polarity: A human enteroid model for host-pathogen interactions. *Cell Rep*. 2019;26(9):2509-20.e4.
326. Aguilar C, Alves da Silva M, Saraiva M, Neyazi M, Olsson IAS, Bartfeld S. Organoids as host models for infection biology – a review of methods. *Exp Mol Med*. 2021; 53(10):1471–82.
327. Li Y, Tang P, Cai S, Peng J, Hua G. Organoid based personalized medicine: from bench to bedside. *Cell Regen*. 2020;9(1):21.

328. Lopez JO, Seguel J, Chamorro A, Ramos KS. Pattern matching for high precision detection of LINE-1s in human genomes. *BMC Bioinformatics*. 2022;23(1):375.
329. Szigeti KA, Kalmár A, Galamb O, Valcz G, Barták BK, Nagy ZB, et al. Global DNA hypomethylation of colorectal tumours detected in tissue and liquid biopsies may be related to decreased methyl-donor content. *BMC Cancer*. 2022;22(1):605.
330. Quintanilla I, Lopez-Cerón M, Jimeno M, Cuatrecasas M, Muñoz J, Moreira L, et al. LINE-1 hypomethylation is neither present in rectal aberrant crypt foci nor associated with field defect in sporadic colorectal neoplasia. *Clin Epigenetics*. 2014;6(1):24.
331. Kraiczky J, Nayak KM, Howell KJ, Ross A, Forbester J, Salvestrini C, et al. DNA methylation defines regional identity of human intestinal epithelial organoids and undergoes dynamic changes during development. *Gut*. 2019;68(1):49–61.
332. Howell KJ, Kraiczky J, Nayak KM, Gasparetto M, Ross A, Lee C, et al. DNA methylation and transcription patterns in intestinal epithelial cells from pediatric patients with inflammatory bowel diseases differentiate disease subtypes and associate with outcome. *Gastroenterology*. 2018;154(3):585–98.
333. Nie K, Ma K, Luo W, Shen Z, Yang Z, Xiao M, et al. Roseburia intestinalis: A beneficial gut organism from the discoveries in genus and species. *Front Cell Infect Microbiol*. 2021;11:757718.
334. Avershina E, Larsen MG, Aspholm M, Lindback T, Storrø O, Øien T, et al. Culture dependent and independent analyses suggest a low level of sharing of endospore-forming species between mothers and their children. *Sci Rep*. 2020;10(1):1832.
335. Parera Olm I, Sousa DZ. Upgrading dilute ethanol to odd-chain carboxylic acids by a synthetic co-culture of Anaerotignum neopropionicum and Clostridium kluyveri. *Biotechnol Biofuels Bioprod*. 2023;16(1):83.
336. Elbing KL, Brent R. Recipes and tools for culture of Escherichia coli. *Curr Protoc Mol Biol*. 2019;125(1):e83.
337. Keitel L, Miebach K, Rummel L, Yordanov S, Büchs J. Process analysis of the anaerobe Phocaeicola vulgatus in a shake flasks and fermenter reveals pH and product inhibition. *Ann Microbiol*. 2024;74(1):7.
338. Keitel L, Braun K, Finger M, Kosfeld U, Yordanov S, Büchs J. Carbon dioxide and trace oxygen concentrations impact growth and product formation of the gut bacterium Phocaeicola vulgatus. *BMC Microbiol*. 2023;23(1):391.
339. Stromberg ZR, Van Goor A, Redweik GAJ, Wymore Brand MJ, Wannemuehler MJ, Mellata M. Pathogenic and non-pathogenic Escherichia coli colonization and host inflammatory response in a defined microbiota mouse model. *Dis Model Mech*. 2018;11(11):dmm035063.
340. Pilarczyk-Zurek M, Strus M, Adamski P, Heczko PB. The dual role of Escherichia coli in the course of ulcerative colitis. *BMC Gastroenterol*. 2016;16(1):128.
341. Kruis W, Fric P, Pokrotnieks J, Lukás M, Fixa B, Kascák M, et al. Maintaining remission of ulcerative colitis with the probiotic Escherichia coli Nissle 1917 is as effective as with standard mesalazine. *Gut*. 2004;53(11):1617–23.
342. Yang H, Mirsepasi-Lauridsen HC, Struve C, Allaire JM, Sivignon A, Vogl W, et al. Ulcerative colitis-associated E. coli pathobionts potentiate colitis in susceptible hosts. *Gut Microbes*. 2020;12(1):1847976.
343. Chloé MLH, Andrew VB, Angeliki KK, Munk PA. Escherichia coli pathobionts associated with inflammatory bowel disease. *Clin Microbiol Rev*. 2019;32(2):e00060-18.

344. Vilardi A, Przyborski S, Mobbs C, Rufini A, Tufarelli C. Current understanding of the interplay between extracellular matrix remodelling and gut permeability in health and disease. *Cell Death Discov.* 2024;10(1):258.
345. Liu L, Xu M, Lan R, Hu D, Li X, Qiao L, et al. *Bacteroides vulgatus* attenuates experimental mice colitis through modulating gut microbiota and immune responses. *Front Immunol.* 2022;13:1036196.
346. Li D, Wu M. Pattern recognition receptors in health and diseases. *Signal Transduct Target Ther.* 2021;6(1):291.
347. Kuo WT, Zuo L, Odenwald MA, Madha S, Singh G, Gurniak CB, et al. The tight junction protein ZO-1 is dispensable for barrier function but critical for effective mucosal repair. *Gastroenterology.* 2021;161(6):1924–39.
348. Wan Q, Song D, Li H, He M liang. Stress proteins: the biological functions in virus infection, present and challenges for target-based antiviral drug development. *Signal Transduct Target Ther.* 2020;5(1):125.
349. Liu L, Yu L, Li Z, Li W, Huang W. Patient-derived organoid (PDO) platforms to facilitate clinical decision making. *J Transl Med.* 2021;19(1):40.
350. Rhodes JM. The role of *Escherichia coli* in inflammatory bowel disease. *Gut.* 2007;56(5):610–2.
351. Chen K, McCulloch J, Das Neves R, Rodrigues G, Hsieh WT, Gong W, et al. The beneficial effects of commensal *E. coli* for colon epithelial cell recovery are related with Formyl peptide receptor 2 (Fpr2) in epithelial cells. *Gut Pathog.* 2023;15(1):28.
352. Natividad JMM, Petit V, Huang X, de Palma G, Jury J, Sanz Y, et al. Commensal and probiotic bacteria influence intestinal barrier function and susceptibility to colitis in *Nod1^{-/-};Nod2^{-/-}* mice. *Inflamm Bowel Dis.* 2012;18(8):1434–46.
353. Török HP, Glas J, Endres I, Tonenchi L, Teshome MY, Wetzke M, et al. Epistasis between Toll-like receptor-9 polymorphisms and variants in NOD2 and IL23R modulates susceptibility to Crohn's Disease. *Am J Gastroenterol.* 2009;104(7):1723–33.
354. Pierik M, Joossens S, Van Steen K, Van Schuerbeek N, Vlietinck R, Rutgeerts P, et al. Toll-like receptor-1, -2, and -6 polymorphisms influence disease extension in inflammatory bowel diseases. *Inflamm Bowel Dis.* 2006;12(1):1–8.
355. Jostins L, Ripke S, Weersma RK, Duerr RH, McGovern DP, Hui KY, et al. Host-microbe interactions have shaped the genetic architecture of inflammatory bowel disease. *Nature.* 2012;491(7422):119–24.
356. Gewirtz AT, Vijay-Kumar M, Brant SR, Duerr RH, Nicolae DL, Cho JH. Dominant-negative TLR5 polymorphism reduces adaptive immune response to flagellin and negatively associates with Crohn's disease. *Am J Physiol Gastrointest Liver Physiol.* 2006;290(6):G1157–63.
357. Franchimont D, Vermeire S, El Housni H, Pierik M, Van Steen K, Gustot T, et al. Deficient host-bacteria interactions in inflammatory bowel disease? The toll-like receptor (TLR)-4 Asp299gly polymorphism is associated with Crohn's disease and ulcerative colitis. *Gut.* 2004;53(7):987–92.
358. Borralho PM, Rodrigues CMP, Steer CJ. Mitochondrial microRNAs and their potential role in cell function. *Curr Pathobiol Rep.* 2014;2(3):123–32.
359. Raval PK, Martin WF, Gould SB. Mitochondrial evolution: Gene shuffling, endosymbiosis, and signaling. *Sci Adv.* 2025;9(32):eadj4493.
360. Viennois E, Chassaing B, Tahsin A, Pujada A, Wang L, Gewirtz AT, et al. Host-derived fecal microRNAs can indicate gut microbiota healthiness and ability to induce inflammation. *Theranostics.* 2019;9(15):4542–57.

361. Chen HM, Chung YCE, Chen HC, Liu YW, Chen IM, Lu ML, et al. Exploration of the relationship between gut microbiota and fecal microRNAs in patients with major depressive disorder. *Sci Rep.* 2022;12(1):20977.
362. Liu L, Xu M, Lan R, Hu D, Li X, Qiao L, et al. *Bacteroides vulgatus* attenuates experimental mice colitis through modulating gut microbiota and immune responses. *Front Immunol.* 2022;13:1036196.
363. Dambal S, Shah M, Mihelich B, Nonn L. The microRNA-183 cluster: the family that plays together stays together. *Nucleic Acids Res.* 2015;43(15):7173–88.
364. Chapman Christopher G, Pekow Joel. The emerging role of miRNAs in inflammatory bowel disease: a review. *Therap Adv Gastroenterol.* 2014;8(1):4–22.
365. Zhao J, Wang X, Mi Z, Jiang X, Sun L, Zheng B, et al. STAT3/miR-135b/NF- κ B axis confers aggressiveness and unfavorable prognosis in non-small-cell lung cancer. *Cell Death Dis.* 2021;12(5):493.
366. Li M, Chen WD, Wang YD. The roles of the gut microbiota – miRNA interaction in the host pathophysiology. *Mol Med.* 2020;26(1):101.
367. Xiao X, Mao X, Chen D, Yu B, He J, Yan H, et al. miRNAs can affect intestinal epithelial barrier in inflammatory bowel disease. *Front Immunol.* 2022;13:868229.
368. Ramadan YN, Kamel AM, Medhat MA, Hetta HF. MicroRNA signatures in the pathogenesis and therapy of inflammatory bowel disease. *Clin Exp Med.* 2024;24(1): 217.
369. Arrieta MC, Finlay BB. The commensal microbiota drives immune homeostasis. *Front Immunol.* 2012;3:33.
370. Serigado JM, Foulke-Abel J, Hines WC, Hanson JA, In J, Kovbasnjuk O. Ulcerative colitis: Novel epithelial insights provided by single cell RNA sequencing. *Front Med.* 2022;9:868508.
371. Ugalde-Silva P, Gonzalez-Lugo O, Navarro-Garcia F. Tight junction disruption induced by type 3 secretion system effectors injected by enteropathogenic and enterohemorrhagic *Escherichia coli*. *Front Cell Infect Microbiol.* 2016;6:87.
372. Maria PA, Hao Z, Qiaojuan S, Xieyue X, Randy L, Lauren BI. Inflammatory bowel disease-associated gut commensals degrade components of the extracellular matrix. *mBio.* 2022;13(6):e02201-22.
373. Ambrozkiwicz F, Karczmariski J, Kulecka M, Paziewska A, Niemira M, Zeber-Lubecka N, et al. In search for interplay between stool microRNAs, microbiota and short chain fatty acids in Crohn’s disease – a preliminary study. *BMC Gastroenterol.* 2020;20(1):307.

PUBLICATIONS

Thesis publications:

1. **Inčiūraitė, R.**, Ramonaitė, R., Kupčinskas, J., Dalgėdienė, I., Kūlokienė, U., Kiudelis, V., Varkalaitė, G., Žvirblienė, A., Jonaitis, L. V., Kiudelis, G., Franke, A., Schreiber, S., Juzėnas, S., Skiecevičienė, J. The microRNA expression in crypt-top and crypt-bottom colonic epithelial cell populations demonstrates cell-type specificity and correlates with endoscopic activity in ulcerative colitis. *Journal of Crohn's and Colitis*. 2024; 18(12): 2033-2044. **IF: 8.3**. Quartile: Q1.
2. **Inčiūraitė, R.**, Steponaitienė, R., Raudžė, O., Kūlokienė, U., Kiudelis, V., Lukoševičius, R., Ugenskienė, R., Adamonis, K., Kiudelis, G., Jonaitis, L. V., Kupčinskas, J., Skiecevičienė, J. Prolonged culturing of colonic epithelial organoids derived from healthy individuals and ulcerative colitis patients results in the decrease of LINE-1 methylation level. *Scientific Reports*. 2024;14(1): 1-10. **IF: 3.8**. Quartile: Q1.
3. **Inčiūraitė, R.**, Gedgaudas, R., Lukoševičius, R., Tilindė, D., Ramonaitė, R., Link, A., Kašėtienė, N., Malakauskas, M., Kiudelis, G., Jonaitis, L. V., Kupčinskas, J., Juzėnas, S., Skiecevičienė, J. Constituents of stable commensal microbiota imply diverse colonic epithelial cell reactivity in patients with ulcerative colitis. *Gut Pathogens*. 2024;16(1): 1-10. **IF: 4.3**. Quartile: Q1.

Other publications:

1. Morkūnas, E., Vaitkevičiūtė, E., **Inčiūraitė, R.**, Kupčinskas, J., Link, A., Skiecevičienė, J., Alunni-Fabbroni, M., Schütte, K., Malfertheiner, P., Varkalaitė, G., Ricke, J. miRNome profiling analysis reveals novel hepatocellular carcinoma diagnostic, prognostic and treatment-related candidate biomarkers: post-hoc analysis of SORAMIC trial. *Digestive Diseases* 2024; 42(4): 336-348. **IF: 2.0**. Quartile: Q3.
2. Šeškutė, M., Žukaitė, D., Laucaitytė, G., **Inčiūraitė, R.**, Malinauskas, M., Jankauskaitė, L. Antiviral Effect of Melatonin on Caco-2 Cell Organoid Culture: Trick or Treat? *International Journal of Molecular Sciences*. 2024;25(22): 1-15. **IF: 4.9**. Quartile: Q1.
3. Varkalaitė, G., Vaitkevičiūtė, E., **Inčiūraitė, R.**, Šaltenienė, V., Juzėnas, S., Petkevičius, V., Gudaitytė, R., Mickevičius, A., Link, A., Kupčinskas, L., Leja, M., Kupčinskas, J., Skiecevičienė, J. Atrophic gastritis and gastric cancer tissue miRNome analysis reveal hsa-miR-129-1 and hsa-

- miR-196a as potential early diagnostic biomarkers. *World Journal of Gastroenterology: WJG*. 2022;28(6): 653-663. IF: 4.3. Quartile: Q2.
4. Vaitiekus, D., Muckienė, G., Vaitiekienė, A., Sereikaitė, L., **Inčiūraitė, R.**, Insodaitė, R., Čepulienė, D., Kupčinskas, J., Ugenskienė, R., Jurkevičius, R., Juozaitytė, E. HFE Gene Variants' Impact on Anthracycline-Based Chemotherapy-Induced Subclinical Cardiotoxicity. *Cardiovascular Toxicology*. 2021;21(1): 59-66. IF: 2.755. Quartile: Q3.
 5. Kūlokienė, U., Lukoševičius, R., **Inčiūraitė, R.**, Varkalaitė, G., Gudoiytė, G., Bekampytė, J., Valentini, S., Šaltenienė, V., Ruzgys, P., Šatkauskas, S., Žvinienė, K., Kupčinskas, J., Skiecevičienė, J. The Role of miR-375-3p and miR-200b-3p in Gastrointestinal Stromal Tumors. *International Journal of Molecular Sciences*. 2020;21(14): 1-12. IF: 5.923. Quartile: Q1.
 6. Varkalaitė, G., **Inčiūraitė, R.**, Juzėnas, S., Šaltenienė, V., Kūlokienė, U., Kiudelis, G., Leja, M., Ruzgys, P., Šatkauskas, S., Kupčinskienė, E., Franke, S., Thon, C., Link, A., Kupčinskas, J., Skiecevičienė, J. miR-20b and miR-451a are involved in gastric carcinogenesis through the PI3K. *International Journal of Molecular Sciences*. 2020;21(3): 1-16. IF: 5.923. Quartile: Q1.

The results of the thesis were presented in national and international scientific conferences:

1. **Inčiūraitė, R.**, Gedgaudas, R., Steponaitienė, R., Tilindė, D., Andziulis, A., Lukoševičius, R., Kiudelis, G., Juzėnas, S., Kupčinskas, J., Skiecevičienė, J. Assessment of colonic epithelial cell reactivity to unaltered fecal microbiota members in ulcerative colitis patients and healthy individuals. *International Health Sciences Conference for All (IHSC for All) „Precision Medicine“: Abstract Book 2024*. 451-452. March 25-26, 2024, Kaunas, Lithuania. Oral presentation.
2. **Inčiūraitė, R.**, Juzėnas, S., Gedgaudas, R., Tilindė, D., Lukoševičius, R., Kiudelis, G., Jonaitis, L. V., Kupčinskas, J., Skiecevičienė, J. Implication of commensal faecal bacteria in regulating the colonic epithelial barrier during ulcerative colitis. *United European Gastroenterology Journal: 32nd United European Gastroenterology Week 2024: Abstract Issue*. 2024;12(Suppl. 8): 100-100. October 12-15, 2024, Vienna, Austria. Oral presentation.
3. **Inčiūraitė, R.**, Steponaitienė, R., Tilindė, D., Šaltenienė, V., Lukoševičius, R., Kiudelis, G., Jonaitis, L. V., Gedgaudas, R., Kiudelis, V., Kupčinskas, J., Skiecevičienė, J. Evaluation of epithelial cell response to

- commensal bacteria in the intestinal organoid model of ulcerative colitis patients. *Microbiota in Health and Disease: EHMSG - 37th International Workshop on Helicobacter and Microbiota in Inflammation and Cancer: Accepted Abstracts*. 2024;6: 138-139. September 12-14, 2024, Porto, Portugal. Poster presentation.
4. **Inčiūraitė, R.**, Gedgaudas, R., Lukoševičius, R., Juzėnas, S., Kiudelis, G., Jonaitis, L. V., Kupčinskas, J., Skiecevičienė, J. Alterations of gut microbiota in ulcerative colitis. *Microbiota in Health and Disease: EHMSG - 36th International Workshop on Helicobacter and Microbiota in Inflammation and Cancer: Accepted Abstracts*. 2023;5: 143-144. September 7-9, 2023, Antwerp, Belgium. Poster presentation.
 5. **Inčiūraitė, R.**, Gedgaudas, R., Lukoševičius, R., Plingytė, K., Muškieta, T., Juzėnas, S., Kupčinskas, J., Skiecevičienė, J. Gut microbiota profile changes in patients with Ulcerative Colitis. *Journal of Crohn's and Colitis – JCC: Abstracts of the 18th Congress of ECCO (European Crohn's and Colitis Organisation)*. 2023;17(Suppl. 1). March 1-4, 2023, Copenhagen, Denmark. Poster presentation.
 6. **Inčiūraitė, R.**, Raudžė, O., Kirilevičiūtė, I., Tumelytė, A., Kiudelis, G., Jonaitis, L. V., Kūlokienė, U., Steponaitienė, R., Skiecevičienė, J. Intestinal organoids as a model system for Ulcerative colitis: evaluation of epigenetic stability. *Health for All: 2023 – International Conference Health for All “Rare diseases”*: Abstract Book. 2023: 21–23. April 19–20, 2023, Kaunas, Lithuania. Oral presentation.
 7. **Inčiūraitė, R.**, Steponaitienė, R., Raudžė, O., Kiudelis, G., Jonaitis, L. V., Kiudelis, V., Ugenskienė, R., Kūlokienė, U., Kupčinskas, J., Skiecevičienė, J. Evaluation of prolonged culturing impact on global methylation level of colon organoids derived from healthy individuals and ulcerative colitis patients. *EMBO | EMBL Symposium: Organoids: modelling organ development and disease in 3D culture: Abstract Book*. 2023. October 18-21, 2024, Heidelberg, Germany. Poster presentation.
 8. **Inčiūraitė, R.**, Steponaitienė, R., Raudžė, O., Kiudelis, G., Jonaitis, L. V., Kiudelis, V., Ugenskienė, R., Kūlokienė, U., Kupčinskas, J., Skiecevičienė, J. Long-term culturing of healthy- and ulcerative colitis patient derived colon organoids is associated with decreased methylation level of LINE-1. *United European Gastroenterology Journal: 31st United European Gastroenterology Week 2023: Abstract Issue*. 2023;11(S8): 805-806. October 14-17, 2023, Copenhagen, Denmark. Poster presentation.
 9. **Inčiūraitė, R.**, Gedgaudas, R., Lukoševičius, R., Juzėnas, S., Kupčinskas, J., Skiecevičienė, J. Sergančiųjų opiniu kolitu žarnyno mikrobiomo analizė. *15-oji Lietuvos jaunujų mokslininkų konferencija BIOATEITIS*:

- Gamtos ir gyvybės mokslų perspektyvos: pranešimų santraukos*. 2022; 34-35. November 24, 2022, Vilnius, Lithuania. Oral presentation.
10. **Inčiūraitė, R.**, Juzėnas, S., Dalgėdienė, I., Ramonaitė, R., Kiudelis, G., Jonaitis, L. V., Kupčinskas, J., Žvirblienė, A., Skiecevičienė, J. Opinio kolito žarnyno epitelinių ląstelių mikroRNR dalyvauja uždegiminių procesų reguliacijoje. *14-oji Lietuvos jaunųjų mokslininkų konferencija BIOATEITIS: Gamtos ir gyvybės mokslų perspektyvos: pranešimų santraukos*. 2021; 23–23. November 25, 2021, Kaunas, Lithuania. Oral presentation.
 11. **Inčiūraitė, R.**, Juzėnas, S., Ramonaitė, R., Skiecevičienė, J. MicroRNA composition of colon crypt-top and crypt-bottom epithelial cells in Ulcerative Colitis. *Journal of Crohn's and Colitis: Abstracts of the 16th Congress of ECCO Virtual*. 2021;15(Suppl. 1). July 2–3, 2021, Virtual. Poster presentation.
 12. **Inčiūraitė, R.**, Juzėnas, S., Ramonaitė, R., Skiecevičienė, J. Profiling of microRNAs in crypt-top and crypt-bottom colonic epithelial cells of patients with active and inactive ulcerative colitis. *Health for All: 2021 – International Conference: Health for All 2021: Abstract Book*. 2021; 18–19. April 7-8, 2021, Virtual. Oral presentation.
 13. **Inčiūraitė, R.**, Juzėnas, S., Ramonaitė, R., Kiudelis, G., Jonaitis, L. V., Kupčinskas, J., Dalgėdienė, I., Žvirblienė, A., Skiecevičienė, J. MicroRNA Profiling on the Levels of Colon Tissue and Epithelial Cell-Populations in Patients with Active and Inactive Ulcerative Colitis. *United European Gastroenterology Journal: 29th United European Gastroenterology Week Virtual: Abstract Issue*. 2021; 9(Suppl. 8): 434-434. October 2-6, 2021, Virtual. Poster presentation.
 14. **Inčiūraitė, R.**, Ramonaitė, R., Juzėnas, S., Skiecevičienė, J. Profiling of microRNAs and their isoforms in differentiated and undifferentiated colonic epithelial cells of patients with active and inactive ulcerative colitis. *Medicina: Abstracts Accepted for the International Scientific Conference on Medicine Organized Within the Frame of the 79th International Scientific Conference of the University of Latvia*. 2021; 57(Suppl. 1): 24-24. April 23-24, 2021, Riga, Latvia. Poster presentation.
 15. **Inčiūraitė, R.** Diferencijuotų ir nediferencijuotų epitelinių storosios žarnos ląstelių mikroRNR ir jų izoformų raiškos profilio pokyčiai sergant opiniu kolitu. *13-oji jaunųjų mokslininkų konferencija BIOATEITIS: Gamtos ir gyvybės mokslų perspektyvos: pranešimų santraukos*. 2020; 46-46. December 4, 2020, Virtual. Oral presentation.

COPIES OF PUBLICATIONS

Publication no. 1

Title: The microRNA expression in crypt-top and crypt-bottom colonic epithelial cell populations demonstrates cell-type specificity and correlates with endoscopic activity in ulcerative colitis

Authors: Inčiūraitė Rūta, Ramonaitė Rima, Kupčinskas Juozas, Dalgėdienė Indrė, Kūlokienė Ugnė, Kiudelis Vytautas, Varkalaitė Greta, Žvirblienė Aurelija, Jonaitis Laimas Virginijus, Kiudelis Gediminas, Franke Andre, Schreiber Stefan, Juzėnas Simonas, Skiecevičienė Jurgita

Journal of Crohn's and Colitis (2024)

Reprinted under a Creative Commons Attribution 4.0 International (CC BY 4.0) licence

The microRNA Expression in Crypt-Top and Crypt-Bottom Colonic Epithelial Cell Populations Demonstrates Cell-Type Specificity and Correlates with Endoscopic Activity in Ulcerative Colitis

Ruta Inciuraite,^{a,*} Rima Ramonaite,^{a,*} Juozas Kupcinskas,^{a,b,*} Indre Dalgediene,^c Ugne Kulokiene,^a Vytautas Kiudelis,^{a,b} Greta Varkalaite,^a Aurelija Zvirbliene,^c Laimas Virginijus Jonaitis,^{a,b} Gediminas Kiudelis,^{a,b} Andre Franke,^d Stefan Schreiber,^d Simonas Juzenas,^{a,c,†} Jurgita Skieceviciene^{a,†}

^aInstitute for Digestive Research, Academy of Medicine, Lithuanian University of Health Sciences, Kaunas, Lithuania

^bDepartment of Gastroenterology, Academy of Medicine, Lithuanian University of Health Sciences, Kaunas, Lithuania

^cInstitute of Biotechnology, Life Sciences Center, Vilnius University, Vilnius, Lithuania

^dInstitute of Clinical Molecular Biology, Christian-Albrechts-University of Kiel, Kiel, Germany

Corresponding author: Jurgita Skieceviciene, PhD, Institute for Digestive Research, Academy of Medicine, Lithuanian University of Health Sciences, Eiveniu st. 4, LT-50161, Kaunas, Lithuania. Email: jurgita.skieceviciene@ismuni.lt

*These authors contributed equally to this work.

†These authors equally supervised this work.

Abstract

Background and Aims: Colonic epithelial barrier dysfunction is one of the early events in ulcerative colitis [UC], and microRNAs [miRNAs] participate in its regulation. However, the cell type-specific miRNome during UC remains unknown. Thus, we aimed to explore miRNA expression patterns in colon tissue and epithelial cells during active and quiescent UC.

Methods: Small RNA-sequencing in colon tissue, crypt-bottom [CD44⁺], and crypt-top [CD66a⁺] colonic epithelial cells from two cohorts of UC patients [*n* = 74] and healthy individuals [*n* = 50] was performed. Data analysis encompassed differential expression, weighted gene co-expression network, correlation, and gene-set enrichment analyses.

Results: Differentially expressed colonic tissue miRNAs showed potential involvement in the regulation of interleukin-4 [IL-4] and IL-13 signalling during UC. As this pathway plays a role in intestinal barrier regulation, consecutive analysis of spatially distinct colonic epithelial cell populations was performed. Cell-type- [crypt-top and crypt-bottom] specific miRNA expression patterns were identified in both active and quiescent UC. Target genes of differentially expressed epithelial miRNAs under different disease activity were overrepresented in epithelial cell migration and therefore intestinal barrier integrity regulation. The pro-inflammatory miRNA co-expression module M1 correlated with endoscopic disease activity and successfully distinguished active and quiescent UC not only in both epithelial cell populations, but also in the colon tissue. The anti-inflammatory module M2 was specific to crypt-bottom cells and was significantly enriched in quiescent UC patients.

Conclusions: miRNA expression was specific to colonic epithelial cell populations and UC state, reflecting endoscopic disease activity. Irrespective of the UC state, deregulated epithelial miRNAs were associated with regulation of intestinal barrier integrity.

Key Words: Colon crypt-bottom epithelial cells; colon crypt-top epithelial cells; microRNA; ulcerative colitis

1. Introduction

Colonic epithelial cells and their secreted products primarily form and maintain frontline intestinal barrier function which deteriorates early in ulcerative colitis [UC].¹ Colonic crypt epithelial cells such as colonocytes, goblet, and epithelial stem cells have been shown to play an important role in UC pathogenesis via reduced epithelial mucus secretion and/or increased barrier permeability.² Since one of the aims in UC management is to induce and then to maintain remission, disentangling the molecular mechanisms regulating epithelial

barrier may help to modulate its permeability and retain long-lasting remission in UC.

Recent studies provide evidence for microRNAs [miRNAs] as being involved in the regulation of intestinal epithelial integrity and barrier permeability via interference with protein-coding genes responsible for tight and adherent junctions,³ also in UC.⁴ However, most of the studies have been based on either immortalized cell cultures or bulk tissue experiments, and thus the exact cellular context of miRNA deregulation during colonic inflammation remains elusive. Therefore, the search for cell type-specific deregulation of miRNAs in UC

might uncover novel aspects of underlying regulatory pathways and molecular targets for therapeutic development.

Here, we report the comprehensive miRNA expression profiling on colon tissue and colonic crypt-bottom [CD44⁻] and crypt-top [CD66a⁺] cell population levels in active and quiescent UC. By using small RNA-sequencing [RNA-seq] we determine UC activity-specific, as well as epithelial cell population-specific, miRNA expression signatures during colonic inflammation. Additionally, we describe the miRNA co-expression network and evaluate its relationships to clinical characteristics of UC. Finally, we explore putative biological pathways in which the deregulated miRNAs are involved and provide potential miRNA candidates for further development of UC management.

2. Materials and methods

2.1. Ethics and consent

The approvals to perform the study was received from Kaunas Regional Biomedical Research Ethics Committee [No. BE-2-31, 22-03-2018, No. BE-2-8, 19-02-2013]. All subjects signed a written informed consent form to participate in the study.

2.2. Study design

The study comprised two distinct yet interconnected parts—Study parts I and II. In Study part I, miRNA profiling was performed in colon tissue samples of Study group I. Then, *IL-4* and *IL-13* expression patterns were analysed in colon tissue samples of Study group III. In Study part II, fluorescence-activated cell sorting [FACS] was performed on colon tissue samples of Study group II to enrich two distinct epithelial cell populations, followed by miRNA expression analysis. Subsequently, miRNA co-expression modules were identified within the epithelial cell populations and finally validated in the colon tissue samples from the first part of the study. The flowchart illustrating the study design and methodology is presented in the Supplementary Figure S1.

2.3. Study samples

Study subject recruitment was conducted at the Department of Gastroenterology, Lithuanian University of Health Sciences [Kaunas, Lithuania] during the period 2011–2014 [Study groups I and III] and 2017–2019 [Study group II]. For miRNA sequencing, colon biopsies were collected from two independent study subject groups (Study group I [$n = 76$] and group II [$n = 48$]). Additionally, colon biopsies for quantitative (q)PCR-based gene expression analysis were collected in the third independent group (Study group III [$n = 200$]). Demographic and clinical characteristics of all study subjects are presented in Table 1. Colon tissue samples of patients with active UC and quiescent UC were collected during routine colonoscopy performed as a part of their planned examination programme. The diagnosis of UC was based on standard clinical, endoscopic, radiological, and histological criteria.⁵ Endoscopic activity was determined using the Mayo endoscopic subscore.⁶ Quiescent UC was confirmed in patients with stool frequency ≤ 3 /day, no rectal bleeding, and healed mucosa at endoscopy [endoscopic Mayo subscore ≤ 1]. The control individuals included in all study groups consisted of healthy subjects who either underwent colonoscopy due to a positive faecal occult blood test or were consulted on functional complaints, but had a normal colonoscopy, uninfamed

mucosa during histopathological examination, and no previous history of intestinal inflammation. All patients enrolled in the study were of European descent.

2.4. Colon tissue disaggregation

Colon biopsies were mechanically and enzymatically separated into single-cell suspensions. Briefly, four to six biopsies [5–10 mg wet weight each] were washed with PBS solution containing 50 IU/mL penicillin, 50 μ g/mL streptomycin, and 0.5 mg/mL gentamicin. Biopsies were minced into small pieces [–1–2 mm³] and incubated in 1 \times trypsin-EDTA solution for 40–45 min at room temperature on an agitator to dissociate single epithelial cells from the lamina propria. After incubation, tissue fragments were gently transferred into PBS and shaken. The isolated cell suspension was filtered and suspended in DMEM/Ham's F-12 medium [1:1] with 15 mM HEPES [Gibco] buffer for flow cytometry procedures.

2.5. Flow cytometry and FACS

To minimize the loss of cell viability, fresh cell suspensions prepared shortly before flow cytometry were used in all cell sorting experiments. Antibody staining was performed in PBS supplemented with 1% heat-inactivated fetal bovine serum. To minimize non-specific binding of antibodies, cells were first incubated with Human TruStain FcX [Fc Receptor Blocking Solution; BioLegend] for 10 min at a concentration of 3–10 $\times 10^5$ cells/100 μ L. Cells were subsequently stained without washing with antibodies at dilutions recommended by the manufacturers. Antibodies used in this study were selected based on previous study⁷ and included: mouse anti-human CD326/EpCAM-FITC [clone VU-1D9, Life Technologies], mouse anti-human CD44-APC [clone G44-26, BD Biosciences], and mouse anti-human CD66a-PE [clone 283340, R&D Systems]. Cells positive for expression of non-epithelial lineage markers were excluded by staining with mouse anti-human CD45-APC-Cy7 [clone 2D1, BioLegend] [see gating strategy in Supplementary Figure S2A]. After 20 min, stained cells were washed of excess unbound antibodies and resuspended in PBS supplemented with 1% heat-inactivated fetal bovine serum. Flow-cytometry analysis was performed using a CyFlow Space cell sorter [Sysmex Partec] [see representative plots of flow cytometry data in Supplementary Figure S2B–D]. In cell sorting experiments, each population of interest was sorted individually, using a protocol already built-in within the CyFlow Space flow cytometer software package [FloMax 2.8], with appropriate adjustments. Data were analysed and visualized using FlowJo v10.7 [BD FlowJo]. Two cell populations [CD45⁻/EpCAM⁺/CD44⁻/CD66a⁺ and CD45⁻/EpCAM⁺/CD44⁺/CD66a⁺] were further described based on the literature and a single-cell RNA-seq dataset of the human colon, available in the GEO database with accession number GSE116222 [see the single-cell RNA-seq data-derived expression plot of three main cell surface markers in Supplementary Figure S3]. The CD45⁻/EpCAM⁺/CD44⁻/CD66a⁺ population was entitled as crypt-bottom cells [consisting of undifferentiated colonic epithelial cells as well as secretory goblet and enteroendocrine cells], while the CD45⁻/EpCAM⁺/CD44⁺/CD66a⁺ population was entitled as crypt-top cells [consisting of absorptive colonocytes and BEST4⁺/OTOP2⁺ cells]. Sorted cell samples were frozen and stored at –70°C prior to total RNA extraction.

Table 1. Demographic and clinical characteristics of the subjects

	Study group I, n = 76		Study group II, n = 48		Study group III, n = 200		
	Active UC, n = 23	Quiescent UC, n = 20	Active UC, n = 16	Quiescent UC, n = 15	Active UC, n = 75	Quiescent UC, n = 50	HC, n = 75
Age, years							
Mean ± SD	43.9 ± 16.1*	47.2 ± 13.5*	58.5 ± 12.7*	41.6 ± 16.3**	57.3 ± 12.1**	50.5 ± 16.1	46.1 ± 13.7
Sex, n [%]							
Female	10 [43.5]	9 [45.0]	21 [73.6]	4 [25.0]***	10 [66.7]***	10 [58.8]***	38 [50.7]
Full Mayo score, n [%]							
Remission [0–2]	0 [0.0]	20 [100.0]	–	0 [0.0]	15 [100.0]	–	–
Mild [3–5]	1 [4.4]	0 [0.0]	–	4 [25.0]	0 [0.0]	–	–
Moderate [6–10]	21 [91.3]	0 [0.0]	–	11 [68.8]	0 [0.0]	–	–
Severe [10–12]	1 [4.4]	0 [0.0]	–	1 [6.3]	0 [0.0]	–	–
Endoscopic Mayo subscore, n [%]							
Normal to mild [0–1]	0 [0.0]	20 [100.0]	33 [100.0]	0 [0.0]	15 [100.0]	17 [100.0]	75 [100.0]
Moderate to severe [2–3]	23 [100.0]	0 [0.0]	–	16 [100.0]	0 [0.0]	–	–
Smoking status, n [%]							
Never	8 [34.8]	11 [55.0]	23 [69.7]	9 [56.3]	10 [66.7]	12 [70.6]	43 [57.3]
Smoking	8 [34.8]	6 [30.0]	5 [15.2]	3 [18.8]	1 [6.7]	3 [17.7]	8 [10.7]
Ex-smoker	3 [13.1]	2 [10.0]	1 [5.0]	4 [25.0]	4 [26.7]	2 [11.8]	22 [29.3]
Unknown	4 [17.4]	1 [5.0]	1 [3.0]	–	–	–	2 [2.7]
BMI, kg/m ²							
Median, [range]	26.8 [18.1–56.2]	26.2 [19.7–31.5]	27.7 [19.6–39.5]	25.5 [18.0–37.2]	28.4 [19.8–32.7]	25.9 [18.9–31.9]	24.9 [16.2–41.5]
Unknown, n [%]	1 [4.4]	1 [5.0]	2 [6.1]	–	1 [6.7]	–	2 [4.0]
							5 [6.7]

*Age differed between both active and quiescent UC groups, and HC, estimated *p* value <0.05 [*t*-test].**Age differed between both active and quiescent UC groups, and HC, estimated *p* value <0.05 [*t*-test].***Sex distribution differed between three groups, estimated *p* value <0.05 [Pearson's chi-squared test].

2.6. Total RNA extraction

Total RNA extraction from colon biopsies and sorted cells was performed using standard protocols of a commercial miRNeasy Mini Kit [Qiagen] and Single Cell RNA Purification Kit [Norgen, Canada], respectively. Total RNA concentration was evaluated via a NanoDrop2000 spectrophotometer [Thermo Scientific] and Qubit 4 fluorometer [Invitrogen]. Total RNA quality was assessed using an Agilent 2100 Bioanalyzer [Agilent Biotechnologies].

2.7. Quantitative reverse transcription PCR [RT-qPCR] and data analysis

To estimate expression of the *IL-4* and *IL-13* genes in colon tissue of UC patients, total RNA from colon tissue samples was reverse transcribed using a High-Capacity cDNA Reverse Transcription Kit [Applied Biosystems]. Further, expression levels were measured using TaqMan Gene Expression Assays [Assay IDs: *IL-4* Hs00174122_m1; *IL-13* Hs00174379_m1] on the 7500 Fast Real-Time PCR System [Applied Biosystems]. The cycle threshold [C_t] values of *IL-4* and *IL-13* were normalized to the value of the *GAPDH* [Assay ID: Hs99999905_m1] reference gene. All procedures were performed in accordance with the manufacturer's protocol. Statistical analysis was performed using R studio software [v.4.0.3]. Data distribution was determined using the Shapiro–Wilk test, and gene expression differences were analysed using the two-sided Mann–Whitney U test. Differences between the values were considered significant at $p < 0.05$.

2.8. Preparation of small RNA libraries and next-generation sequencing

Small RNA libraries from tissue samples were prepared using the TruSeq Small RNA Sample Preparation Kit [Illumina] with 1 μg of total RNA input per sample. Small RNA libraries from sorted cells were prepared using the NEXTFLEX Small RNA-seq Kit v.3 [Bioo Scientific] with up to 50 ng of total RNA input per sample. Procedures were conducted according to the manufacturers' protocols. The yield of sequencing libraries was assessed using the Agilent 2200 TapeStation system [Agilent Biotechnologies]. Subsequently, the TruSeq libraries were pooled with around 24 samples per lane, while the NEXTFLEX libraries were pooled with around 16 samples per lane and then sequenced on a HiSeq 4000 [Illumina] next-generation sequencing platform.

2.9. Bioinformatics and statistical analysis of small RNA-seq data

The demultiplexed raw reads [.fastq] were processed with the nf-core/smrnaseq v.1.0.0 best-practice analysis pipeline using default parameters [Nextflow v.20.01.0].⁵ The pipeline was executed within a Docker container. Briefly, depending on the small RNA-seq library preparation kits, the 'illumina' or 'nextflex' protocol was selected for processing of the libraries generated from tissue and sorted cell samples, respectively. First, Trim Galore [v.0.6.3] was used to remove 3' adapter [5'-TGGAATTCTCGGGTCCAAGG-3' for both 'illumina' and 'nextflex' protocols] sequences from the reads and an additional four nucleotides from both the 5' and 3' ends of reads [only for the 'nextflex' protocol]. Second, to reduce computational time, the reads with identical sequences were collapsed using seqcluster⁹ while saving read count information. Third, Bowtie1 v.1.2.2¹⁰ was used to perform the alignment of collapsed reads against mature and hairpin miRNA

sequences in miRbase database v.22.1.¹¹ Finally, miRNA annotation was performed using mirTOP v.0.4.23.¹² Further, sample and miRNA quality control [QC] was performed: samples with initial read count < 1.5 interquartile range [IQR] and number of detected miRNAs $< .5$ IQR on \log_2 scale as well as non-expressed [mean raw count < 1] and non-variable miRNAs were excluded from further analysis. Subsequently, to perform differential expression analyses of the size factor-normalized counts of mature miRNAs between samples, negative binomial generalized linear models implemented in the R package DESeq2¹³ were used including age [scaled and centred] and sex as covariates in the model. The p -values resulting from Wald tests were corrected for false discovery rate [FDR] according to Benjamini and Hochberg. miRNAs with FDR < 0.05 and absolute value of $\log_2 FC > 1$ were considered to be significantly differentially expressed. A multidimensional scaling [MDS] analysis using Euclidean distance was performed on variance stabilizing transformation [VST] normalized miRNA count data. Additionally, Spearman's rank correlation analysis was performed between sex- and age-adjusted normalized miRNA read counts and endoscopic Mayo subscore. FDR < 0.05 was considered statistically significant. Removal of sex and age effects from normalized data was performed using the removeBatchEffect function from the limma R package.¹⁴ Statistical analyses and data processing were performed using R v.4.0.3.¹⁵ Visualization of graphs was performed using the ggplot2 package.¹⁶

2.10. Gene set enrichment analysis

To obtain putative biological functions of differentially expressed miRNAs, gene set enrichment analysis [GSEA] was performed using Reactome pathways¹⁷ and Gene Ontology [GO] categories.¹⁸ More specifically, luciferase assay-validated miRNA-target interactions [MTIs] were obtained from miRecords,¹⁹ miRTarBase,²⁰ and TarBase²¹ using the multiMiR package.²² The retrieved MTIs were then submitted to a hypergeometric test implemented in the enrichPathway [from the ReactomePA package²³] and enrichGO [from the clusterProfiler package²⁴] functions using genes that are expressed in colon crypt-bottom [CD44⁺] and crypt-top [CD66a⁺] cells as a background reference [defined as universe]. The universe genes were obtained from single-cell RNA-seq data of the human colon, available in the GEO database with accession number GSE116222.²⁵ Pathways with FDR < 0.05 were considered to be significantly deregulated. The expression of *IL-4* and *IL-13* signalling pathway-related genes in different human colonic cell populations was also analysed using the GSE116222 dataset.

2.11. miRNA co-expression analysis

Samples of study group II were used for weighted gene co-expression network analysis [WGCNA] aiming to identify modules of co-expressed miRNAs using the CEMiTool package²⁶ [v.1.22.0] for R. A VST normalized miRNA count table was used to generate the co-expression modules. Filtering based on variance was applied on the gene expression table prior to identification of miRNA co-expression modules. The minimal number of miRNAs per submodule as well as minimum size of gene sets for GSEA was set to five, while the p -value threshold for filtering was set to 0.1. Further, the eigengene value of the co-expression module identified in colonic epithelial cells was also calculated in colon tissue data using the expression table of co-expressed

miRNAs and WGCNA package²⁷ [v.1.72-1] for R. Next, Spearman's rank correlation coefficients were calculated between module eigengene values and endoscopic Mayo subscore in both colonic epithelial cell populations as well as in colon tissue. $FDR < 0.05$ was considered statistically significant. Finally, to assess the performance of the identified module eigengene value for distinguishing between active and quiescent UC in both colon tissue and distinct colonic epithelial cell populations, analysis of area under the receiver operating characteristic curve [AUC-ROC] was applied using the pROC package²⁸ [v.1.18.4] for R.

3. Results

3.1. Differentially expressed miRNAs in active and quiescent UC tissues are involved in regulation of inflammation-related pathways

To identify differentially expressed miRNAs and their putative regulatory processes during chronic colon inflammation, small RNA-seq was performed on inflamed [active] and non-inflamed [quiescent] colonic mucosal biopsies of UC patients and healthy controls [HC] [Figure 1].

After count data normalization and QC, 573 unique miRNAs were found to be expressed in colon tissue samples. The overall similarity structure [based on MDS analysis; see Methods] of colon miRNA transcriptomes revealed two clearly resolved clusters corresponding to active UC and HC tissues, while the third cluster corresponding to quiescent UC overlapped with both active UC and HC clusters, suggesting a shift of miRNA expression from a healthy to inflammatory state [Figure 1A]. To evaluate expression of specific miRNAs in active and quiescent UC, differential gene expression analysis was performed. As expected, the most profound miRNA deregulation was observed comparing active UC to HC or to quiescent UC (93 and 59 differentially expressed miRNAs [$FDR < 0.05$ and $\log_2FCI > 1$], respectively). Interestingly, although substantially lower than in active UC, a differential expression of miRNAs [$n = 32$] was also observed in quiescent UC compared to HC [Figure 1B; Supplementary Table S1]. Among the differentially expressed miRNAs, a considerable number [$n = 13$] of molecules were deregulated in both active and quiescent UC compared to HC. In addition, the gradual decrease in miR-1-3p expression was found in all pairwise comparisons [Supplementary Table S1].

To further determine the biological function of differentially expressed miRNAs in the pathogenesis of UC, GSEA was performed for each pairwise comparison using validated target genes of significantly deregulated miRNAs and Reactome pathways [Supplementary Figure S4 and Table S2]. Intriguingly, both active UC and quiescent UC, compared to HC, had overrepresented interleukin signalling-related pathways among the top significant ones, such as 'Signaling by Interleukins' [R-HSA-449147], 'Interleukin-4 and Interleukin-13 signaling' [R-HSA-6785807], 'Intracellular signaling by second messengers' [R-HSA-9006925], and 'Diseases of signal transduction by growth factor receptors and second messengers' [R-HSA-5663202]. Based on the highest number of target genes, we identified 20 major miRNAs, including miR-223-3p, miR-20a-5p, miR-155-5p, miR-146a-5p, miR-1-3p, miR-31-5p, miR-10b-5p, and miR-205-5p, that were involved in these pathways [Figure 1C].

To explore the genes related to the interleukin-4 [IL-4] and IL-13 signalling pathway in colonic tissue more deeply, the expression patterns of two main cytokines, IL-4 and IL-13, were analysed using targeted RT-qPCR. A gradual increase in *IL-13* expression was observed between UC patients and HC individuals (2.19-fold [$p = 0.031$] increase in quiescent UC vs. HC, 2.91-fold [$p = 0.0007$] increase in active UC vs. quiescent UC, 6.38-fold [$p = 2 \times 10^{-10}$] increase in active UC vs. HC), whereas the expression of *IL-4* did not differ between the groups [Figure 1D]. Subsequently, the GSE116222 dataset was used to explore the expression signatures of IL-4 and IL-13 signalling-related genes, also identified as validated target genes of differentially expressed colonic tissue miRNAs in different colonic cell populations [both epithelial and immune subsets] during active and quiescent UC as well as in HC [Figure 1E]. Briefly, downstream genes of the IL-4 and IL-13 pathway, including cytokine receptors [in particular *IL13RA1* and *IL4R*] and signal regulators [*JAK1*, *SOCS1*, *STAT3*, and *STAT6*] were detectable in a larger proportion of cells with potentially altered expression in active UC compared to HC.

Collectively, differentially expressed colonic tissue miRNAs [including miR-223-3p, miR-20a-5p, miR-155-5p, miR-146a-5p, and miR-1-3p] showed potential involvement in regulation of the IL-4 and IL-13 signalling pathway in both active and quiescent UC, dysregulation of which was further supported by the pathway-specific gene expression analysis.

3.2. Sequencing of FACS-enriched colonic epithelial cells shows cell type-specific miRNA expression during colonic inflammation in UC

The role of IL-4 and IL-13 in mediating permeability of the epithelial barrier, as well as their relationship to the pathogenesis of UC, has been previously described.²⁹ Additionally, colonic biopsies largely consist of epithelial cells, with comparatively fewer cells of other lineages.²⁵ Therefore, as we have shown that the key player *IL-13* was overexpressed during active and quiescent UC in the colonic tissue, and different epithelial cell populations [such as differentiated and undifferentiated colonocytes, as well as goblet and enteroendocrine cells] expressed downstream genes of this signalling pathway, we further explored colonic epithelial cells during UC more deeply by analysing miRNA dysregulation in two distinct cell populations—crypt-top [CD66a+] and crypt-bottom [CD44+] colonic epithelial cells.

FACS was applied to select and enrich for crypt-bottom and crypt-top colonic epithelial cells from active and quiescent UC patients and healthy controls using CD44⁺ and CD66a⁺ surface markers [Supplementary Figures S2 and S3]. Interestingly, analysis of flow cytometry showed a significant [$FDR < 0.05$] increase in crypt-bottom [CD44⁺] cells in active UC compared to HC [Figure 2A], suggesting a potential inflammation-stimulated cell proliferation.^{30,31}

Using sequencing, 436 unique miRNAs were found to be expressed in crypt-bottom [CD44⁻] and crypt-top [CD66a⁺] epithelial cells. Although the miRNA transcriptomes of these colonic epithelial cell populations were rather similar [Figure 2B], significant changes in expression profiles were observed within and between cell populations in different stages of the disease [Figure 2C and D; Supplementary Table S3]. Initially, pairwise comparisons were performed in the same epithelial cell population to identify UC inflammation-associated miRNAs. As in the tissue data, the number of differentially

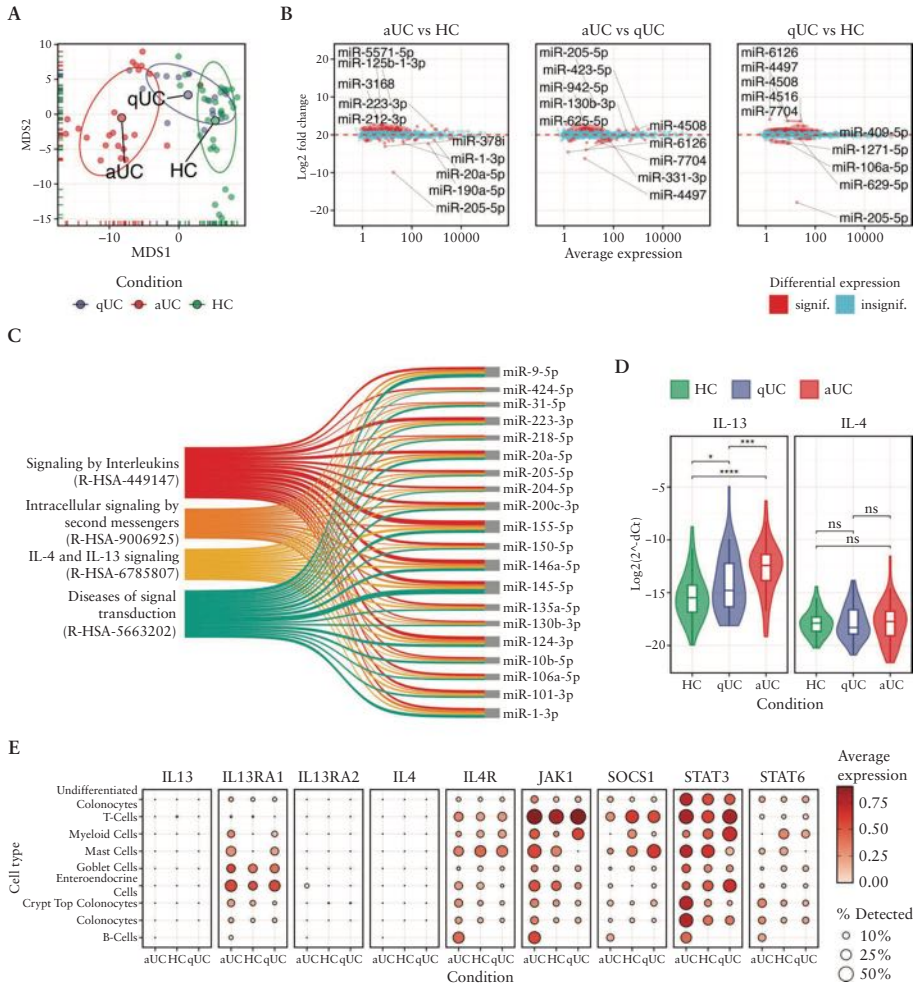


Figure 1. Small RNA-seq defines differentially expressed miRNAs involved in inflammation-associated pathways in active and quiescent UC tissues. [A] MDS plot showing the similarity structure of the miRNA transcriptomes in active UC [aUC] ($n = 23$), quiescent UC [qUC] ($n = 20$), and HC ($n = 30$) tissue samples based on normalized expression values. The dots represent samples coloured by group. The centroid of ellipses corresponds to the group mean; the shapes are defined by covariance within a given group. [B] Differentially expressed miRNAs in aUC ($n = 23$) and qUC ($n = 20$). The red colour represents significantly [FDR < 0.05] differentially expressed miRNAs with an absolute value of $\log_2FC > 1$, while the blue colour represents non-differentially expressed miRNAs. [C] Sankey plot showing the overlapping significantly enriched [FDR < 0.05] Reactome pathways among the pairwise comparisons of aUC and qUC with HC tissues identified by miRNA set enrichment analysis [left side], and highlighting the top 20 miRNAs with the highest count of target genes within these pathways [right side]. Line width reflects the number of miRNA–target gene counts in the pathways. Line colour represents a distinct Reactome pathway. [D] Violin plots showing expression levels of *IL-4* and *IL-13* genes measured by RT-qPCR in colon tissue samples of an independent cohort of HC ($n = 75$), aUC ($n = 75$), and qUC ($n = 50$) individuals. Violin colour represents study group. Median of each group is represented by a vertical line. Quartiles of each group are represented by whiskers. Gene expression is represented on a logarithmic scale, and ΔCt values are inverted in order to show the true direction of the expression. Significance levels: * $p \leq 0.05$, *** $p \leq 0.001$, **** $p \leq 0.0001$, ns—not significant. [E] Dot plot showing the expression of *IL-4* and *IL-13* signalling pathway-related genes in distinct epithelial and immune cell populations of human colon [dataset GEO accession number: GSE116222] within the aUC, qUC, and HC groups. The size of the dot represents the fraction of cells expressing a particular gene in each group [%]. The colour of the dot represents average expression of the gene.

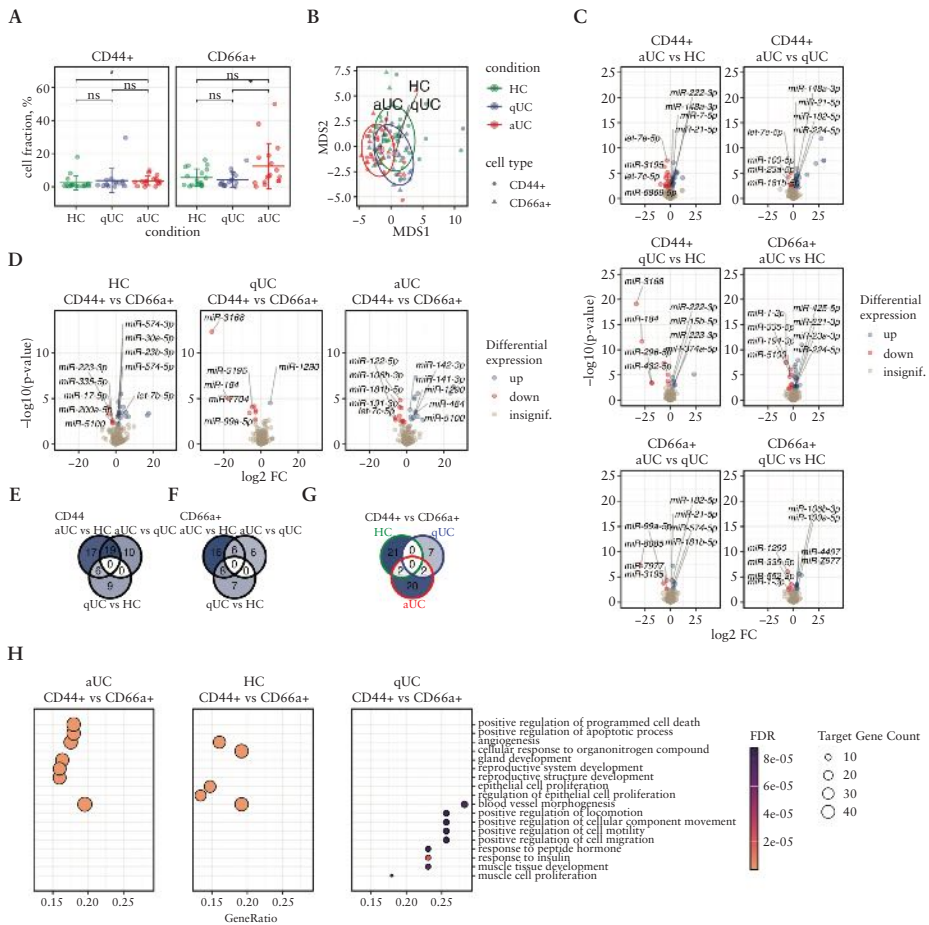


Figure 2. Sequencing data reveal differentially expressed miRNAs in colonic epithelial cells of patients with active and quiescent UC. [A] FACS of colonic epithelial cells and distribution of crypt-top CD44⁺CD66a⁻ and crypt-bottom CD44⁻CD66a⁺ epithelial cell types in inflammatory [aUC] (*n* = 16) and non-inflammatory [qUC and HC] (*n* = 15 and 17) colon tissues. Each dot represents a sample from the patients of the second study group. Mean ± SD of each group is represented by vertical lines. To compare the groups a non-parametric Mann–Whitney U test was performed, **p* < 0.05. [B] MDS plot showing the similarity structure of the miRNA transcriptomes in crypt-top [CD66a⁺] and crypt-bottom [CD44⁺] colonic epithelial cell populations in active UC [aUC] (*n* = 16), quiescent UC [qUC] (*n* = 15), and HC (*n* = 17) based on normalized expression values. Dots represent samples shaped by cell population. Dot colours represent condition. The centroid of ellipses corresponds to the condition group mean; the shapes are defined by covariance within the group. [C, D] Volcano plots of differentially expressed miRNAs in crypt-top [CD66a⁺] and crypt-bottom [CD44⁺] colonic epithelial cell populations in aUC (*n* = 16), qUC (*n* = 15), and HC (*n* = 17). Colours indicate significantly [FDR < 0.05] differentially expressed miRNAs with an absolute value of $\log_2FC > 1$ between compared groups. [E–G] Venn diagrams representing the numbers of commonly and uniquely differentially expressed miRNAs in [E] crypt-bottom [CD44⁺] and [F] crypt-top [CD66a⁺] epithelial cell populations in different UC activity, and [G] between crypt-bottom and crypt-top cells in the same condition. [H] Overrepresented pathways with the top five FDR values between crypt-top [CD66a⁺] and crypt-bottom [CD44⁺] colonic epithelial cell populations during aUC (*n* = 16), qUC (*n* = 15), and HC (*n* = 17) identified by miRNA–target gene set enrichment analysis. Dot size represents the number of miRNA–target counts in the significantly enriched [FDR < 0.05] GO categories.

expressed miRNAs [FDR < 0.05 and $|\log_2FC| > 1$] in both colonic epithelial cell populations were gradually increased depending on disease activity [Figure 2C]. Among deregulated molecules, no miRNAs were commonly differentially

expressed across all three comparisons [active UC vs HC; quiescent UC vs HC; active UC vs quiescent UC] in both crypt-bottom [CD44⁺] and crypt-top [CD66a⁺] colonic epithelial cells. However, six miRNAs [miR-15b-5p, miR-222-3p,

miR-223-3p, miR-194-3p, miR-3195, and miR-574-3p] were identified as commonly differentially expressed in crypt-bottom [CD44⁺] cells and eight miRNAs [let-7c-5p, miR-106b-3p, miR-125b-5p, miR-1-3p, miR-1290, miR-194-3p, miR-335-5p, and miR-552-3p] in crypt-top [CD66a⁺] cells in active and quiescent UC when compared to HC [Figure 2E and F]. Similar to the colonic tissue data, the majority of the overrepresented pathways in both colonic epithelial cell populations at both stages of disease activity overlapped and included signalling pathways such as ‘Signaling by Interleukins’ [R-HSA-449147], ‘Interleukin-4 and Interleukin-13 signaling’ [R-HSA-6785807], and ‘Signaling by Receptor Tyrosine Kinases’ [R-HSA-9006934] [Supplementary Figure S5 and Table S4]. This supports that observations in the colon biopsy samples were mainly driven by colonic epithelial cells.

Further, the response of distinct epithelial cell populations to inflammation was determined by performing pairwise comparisons with the separate populations of colonic epithelial cells. Interestingly, 24 miRNAs were identified to be differentially expressed in active UC, nine miRNAs in quiescent UC, and 22 miRNAs in HC when compared crypt-bottom [CD44⁺] and crypt-top [CD66a⁺] colonic epithelial cells [Figure 2D; Supplementary Table S3]. Notably, the vast majority of identified differentially expressed miRNAs between distinct epithelial cell types in different stages of inflammation were found to be uniquely dysregulated. Only two commonly differentially expressed miRNAs were observed in each of the two comparison groups: miR-106b-3p and miR-1290 in active UC CD44⁺ vs CD66a⁺ and quiescent UC CD44⁺ vs CD66a⁺, and miR-296-5p and miR-432-5p in active UC CD44⁺ vs CD66a⁺ and HC CD44⁺ vs CD66a⁺ [Figure 2G]. This suggests that even at different disease activity stages there are cell population-specific responses, in terms of miRNA expression. The results of GSEA [using GO terms] of deregulated miRNAs in the active UC, quiescent UC, and HC groups revealed that overrepresented processes between crypt-bottom [CD44⁺] compared to crypt-top [CD66a⁺] cells were mainly related to cell differentiation and motility in both active UC and HC [Figure 2H], suggesting that in inflamed and healthy colon mucosa these pathways are differentially regulated between the cell types. Additionally, significant enrichment in ‘epithelium migration’ [GO:0090132] and ‘epithelial cell migration’ [GO:0010631] between crypt-bottom [CD44⁺] and crypt-top [CD66a⁺] cells was uniquely identified only in active UC among the most overrepresented biological processes. Target genes of differentially expressed miRNAs between cell populations in the quiescent UC group were mainly related to cell migration and were least different between those populations.

In summary, despite the significant overlap of aberrantly expressed miRNAs in both colonic epithelial cell populations within regulatory signalling pathways, GSEA results revealed unique involvement of differentially expressed miRNAs between cell populations in processes related to intestinal barrier integrity.

3.3. miRNAs in crypt-top [CD66a⁺] and crypt-bottom [CD44⁺] colonic epithelial cells exhibit a co-expression pattern which is related to UC activity

First, to reveal the relationship between individual miRNA expression levels and endoscopic Mayo subscore in crypt-top [CD66a⁺] and crypt-bottom [CD44⁺] colonic epithelial cells,

Spearman correlation analysis was used. In crypt-bottom [CD44⁺] and crypt-top [CD66a⁺] colonic epithelial cells, a number [$n = 34$ and $n = 23$, respectively] of moderate positive [$0.4 < \rho < 0.7$; FDR < 0.05] and a few [$n = 6$ and $n = 7$, respectively] moderate negative [$-0.7 < \rho < -0.4$; FDR < 0.05] correlations were observed among the normalized miRNA expression levels and endoscopic Mayo subscore [Supplementary Figure S6; Supplementary Tables S5 and S6]. Notably, analysis not only resulted in a substantial overlap in disease activity-associated miRNAs between both colonic epithelial cell populations [29 common moderately correlating miRNAs], but also revealed a few cell population-unique correlations.

Subsequently, we performed more complex analysis and evaluated if certain colonic epithelial cell miRNAs of both populations are co-expressed together. First, WGCNA performed on all miRNAs of colonic epithelial cell populations uncovered the miRNA co-expression network [Figure 3A] and identified two co-expression modules [M1 and M2]. Module M1 comprised 13 miRNAs [miR-10b-5p, miR-182-5p, miR-146a-5p, miR-196b-5p, miR-222-3p, miR-27a-3p, miR-221-3p, miR-194-3p, miR-183-5p, miR-223-3p, miR-574-5p, miR-135b-5p, and miR-31-5p], while module M2 consisted of 11 miRNAs [let-7b-5p, miR-143-3p, miR-125a-5p, miR-15b-5p, let-7e-5p, miR-5100, miR-181b-5p, miR-1-3p, miR-125b-5p, miR-100-5p, and miR-195-5p]. Notably, certain miRNAs in module M1 [e.g. miR-31-5p, miR-223-3p, and miR-10b-5p] were also previously identified as important regulators of genes involved in interleukin signalling pathways [Figure 2H]. Subsequent module enrichment analysis based on the evaluation of normalized enrichment score [NES] [Figure 3B] further revealed that module M1 was significantly enriched in both crypt-top [CD66a⁺] and crypt-bottom [CD44⁺] epithelial cells of patients with active UC (NES = 1.71 [$p_{\text{adj.}} = 9.7 \times 10^{-3}$] and 1.67 [$p_{\text{adj.}} = 2.9 \times 10^{-2}$], respectively), while in both cell populations of control group individuals it was decreased [NES = -1.79 [$p_{\text{adj.}} = 7.7 \times 10^{-3}$] and -1.74 [$p_{\text{adj.}} = 5.0 \times 10^{-2}$], respectively]. Interestingly, the enrichment values for module M2 were opposite to that observed for M1, meaning the normalized expression of module M2 in both crypt-top [CD66a⁺] and crypt-bottom [CD44⁺] epithelial cell populations of patients with active UC was significantly decreased (NES = -1.84 [$p_{\text{adj.}} = 9.7 \times 10^{-3}$] and -1.80 [$p_{\text{adj.}} = 2.9 \times 10^{-2}$], respectively), while it was significantly enriched exclusively in crypt-bottom [CD44⁺] cells of patients with quiescent UC (NES = 2.08 [$p_{\text{adj.}} = 3.3 \times 10^{-4}$]).

Further, we focused on the potentially pro-inflammatory module M1 and explored whether the expression of this module in each of the studied epithelial cell populations is associated with clinical characteristics of UC. Therefore, Spearman correlation analysis was used to check for an association between endoscopic Mayo subscore and module M1 eigengene value [summarized module expression value]. Analysis showed a significant moderate positive correlation in both crypt-top [CD66a⁺] and crypt-bottom [CD44⁺] cells ($\rho = 0.68$ [$p = 1.08 \times 10^{-7}$] and 0.60 [$p = 1.07 \times 10^{-3}$], respectively) [Figure 3C]. Next, AUC-ROC analysis was used to assess the performance of the module M1 eigengene value in distinguishing between active and quiescent UC in each of the studied colonic epithelial cell populations. In crypt-bottom [CD44⁺] cells, analysis gave an AUC value of 80.0% (confidence interval [CI]: 63.6–96.4%), while in the crypt-top [CD66a⁺] cells M1 eigengene expression value demonstrated

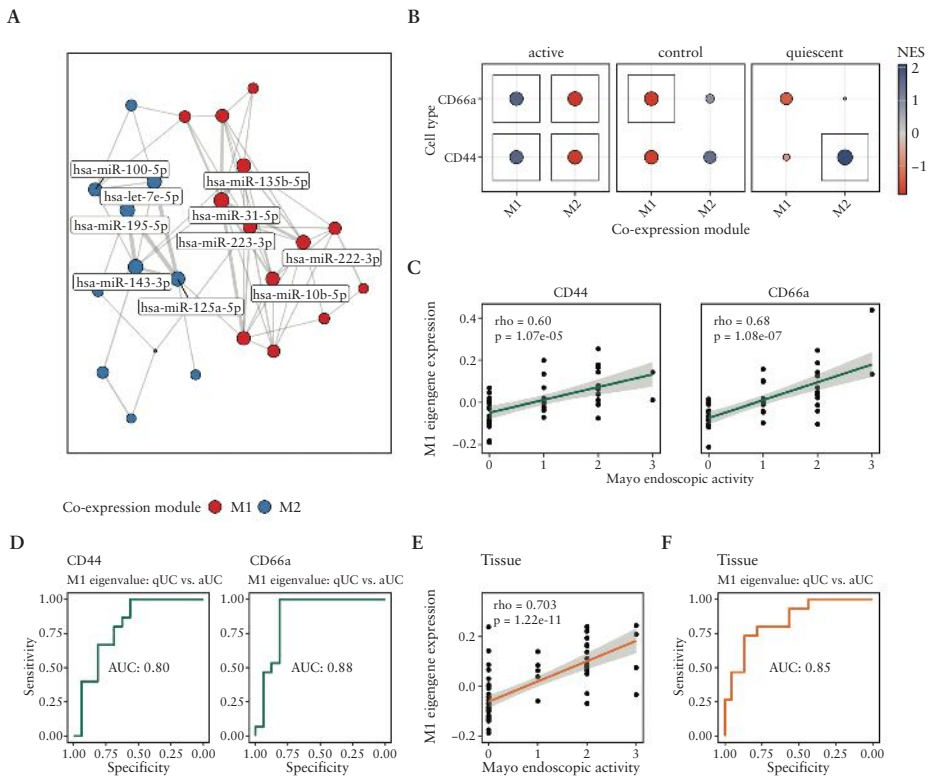


Figure 3. WGCNA in colonic epithelial cell populations reveals miRNA co-expression modules which reflect endoscopic activity of UC. [A] Network displaying identified co-expression modules [M1 and M2] in crypt-top [CD66a⁺] and crypt-bottom [CD44⁻] colonic epithelial cells of patients with active [aUC] ($n = 16$), quiescent UC [qUC] ($n = 15$), and control individuals ($n = 17$). The colour and size of the node represents distinct modules and strength of connectivity, respectively. [B] Dot plot showing normalized enrichment score [NES] of modules M1 and M2 in crypt-top [CD66a⁺] and crypt-bottom [CD44⁻] colonic epithelial cells of patients with active UC, quiescent UC, and control individuals. The colour and size of the dot represents the value and absolute value of NES, respectively. The box marks significant value [$p_{adj} < 0.05$]. Plots [C] and [E] show the correlation between module M1 eigengene value and Mayo endoscopic activity in crypt-bottom [CD44⁻] and crypt-top [CD66a⁺] colonic epithelial cells as well as colon tissue, respectively. Spearman correlation coefficient. Each dot represents a different sample. Plots [D] and [F] show the AUC-ROC curves reflecting the performance of M1 module eigengene value at distinguishing between active UC [aUC] and quiescent UC [qUC] in crypt-bottom [CD44⁻] and crypt-top [CD66a⁺] colonic epithelial cells as well as in colon tissue, respectively.

even better performance with an AUC value of 87.9% [CI: 74.0–100.0%] when separating quiescent vs active UC [Figure 3D]. To evaluate the concordance of the epithelial cell population-derived data with the situation in colon tissue, we calculated module M1 eigengene values in the tissue and performed analogous analysis as in the crypt-top and crypt-bottom cell populations. In colon tissue, the module M1 eigengene showed strong a positive correlation with endoscopic Mayo subscore ($\rho = 0.703$ [$p = 1.22 \times 10^{-11}$]) [Figure 3E] with an AUC of 85.0% [CI: 72.2–97.1%] [Figure 3F]. These results indicated high resemblance between whole tissue and colonic crypt-top [CD66a⁺] epithelial cells.

Generally, the results uncovered potential UC endoscopic activity-related miRNA co-expression patterns that are not only characteristic for both crypt-top and crypt-bottom

colonic epithelial cell populations, but also reflect the overall situation in the more heterogeneous colon tissue during UC.

4. Discussion

Although UC is a well-studied complex disease and huge efforts have been made to explore its molecular mechanisms, the disease pathogenesis remains largely unclear.³² In particular, there is a substantial knowledge gap regarding expression patterns of regulatory non-coding miRNA in UC in a cell type-specific context. Thus, here we provide an overview of the miRNA expression in unsorted whole colonic mucosa samples of UC patients, present detailed colonic epithelial cell population-specific miRNA expression profiles from active and quiescent UC patients, and describe differences in

miRNA expression patterns between two distinct—crypt-bottom [CD44⁺] and crypt-top [CD66a⁺]—cell populations. Furthermore, we describe putative biological pathways in which deregulated miRNAs of UC colonic epithelial cell populations might be involved, identify a potential inflammatory miRNA co-expression module, determine its associations with endoscopic disease activity, and evaluate its performance in distinguishing between active and quiescent stages of UC.

Most importantly, we determined distinct responses in miRNA expression of different colonic epithelial cell populations during UC. Our findings showed that in colon crypt-bottom [CD44⁺] cells (compared to crypt-top [CD66a⁺] cells) inflammation promoted/suppressed the expression of several miRNAs possibly involved in cell proliferation, differentiation, and/or permeability of the intestinal barrier. For example, let-7c-5p showed considerable down-regulation and miR-501-3p up-regulation in crypt-bottom [CD44⁺] cells during active UC. It has previously been shown that overexpression of let-7c-5p as well as inhibition of miR-501-3p can reduce the proliferation of colorectal cancer cells.^{33,34} Thus, deregulation of these miRNAs might be related to the relative increase of crypt-bottom [CD44⁺] cells in active UC when compared to controls, as has been shown in our flow cytometry experiment. On the other hand, we observed increased expression of miR-1-3p and decreased expression of miR-125b-5p in crypt-bottom compared to crypt-top cells only during active UC. Both miRNAs were shown to be involved in barrier function dysregulation, where a decrease of miR-125b-5p³⁵ and increase of miR-1-3p³⁶ contribute to disruption of the epithelial barrier in colon tissue. This would suggest that the epithelial barrier is already impaired in crypt-bottom epithelial cells during active UC; however, it remains unclear if this is a UC-specific event or rather a normal cell response to inflammation in the gut.

Furthermore, our analysis showed that not only are certain individual miRNAs associated with the endoscopic Mayo subscore, but they also form an inflammation-related co-expression network, which directly correlates with clinical disease activity. Of two identified miRNA co-expression modules in both crypt-bottom [CD44⁺] and/or crypt-top [CD66a⁺] cells, module M1 was significantly enriched in both epithelial cell populations of active UC patients and comprised miRNAs such as miR-31-5p, miR-135b-5p, miR-27a-3p, miR-222-3p, and miR-223-3p. In the literature, these small non-coding RNAs are also reported to be up-regulated in inflamed, non-inflamed and/or pre-cancerous colon tissues as well as in faeces [specifically, miR-223-3p] of UC patients^{37–42} and are involved in the regulation of inflammatory response [e.g. miR-222-3p targets *SOCS1* and activates *STAT3* signalling].^{43–45} Additionally, we observed that all miRNAs belonging to module M1 were involved in Reactome pathways related to interleukin signalling by targeting various validated genes [e.g. *FOXO3*, *IGF1R*, *ICAM1*, *STAT6*, *STAT1*, *STAT5A*, and *CCND1*]. Interestingly, when comparing crypt-top and crypt-bottom cell population-derived module M1 performance and association results to colon tissue, both the correlation coefficient and AUC values in tissue were more like those observed in crypt-top [CD66a⁺] cells. This may be at least partially explained by the cellular composition of the colon mucosa, the most abundant cell type in the mucosal layer being absorptive colonocytes.⁴⁶ By contrast, the second identified miRNA co-expression module M2 showed an inverse correlation with the endoscopic Mayo subscore and was exclusively enriched

in crypt-bottom [CD44⁺] colonic epithelial cells of quiescent UC patients, suggesting its anti-inflammatory properties. For example, among module M2 miRNAs we identified let-7e-5p, which, together with other let-7 miRNAs, has been previously shown to affect maintenance of cell differentiation.⁴⁷ Additionally, in the intestinal epithelium let-7 family member let-7b appears to be among the highest-expressed miRNAs in the let-7 group/family [Supplementary Figure S6]. Together, these observations suggest the relevance of let-7 miRNAs during intestinal inflammation via maintenance of stemness of crypt-bottom [CD44⁺] cells and thereby explain their expression correlation with disease activity, exclusively in undifferentiated colonic epithelial cells.

Finally, we described potential involvement of differentially expressed miRNAs in regulatory biological pathways. Our initial small RNA-seq of colonic mucosa biopsies from active and quiescent UC compared to healthy controls, at first, revealed multiple deregulated miRNAs, which were significantly enriched in inflammation- and intestinal epithelial barrier function-related biological pathways. Interestingly, miRNAs enriched in interleukin biological pathways, such as IL-4 and IL-13 signalling, were deregulated not only in active but also in quiescent UC, suggesting lasting derangement of this pathway in UC mucosa. The IL-4 and IL-13 pathway is known to differentially regulate epithelial chloride secretion and cause epithelial barrier dysfunction.⁴⁸ It has been shown that large amounts of IL-13 are produced in colon mucosa of UC patients and thereby impair epithelial barrier function by affecting epithelial apoptosis, tight junctions, and restitution velocity.^{29,49} We also confirmed the increased expression of the IL-13 gene during the course of UC when analysing active and quiescent UC patient colon tissue samples. By contrast, some studies report decreased mucosal amounts of IL-13 in active UC.⁵⁰ Nevertheless, attempts are still being made to adapt the inhibition of IL-13-based treatment to induce UC remission (e.g. clinical trials of anti-IL-13 monoclonal antibodies [tralokinumab and anrukinzumab]⁵¹ and preclinical studies of anti-IL-Rα2⁵²). Similar to the results in colonic biopsies, both crypt-bottom [CD44⁺] and crypt-top [CD66a⁺] epithelial cell populations showed deregulation in miRNAs during UC, the targets of which were significantly enriched in the IL-4 and IL-13 signalling pathway. Since IL-4 and IL-13 cytokines are predominantly produced by immune cells,⁵³ the expected regulatory action of deregulated miRNAs in colonic epithelial cells would be downstream targets of the pathway, such as *STAT3*, *FOXO3*, and *SOCS1*. During active UC in both crypt-bottom [CD44⁺] and crypt-top [CD66a⁺] cells, we found miR-221-3p, miR-182-6p, miR-222-3p, and miR-31-5p to be up-regulated, which are known to target the *FOXO3* gene.²² Up-regulation of the aforementioned miRNAs, theoretically, would lead to decreased expression of the *FOXO3* gene, as already observed in colonic mucosa of UC patients.⁵⁴ This, in turn, may lead to more severe colonic inflammation during UC.⁵⁵ Additionally, both crypt-bottom [CD44⁺] and crypt-top [CD66a⁺] cells of patients with active UC had increased expression of hsa-miR-221-3p and hsa-miR-21-5p, which target the *SOCS1* gene.²² *SOCS1* is an important regulator of IL-4 signalling, and its forced expression was shown to inhibit IL-13 signalling in epithelial cells.⁵⁶ In addition to involvement in interleukin signalling pathways, we observed a few aberrantly expressed miRNAs between crypt-bottom [CD44⁺] and crypt-top [CD66a⁺]

cells in active UC that possibly exert their biological function through regulation of epithelial cell migration, which is known to occur along the crypt-villus axis⁵⁷ and is increased during inflammatory bowel disease.⁵⁸ Noteworthy, the GSEA results should be treated with caution, since the selection of miRNA targets significantly affects the results.⁵⁹ However, currently, there are no methods to solve this issue, since miRNA target prediction as well as its dosage to affect target expression remain unsolved problems in the field.

In summary, our study determined crypt-bottom [CD44⁺] and crypt-top [CD66a⁺] colonic epithelial cell-specific miRNA deregulation in UC in a cell type- and disease stage-dependent manner. We also revealed cell population-specific miRNA expression patterns and networks as well as their associations with clinical disease activity. Furthermore, we unveiled the potential functional role of differentially expressed miRNAs and observed their possible involvement in biological pathways associated with maintenance of intestinal barrier function in active as well as quiescent UC, in both epithelial cell populations. Together, these observations not only highlight the regulatory importance of miRNAs in distinct colonic epithelial cell populations during the pathogenesis of UC, but also provide potential miRNA candidates for the development of new treatment strategies to maintain the remission of mucosal inflammation.

Conference Presentation

Part of this work was presented at the 16th Congress of ECCO Virtual—Inflammatory Bowel Diseases 2021, July 2–3 & 8–10, 2021.

Funding

This work was supported by the Research Council of Lithuania and European Crohn's and Colitis Organisation [grant number S-MIP-20-56 and ECCO Grant 2016, respectively].

Conflict of Interest

The authors declare no conflict of interest.

Author Contributions

JS, SJ, and JK participated in the concept and design of the study. JK, LVJ, VK, UK, GV, and GK participated in patient recruitment, material collection and sample processing. RR, ID, and AZ were responsible for fluorescence-activated cell sorting. AF and SS provided infrastructure for small RNA library preparation and sequencing. RI and SJ were responsible for bioinformatics, statistical analysis, data interpretation, and writing the first draft of the manuscript. All authors were members of the writing group and participated in the drafting revision of the manuscript.

Data Availability

The small RNA-seq data underlying this article are available in the Gene Expression Omnibus [GEO] Database and can be accessed with accession numbers GSE185101 and GSE185102. Supplementary Tables S1–S6 are available upon request from the corresponding author.

Supplementary Data

Supplementary data are available online at ECCO-JCC online.

References

1. Antoni L, Nuding S, Wehkamp J, Stange EF. Intestinal barrier in inflammatory bowel disease. *World J Gastroenterol* 2014;20:1165–79.
2. Nyström EEL, Martínez-Abad B, Arike L, et al. An intercrypt subpopulation of goblet cells is essential for colonic mucus barrier function. *Science* 2021;372:eabb1590.
3. Cichon C, Sabharwal H, Rüter C, Schmidt MA. MicroRNAs regulate tight junction proteins and modulate epithelial/endothelial barrier functions. *Tissue Barriers* 2014;2:e944446.
4. Ye D, Guo S, Alsadi R, Ma TY. MicroRNA regulation of intestinal epithelial tight junction permeability. *Gastroenterology* 2011;141:1323–33.
5. Magro F, Gionchetti P, Eliakim R, et al.; European Crohn's and Colitis Organisation [ECCO]. Third European Evidence-based consensus on diagnosis and management of ulcerative colitis. Part 1: definitions, diagnosis, extra-intestinal manifestations, pregnancy, cancer surveillance, surgery, and ileo-anal pouch disorders. *J Crohns Colitis* 2017;11:649–70.
6. Schroeder KW, Tremaine WJ, Ilstrup DM. Coated oral 5-aminosalicylic acid therapy for mildly to moderately active ulcerative colitis. A randomized study. *N Engl J Med* 1987;317:1625–9.
7. Dalerba P, Kalisky T, Sahoo D, et al. Single-cell dissection of transcriptional heterogeneity in human colon tumors. *Nat Biotechnol* 2011;29:1120–7.
8. Ewels PA, Peltzer A, Fillinger S, et al. The nf-core framework for community-curated bioinformatics pipelines. *Nat Biotechnol* 2020;38:276–8.
9. Pantano L, Estivill X, Martí E. A non-biased framework for the annotation and classification of the non-miRNA small RNA transcriptome. *Bioinformatics* 2011;27:3202–3.
10. Langmead B, Trapnell C, Pop M, Salzberg SL. Ultrafast and memory-efficient alignment of short DNA sequences to the human genome. *Genome Biol* 2009;10:R25–10.
11. Kozomara A, Birgaoanu M, Griffiths-Jones S. miRBase: from microRNA sequences to function. *Nucleic Acids Res* 2019;47:D155–62.
12. Desvignes T, Loher P, Eilbeck K, et al. Unification of miRNA and isomiR research: the mirGFF3 format and the mirtop API. *Bioinformatics* 2020;36:698–703.
13. Love MI, Huber W, Anders S. Moderated estimation of fold change and dispersion for RNA-seq data with DESeq2. *Genome Biol* 2014;15:1–21.
14. Ritchie ME, Phipson B, Wu D, et al. limma powers differential expression analyses for RNA-seq and microarray studies. *Nucleic Acids Res* 2015;43:e47.
15. R Foundation for Statistical Computing. R Core Team. R: a language and environment for statistical computing 2021. <https://www.r-project.org/>. Accessed 10 September 2019.
16. Wickham H. Getting Started with ggplot2. ggplot2: elegant graphics for data analysis. Springer Cham 2016; 11–31.
17. Jassal B, Matthews L, Viteri G, et al. The reactome pathway knowledgebase. *Nucleic Acids Res* 2020;48:D498–503.
18. Thomas PD, Ebert D, Muruganujan A, Mushayahama T, Albou LP, Mi H. PANTHER: making genome-scale phylogenetics accessible to all. *Protein Sci* 2022;31:8–22.
19. Xiao F, Zuo Z, Cai G, Kang S, Gao X, Li T. miRecords: an integrated resource for microRNA-target interactions. *Nucleic Acids Res* 2009;37:D105–10.
20. Hsu S-D, Lin F-M, Wu W-Y, et al. miRTarBase: a database curates experimentally validated microRNA-target interactions. *Nucleic Acids Res* 2011;39:D163–9.
21. Karagkouni D, Paraskevopoulou MD, Chatzopoulos S, et al. DIANA-TarBase v8: a decade-long collection of experimentally

- supported miRNA-gene interactions. *Nucleic Acids Res* 2018;**46**:D239–45.
22. Ru Y, Kechris KJ, Tabakoff B, et al. The multiMiR R package and database: integration of microRNA-target interactions along with their disease and drug associations. *Nucleic Acids Res* 2014;**42**:e133.
 23. Yu G, He Q-Y. ReactomePA: an R/Bioconductor package for reactome pathway analysis and visualization. *Mol Biosyst* 2016;**12**:477–9.
 24. Wu T, Hu E, Xu S, et al. clusterProfiler 4.0: a universal enrichment tool for interpreting omics data. *Innovation (Camb)*. 2021;**2**:100141.
 25. Parikh K, Antanaviciute A, Fawcner-Corbett D, et al. Colonic epithelial cell diversity in healthy and inflammatory bowel disease. *Nature* 2019;**567**:49–55.
 26. Russo PST, Ferreira GR, Cardozo LE, et al. CEMiTool: a bioconductor package for performing comprehensive modular co-expression analyses. *BMC Bioinf* 2018;**19**:56.
 27. Langfelder P, Horvath S. WGCNA: an R package for weighted correlation network analysis. *BMC Bioinf* 2008;**9**:559.
 28. Robin X, Turck N, Hainard A, et al. pROC: an open-source package for R and S+ to analyze and compare ROC curves. *BMC Bioinf* 2011;**12**:77.
 29. Heller F, Florian P, Bojarski C, et al. Interleukin-13 is the key effector Th2 cytokine in ulcerative colitis that affects epithelial tight junctions, apoptosis, and cell restitution. *Gastroenterology* 2005;**129**:550–64.
 30. Yao D, Dong M, Dai C, Wu S. Inflammation and inflammatory cytokine contribute to the initiation and development of ulcerative colitis and its associated cancer. *Inflamm Bowel Dis* 2019;**25**:1595–602.
 31. MacDonald TT. Epithelial proliferation in response to gastrointestinal inflammation. *Ann N Y Acad Sci* 1992;**664**:202–9.
 32. Ungaro R, Mehandru S, Allen PB, Peyrin-Biroulet L, Colombel J-F. Ulcerative colitis. *Lancet* 2017;**389**:1756–70.
 33. Wu F, Xing T, Gao X, Liu F. miR-501-3p promotes colorectal cancer progression via activation of Wnt/ β -catenin signaling. *Int J Oncol* 2019;**55**:671–83.
 34. Akao Y, Nakagawa Y, Naoe T. let-7 microRNA functions as a potential growth suppressor in human colon cancer cells. *Biol Pharm Bull* 2006;**29**:903–6.
 35. Martínez C, Rodiño-Janeiro BK, Lobo B, et al. miR-16 and miR-125b are involved in barrier function dysregulation through the modulation of claudin-2 and cingulin expression in the jejunum in IBS with diarrhoea. *Gut* 2017;**66**:1537–8.
 36. Sun T-Y, Li Y-Q, Zhao F-Q, et al. MiR-1-3p and MiR-124-3p synergistically damage the intestinal barrier in the ageing colon. *J Crohns Colitis* 2022;**16**:656–67.
 37. Tian Y, Xu J, Li Y, et al. MicroRNA-31 reduces inflammatory signaling and promotes regeneration in colon epithelium, and delivery of mimics in microspheres reduces colitis in mice. *Gastroenterology* 2019;**156**:2281–96.e6.
 38. Masi L, Capobianco I, Magri C, Marafini I, Petito V, Scaldaferrri F. MicroRNAs as innovative biomarkers for inflammatory bowel disease and prediction of colorectal cancer. *Int J Mol Sci* 2022;**23**:7991.
 39. Su C, Huang D-P, Liu J-W, Liu W-Y, Cao Y-O, Cao Y-O. miR-27a-3p regulates proliferation and apoptosis of colon cancer cells by potentially targeting BTG1. *Oncol Lett* 2019;**18**:2825–34.
 40. Zhou J, Liu J, Gao Y, Shen L, Li S, Chen S. miRNA-based potential biomarkers and new molecular insights in ulcerative colitis. *Front Pharmacol* 2021;**12**:707776.
 41. Béres NJ, Szabó D, Kocsis D, et al. Role of altered expression of miR-146a, miR-155, and miR-122 in pediatric patients with inflammatory bowel disease. *Inflamm Bowel Dis* 2016;**22**:327–35.
 42. Neudecker V, Haneklaus M, Jensen O, et al. Myeloid-derived miR-223 regulates intestinal inflammation via repression of the NLRP3 inflammasome. *J Exp Med* 2017;**214**:1737–52.
 43. Gwiggner M, Martinez-Nunez RT, Whiteoak SR, et al. MicroRNA-31 and MicroRNA-155 are overexpressed in ulcerative colitis and regulate IL-13 signaling by targeting interleukin 13 receptor α -1. *Genes (Basel)* 2018;**9**:85.
 44. Xia F, Bo W, Ding J, Yu Y, Wang J. MiR-222-3p aggravates the inflammatory response by targeting SOCS1 to activate STAT3 signaling in ulcerative colitis. *Turk J Gastroenterol* 2022;**33**:934–44.
 45. Wang H, Chao K, Ng SC, et al. Pro-inflammatory miR-223 mediates the cross-talk between the IL23 pathway and the intestinal barrier in inflammatory bowel disease. *Genome Biol* 2016;**17**:58.
 46. Allaire JM, Crowley SM, Law HT, Chang S-Y, Ko H-J, Vallance BA. The intestinal epithelium: central coordinator of mucosal immunity. *Trends Immunol* 2018;**39**:677–96.
 47. Chirshv E, Oberg KC, Ioffe YJ, Unteraehrer JJ, Unteraehrer JJ. Let-7 as biomarker, prognostic indicator, and therapy for precision medicine in cancer. *Clin Transl Med* 2019;**8**:24.
 48. Saatian B, Rezaee F, Desando S, et al. Interleukin-4 and interleukin-13 cause barrier dysfunction in human airway epithelial cells. *Tissue Barriers* 2013;**1**:e24333.
 49. Rosen MJ, Frey MR, Washington MK, et al. STAT6 activation in ulcerative colitis: a new target for prevention of IL-13-induced colon epithelial cell dysfunction. *Inflamm Bowel Dis* 2011;**17**:2224–34.
 50. Kadivar K, Ruchelli ED, Markowitz JE, et al. Intestinal interleukin-13 in pediatric inflammatory bowel disease patients. *Inflamm Bowel Dis* 2004;**10**:593–8.
 51. Giuffrida P, Caprioli F, Facciotti F, Di Sabatino A. The role of interleukin-13 in chronic inflammatory intestinal disorders. *Autoimmun Rev* 2019;**18**:549–55.
 52. Karnele EP, Pasricha TS, Ramalingam TR, et al.; 23andMe Research Team. Anti-IL-13R α 2 therapy promotes recovery in a murine model of inflammatory bowel disease. *Mucosal Immunol* 2019;**12**:1174–86.
 53. Junttila IS. Tuning the cytokine responses: an update on interleukin (IL)-4 and IL-13 receptor complexes. *Front Immunol* 2018;**9**:888.
 54. Min M, Yang J, Yang Y-S, Liu Y, Liu L-M, Xu Y. Expression of transcription factor FOXO3a is decreased in patients with ulcerative colitis. *Chin Med J (Engl)* 2015;**128**:2759–63.
 55. Snoeks L, Weber CR, Wasland K, et al. Tumor suppressor FOXO3 participates in the regulation of intestinal inflammation. *Lab Invest* 2009;**89**:1053–62.
 56. Doran E, Choy DF, Shikotra A, et al. Reduced epithelial suppressor of cytokine signalling 1 in severe eosinophilic asthma. *Eur Respir J* 2016;**48**:715–25.
 57. Krndija D, El Marjou F, Guirao B, et al. Active cell migration is critical for steady-state epithelial turnover in the gut. *Science* 2019;**365**:705–10.
 58. Martini E, Krug SM, Siegmund B, Neurath MF, Becker C. Mend your fences: the epithelial barrier and its relationship with mucosal immunity in inflammatory bowel disease. *Cell Mol Gastroenterol Hepatol* 2017;**4**:33–46.
 59. Godard P, van Eyll J. Pathway analysis from lists of microRNAs: common pitfalls and alternative strategy. *Nucleic Acids Res* 2015;**43**:3490–7.

Publication no. 2

Title: Constituents of stable commensal microbiota imply diverse colonic epithelial cell reactivity in patients with ulcerative colitis

Authors: Inčiūraitė Rūta, Gedgaudas Rolandas, Lukoševičius Rokas, Tilindė Deimantė, Ramonaitė Rima, Link Alexander, Kašėtienė Neringa, Malakauskas Mindaugas, Kiudelis Gediminas, Jonaitis Laimas Virginijus, Kupčinskas Juozas, Juzėnas Simonas, Skiecevičienė Jurgita

Gut Pathogens (2024)

Reprinted under a Creative Commons Attribution 4.0 International (CC BY 4.0) licence

RESEARCH

Open Access



Constituents of stable commensal microbiota imply diverse colonic epithelial cell reactivity in patients with ulcerative colitis

Ruta Inciuraitė^{1*}, Rolandas Gedgaudas^{1,2}, Rokas Lukosevicius¹, Deimante Tilinde¹, Rima Ramonaite¹, Alexander Link³, Neringa Kasetiene⁴, Mindaugas Malakauskas⁴, Gediminas Kiudelis^{1,2}, Laimas Virginijus Jonaitis^{1,2}, Juozas Kupcinskis^{1,2}, Simonas Juzenas^{1,5} and Jurgita Skieceviciene^{1*}

Abstract

Background Despite extensive research on microbiome alterations in ulcerative colitis (UC), the role of the constituent stable microbiota remains unclear.

Results This study, employing 16S rRNA-gene sequencing, uncovers a persistent microbial imbalance in both active and quiescent UC patients compared to healthy controls. Using co-occurrence and differential abundance analysis, the study highlights microbial constituents, featuring *Phocaeicola*, *Collinsella*, *Roseburia*, *Holdemanella*, and *Bacteroides*, that are not affected during the course of UC. Co-cultivation experiments, utilizing commensal *Escherichia coli* and *Phocaeicola vulgatus*, were conducted with intestinal epithelial organoids derived from active UC patients and controls. These experiments reveal a tendency for a differential response in tight junction formation and maintenance in colonic epithelial cells, without inducing pathogen recognition and stress responses, offering further insights into the roles of these microorganisms in UC pathogenesis. These experiments also uncover high variation in patients' response to the same bacteria, which indicate the need for more comprehensive, stratified analyses with an expanded sample size.

Conclusion This study reveals that a substantial part of the gut microbiota remains stable throughout progression of UC. Functional experiments suggest that members of core microbiota – *Escherichia coli* and *Phocaeicola vulgatus* – potentially differentially regulate the expression of tight junction gene in the colonic epithelium of UC patients and healthy individuals.

Keywords Ulcerative colitis, Gut microbiota, *Escherichia coli*, *Phocaeicola vulgatus*, Colonic epithelial organoids, Colonic epithelial barrier, Crosstalk

*Correspondence:

Ruta Inciuraitė
ruta.inciuraitė@smu.lt
Jurgita Skieceviciene
jurgita.skieceviciene@smu.lt

¹Institute for Digestive Research, Academy of Medicine, Lithuanian University of Health Sciences, Kaunas, Lithuania

²Department of Gastroenterology, Academy of Medicine, Lithuanian University of Health Sciences, Kaunas, Lithuania

³Department of Gastroenterology, Hepatology and Infectious Diseases, Otto-von-Guericke University Hospital Magdeburg, Magdeburg, Germany

⁴Department of Food Safety and Quality, Academy of Veterinary, Lithuanian University of Health Sciences, Kaunas, Lithuania

⁵Institute of Biotechnology, Life Sciences Center, Vilnius University, Vilnius, Lithuania



© The Author(s) 2024. **Open Access** This article is licensed under a Creative Commons Attribution 4.0 International License, which permits use, sharing, adaptation, distribution and reproduction in any medium or format, as long as you give appropriate credit to the original author(s) and the source, provide a link to the Creative Commons licence, and indicate if changes were made. The images or other third party material in this article are included in the article's Creative Commons licence, unless indicated otherwise in a credit line to the material. If material is not included in the article's Creative Commons licence and your intended use is not permitted by statutory regulation or exceeds the permitted use, you will need to obtain permission directly from the copyright holder. To view a copy of this licence, visit <http://creativecommons.org/licenses/by/4.0/>. The Creative Commons Public Domain Dedication waiver (<http://creativecommons.org/publicdomain/zero/1.0/>) applies to the data made available in this article, unless otherwise stated in a credit line to the data.

Background

Ulcerative colitis (UC) is a complex, chronic inflammatory disorder, characterized by periods of relapse and remission, often leading to significant morbidity and reduced quality of life [1]. While the exact etiology of UC remains elusive, emerging evidence points towards an important role for the gut microbiota in disease pathogenesis [2]. The interplay between the host and its microbial inhabitants is known to be a crucial factor of intestinal homeostasis, which is commonly impaired in UC [3].

In this study we aim to investigate the relationship between gut microbiota dynamics as well as epithelial cell response to commensal bacteria in patients with UC and healthy individuals. Specifically, we explore the alterations as well as consistencies in the composition of the gut microbiota in the individuals afflicted with UC. Additionally, we focus on how co-cultivation of stable, rather than altered, predominantly commensal bacteria (such as *Escherichia coli* and *Phocaeicola vulgatus*) [4, 5] with healthy or UC patient-derived colonic epithelial organoids affect host gene expression responsible for pathogen recognition, tight junction regulation and stress stimuli indication, and how this response differs between UC-afflicted and healthy colonic epithelial cells. Understanding the intricate crosstalk between the host response and the consistently resident microbiota holds the potential to uncover novel insights into the mechanisms underlying UC pathogenesis.

In this context, we present a comprehensive analysis of gut microbiota profiles in active and quiescent UC patients as well as healthy individuals, shedding light on altered and stable microbiota. Importantly, we focus on the bacteria that remain unaltered after undergoing the reduction of diversity during the pathogenesis of UC. Furthermore, we delve into the putative functional consequences of these unaltered and predominantly commensal bacteria to discern their potential implications for disease progression, including their capacity to trigger UC relapses.

Methods

Study samples

Study subject recruitment was conducted at the Department of Gastroenterology, Lithuanian University of Health Sciences (Kaunas, Lithuania) during the period of 2020–2022. The study was approved by the Kaunas Regional Biomedical Research Ethics Committee (Protocol No. BE-2-31) and all subjects signed written informed consent to participate in the study. All procedures were performed in accordance with relevant guidelines and regulations. Colonic biopsies were obtained from patients with a previously established diagnosis of UC (based on clinical, endoscopic, and histological examinations). Individuals without inflammatory, oncological, or other gastrointestinal diseases were enrolled in the study as controls. UC patients underwent colonoscopy procedures either because of a disease flare or for screening purposes, while control individuals underwent colonoscopy procedure through colorectal cancer screening program. The study included two cohorts of samples (Table 1). UC patients were subgrouped based on endoscopic Mayo score (score of 0–1 was considered mild disease (healed mucosa), 2 reflected moderate severity of UC, and 3 was considered as an indicator for severe UC (with spontaneous bleeding and ulcerations in the colon) [6]. Individuals with an endoscopic Mayo score >1 were classified as active UC patients, while those with endoscopic Mayo score ≤1 were considered as a quiescent UC (in remission) group. The age and sex of individuals did not differ significantly between patient groups of each cohort (cohort 1 and 2).

Nucleic acid extraction

For gut microbiota analysis, nucleic acids were extracted from fecal samples using the AllPrep PowerFecal DNA/RNA kit (Qiagen) following the manufacturer's protocol. In brief, up to 200 mg of fresh-frozen fecal samples were lysed using chemical and mechanical homogenization and DNA was eluted into 30 µl of elution buffer. For colonic epithelial cell gene expression analysis, intestinal monolayer cultures were processed using AllPrep DNA/RNA Micro Kit (Qiagen). Cells were lysed and homogenized chemically, using denaturing guanidine isothiocyanate-containing buffer. Purified RNA was eluted into 14 µl of RNase and DNase-free water. Purity and concentration of extracted nucleic acids were evaluated using Qubit 4 (Invitrogen) fluorometer and respective assay kits.

16S rRNA-gene library preparation and sequencing

The isolated DNA underwent amplification with the specific primer pair set 27F 5'-AGAGTTTGATCCTGGCT CAG-3' and 338R 5'-TGCTGCCTCCCGTAGGAGT-3', using dual-indexing during the PCR process. Cycling

Table 1 Demographic and clinical characteristics of the study subjects

	Cohort 1, n = 72			Cohort 2, n = 17	
	Control, n = 25	Active UC, n = 27	Quiescent UC, n = 20	Control, n = 8	Active UC, n = 9
Age					
Mean ± SD	40.9 ± 13.2	43.3 ± 17.3	45.8 ± 15.3	56.9 ± 7.3	44.2 ± 15.9
Sex, n (%)					
Female	3 (50.0)	3 (50.0)	3 (43.0)	4 (50.0%)	4 (44.4%)
Endoscopic Mayo score					
Min-max	-	2–3	0–1	-	2–3

SD – standard deviation, UC – ulcerative colitis

conditions: 1×98 °C 30 s.; 34×98 °C 9 s., 50 °C 1 min., 72 °C 20 s.; 1×72 °C 10 min; 1×10 °C ∞. Purification and normalization of the PCR products were carried out using the Invitrogen SequalPrep Normalization Plate Kit (Thermo Fisher Scientific). After the preparation, 16S rRNA gene sequencing was conducted on the Illumina MiSeq platform in accordance with the manufacturer's instructions, utilizing MiSeq Reagent Kit v3 (2×300 bp) (Illumina).

16S rRNA-gene sequencing data analysis

The obtained sequencing data were processed into amplicon sequencing variants and taxonomically annotated against the RDP v18 database [7] using the 'DADA2' (V.1.10) [8] software package in R, following the DADA2 workflow. Specifically, reads were truncated to 200 base pairs for forward and 150 base pairs for reverse using the `truncLen` parameter, while the maximum number of expected errors (`maxEE` parameter) was set to 3 for both directions. Additionally, trimming of the first 5 bases from both forward and reverse reads (`trimLeft` parameter) was performed to enhance overall quality, with primer sequences already removed from the fastQ files. The `maxN` parameter was set to 0, indicating the exclusion of reads containing ambiguous base calls (N's). Reads were truncated at the first instance of a quality score equal to or lower than 5 using the `truncQ` parameter. These parameter configurations were chosen to ensure the retention of high-quality reads while effectively filtering out artifacts and low-quality regions. Rarefaction was used as a measure of normalization, with all samples rarefied to 22,032 reads per sample. Rare taxa, defined as ASVs with fewer than 10 counts and present in less than 10% of total samples were filtered before performing α -diversity, β -diversity and compositional analyses. Alpha diversity was assessed using the Chao1, Simpson and Shannon index, while Bray Curtis dissimilarity on taxa relative abundances was used as a measure of β -diversity. Permutational analysis of variance (PERMANOVA) within the `vegan` package was employed to identify significant changes in Bray-Curtis dissimilarity. For core microbiome analysis, a minimum relative abundance of 0.1% in at least 50% of samples was applied. Differential abundance analysis was conducted on the taxa count matrix utilizing the Wilcoxon rank-sum test. This analysis focused only on taxa that had a minimum count of 10 and appeared in more than 20% of the samples. The *P* values obtained from the Wilcoxon rank-sum test underwent Benjamini-Hochberg (BH) correction to control the false discovery rate. A corrected *P* value (BH adjusted P_{Wilcoxon}) threshold of 0.05 was set to determine statistical significance in the differential abundance analysis. Compositional plots were generated using `microViz` package [9].

Establishment and expansion of 3D colonic epithelial organoids

3D undifferentiated colonic epithelial organoids from adult intestinal stem cells were established and cultured according to the protocol of IntestiCult Organoid Growth Medium (Human) (OGMH) (StemCell Technologies) with slight adjustments. Briefly, colon biopsies were minced and digested using Gentle Cell Dissociation reagent (StemCell Technologies). To further isolate colonic crypts from tissue homogenate, samples were vigorously pipetted in cold DMEM/F-12 (supplemented with 1% BSA and 15 mM HEPES) medium, passed through a 70 μm pore filter and centrifuged. Isolated colonic crypts were mixed with extracellular matrix (Matrigel Matrix Phenol Red-free, LDEV-Free (Corning)). The volume of 50 μl of crypt-Matrigel mixture was used to form domes in a 24-well cell culture plate. Colon organoids were cultured in OGMH medium supplemented with penicillin/streptomycin (100 $\mu\text{g}/\text{ml}$) (Gibco). Medium also contained RHO/ROCK signaling pathway inhibitor Y-27,632 (10 μM) (Stemcell Technologies) for the first two days of culturing. Colonic epithelial organoids were incubated at 37 °C with 5% CO_2 . Undifferentiated 3D organoids were microscopically evaluated using ZEISS Axio Observer 7 and ZEISS ZEN 3.1 (blue edition) software (ZEISS). The primary splitting of colonic epithelial organoids was performed after 1–2 weeks from culture establishment. Subsequent passaging of cultures was performed every 7–10 days depending on the maturity of organoids (usually, 7–10 days post-passage).

Establishment of colonic epithelial cell monolayers

Human colonic epithelial cell monolayers were established from expanded 3D colonic epithelial organoids in 24-well cell culture plates (Falcon). Briefly, each well of the cell culture plate was coated with Collagen I, Rat tail (Gibco) ($\approx 5 \mu\text{g}/\text{cm}^2$) for 2 hours at 37°C, then washed with PBS. Simultaneously, undifferentiated 3D colonic epithelial organoids were reduced into single cell suspensions. Organoids were disrupted by adding TrypLE Express (Gibco) supplemented with Y-27632 (StemCell Technologies) and incubating suspensions at 37°C for 10 min. The suspension was pipetted every 5 min to ensure the appropriate cell separation. TrypLE Express was blocked by addition of equal volume of DMEM/F-12 (StemCell Technologies) and suspension was centrifuged at 400 $\times\text{g}$ for 5 min. Pellet was resuspended in DMEM/F-12, passed through a 40 μm cell strainer and centrifuged again. Colonic epithelial cells were resuspended in IntestiCult OGMH (StemCell Technologies) supplemented with penicillin/streptomycin (100 $\mu\text{g}/\text{ml}$) (Gibco) and Y-27632 (10 μM) (Stemcell Technologies) and plated on the Collagen I-coated wells. The number

of 5×10^5 cells was used per well for seeding monolayers. Monolayers were incubated at 37 °C with 5% CO₂. The growth of 3D organoid-derived colonic epithelial cell monolayers was monitored under the microscope every day. Cell culture medium (IntestiCult OGMH supplemented with penicillin/streptomycin and Y-27632) was changed every 2–3 days until monolayer reached 100% confluency. Then, culturing medium was changed into cell differentiation medium (IntestiCult Organoid Differentiation Medium (Human) (ODMH) (StemCell Technologies)) supplemented with DAPT (5 μM), penicillin/streptomycin (100 μg/ml) (Gibco) and Y-27632 (10 μM) for 5 days to induce stem cell transition into specialized colonic epithelial cell types. Medium change was performed every 2 days. Monolayers were microscopically evaluated using ZEISS Axio Observer 7 and ZEISS ZEN 3.1 (blue edition) software (ZEISS).

Immunofluorescence microscopy

The cellular and structural composition of the established patient organoid-derived differentiated colonic epithelial cell monolayers was evaluated by immunofluorescence microscopy. First, monolayers were formed on 8-well format Collagen I-coated Nunc Lab-Tek II Chamber Glass slides (Thermo Scientific) and grown until full confluency and then differentiated as described above. Further, monolayers were fixed by incubating them in 4% paraformaldehyde (Sigma-Aldrich) solution for 30 min at RT. Further, colonic epithelial cell monolayers were permeabilized by using 0.5% Triton-X (Sigma-Aldrich) solution and blocked with 2% BSA blocking solution. Finally, conjugated monoclonal antibodies were diluted in antibody dilution solution (dilution ratio 1:50–1:500), applied to the processed monolayers and incubated for 60 min at RT. Conjugated antibodies for (i) tight-junction marker (Anti-ZO-1-Alexa Fluor 555 (MA3-39100-A555, Invitrogen)), (ii) proliferating cell marker (Anti-ki67-Alexa Fluor 488 (ab206633, Abcam)), differentiated/specialized cell markers (for Goblet cells, colonocytes, enteroendocrine cells) (Anti-Mucin2-Alexa Fluor 555 (bs-1993R-A555, Biocompare), anti-Cytokeratin 20-Alexa Fluor 488 (ab275988, Abcam), anti-Chromogranin A-Alexa Fluor 488 (ab199192, Abcam), respectively) were used. Hoechst 33342 (Invitrogen) was used as a counterstain for cell nuclei. All images were acquired with ZEISS Axio Observer 7 inverted fluorescence microscope using 5x and 10x objectives and analyzed by ZEISS ZEN 3.1 (blue edition) software (ZEISS).

Bacteria cultivation and preparation for co-culturing

Reference strains used for the tests were *Escherichia coli* ATCC 25,922 (Thermo Scientific) and *Phocaeicola vulgatus* ATCC 8482 (ATCC). Before assembling the co-culture system, bacteria were kept at -80°C in Brain Heart

Infusion Broth with glycerol (30%). At first, bacteria were inoculated on agar. Specifically, Trypton Soy Agar (TSA) (Sigma-Aldrich) was used for *Escherichia coli*, while Trypton Soy Agar supplemented with Defibrinated Sheep blood (5%) (Liofilchem) was used for *Phocaeicola vulgatus*. Both strains were cultivated for 24 h at 37°C; *Escherichia coli* were cultured under aerobic conditions, while anaerobic conditions were used for *Phocaeicola vulgatus*. Bacterial suspensions were prepared using phosphate-buffered saline solution (Invitrogen).

Colonic epithelial cell and bacteria co-culturing

Differentiated patient-derived colonic epithelial cell monolayers and two bacterial strains - *Escherichia coli* and *Phocaeicola vulgatus* - were used to establish a co-culture systems. Monolayers cultured without bacteria were used as control samples. First, to assemble co-cultures, cell differentiation medium was removed, and epithelial cell monolayers were washed twice with 500 μl of pre-warmed D-PBS (StemCell Technologies). Bacterial suspensions were centrifuged, and pellet was resuspended in a differentiation medium without antibiotics (IntestiCult ODMH supplemented with DAPT (5 μM) and Y-27632 (10 μM)). 2×10^6 of bacteria (*Escherichia coli* or *Phocaeicola vulgatus*) were added into respective wells with epithelial cell monolayers and co-cultures were incubated for 2 h at 37°C with 5% CO₂. After incubation, cell culture medium containing bacteria was discarded, epithelial cell monolayers were washed twice with 500 μl of D-PBS. Then, 500 μl of pre-warmed IntestiCult ODMH (StemCell Technologies) supplemented with DAPT (5 μM), penicillin/streptomycin (100 μg/ml) (Gibco) and Y-27632 (10 μM) was added into each well and monolayers were cultured for additional 24 h at 37°C with 5% CO₂. After incubation, monolayers were washed with 500 μl of D-PBS and lysed using 350 μl of RLT Plus buffer (supplemented with 1% of β-mercaptoethanol) (Qiagen). Lysates were stored at -80°C until further use for nucleic acid extraction.

Targeted gene expression analysis using RT-qPCR

To evaluate the expression of *TLR4*, *ZOI1*, *HSPA1A* and *HSPB1* genes in patient organoid-derived colonic epithelial cell monolayers, total RNA from these samples was reverse transcribed using High-Capacity cDNA Reverse Transcription Kit (Applied Biosystems). Up to 500 ng of total RNA was used per reaction to synthesize first strand cDNA. Further, the measurement of gene expression was based on SYBR Green chemistry by using SYBR Green PCR Master Mix (Applied Biosystems) and pairs of gene-specific primers (final concentration of each primer –300 nM). Primers used for amplification and amplicon size are listed in Table 2. Cycling conditions: 1×95 °C 10 min.; 40×95 °C 15 s., 60 °C 1 min. Analysis

Table 2 Primers used for targeted gene expression analysis

Gene	Transcript ID	Forward primer sequence (5'-3')	Reverse primer sequence (5'-3')	Amplicon size, bp
<i>ACTB</i>	NM_001101.5	GGACTTCGAGCAAGAGATGG	TGTGTTGGCGTACAGGCTTTG	229
<i>TLR4</i>	NM_138554.5	ATATTGACAGGAAACCCCATCCA	AGAGAGATTGAGTAGGGCATTT	300
<i>HSPA1A</i>	NM_005345.6	CCCCACCATTTGAGGAGGTAG	ACATTGCAAAACACAGAAATTGA	124
<i>HSPB1</i>	NM_001540.5	AAGCTAGCCACGCAGTCCAA	CGACTCGAAGGTGACTGGGA	51
<i>ZOI1</i>	NM_003257.5	CGGCTCCTGAGCCTGTAAG	GGATCTACATGCCAGACAA	371

was performed on the 7500 Fast Real-Time PCR System (Applied Biosystems). The amount of 4 ng of template DNA was used for each reaction. The cycle threshold (C_T) values of genes-of-interest were normalized to the value of *ACTB* reference gene. All the procedures were performed in accordance with the manufacturer's protocol and recommendations.

Statistical analysis

Statistical gene expression analysis was performed using R Studio software (version 4.3.2). Data distribution was determined using the Shapiro-Wilk test, gene expression differences were analyzed using the Wilcoxon rank-sum test. The difference between the values was considered significant when $P < 0.05$.

Results

UC harbors reduced diversity of gut microbiota

To resolve the composition of gut microbiota, we performed 16S rRNA-gene sequencing of fecal microbiomes in active and quiescent UC as well as in healthy individuals. To ensure data quality, we rigorously preprocessed sequencing reads by implementing strict quality control parameters (see Methods and Supplementary Table S1). Bacterial diversity (α -diversity), assessed by Chao1, Shannon and Simpson diversity indices, indicated that control individuals exhibited significantly greater species richness and diversity in comparison to those with active or quiescent UC (Fig. 1A). Interestingly, there were no differences between UC disease activity states, showing that UC patients, that are in remission, already harbor less diverse microbiomes than healthy individuals (Fig. 1B). Similarly, microbial community clusters (β -diversity), evaluated using the Bray-Curtis dissimilarity index, significantly differed between control subjects and patients with active or quiescent UC ($P_{\text{PERMANOVA}} = 0.008$ (R-squared value=0.047) and $P_{\text{PERMANOVA}} = 0.01$ (R-squared value=0.052), respectively). Notably, no significant clusters were identified among different disease activity states ($P_{\text{PERMANOVA}} = 0.49$) (Fig. 1C). Reflecting similar patterns, in-between sample dissimilarity also assessed by Bray-Curtis dissimilarity index showed that samples from control subjects had significantly higher in-between sample similarity (mean 0.548 ± 0.118) than patients with active disease (mean 0.640 ± 0.168) and patients in remission (0.607 ± 0.148). Quiescent UC

patients also bore significantly higher similarity than patients with active UC (Fig. 1D).

Taken together, the results show decreased diversity and altered microbiota not only in the active, but also in quiescent UC patients compared to healthy controls.

Common core microbiome among UC and healthy controls

To investigate not only the altered taxa, but more importantly, the stable (common) core microbiota across different stages of UC and healthy individuals, multiple analyses, including co-occurrence and differential abundance were performed. In total, 27 genera (such as *Intestinibacter*, *Phocaeicola*, *Ligilactobacillus*, *Bacteroides*, *Escherichia/Shigella*, etc.) were identified to be shared and consistently present in the feces of active and quiescent UC patients as well as healthy controls (Fig. 2A). Compared to healthy individuals, UC patients contained 5 genera (such as *Alistipes*, *Mediterraneibacter*, *Paraprevotella*, etc.), that showed statistical significance (BH adjusted $P_{\text{Wilcoxon}} < 0.05$) in relative abundance, while 35 genera were present at similar levels (Fig. 2B and Supplementary Table S2). Among the commonly present and non-altered taxa, the most abundant ones were *Phocaeicola*, *Collinsella*, *Roseburia*, *Holdemanella* and *Bacteroides* (Supplementary Table S2), and most of which are known to be predominantly commensal bacteria as well as considered as a core microbiome to sustain intestinal homeostasis [10].

Collectively, the results indicate that a substantial portion of the gut microbiota is consistently present and remains unchanged throughout the pathogenesis of UC. It is meaningful to acknowledge that the stability of these bacteria might be important in understanding the condition.

UC patient-derived colonic epithelial cells show diverse reactivity to constituent bacteria

To gain some functional insights on the stable core gut microbiome and how colonic epithelial cells respond and react to their presence as well as how this response is different in the cells from healthy and UC-afflicted individuals, co-cultivation experiments were performed. Specifically, we employed patient-derived 3D colonic epithelial organoid technology to further establish organoid-derived epithelial monolayers (2D cultures) from healthy ($N=8$) and UC-afflicted ($N=9$) individuals (Fig. 3A-B).

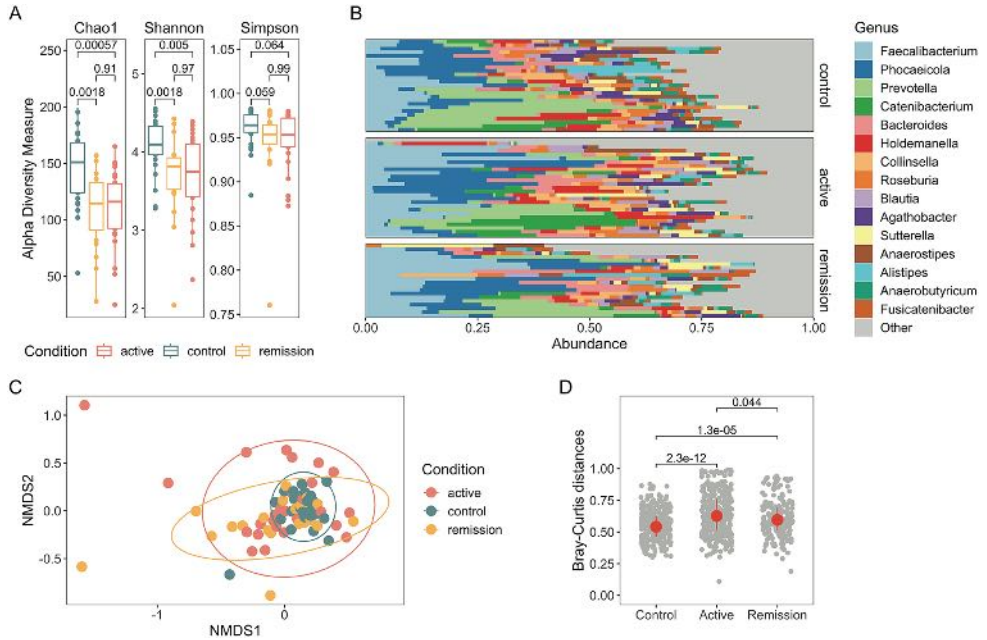


Fig. 1 Composition of microbiome in active and quiescent (remission) UC compared to healthy controls. **(A)** Boxplots representing median and Q1-Q3 values of alpha diversity metrics. Numbers indicate p value between the groups assessed by Wilcoxon rank-sum test. **(B)** Bar plots displaying relative abundances of top 15 most abundant genera in the study cohort, genera not in the top 15 are marked as Other. **(C)** Non-metric multidimensional scaling (NMDS) plot of complete dataset based on Bray-Curtis distances showing compositional differences between groups. **(D)** Scatter plot comparing in-between sample similarity in respective condition groups based on Bray-Curtis dissimilarity index

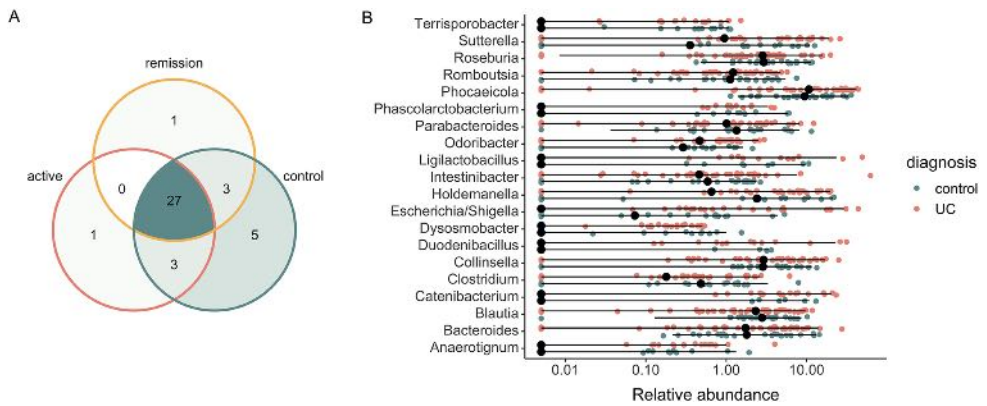


Fig. 2 Fecal core microbiome among active and quiescent (remission) UC patients and healthy controls. **(A)** Venn diagram of exclusive and shared core taxa at genus level (minimum prevalence – 0.1% in at least 20% of samples in each group) based on respective condition. **(B)** Most constituently abundant ($N=20$) genera between healthy controls and active UC groups

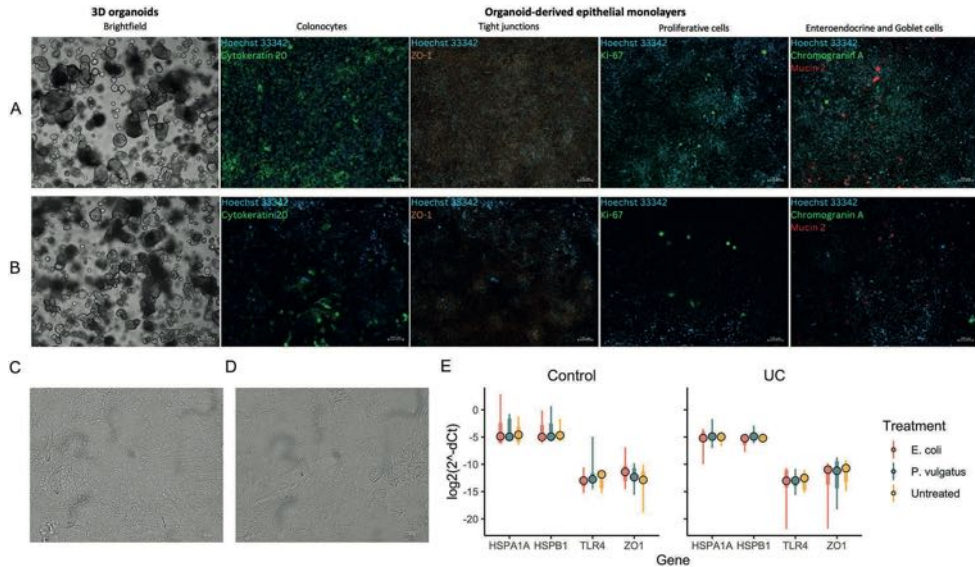


Fig. 3 3D colon organoids and organoid-derived colonic epithelial monolayers resemble the typical appearance of colonic epithelium and empower co-cultivation with commensal bacteria. **(A–B)** Representative pictures of 3D colonic epithelial organoids (colonoids) and cellular composition of organoid-derived monolayers of control individual **(A)** and patient with active UC **(B)**. Hoechst 33,342 (blue) was used in all cases as a counterstain for cell nuclei. Areas of proliferation are identified by Ki67 (green) expressing proliferating cells. Epithelial barrier integrity is defined by detection of tight junction protein ZO-1 (orange). Absorptive colonocytes are defined by positive Cytokeratin 20 (green) staining. Mucin-producing enteroendocrine cells are identified by positive Mucin 2 (red) staining. Hormone-producing enteroendocrine cells are defined by positive Chromogranin A (green) staining. **(C–D)** Representative pictures of colonic epithelial monolayers co-cultured with *Escherichia coli* **(C)** and *Phocaeicola vulgatus* **(D)**. **(E)** Expression analysis of marker genes (x-axis), representing host response to pathogen recognition (*TLR4*), tight junction regulation (*ZO1*) and stress stimuli indication (*HSPA1A* and *HSPB1*). Expression estimates (Ct) were normalized to *ATCB* ($\Delta\Delta Ct$) and were inverted (as $\log_2(2^{\Delta\Delta Ct})$) to recapitulate direction of the effect

These intestinal cell monolayers were then used for co-cultivation with *Escherichia coli* and *Phocaeicola vulgatus* (Fig. 3C–D). The selection of these bacteria was based on the fecal microbiota sequencing results showing that these species belonged to the ones of the most constituent genus among healthy and UC-afflicted individuals. Host response to bacteria was evaluated using targeted gene expression analyses of markers responsible for pathogen recognition (*TLR4*), tight junction regulation (*ZO1*) and stress stimuli indication (*HSPA1A* and *HSPB1*). Upon examining the marker gene expression, we observed insightful trends in the exposed cultures. First, neither *E. coli*, nor *P. vulgatus* were recognized as pathogens or induced stress response as assessed from the expression of *TLR4*, *HSPA1A* and *HSPB1* in the epithelial cells of healthy controls and UC patients (Fig. 3E). Interestingly, there was a trend for an increase in *ZO1* expression in control-derived monolayers ($\log_2FC=1.8$ [*E. coli*] and $\log_2FC=0.85$ [*P. vulgatus*]), while a trend for decrease was observed in UC-afflicted colonic epithelial cells compared to mock (untreated) versus co-cultured

cells ($\log_2FC = -1.25$ [*E. coli*] and $\log_2FC = -0.47$ [*P. vulgatus*]), suggesting a putative differential response in tight junction formation and integrity, which is suggestively reduced in the UC-derived epithelial cells (Fig. 3E). However, we could not identify any statistically significant changes in response to bacteria between UC and controls due to a relatively small sample size and huge patient-specific variation in response to co-cultivation with bacteria, even in the control individuals. For example, an average variance of normalized gene expression values between biological groups were reaching up to 11.4 and 18.8, respectively, for control- and UC-derived organoids co-cultured with *P. vulgatus* (Supplementary Table S3).

To summarize, the results show a tendency to differential response to *E. coli* and *P. vulgatus* in tight junction formation between control- and UC patient-derived colonic epithelial cell monolayers. Results also show that a host response to intestinal bacteria is very patient-specific, and that patients' colonic epithelial cells react very differently to the same bacteria.

Discussion

Typically, the changes in the gut microbiome are deemed as functionally relevant, while unaltered and consistent taxa are often overlooked as irrelevant. For example, several studies have focused on microbiome alterations and their putative functional implications rather than delving into characteristics of the preserved microbiome [11–15]. Indeed, dysbiotic changes in microbiota composition are certainly important and have been shown to provide decisive insights into the pathogenesis of UC as well as being utilized to monitor disease activity or even to treat patients (using such procedures as fecal microbial transplantation) [16]. However, it is still unknown whether the so-called core microbiome, which remains stable amid the ongoing reduction in diversity during UC pathogenesis, can potentially trigger or contribute to the relapse of the disease. To get more insights of the enduring microbial constituents, in this study we used 16S rRNA-gene sequencing to determine the composition of gut microbiota in UC as well as constituent genera. Additionally, we explored the impact of commensal bacteria from these unaltered genera, specifically, *Escherichia coli* and *Phocaeicola vulgatus*, on the colonic epithelial cells of healthy individuals and patients with UC through co-cultivation experiments.

Our findings on microbial composition align with previous research, indicating a substantial decrease in microbial diversity in UC patients when compared to healthy controls [14, 17]. However, our study extends this understanding to include alterations in quiescent patients, suggesting a persistent imbalance in microbial composition even during seemingly inactive phases of the disease. This observation supports the results of Öhman et al., who demonstrated in a follow-up study that the gut microbiota of UC patients remains remarkably stable regardless of disease stage, activity, or treatment escalation [18]. Our next focus was to establish the so-called stable core microbiome among the UC patients and control individuals. For this purpose, we combined co-occurrence and differential abundance analysis (to omit differentially abundant), and have identified the most consistent genera, including *Phocaeicola*, *Collinsella*, *Roseburia*, *Holdemanella* and *Bacteroides*. Although we identified *Phocaeicola*, *Bacteroides*, and *Roseburia* genera as constituent, there are studies showing their altered abundance in UC [15, 19, 20]. This might be due to various reasons, including demographics and diet habits of the enrolled individuals, since it is known that the major factor defining microbiome is environment [20]. Generally, it is rather challenging to compare our results from this analysis with other studies, primarily due to the predominant focus of other studies on describing microbiome alterations rather than uniformity. Although our primary focus was on the stable core microbiota, it is

noteworthy that our identified differentially abundant genera (*Alistipes*, *Mediterraneibacter*, *Paraprevotella*) were previously shown to be also altered in IBD by other authors [21–23]. Further, we have selected two bacteria, namely, *Escherichia coli* and *Phocaeicola vulgatus* (formerly, *Bacteroides vulgatus*), which belong to our identified stable core genera among UC patients and control individuals. The selection of these two specific bacteria was mainly based on the availability of techniques and validated protocols for maintaining bacteria species in culture [24, 25] well as in the co-culture with colonic epithelial cells [26, 27]. Moreover, both *Escherichia coli* and *Phocaeicola vulgatus* are known as life-long highly abundant residents of normal intestinal microbiota in humans [28–30]. Therefore, to finally evaluate if these bacteria can trigger different responses in UC patients than in controls, we performed co-cultivation experiments using intestinal organoid monolayers derived from tissue-resident adult stem cells. Precisely, we evaluated the changes in gene expression of established markers for pathogen recognition (*TLR4*) [20], tight junction regulation (*ZO1*) [31] and stress stimuli indication (*HSPA1A* and *HSPB1*) [32]. Our investigation into the interaction between the gut microbiota and colonic epithelial cells revealed intriguing insights into host responses. We observed a trend to a differential response in tight junction maintenance (based on *ZO1* gene expression) between control- and UC-derived epithelial monolayers co-cultivated with both *Escherichia coli* and *Phocaeicola vulgatus*. Even though controversially, both bacteria were previously described to be functionally relevant in the pathogenesis of the UC. Mills et al. has shown that proteases released by *Phocaeicola vulgatus* are involved in the dysfunction of epithelial barrier during UC pathogenesis [20], which could be related with our suggestive observations related to the tight junction formation. While other studies, such as Liu et al., were showing its protective effect on UC, since it has significantly attenuated symptoms of DSS-induced colitis in mice [33]. One of the probiotic *Escherichia coli* strains (Nissle 1917) has been shown to be efficient and safe in maintaining remission equivalent to the gold standard mesalazine in patients with ulcerative colitis [34]. However, there are reports, such as Yang et al., showing possible pathological effects of this bacteria in the pathogenesis of UC [6].

Furthermore, our results emphasize the patient-specific nature of the host response to intestinal bacteria, as evidenced by the varied reactions of patients' colonic epithelial cells to the same bacteria. Therefore, more samples are needed and various stratifications of those to acquire significant and in-depth observations.

Conclusions

Despite the decreased bacterial diversity and alterations in gut microbiota during UC, a significant portion of these microorganisms are consistently present and remain unchanged throughout the pathogenesis of the disease. Two species - *E. coli* and *P. vulgatus* - belonging to the most stable and unaltered commensal genera of the gut do not cause colonic epithelial stress and are not recognized as pathogens. Nevertheless, both species show a tendency to differentially regulate the tight junction formation in the control- as well as UC patient-derived colonic epithelial cell monolayers.

Supplementary Information

The online version contains supplementary material available at <https://doi.org/10.1186/s13099-024-00612-0>.

Supplementary Material 1

Author contributions

RI conceptualized the study, planned, and performed experimental work with fecal samples, organoids and co-cultures, analyzed the data, interpreted the results, wrote the initial and edited the final draft. RG performed 16S rRNA-gene NGS data analysis. RL prepared libraries for 16S rRNA-gene NGS. DT, RR performed co-culturing experiments. AL provided scripts for NGS data analysis. NK recovered and prepared bacterial cultures for co-cultivation experiments. MM provided the facilities for bacteria cultivation under anaerobic conditions. GK, LVJ, JK provided biological samples (feces and biopsies) and collected clinical patient data. SJ conceptualized the study, interpreted the results, wrote the initial and edited the final draft. JS conceptualized the study and edited the final draft. All authors read and approved the final manuscript.

Funding

This work was funded by the Research Council of Lithuania (Grant number S-MIP-20-56).

Data availability

The 16S rRNA coding gene sequencing data was deposited into OSG database and is available under the accession number: 10.17605/OSFIO/J3PC6. The qPCR datasets supporting the conclusions of this article are available from the corresponding author upon reasonable request.

Declarations

Ethics approval and consent to participate

The approval to perform the study was received from Kaunas Regional Biomedical Research Ethics Committee (No. BE-2-31, 22-03-2018). All subjects have signed a written informed consent form to participate in the study.

Competing interests

The authors declare no competing interests.

Received: 5 January 2024 / Accepted: 15 March 2024

Published online: 23 March 2024

References

1. GBD 2017 Inflammatory Bowel Disease Collaborators. The global, regional, and national burden of inflammatory bowel disease in 195 countries and territories, 1990–2017: a systematic analysis for the global burden of Disease Study 2017. *Lancet Gastroenterol Hepatol*. 2020;5:17–30.
2. Ungaro R, Mehandru S, Allen PB, Peyrin-Boulet L, Colombel JF. Ulcerative colitis. *Lancet*. 2017;389:1756–70.

3. Okumura R, Takeda K. Maintenance of gut homeostasis by the mucosal immune system. *Proc Jpn Acad Ser B Phys Biol Sci*. 2016;92:423–35.
4. Rendón MA, Saldaña Z, Erdem AL, Monteiro-Neto V, Vázquez A, Kaper JB, et al. Commensal and pathogenic *Escherichia coli* use a common pilus adherence factor for epithelial cell colonization. *Proc Natl Acad Sci U S A*. 2007;104:10637–42.
5. Scott H, Davies GJ, Armstrong Z. The structure of Phocaeicola Vulgatus sialic acid acetyltransferase. *Acta Crystallogr Sect D Struct Biol*. 2022;78:647–57.
6. Yang H, Mirsepasi-Lauridsen HC, Struve C, Allaire JM, Sivignon A, Vogl W, et al. Ulcerative Colitis-associated *E. Coli* pathobionts potentiate colitis in susceptible hosts. *Gut Microbes*. 2020;12:1847976.
7. Maidak BL, Olsen GJ, Larsen N, Overbeek R, McCaughey MJ, Woese CR. The RDP (ribosomal database project). *Nucleic Acids Res*. 1997;25:109–11.
8. Callahan BJ, McMurdie PJ, Rosen MJ, Han AW, Johnson AJA, Holmes SP. DADA2: high-resolution sample inference from Illumina amplicon data. *Nat Methods*. 2016;13:581–3.
9. Barnett D, Arts I, Penders J. microViz: an R package for microbiome data visualization and statistics. *J Open Source Softw*. 2021;6:3201.
10. Fung TC, Artis D, Sonnenberg GF. Anatomical localization of commensal bacteria in immune cell homeostasis and disease. *Immunol Rev*. 2014;260:35–49.
11. Santoru ML, Piras C, Murgia A, Palmas W, Camboni T, Liggi S, et al. Cross sectional evaluation of the gut-microbiome metabolome axis in an Italian cohort of IBD patients. *Sci Rep*. 2017;7:9523.
12. Moen AEF, Lindström JC, Tannaes TM, Vatn S, Ricanek P, Vatn MH, et al. The prevalence and transcriptional activity of the mucosal microbiota of ulcerative colitis patients. *Sci Rep*. 2018;8:17278.
13. Lo Sasso G, Khachatryan L, Kondylis A, Battey JND, Siero N, Danilova NA, et al. Inflammatory bowel Disease-Associated Changes in the gut-focus on Kazan Patients. *Inflamm Bowel Dis*. 2021;27:418–33.
14. Alam MT, Amos GCA, Murphy ARJ, Murch S, Wellington EMH, Arasaradnam RP. Microbial imbalance in inflammatory bowel disease patients at different taxonomic levels. *Gut Pathog*. 2020;12:1.
15. Machiels K, Joossens M, Sabino J, De Preter V, Arijis I, Eeckhaut V, et al. A decrease of the butyrate-producing species *Roseburia hominis* and *Faecalibacterium prausnitzii* defines dysbiosis in patients with ulcerative colitis. *Gut*. 2014;63:1275–83.
16. Shen Z-H, Zhu C-X, Quan Y-S, Yang Z-Y, Wu S, Luo W-W, et al. Relationship between intestinal microbiota and ulcerative colitis: mechanisms and clinical application of probiotics and fecal microbiota transplantation. *World J Gastroenterol*. 2018;24:5–14.
17. Nishihara Y, Ogino H, Tanaka M, Ihara E, Fukaura K, Nishioka K, et al. Mucosa-associated gut microbiota reflects clinical course of ulcerative colitis. *Sci Rep*. 2021;11:13743.
18. Ohman L, Lansson A, Strömbeck A, Isaksson S, Hesselmar M, Simrén M, et al. Fecal microbiota dynamics during disease activity and remission in newly diagnosed and established ulcerative colitis. *Sci Rep*. 2021;11:8641.
19. Zhou Y, Zhi F. Lower Level of Bacteroides in the gut microbiota is Associated with Inflammatory Bowel Disease: a Meta-analysis. *Biomed Res Int*. 2016;2016:5828959.
20. Mills RH, Dulai PS, Vázquez-Baeza Y, Saucedo C, Daniel N, Gerner RR, et al. Multi-omics analyses of the ulcerative colitis gut microbiome link *Bacteroides vulgatus* proteases with disease severity. *Nat Microbiol*. 2022;7:262–76.
21. de Meij TGJ, de Groot EFJ, Peeters CFW, de Boer NKH, Kneepkens CMF, Eck A, et al. Variability of core microbiota in newly diagnosed treatment-naïve paediatric inflammatory bowel disease patients. *PLoS ONE*. 2018;13:e0197649.
22. Elmassry MM, Sugihara K, Chankhamjon P, Camacho FR, Wang S, Sugimoto Y, et al. A meta-analysis of the gut microbiome in inflammatory bowel disease patients identifies disease-associated small molecules. *bioRxiv Prepr. Serv. Biol. United States*; 2024.
23. Zakerska-Banaszak O, Tomczak H, Gabryel M, Baturo A, Wolko L, Michalak M, et al. Dysbiosis of gut microbiota in Polish patients with ulcerative colitis: a pilot study. *Sci Rep*. 2021;11:2166.
24. Elbing KL, Brent R. Recipes and tools for culture of *Escherichia coli*. *Curr Protoc Mol Biol*. 2019;125:e83.
25. Keitel L, Miebach K, Rummel L, Yordanov S, Büchs J. Process analysis of the anaerobe *Phocaeicola vulgatus* in a shake flasks and fermenter reveals pH and product inhibition. *Ann Microbiol*. 2024;74:7.
26. Puschhof J, Pleguezuelos-Manzano C, Martinez-Silgado A, Akkerman N, Safien A, Boot C, et al. Intestinal organoid cocultures with microbes. *Nat Protoc*. 2021;16:4633–49.

27. Keitel L, Braun K, Finger M, Kosfeld U, Yordanov S, Büchs J. Carbon dioxide and trace oxygen concentrations impact growth and product formation of the gut bacterium *Phocaeicola vulgatus*. *BMC Microbiol.* 2023;23:391.
28. MJN V. T. WS. *Escherichia coli* residency in the gut of healthy human adults. *EcoSal Plus.* 2020;9.
29. Stromberg ZR, Van Goor A, Redweik GAJ, Wymore Brand MJ, Wannemuehler MJ, Mellata M. Pathogenic and non-pathogenic *Escherichia coli* colonization and host inflammatory response in a defined microbiota mouse model. *Dis Model Mech.* 2018;11.
30. Neff A, Lück R, Hövels M, Deppenmeier U. Expanding the repertoire of counterselection markers for markerless gene deletion in the human gut bacterium *Phocaeicola vulgatus*. *Anaerobe.* 2023;81:102742.
31. Guttman JA, Finlay BB. Tight junctions as targets of infectious agents. *Biochim Biophys Acta.* 2009;1788:832–41.
32. Gong M, Zhang F, Miao Y, Niu J. Advances of heat shock family in Ulcerative Colitis. *Front Pharmacol.* 2022;13:869930.
33. Liu L, Xu M, Lan R, Hu D, Li X, Qiao L, et al. *Bacteroides vulgatus* attenuates experimental mice colitis through modulating gut microbiota and immune responses. *Front Immunol.* 2022;13:1036196.
34. Kruis W, Fric P, Pokrotnieks J, Lukás M, Fixa B, Kascák M, et al. Maintaining remission of ulcerative colitis with the probiotic *Escherichia coli* Nissle 1917 is as effective as with standard mesalazine. *Gut.* 2004;53:1617–23.

Publisher's Note

Springer Nature remains neutral with regard to jurisdictional claims in published maps and institutional affiliations.

Publication no. 3

Title: Prolonged culturing of colonic epithelial organoids derived from healthy individuals and ulcerative colitis patients results in the decrease of LINE-1 methylation level

Authors: Inčiūraitė Rūta, Steponaitienė Rūta, Raudžė Odeta, Kūlokienė Ugnė, Kiudelis Vytautas, Lukoševičius Rokas, Ugenskienė Rasa, Adamonis Kęstutis, Kiudelis Gediminas, Jonaitis Laimas Virginijus, Kupčinskas Juozas, Skiecevičienė Jurgita

Scientific Reports (2024)

Reprinted under a Creative Commons Attribution 4.0 International (CC BY 4.0) licence



OPEN Prolonged culturing of colonic epithelial organoids derived from healthy individuals and ulcerative colitis patients results in the decrease of LINE-1 methylation level

Ruta Inciuraite^{1,4}, Ruta Steponaitiene^{1,4}, Odeta Raudze¹, Ugne Kulokiene¹, Vytautas Kiudelis², Rokas Lukosevicius¹, Rasa Ugenskiene³, Kestutis Adamonis², Gediminas Kiudelis^{1,2}, Laimas Virginijus Jonaitis^{1,2}, Juozas Kupcinskas^{1,2} & Jurgita Skieceviciene¹✉

Patient-derived human intestinal organoids are becoming an indispensable tool for the research of digestive system in health and disease. However, very little is still known about the long-term culturing effect on global genomic methylation level in colonic epithelial organoids derived from healthy individuals as well as active and quiescent ulcerative colitis (UC) patients. In this study, we aimed to evaluate the epigenetic stability of these organoids by assessing the methylation level of LINE-1 during prolonged culturing. We found that LINE-1 region of both healthy control and UC patient colon tissues as well as corresponding epithelial organoids is highly methylated (exceeding 60%). We also showed that long-term culturing of colonic epithelial organoids generated from stem cells of healthy and diseased (both active and quiescent UC) individuals results in decrease of LINE-1 (up to 8%) methylation level, when compared to tissue of origin and short-term cultures. Moreover, we revealed that LINE-1 methylation level in sub-cultured organoids decreases at different pace depending on the patient diagnosis (healthy control, active or quiescent UC). Therefore, we propose LINE-1 as a potential and convenient biomarker for reliable assessment of global methylation status of patient-derived intestinal epithelial organoids in routine testing of ex vivo cultures.

The term 'organoid' refers to cells growing in a defined three-dimensional (3D) environment in vitro that form clusters of cells capable of self-organization and differentiation into functional cell types¹, and mirroring the structure and functions of an in vivo organ². The mini-gut culture system, referred as human intestinal epithelial organoid³, derived from highly Lgr5 (Leucine-rich repeat-containing G-protein coupled receptor 5) expressing intestinal stem cells⁴ is one of the most widely used model systems for a broad range of scientific applications, including, but not limited to modeling of intestinal diseases pathogenesis mechanisms (such as ulcerative colitis (UC)), tissue development research, development of new treatment tools for personalized medicine, etc.⁵⁻⁷.

Epigenetic processes, such as global DNA methylation, gene-specific DNA methylation, modifications of histone proteins and chromatin, etc., are crucial in regulating gene expression, development, maintaining and transforming genome stability and genomic integrity in health and disease (incl. cancer and inflammatory diseases)^{8,9}. Long Interspersed Nucleotide Element 1 (LINE-1) is a widely accepted universal surrogate genomic

¹Institute for Digestive Research, Academy of Medicine, Lithuanian University of Health Sciences, A. Mickevieciaus St. 9, 44307 Kaunas, Lithuania. ²Department of Gastroenterology, Academy of Medicine, Lithuanian University of Health Sciences, A. Mickevieciaus St. 9, 44307 Kaunas, Lithuania. ³Department of Genetics and Molecular Medicine, Academy of Medicine, Lithuanian University of Health Sciences, A. Mickevieciaus St. 9, 44307 Kaunas, Lithuania. ⁴These authors contributed equally: Ruta Inciuraite and Ruta Steponaitiene. ✉email: jurgita.skieceviciene@ismuni.lt

DNA methylation marker correlating with the global DNA methylation levels¹⁰. In normal state LINE-1 CpG content is hypermethylated¹¹ and under specific circumstances, such as disease development (various cancers, autoimmune diseases, etc.), harsh external influences, the level of methylation within LINE-1 elements decreases^{12–14}. Accordingly, previously conducted study focusing on DNA methylation in UC reveals the relation between colon tissue inflammation and hypomethylated DNA spectrum¹⁵.

UC, a state referred as idiopathic chronic, progressive immune-mediated inflammatory bowel disease (IBD) characterized by fluctuating periods of mucosal inflammation activity followed by phases of endoscopic remission and mucosal healing^{16,17} was extensively studied in the context of epigenetic and genetic background. Panels of differentially expressed genes in correlation with methylation patterns related to UC were identified (summarized by Annesi¹⁸ and Gould et al.¹⁹), however alterations of genome-wide methylation in repetitive transposable elements in UC is still scarcely explored.

The importance of methylation alterations in ageing and regional identity of intestinal epithelial organoid system has been studied on regional and genome-wide levels. A very recent study by Edgar et al. also showed that genome-wide methylation status of intestinal epithelial organoids cultured for an extended period of time decreases²⁰. However, up to date most of the epigenetic studies were conducted using murine intestinal organoid models, or healthy human intestinal organoid models, whereas studies analyzing the epigenetic stability of epithelial organoids derived from UC patients are still lacking.

The aim of current study was to evaluate the epigenetic stability of human intestinal epithelial organoids obtained and cultured from colonic biopsies of UC patients and healthy controls during long-term culture using quantitative methylation level of LINE-1 as a surrogate global genomic methylation marker. Our study design allowed us to not only evaluate whether the generated ex vivo epithelial organoid model systems have a stable DNA methylation profile compared to their original source (colon biopsy and colonic crypts) in the context of both active and quiescent UC, and healthy control conditions, but also let us to assess if long-term culturing of these healthy- and diseased patients-derived epithelial organoids introduces the changes in LINE-1 methylation intensity. Collectively, our study allowed us to fill the knowledge gap regarding dynamics of LINE-1 methylation in the UC patient-derived colon epithelial organoids cultured for prolonged time.

Results

Healthy- and UC patient-derived colonic epithelial organoids exhibit stable characteristic morphological phenotype during long-term culturing

3D epithelial organoids of control (CON) individuals as well active (aUC) and quiescent (qUC) ulcerative colitis patients were grown in primary culture for 7–14 days before passaging. The growth dynamic of patient-derived colonic organoids was assessed microscopically, observing the transition from freshly isolated crypts (day 0 in culture) to small (5–8 days in culture) and large (8–14 days in culture) cystic structures in all study groups. Neither the patient diagnosis, nor the duration of cultivation affected the cell behavior, or the microscopic appearance of intestinal epithelial organoids and typical cystic appearance of colonic organoids was retained in high-passage number (Passage 5) cultures (Supplementary Fig. 1A). Additionally, immunofluorescence characterization of generated organoids confirmed the proper polarity of organoid-forming epithelial cells, assessed as the basolateral expression of β -catenin and apical expression of F-actin (Phalloidin) (Supplementary Fig. 1B), defining the central lumen. Furthermore, undifferentiated patient-derived 3D epithelial organoids also mimicked the cellular composition and architecture of human colon epithelium. High expression of proliferating cell marker Ki-67, as well as tight junction protein ZO-1 was observed, while the levels of specialized intestinal cell markers (colonocytes—Cytokeratin 20, Goblet cells—Mucin 2, and enteroendocrine cells—Chromogranin A) were comparably lower (Supplementary Fig. 1C–G).

Our results, namely the timing of epithelial organoid formation, epithelial polarization, and cellular composition, are in agreement with studies by other research groups, where they also described adult human stem cell-generated ex vivo experimental models for studies of the intestinal system^{21,22}.

Healthy and diseased human colon tissues and respective epithelial organoids have a highly methylated LINE-1 region

Quantitative evaluation of LINE-1 region methylation level was performed in the control (CON), active (aUC) and quiescent (qUC) ulcerative colitis groups at each point of the biological sample studied—colon biopsies, isolated crypts, primary epithelial organoids (P0), short-term (P1) and long-term (P5) cultured epithelial organoids. The presented methylation estimates show that the LINE-1 region was highly methylated in all studied biological sample groups for all conditions (Fig. 1). The methylation level of our selected LINE-1 region varied at certain level both when comparing different study groups (CON, aUC, qUC) and between different biological samples (biopsies, crypts, organoids) (Table 1). The observed average (\pm SD) percentage values of LINE-1 methylation level in the entire study cohort ranged between $69.4 \pm 2.9\%$ (in the group of qUC Biopsy) and $61.8 \pm 3.8\%$ (in the group of aUC Organoids, P1).

Average (\pm SD) LINE-1 methylation level was almost the same in the colon biopsy samples of control and qUC groups and reached $68.7 \pm 4.3\%$ and $69.4 \pm 2.9\%$ ($p_{\text{adj.}} = 0.61$), respectively, while it was slightly lower in the group of aUC ($66.7 \pm 4.4\%$, $p_{\text{adj.}} = 0.47$ and $p_{\text{adj.}} = 0.15$, compared to CON and qUC, respectively). The observed percentage methylation values in the colonic crypts showed the same tendency as in the biopsies, being more similar between CON and qUC groups ($68.6 \pm 4.9\%$ and $67.9 \pm 3.7\%$, $p_{\text{adj.}} = 0.59$) and lower in the aUC group ($66.3 \pm 4.6\%$, $p_{\text{adj.}} = 0.52$ and $p_{\text{adj.}} = 0.52$, compared to CON and qUC, respectively). Finally, primary cultures of generated organoids also followed the trend and revealed minor decrease in LINE-1 methylation in all groups, when compared to biopsy samples. The LINE-1 region methylation percentage in CON and qUC groups was

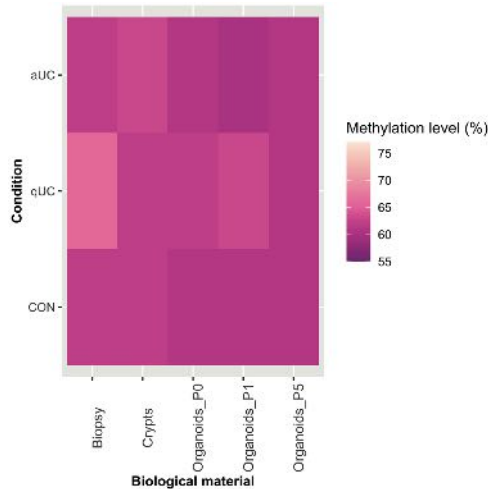


Figure 1. Heatmap showing average LINE-1 region methylation level of different biological samples in UC patients with active and quiescent disease and control subjects. The colour of the box represents the average methylation level (%) in each study group. CON—control (n = 6), qUC (n = 7)—quiescent ulcerative colitis, aUC (n = 6)—active ulcerative colitis.

	CON	Active UC	Quiescent UC
Biopsy, %			
Mean ± SD	68.7 ± 4.3	66.7 ± 4.4	69.4 ± 2.9
Crypts, %			
Mean ± SD	68.6 ± 4.9	66.3 ± 4.6	67.9 ± 3.7
Organoids_P0			
Mean ± SD	66.9 ± 4.1	65.6 ± 4.2	66.0 ± 3.9
Organoids_P1			
Mean ± SD	66.5 ± 5.4	61.8 ± 3.8	65.5 ± 3.7
Organoids_P5			
Mean ± SD	60.6 ± 2.3	62.6 ± 4.8	64.4 ± 3.9

Table 1. The summary table of average LINE-1 region methylation level in study cohort. SD—standard deviation, CON—control, UC—ulcerative colitis.

66.9 ± 4.1% and 66.0 ± 3.9% ($p_{\text{adj}} = 1.00$), and in aUC group in was 65.6 ± 4.2% ($p_{\text{adj}} = 0.84$ and $p_{\text{adj}} = 1.00$, compared to CON and qUC, respectively).

Hence, our initial observations did not reach statistical significance but clearly showed similar trends to previous studies that associate active UC with DNA hypomethylation¹⁵.

LINE-1 methylation level of healthy and diseased individual-derived colonic epithelial organoids decreases over long-term culturing

Analysis of DNA methylation level revealed that methylation level of the initial colon biopsy samples in all study groups (control/active/quiescent UC) differed significantly compared to the respective pure epithelial colon organoid cultures (Fig. 2). In the control group (CON) representing the healthy colon, LINE-1 methylation level of late-passage organoids (P5) decreased significantly compared to colon biopsy (8.1%, $p_{\text{adj}} = 1.04 \times 10^{-4}$), crypts (8.0%, $p_{\text{adj}} = 2.48 \times 10^{-4}$), and early-passage P0 (6.3%, $p_{\text{adj}} = 2.00 \times 10^{-3}$) and P1 organoids (5.9%, $p_{\text{adj}} = 0.019$). Significant differences, in terms of LINE-1 methylation level, were also observed when comparing P1 and P5 epithelial organoids generated from patients with quiescent UC (qUC) to primary tissue, i.e., biopsies. In this group, methylation level of analyzed LINE-1 region dropped down by approx. 4.0% ($p_{\text{adj}} = 6.00 \times 10^{-3}$) and 5.0% ($p_{\text{adj}} = 1.00 \times 10^{-3}$) in P1 and P5 organoids, respectively, when compared to biopsy samples. Similar observations

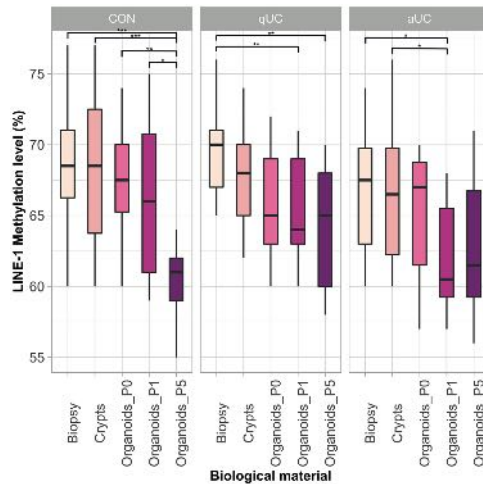


Figure 2. Boxplots showing comparisons of LINE-1 methylation level of different biological samples in healthy controls and patients with active and quiescent UC. The colour of the boxes represents different biological material. Distinct panels correspond to different health conditions. CON—control (n=6), qUC (n=7)—quiescent ulcerative colitis, aUC (n=6)—active ulcerative colitis. * $p_{\text{adj.}} \leq 0.05$, ** $p_{\text{adj.}} \leq 0.01$, *** $p_{\text{adj.}} \leq 0.001$.

were made in group of patients with active UC (aUC), where LINE-1 methylation level of P1 organoids decreased significantly by approx. 4.9% and 4.6% when compared to colon biopsy ($p_{\text{adj.}} = 0.012$) and crypts ($p_{\text{adj.}} = 0.019$) samples, respectively. Analogous trend of considerable LINE-1 methylation level decrease (by approx. 4.0%) was also noticed in group of late-passage epithelial organoids (P5) of aUC patients compared to respective colon tissue samples, however, differences did not reach the statistical significance ($p = 0.102$).

Altogether, our results reveal that establishment and long-term culturing of colonic epithelial organoid cultures derived from both healthy controls and UC patients is associated with epigenetic changes, namely the LINE-1 hypomethylation.

The LINE-1 methylation dynamic differs in epithelial organoids generated from healthy control, and healed and inflamed colon of UC patients

Additionally, our study design also allowed us to evaluate whether the changes in DNA methylation intensity differ in sub-cultured epithelial organoids depending on the colon inflammation activity. LINE-1 methylation level comparisons of early- and late-passage organoids-derived data revealed significant differences between health conditions (Fig. 3). Methylation level of LINE-1 region was lower by approx. 4.7% and 3.7% in the P1 organoids of aUC patients when compared to either CON ($p_{\text{adj.}} = 0.018$) or qUC ($p_{\text{adj.}} = 0.010$) group, respectively. Interestingly, sizable decrease in LINE-1 methylation level (reaching the value of aUC group) was observed in the late-passage (P5) organoids of CON group, which, in turn, resulted in significant difference (by 3.8%) when compared to qUC P5 organoids ($p_{\text{adj.}} = 0.024$).

To sum up, our results suggest that long-term culturing of colonic epithelial organoids of healthy individuals and active and quiescent UC patients results in different pace of LINE-1 methylation decrease.

Discussion

Since the development of human intestinal epithelial cell-derived organoids over a decade ago²³, their use as powerful translational research tool to study intestinal epithelial cell biology and pathophysiology has continued to expand rapidly. However, in vitro culturing of intestinal organoids lacks in vivo environment, such as gut microbiota or signals from other cell types. Therefore, some of their initial characteristics may be altered due to prolonged culturing which is required not only for expansion and maintaining organoids in culture, but also for specific experiments (e.g., focusing on development, long-term effect of stimulation, etc.). Even though it has already been shown that intestinal organoids maintain genetic stability²⁴, very little is known about the epigenetic regulation, especially in the context of IBD. Thus, here we provide the evidence for global DNA methylation level changes in human adult stem cell-derived 3D colonic epithelial organoids during long-term culturing. We not only describe LINE-1 methylation level fluctuations in epithelial organoids representing healthy colon, but

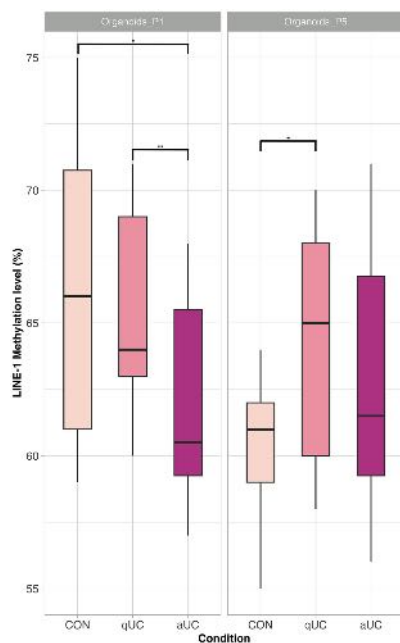


Figure 3. Boxplots comparing LINE-1 methylation level in early- and late-passage epithelial organoids between healthy controls and patients with active and quiescent UC. The colour of the boxes represents different health conditions. Distinct panels correspond to different organoid passage number. CON—control (n = 6), qUC (n = 7)—quiescent ulcerative colitis, aUC (n = 6)—active ulcerative colitis. * $p_{adj.} \leq 0.05$, ** $p_{adj.} \leq 0.01$.

also determine changes in the cultures originated from inflamed and non-inflamed colon sites of patients with UC over time.

First, our study provides a detailed characterization of quantitative LINE-1 methylation status across different levels of studied samples—ranging from whole colon biopsy, narrowing the analysis to epithelial cells in colonic crypts and ending with crypt-generated pure colonic epithelial organoids during prolonged (up to 5th passage) *in vitro* cultivation. We found that LINE-1 region is highly methylated (exceeding 60% in all cases) in human colon tissue, isolated crypts, and epithelial cell-derived early- and late-passage colonic organoids derived from either healthy control patients or patients with active and quiescent UC. High level of LINE-1 methylation in colon tissue also has been revealed in previous reports^{14,25,26}. In our study, when assessing all biological material collectively, we determined the highest methylation of LINE-1 in the control group, while hypomethylation was observed in case of active UC. This observation of altered LINE-1 methylation in UC when compared to healthy colon confirms findings of previous studies reporting gene hypomethylation as a signature feature of UC¹⁵. However, there is some controversy in the literature when comparing global methylation level data (assessed by quantitative LINE-1) to data originating from gene-level methylation profiling studies. For example, in contrast to the reported gene-level specific methylation level decrease during UC¹⁵, recently Szigeti et al. reported equally high methylation level of LINE-1 region for colon tissue from healthy subjects and IBD patients¹⁴. What is more, Quintanilla et al. found different LINE-1 methylation levels in normal mucosa across distinct segments of large intestine²⁶. Together, these data suggest different but still high genome-wide methylation levels between healthy and inflamed large intestine and its sites. Similarly, results of our present study also demonstrate high LINE-1 methylation level in both healthy and diseased colon tissue and besides that, such readout is in line with the results from previous study of our group, where we found an average $67.17 \pm 4.84\%$ methylated LINE-1 region in endoscopically normal colon mucosa²⁵.

Most importantly, our study design enabled the determination of the changes in overall DNA methylation level during prolonged culturing of colonic epithelial organoids derived from either healthy control, healed, or inflamed UC patients' mucosa. We used LINE-1 as a global genome methylation marker, as LINE-1 elements comprise at least 17–18% of the human genome, are generally highly methylated in somatic tissue and their methylation level correlates significantly with genome-wide 5-methylcytosine content¹⁰. To the best of our knowledge,

there are no previous studies where LINE-1 was used as a surrogate index mirroring global DNA methylation status in human intestinal organoid models. We compared not only colon tissue and primary epithelial organoids (P0), but also involved further cultures, i.e., early passage (P1) and late passage (P5) colonic epithelial organoids, which were cultured for approx. 2–3 weeks and 2 months, respectively. This led us to observation that LINE-1 methylation level of the colon crypt-derived epithelial organoids was lower than initial colon biopsy samples used for ex vivo culture establishment. What is more, our data revealed the different patterns in the decrease pace of LINE-1 methylation level, when comparing healthy control subjects and UC patients. In our data LINE-1 methylation level of healthy control colon-derived epithelial organoids tends to decrease more drastically than in active and quiescent UC patients' groups. Therefore, we suggest that experimental data derived from late-passage organoids of individuals with different diagnosis should be compared with caution. Even though the epigenetic changes in global DNA methylation context in human intestinal epithelial organoid model (healthy or IBD) during short- or long-term *in vitro* culture have already been revealed in several publications^{20,27,28}, the reported findings remain ambiguous. For example, in a study which used a small subset of pediatric IBD patients and healthy subjects, authors established ex vivo intestinal epithelial organoids and profiled epigenotype by assessing disease-associated differentially methylated positions (DMPs) and compared them with DNA methylation profile of highly purified intestinal epithelial cells. Distinct disease-specific epigenetic profile was identified in intestinal epithelium of children with IBD, and organoid cultures partially reflected the methylation profile of purified intestinal epithelium²⁸. However, the long-term culturing impact on the methylation profile changes was not evaluated within the frames of this study. Another study using microarray technology (Infinium HumanMethylation450 BeadChip), showed that intestinal epithelial organoid cultures generated from biopsies of different intestinal segments maintain gut site-specific genome-wide DNA methylation profile (i.e., site-specific DMPs) during long-term culturing (up to 3 months)²⁷. On the other hand, in the most recent large-scale study, including healthy pediatric and adult subjects, authors evaluated global changes in DNA methylation, gene expression and cellular function induced by human intestinal epithelial organoids culturing over time. The results of this study suggested a shifted epigenetic profile in organoids cultured for an extended period²⁹. Accordingly, our results fall in concordance with findings of this study and also indicate that LINE-1 methylation level tends to decrease over prolonged cultivation. Together, our study revealed that methylation pattern differs significantly between primary biopsy sample and colonic epithelial organoids culture (i.e., the longer organoids are cultured, the lower LINE-1 methylation level is) regardless the inflamed (aUC) or non-inflamed (qUC, CON) origin of the biopsy, but the pace of the DNA methylation reduction is diagnosis dependent.

To conclude, our results show that LINE-1 region of both healthy control and UC patients colon tissues and corresponding intestinal epithelial organoids is highly methylated and long-term culturing of these organoids results in decrease of LINE-1 methylation level which proceeds at different pace depending on the inflammation status of primary tissue. Therefore, we suggest that LINE-1 region could potentially be used as an additional routine biomarker in epithelial organoid characterization to assess methylation status, as it resembles the global methylation status results published in previous studies.

Methods

Patient cohort description and pathology classification

The present study was approved by the Kaunas Regional Biomedical Research Ethics Committee (Protocol No. BE-2-31) and written informed consent was obtained from each subject who participated in the study. All research was performed in accordance with relevant guidelines and regulations. This study consisted of three age- and sex-matched groups (Fig. 4). It enrolled 13 age- and sex-matched patients (7 males, 6 females, mean age of patients group 41.9 ± 15.4 years) with a previously established diagnosis of UC based on clinical, endoscopic, and histological examinations, that were scheduled for a colonoscopy either because of a disease flare or for screening purposes. 6 subjects who underwent colonoscopy procedure through colorectal cancer screening program (3 males, 3 females, mean age of control group 53.2 ± 8.5 years) without inflammatory, oncological, or other gastrointestinal diseases were enrolled as controls. Colon biopsy samples from sigmoid colon, rectum, or descending colon were obtained during standard colonoscopy procedure from control group individuals and subjects with active UC (aUC) or UC in remission (quiescent—qUC) who were examined at the Department of Gastroenterology, Hospital of Lithuanian University of Health Sciences. Remission of ulcerative colitis was confirmed in patients with stool frequency ≤ 3 /day, no rectal bleeding, and healed mucosa at endoscopy (Endoscopic Mayo score ≤ 1). The biopsies for tissue level methylation analysis were immediately flash frozen, whereas biopsies for organoid establishment were placed in DMEM/F-12 medium and processed immediately. Table 2 represents other summarized clinical and demographic data of the study subjects.

Establishment and expansion of human colonic epithelial organoid cultures

3D undifferentiated colonic epithelial organoids from adult intestinal stem cells were established and cultured according to the protocol of IntestiCult Organoid Growth Medium (Human) (OGMH) (06010, StemCell Technologies) with slight adjustments. Briefly, colon biopsies were first minced with sterile scalpel and incubated in Gentle Cell Dissociation reagent (100–0485, StemCell Technologies) to digest colon tissue. After centrifugation and removal of the supernatant, crypts containing intestinal stem cells were removed from biopsies by vigorous pipetting in cold DMEM/F-12 (supplemented with 1% BSA and 15 mM HEPES) medium, passed through a 70 μ m pore filter, and the number of isolated crypts was estimated. After centrifugation and removal of the supernatant, isolated colonic crypts were mixed with basement membrane matrix Matrigel (356231, Corning) and seeded into a 24-well cell culture plate, forming 50 μ l volume domes. Colon epithelial organoids were cultured in OGMH medium containing factors necessary for structure formation and stem cell renewal, supplemented with antibiotics (penicillin/streptomycin (100 μ g/ml) (15140122, Gibco) and the RHO/ROCK

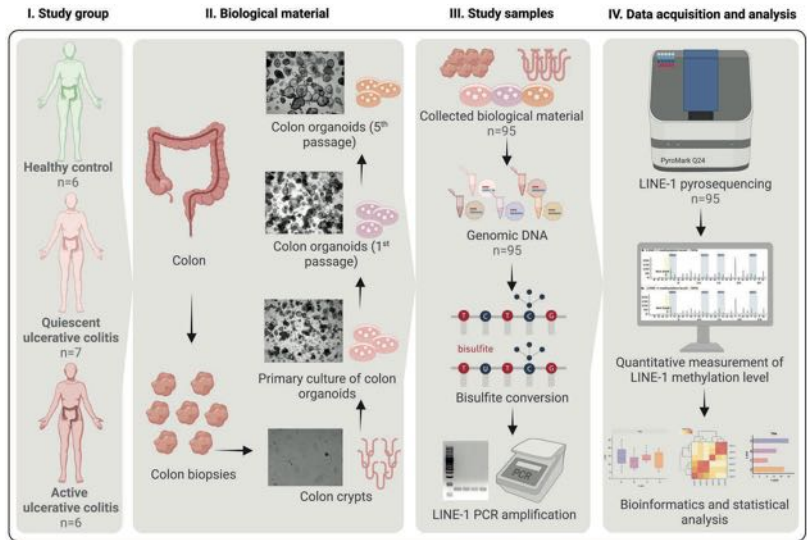


Figure 4. Scheme representing experimental study design and workflow (created with BioRender.com).

	CON, n = 6	Active UC, n = 6	Quiescent UC, n = 7
Age			
Mean ± SD	53.2 ± 8.5	43.7 ± 19.3	40.4 ± 12.7
Sex, n (%)			
Female	3 (50.0)	3 (50.0)	3 (43.0)
Full Mayo score			
Min–max	-	4–8	0–2
Biopsy site, n (%)			
Sigmoid colon	3 (50.0)	2 (33.0)	5 (71.00)
Rectum	2 (33.0)	2 (33.0)	1 (14.0)
Descending colon	1 (17.0)	2 (33.0)	1 (14.0)
Extent of UC, n (%)			
Proctitis (E1)	-	0 (0.0)	1 (14.0)
Left-sided colitis (E2)	-	1 (17.0)	2 (28.0)
Extensive colitis (E3)	-	5 (83.0)	4 (57.0)
Previous treatment (Yes/No)			
Immunosuppressants	-	No	Yes
Anti-inflammatory agents	-	Yes	Yes

Table 2. Demographic and clinical characteristics of the subjects. SD—standard deviation, CON—control, UC—ulcerative colitis.

signaling pathway inhibitor Y-27632 (for the first two days after seeding). OGMH was changed every 2 days. Colonic organoids were incubated at 37 °C with 5% CO₂. The growth of undifferentiated 3D colonic organoids was evaluated microscopically (inverted fluorescent microscope ZEISS Axio Observer 7, ZEISS ZEN 3.1 (blue edition) software). The first splitting of the organoid culture was performed after 7–14 days. Each subsequent passage of organoids was performed once the organoids were mature (7–10 days post-passage) until the fifth passage. A portion of fully formed undifferentiated colonic organoids after passage 0, 1, and 5 and portion of initial samples of isolated colon crypts were cryopreserved using CryoStor® CS10 (07930, StemCell Technologies) cell storage reagent. The suspension was transferred to a cryotube and immediately placed at –80 °C. See Fig. 4 for the overview of study design.

Microscopical characterization of colonic epithelial organoids

The morphology, cellular composition and functional parameters of the formed 3D intestinal epithelial organoids were evaluated by brightfield and immunofluorescence microscopy. Organoid growth dynamics were monitored daily. For immunofluorescence microscopy, undifferentiated organoids were fixed in 4% paraformaldehyde (1.00496.0700, Sigma-Aldrich) solution, incubated for 30 min, thus releasing them from the *Matrigel matrix*. Further organoid cells were permeabilized with 0.5% Triton-X (9002-93-1, Sigma-Aldrich) solution and blocked with 2% BSA blocking solution. Finally, fluorochrome-conjugated monoclonal antibodies diluted in antibody dilution solution (1:50–1:500) were added to the prepared organoids and incubated for 60 min at RT. Antibodies were applied that are specifically directed against: 1. cell polarity markers (*Anti-beta-catenin-Alexa Fluor 488* (53-2567-42, eBioscience), *F-actin phalloidin-Alexa Fluor 660* (A22285, Invitrogen)); 2. tight-junction marker (*Anti-ZO-1-Alexa Fluor 555* (MA3-39100-A555, Invitrogen)); 3. proliferating cell marker (*Anti-ki67-Alexa Fluor 488* (ab206633, Abcam)); 4. markers to identify differentiated/specialized cells (Goblet cells, colonocytes, enteroendocrine cells) (*Anti-Mucin2-Alexa Fluor 555* (bs-1993R-A555, Biocompare), *anti-Cytokeratin 20-Alexa Fluor 488* (ab275988, Abcam), *anti-Chromogranin A-Alexa Fluor 488* (ab199192, Abcam), respectively). Cell nuclei were labeled with the fluorescent dye *Hoechst 33342* (R37605, Invitrogen). Both brightfield and immunofluorescence microscopy of the samples were performed with 5 \times , 10 \times and 40 \times objectives using an inverted fluorescence microscope ZEISS Axio Observer with ZEISS ZEN 3.1 (blue edition) software.

DNA isolation from biopsies, crypts, and organoids samples

DNA from fresh frozen biopsy samples, cryopreserved crypts and organoid specimens was extracted using *AllPrep DNA/RNA Mini Kit* (80204, Qiagen). Briefly, frozen biopsy samples were lysed on *MagNA Lyser* (Roche Diagnostics) (6000 rpm, twice for 15 s with a 15 s break) using *Lysing Matrix D* tubes (116913050-CF, MP Bio-medicals) and 350 μ l buffer RLT Plus. Cryopreserved pellets of crypts and organoids in *CryoStor[®] CS10* medium (07930, StemCell Technologies) were gently thawed at +4 °C and centrifuged for 5 min at 400 \times g at +4 °C. Supernatant was removed and pellets were lysed in 350 μ l buffer RLT Plus. The following steps of DNA extraction from the lysates of biopsies, crypts and organoids were performed in line with the manufacturer's instructions.

Bisulfite conversion and PCR Amplification

In total 200 ng of the isolated genomic DNA was bisulfite converted using *MethylCode[™] Bisulfite Conversion Kit* (MECOV50, Applied Biosystems) and applied for 146 bp size LINE-1 region amplification via PCR. Samples containing no template were used for PCR contamination control. Custom-made primers set (F: 5'-TTTGA GTTAGGTGTGGGATATA-3', R: 5'-biotin-AAAATCAAAAATTCCTTTC-3') (final concentration of each 0.2 μ M) and *PyroMark[®] PCR Kit* (978703, Qiagen) was used for PCR amplification. Thermal-cycling conditions: 95 °C for 15 min; 45 cycles of 94 °C for 30 s, 56 °C for 30 s, 72 °C for 30 s; 72 °C for 10 min cycling mode. The specificity of PCR amplicon was verified using 2% agarose gel.

LINE-1 methylation analyses

Methylation level of three CpG islands in amplified LINE-1 region was analyzed using *PyroMark Q24* (Qiagen) pyrosequencing system. Briefly, 20 μ l of PCR product was immobilized to *Streptavidin Sepharose HP beads* (17-5113-01, Cytiva), processed with the *PyroMark Q24 Vacuum Workstation* and annealed to the sequencing primer 5'-AGTTAGGTGTGGGATATAGT-3'. Sequence analysis was performed by applying *PyroMark Gold Q24 reagents* (970802, Qiagen). All samples were analyzed in duplicates. Positive control *CpG Methylated Human Genomic DNA* (SD1131, Thermo Scientific) and PCR negative control were used in each sequencing run. Methylation level of 60% and higher value was considered as high LINE-1 methylation based on the previous publications^{25,29,30}.

Statistical analysis

The pyrograms of LINE-1 region were analyzed using the *PyroMark Q24 software* (v. 2.0.8, Qiagen). Statistical analysis of methylation data results and data visualization were performed using *R studio* (R version 4.0.3) software and its packages (ggplot2, ggsignif, ggpubr, scales, base, stats, tidyverse). Differences between groups were considered statistically significant when the calculated p-value was equal to or lower than the critical level ($p \leq 0.05$). The distribution of data in groups according to the normal (Gaussian) distribution was assessed by the Shapiro–Wilk normality test. Since the data in the study groups were not normally distributed, the Wilcoxon signed-rank test was used for statistical analysis.

Data availability

The data presented in the current study are available on reasonable request from the corresponding author.

Received: 12 June 2023; Accepted: 19 February 2024
Published online: 23 February 2024

References

- Wang, Y. *et al.* Self-renewing monolayer of primary colonic or rectal epithelial cells. *Cell. Mol. Gastroenterol. Hepatol.* **4**, 165–182. e7 (2017).
- Corrò, C., Novellademunt, L. & Li, V. S. W. A brief history of organoids. *Am. J. Physiol. Cell Physiol.* **319**, C151–C165 (2020).
- Barchitta, M., Quattrocchi, A., Mangeri, A., Vinciguerra, M. & Agodi, A. LINE-1 hypomethylation in blood and tissue samples as an epigenetic marker for cancer risk: A systematic review and meta-analysis. *PLoS One* **9**, e109478 (2014).
- Barker, N. *et al.* Identification of stem cells in small intestine and colon by marker gene *Lgr5*. *Nature* **449**, 1003–1007 (2007).

5. Xu, L., Lin, W., Wen, L. & Li, G. Lgr5 in cancer biology: Functional identification of Lgr5 in cancer progression and potential opportunities for novel therapy. *Stem Cell Res. Ther.* **10**, 219 (2019).
6. Artegiani, B. & Clevers, H. Use and application of 3D-organoid technology. *Hum. Mol. Genet.* **27**, R99–R107 (2018).
7. Clevers, H. Modeling development and disease with organoids. *Cell* **165**, 1586–1597 (2016).
8. Tammen, S. A., Friso, S. & Choi, S.-W. Epigenetics: The link between nature and nurture. *Mol. Aspects Med.* **34**, 753–764 (2013).
9. Karatzas, P. S., Gazouli, M., Safioleas, M. & Mantzaris, G. J. DNA methylation changes in inflammatory bowel disease. *Ann. Gastroenterol.* **27**, 125–132 (2014).
10. Weisenberger, D. J. *et al.* Analysis of repetitive element DNA methylation by MethylLight. *Nucleic Acids Res.* **33**, 6823–6836 (2005).
11. Tse, J. W. T., Jenkins, L. J., Chionh, F. & Mariadason, J. M. Aberrant DNA methylation in colorectal cancer: What should we target?. *Trends Cancer* **3**, 698–712 (2017).
12. Lakatos, P.-L. & Lakatos, L. Risk for colorectal cancer in ulcerative colitis: Changes, causes and management strategies. *World J. Gastroenterol.* **14**, 3937–3947 (2008).
13. Yashiro, M. Ulcerative colitis-associated colorectal cancer. *World J. Gastroenterol.* **20**, 16389–16397 (2014).
14. Szegedi, K. A. *et al.* Global DNA hypomethylation of colorectal tumours detected in tissue and liquid biopsies may be related to decreased methyl-donor content. *BMC Cancer* **22**, 605 (2022).
15. Arasaradnam, R. P., Khoo, K., Bradburn, M., Mathers, J. C. & Kelly, S. B. DNA methylation of ESR-1 and N-33 in colorectal mucosa of patients with ulcerative colitis (UC). *Epigenetics* **5**, 422–426 (2010).
16. Mulder, D. J., Noble, A. J., Justinich, C. J. & Duffin, J. M. A tale of two diseases: The history of inflammatory bowel disease. *J. Crohns. Colitis* **8**, 341–348 (2014).
17. Dotti, I. *et al.* Alterations in the epithelial stem cell compartment could contribute to permanent changes in the mucosa of patients with ulcerative colitis. *Gut* **66**, 2069–2079 (2017).
18. Anese, V. Genetics and epigenetics of IBD. *Pharmacol. Res.* **159**, 104892 (2020).
19. Gould, N. J., Davidson, K. L., Nwokolo, C. U. & Arasaradnam, R. P. A systematic review of the role of DNA methylation on inflammatory genes in ulcerative colitis. *Epigenomics* **8**, 667–684 (2016).
20. Edgar, R. D. *et al.* Culture-associated DNA methylation changes impact on cellular function of human intestinal organoids. *Cell. Mol. Gastroenterol. Hepatol.* **14**, 1295–1310 (2022).
21. Co, J. Y. *et al.* Controlling epithelial polarity: A human enteroid model for host-pathogen interactions. *Cell Rep.* **26**, 2509–2520.e4 (2019).
22. d'Aldebert, E. *et al.* Characterization of human colon organoids from inflammatory bowel disease patients. *Front. Cell Dev. Biol.* **8**, 363 (2020).
23. Sato, T. *et al.* Single Lgr5 stem cells build crypt-villus structures in vitro without a mesenchymal niche. *Nature* **459**, 262–265 (2009).
24. Li, Y., Tang, P., Cai, S., Peng, J. & Hua, G. Organoid based personalized medicine: from bench to bedside. *Cell Regen. (London England)* **9**, 21 (2020).
25. Kupcinskas, J. *et al.* LINE-1 hypomethylation is not a common event in preneoplastic stages of gastric carcinogenesis. *Sci. Rep.* **7**, 4828 (2017).
26. Quintanilla, I. *et al.* LINE-1 hypomethylation is neither present in rectal aberrant crypt foci nor associated with field defect in sporadic colorectal neoplasia. *Clin. Epigenet.* **6**, 24 (2014).
27. Krafczy, J. *et al.* DNA methylation defines regional identity of human intestinal epithelial organoids and undergoes dynamic changes during development. *Gut* **68**, 49–61 (2019).
28. Howell, K. J. *et al.* DNA methylation and transcription patterns in intestinal epithelial cells from pediatric patients with inflammatory bowel diseases differentiate disease subtypes and associate with outcome. *Gastroenterology* **154**, 585–598 (2018).
29. Scherhammer, E. S. *et al.* Dietary folate, alcohol and B vitamins in relation to LINE-1 hypomethylation in colon cancer. *Gut* **59**, 794LP–799 (2010).
30. Ogino, S. *et al.* Prospective study of family history and colorectal cancer risk by tumor LINE-1 methylation level. *J. Natl. Cancer Inst.* **105**, 130–140 (2013).

Author contributions

Conceptualization, R.I., U.K. and J.S.; methodology, R.I., R.S., U.K. and J.S.; formal analysis, R.I., R.S. and J.S.; investigation, R.I., R.S., and O.R.; patient material collection, V.K., G.K., L.V.J., K.A. and J.K.; data curation, R.I. and R.S.; writing-original draft preparation, R.I. and R.S.; writing-review and editing, R.I., R.L., R.S., R.U. and J.S.; visualization, R.I.; supervision, J.S. and J.K.; project administration, J.S. and R.I.; funding acquisition, J.S. and R.I. All authors have read and agreed to the published version of the manuscript.

Funding

This study is a part of IBD.ORG project (measure “Parallel laboratories”) which has received funding from European Structural Fund (Grant Number 01.2.2-LMT-K-718-04-0003) under grant agreement with the Research Council of Lithuania (LMTLT).

Competing interests

The authors declare no competing interests.

Additional information

Supplementary Information The online version contains supplementary material available at <https://doi.org/10.1038/s41598-024-55076-8>.

Correspondence and requests for materials should be addressed to J.S.

Reprints and permissions information is available at www.nature.com/reprints.

Publisher's note Springer Nature remains neutral with regard to jurisdictional claims in published maps and institutional affiliations.



Open Access This article is licensed under a Creative Commons Attribution 4.0 International License, which permits use, sharing, adaptation, distribution and reproduction in any medium or format, as long as you give appropriate credit to the original author(s) and the source, provide a link to the Creative Commons licence, and indicate if changes were made. The images or other third party material in this article are included in the article's Creative Commons licence, unless indicated otherwise in a credit line to the material. If material is not included in the article's Creative Commons licence and your intended use is not permitted by statutory regulation or exceeds the permitted use, you will need to obtain permission directly from the copyright holder. To view a copy of this licence, visit <http://creativecommons.org/licenses/by/4.0/>.

© The Author(s) 2024

SUPPLEMENTS



KAUNO REGIONINIS BIOMEDICININIŲ TYRIMŲ ETIKOS KOMITETAS

KMUK Eivenių 2, Centrinis korpusas 71 kab., 50009 Kaunas, tel. +370 37 326168; faks. +370 37 326901, e-mail: cmeinfo@kmu.lt

LEIDIMAS ATLIKTI BIOMEDICININĮ TYRIMĄ

2011-03-08 Nr. BE-2-10

Biomedicininio tyrimo pavadinimas: „Virškinimo sistemos ligų tiriamosios medžiagos biobankas“.	
Protokolo Nr.:	1
Data:	2010-12-27
Versija:	1
Pagrindinis tyrėjas:	Prof. habil. dr. Limas Kupčinskas Prof. habil. dr. Juozas Pundzius
Biomedicininio tyrimo vieta: Įstaigos pavadinimas: Adresas:	LSMU MA Gastroenterologijos klinika LSMU MA Chirurgijos klinika Eivenių g. 2, LT-50009 Kaunas

Išvada:

Kauno regioninio biomedicininis tyrimų etikos komiteto posėdžio, įvykusio 2011 m. sausio 4 d. (protokolo Nr. 8/2011) sprendimu pritarta biomedicininio tyrimo vykdymui.

Mokslinio eksperimento vykdytojai įsipareigoja: (1) nedelsiant informuoti Kauno Regioninį biomedicininis Tyrimų Etikos komitetą apie visus nenumatytus atvejus, susijusius su studijos vykdymu, (2) iki sausio 15 dienos – pateikti metinį studijos vykdymo apibendrinimą bei, (3) per mėnesį po studijos užbaigimo, pateikti galutinį pranešimą apie eksperimentą.

Kauno regioninio biomedicininis tyrimų etikos komiteto nariai			
Nr.	Vardas, Pavardė	Veiklos sritis	Dalyvavo posėdyje
1.	Doc. Irena Marchertienė	anesteziologija	taip
2.	Doc. Romaldas Mačiulaitis	klinikinė farmakologija	taip
3.	Prof. Nijolė Dalia Bakšienė	pediatrija	taip
4.	Prof. Irayda Jakušovaitė	filosofija	ne
5.	Dr. Eimantas Pečiūš	filosofija	taip
6.	Laima Vasiliauskaitė	psichoterapija	taip
7.	Gintaras Česnauskas	chirurgija	ne
8.	Zelmanas Šapiro	terapija	ne
9.	Jurgita Laurinaitytė	bioteisė	ne

Kauno regioninis biomedicininis tyrimų etikos komitetas dirba vadovaudamasis etikos principais nustatytais biomedicininis tyrimų Etikos įstatyme, Helsinkio deklaracijoje, vaistų tyrinėjimo Geros klinikinės praktikos taisyklėmis.

Pirmininkė



Irena Marchertienė

KAUNAS REGIONAL BIOMEDICAL RESEARCH ETHICS COMMITTEE

LUHS Eivenių str. 2, central body 71 cab., 5009 Kaunas, Tel. +370 37 326168; Fax +370 37 326901, e-mail: cmeinfo@kmu.lt

AUTHORIZATION FOR BIOMEDICAL RESEARCH

08/03/2011 No. BE-2-10

Biomedical research name: “Research Material Biobank of Digestive System Diseases”	
Protocol No.:	1
Date:	27/12/2010
Version:	1
Principal Investigator:	prof. habil. dr. Limas Kupčinskas prof. habil. dr. Juozas Pundzius
Biomedical Research Location: Institution Name: Address:	LUHS MA Gastroenterology Clinic LUHS MA Surgery Clinic LUHS Eivenių str. 2, LT-50009 Kaunas

Conclusion:

Under the decision of the meeting of Kaunas Regional Biomedical Research Ethics Committee, held on the **4th January 2011** (Protocol No. 8/2011), biomedical research execution was supported.

Scientific experiment promoters undertake: (1) to inform immediately Kaunas Regional Biomedical Research Ethics Committee of all unforeseen cases relating to the implementation of the study, (2) until the 15th January to submit an annual summary of the implementation of the study, (3) and one month after the completion of the study to submit a final report on the experiment.

Members of Kaunas Regional Biomedical Research Ethics Committee			
No.	Name	Activity Area	Participated in the meeting
1.	Assoc.Prof. Irena Marchertienė	Anesthesiology	yes
2.	Assoc. Prof. Romaldas Mačiulaitis	Clinical Pharmacology	yes
3.	Prof. Nijolė Dalia Bakšienė	Pediatrics	yes
4.	Prof. Irayda Jakušvaitė	Philosophy	no
5.	Dr. Eimantas Peičius	Philosophy	yes
6.	Laima Vasiliauskaitė	Psychotherapy	yes
7.	Gintaras Česnauskas	Surgery	no
8.	Zelmanas Šapiro	Therapy	no
9.	Jurgita Laurinaitytė	Biolaw	no

Kaunas Regional Biomedical Research Ethics Committee works in accordance with the ethical principles laid down in the Law on Ethics of Biomedical Research, in Helsinki Declaration, and drug exploration of Good Clinical Practice (GCP).

Chairwoman

/signature/

Irena Marchertienė

Seal: /Lithuanian University of Health Sciences
Kaunas Regional Biomedical Research Ethics Committee/

18 September 2014

I, Rūta Palšauskienė, the Notary of Kaunas city Notary's Office No. 5 hereby confirm that this to a true copy of the original document submitted.

Notary's register No. 5-2-7026

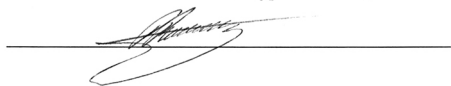
Notary's fee 3,087 Lt

Payment for other services provided on the request of the client _____

Notary's signature, seal

Aš, Renata Plukienė, patvirtinu, kad priimu atsakomybę už šio dokumento vertimo iš lietuvių kalbos į anglų kalbą teisingumą.

Renata Plukienė, asmens kodas 47905060416, asmens tapatybės kortelės Nr.11673422-, darbovietės adresas Savanorių pr. 192-811, Kaune.



Kaunas, du tūkstančiai keturioliktųjų metų rugsėjo mėnesio 18 diena

I, Renata Plukienė, confirm that I take the responsibility for the translation of this document from Lithuanian into English.

Renata Plukienė, personal code 47905060416, Identity Card No. 11673422-, workplace address Savanorių pr. 192-811, Kaunas.



Kaunas, the 18 of September, two thousand and fourteenth

Rūta Palšauskienė
Aš, _____, Kauno m. 5-ojo notarų biuro notarė (-as) -, Renatos Plukienės parašo tikrumą liudiju.

Rūta Palšauskienė
I, _____, the Notary of Kaunas city Notary's Office No. 5 -, hereby witness that the signature of Renata Plukienė is true.

Notarinio registro Nr. 5-2-7026
Notaro atlyginimas: 3,- Lt / 0,87 EUR
Atlyginimas už dokumento parengimą:-
Kompensacijos už patikrą registruose dydis:-
Kompensacijos (-ų) už kitas kliento prašymu notaro atliktas paslaugas dydis:-

Notary's register No. 5-2-7026
Notary's fee: 3,- Lt / 0,87 EUR
Fee for preparing the document: -
Fee for Registry review:-
Payment for other services provided on the request of the client:-

Notaro parašas



Notary's signature



KAUNO REGIONINIS BIOMEDICININIŲ TYRIMŲ ETIKOS KOMITETAS

Lietuvos sveikatos mokslų universitetas, A. Mickevičiaus g. 9, LT 44307 Kaunas, tel. (+370) 37 32 68 89; el.paštas: kaunorbtek@lsmuni.lt

LEIDIMAS ATLIKTI BIOMEDICININĮ TYRIMĄ

2018-03-22 Nr. BE-2-31

Biomedicininio tyrimo pavadinimas: „**Daugiapakopis molekulinis virškinimo sistemos ligų tyrimas: genetinių, proteominių, epigenetinių ir mikrobiomo žymenų nustatymas**“.

Protokolo Nr.:	1
Data:	2018-02-14
Versija:	2
Asmens informavimo forma	Versija nr. 2, data 2018-03-14
Pagrindinis tyrėjas:	Prof.dr. Limas Kupčinskas
Biomedicininio tyrimo vieta:	LSMUL Kauno Klinikos,
Įstaigos pavadinimas:	Chirurgijos klinika,
Adresas:	Gastroenterologijos klinika, Eivenių g. 2, LT-50161, Kaunas

Išvada:

Kauno regioninio biomedicininis tyrimų etikos komiteto posėdžio, įvykusio **2018 m. kovo mėn. 7 d.** (protokolo Nr. BE-10-6) sprendimu pritarta biomedicininio tyrimo vykdymui.

Mokslinio eksperimento vykdytojai įsipareigoja: (1) nedelsiant informuoti Kauno Regioninį biomedicininis Tyrimų Etikos komitetą apie visus nenumatytus atvejus, susijusius su studijos vykdymu, (2) iki sausio 15 dienos – pateikti metinį studijos vykdymo apibendrinimą bei, (3) per mėnesį po studijos užbaigimo, pateikti galutinį pranešimą apie eksperimentą.

Kauno regioninio biomedicininis tyrimų etikos komiteto nariai

Nr.	Vardas, Pavardė	Veiklos sritis	Dalyvavo posėdyje
1.	Prof. Edgaras Stankevičius	Fiziologija, farmakologija	Taip
2.	Prof. Skaidrius Miliuskas	Pulmunologija, vidaus ligos	Ne
3.	Med. dr. Jonas Andriuškevičius	Chirurgija	Ne
4.	Doc. Gintautas Gumbrevičius	Klinikinė farmakologija	Taip
5.	Prof. Kęstutis Petrikonis	Neurologija	Taip
6.	Dr. Ramunė Kasperavičienė	Filologija	Taip
7.	Eglė Vaižgelienė	Visuomenės sveikata	Ne
8.	Žydrūnė Luneckaitė	Visuomenės sveikata	Taip
9.	Jurgita Laurinaitytė	Teisė	Ne

Kauno regioninis biomedicininis tyrimų etikos komitetas dirba vadovaudamasis etikos principais nustatytais biomedicininis tyrimų Etikos įstatyme, Helsinkio deklaracijoje, vaistų tyrinėjimo Geros klinikinės praktikos taisyklėmis.

Kauno RBTEK Pirmininkas

Prof. Edgaras Stankevičius



KAUNAS REGION BIOMEDICAL RESEARCH ETHICS COMMITTEE

Lithuanian University of Health Sciences. A. Mickevičiaus g. 9, LT-44307 Kaunas, tel. (+370) 37 32 68 89 email: kaunorbtek@lsmuni.lt

PERMIT FOR BIOMEDICAL STUDY

22-03-2018 No BE-2-31

Title of the biomedical research: “ Multilevel molecular study of the gastrointestinal system: determination of genetic, proteomic, epigenetic and microbiomic signs ”	
Minutes No:	1
Date:	14-02-2018
Version:	2
Personal information form:	Version No 2 date 14-03-2018
Principal investigator:	Prof. Dr. Limas Kupčinskas
Location of the biomedical study: Name of the establishment: Address:	Hospital of Lithuanian University of Health Sciences Kauno klinikos Department of Surgery, Departed of Gastroenterology, Eivenių g. 2, LT-50161 Kaunas

Findings:

The biomedical study was approved by the decision of Kaunas Regional Biomedical Research Ethics Committee (minutes No BE-10-6) at the meeting held on **7 March 2018**.

The operators of the scientific experiment undertake: (1) to inform Kaunas Regional Biomedical Research Ethics Committee immediately on the occurrence of any study-related emergence cases, (2) to provide an annual summary of the study until 15 January, (3) to provide a final report on the experiment within one month after completion.

Members of Kaunas Regional Biomedical Research Ethics Committee			
No	Full name	Field of operations	Presence at the meeting
1	Prof. Edgaras Stankevičius	Physiology, Pharmacology	Present
2	Prof. Skaidrius Miliuskas	Pulmonology, internal diseases	Absent
3	Med. Dr. Jonas Andriuškevičius	Surgery	Absent
4	Ass. Prof. Gintautas Gumbrevičius	Clinical Pharmacology	Present
5	Prof. Kęstutis Petrikonis	Neurology	Present
6	Dr. Ramūbė Kasperavičienė	Phytology	Present
7	Eglė Vaižgelienė	Public Health	Absent
8	Žydrūnė Luneckaitė	Public Health	Present
9	Jurgita Laurinaitytė	Law	Absent

The activities of Kaunas Regional Biomedical Research Ethics Committee are based on the principles of ethics defined in the Law on Biomedical Research, Declaration of Helsinki, GMP rules for the research of medicines

Prof. Edgaras Stankevičius /signed/

Chairperson of Kaunas Regional Biomedical Research Ethics Committee

/Seal of the issuing authorities/

*Vertimas atliktas vertimų biure „AIRV“, į. k. 134819573, Taikos pr. 2-29, Kaunas
Vertimo tikrumą ir atitikimą originaliam tekstui liudiju.*

*The above text was translated in the translation agency AIRV, company code 134819573, Taikos pr.
2-29, Kaunas. I hereby witness that the translation conforms the original text.*



Office in **Vilnius**
Raugyklos g. 4A, LT-01139
Tel./fax +370 5 2122496
Mob. 370 612 73093
E-mail: vilnius@airv.lt

Office in **Kaunas**
Taikos pr. 2, LT-50187
Tel./fax +370 37 313455, 313258
Mob. +370 65051544
E-mail: kaunas@airv.lt

Office in **Klaipėda**
Taikos pr. 29, LT-91145
Tel./fax +370 46 210588
Mob. +370 650 58996
E-mail: klaipeda@airv.lt

CURRICULUM VITAE

Name, Surname: Rūta Inčiūraitė
E-mail address: ruta.inciuraite@lsmu.lt

Education:

2019–2025 **Ph.D. studies in Natural sciences**
Lithuanian University of Health Sciences, Kaunas, Lithuania

2017–2019 **M.S. in Biology of Laboratory Medicine**
Lithuanian University of Health Sciences, Kaunas, Lithuania

2013–2017 **B.S. in Medical and Veterinary Genetics**
Lithuanian University of Health Sciences, Kaunas, Lithuania

Research experience:

03/2020–present **Junior Researcher**
Laboratory of Clinical and Molecular Gastroenterology, Institute for Digestive Research, Faculty of Medicine, Lithuanian University of Health Sciences, Kaunas, Lithuania

03/2017–03/2020 **Senior Laboratory Technician**
Laboratory of Clinical and Molecular Gastroenterology, Institute for Digestive Research, Faculty of Medicine, Lithuanian University of Health Sciences, Kaunas, Lithuania

Research projects:

09/2024–present **Project Junior Researcher**
“Microscopic colitis: from single cell to complex model system (M.C.ell)“, funded by Research Council of Lithuania (grant no. S-MIP-24-133; project leader: dr. Greta Gedgaudienė)

09/2023–present **Project Junior Researcher**
Project “Personalised blueprint of Intestinal Health (miGut-Health)“, funded by HORIZON EUROPE (grant no. 101095470; project leader: prof. dr. Jurgita Skiecevičienė)

10/2023–present **Project Junior Researcher**
Project “Evidence-based Participatory Decision Making for Cancer Prevention through implementation research (ONCODIR)“, funded by HORIZON EUROPE (grant no. 101104777); project leader: prof. dr. Juozas Kupčinskas)

04/2023–present **Project Junior Researcher**
“Diet-microbiome-gut axis: the effect of microbiome derived nutrition associated metabolites on inflammatory processes in the gut (Foodflammation)” funded by Research Council of Lithuania (grant no. S-MIP-23-101; project leader: prof. dr. Jurgita Skiecevičienė)

- 12/2021–08/2023 **Project Junior Researcher**
 “SARS-CoV-2 genomics: providing a tool for viral evolution rate assessment, to inform exploratory modelling of immune and clinical response (evoCOVID)“, funded by EU structural fund (grant no. 13.1.1-LMT-K-718-05-0023 / DOTSUT-403; project leader: prof. habil. dr. Limas Kupčinskas)
- 04/2023–08/2023 **Project Junior Researcher**
 “Intestinal Organoid Model: Platform for Drug Testing and Personalized Therapy in Inflammatory bowel diseases (IBD.ORG)” funded by EU structural fund (grant no. 01.2.2-LMT-K-718-04-0003; project leader: prof. dr. Jurgita Skiecevičienė)
- 08/2019–06/2022 **Project Junior Researcher**
 “Multi-layer omics approach to gastric cancer: circulating biomarker profiling in the blood on genetic, epigenetic and microbiome levels (MULTIOMICS)” funded by EU structural fund (grant no. 09.3.3-LMT-K-712-01-0130; project leader: prof. dr. Jurgita Skiecevičienė)
- 03/2021–12/2023 **Project Junior Researcher**
 “Gut-Blood-Liver Axis: Circulating microbiome as non-invasive biomarker for Inflammatory Bowel Disease (IBD) and Primary Sclerosing Cholangitis (PSC) (BLOOD-BIOME)” funded by EEA financial mechanism (grant no. S-BMT-21-11 (LT08-2-LMT-K-01-060); project leader: prof. dr. Gediminas Kiudelis)
- 03/2021–12/2023 **Project Junior Researcher**
 “Molecular test for non-invasive screening of colorectal cancer (MOL-CRC-SCREEN)” funded by EU structural fund (grant no. 01.2.2-LMT-K-718-03-0086; project leader: prof. dr. Juozas Kupčinskas)
- 06/2020–12/2022 **Project Junior Researcher**
 “Crosstalk of gut microbiota and host-derived fecal microRNAs in ulcerative colitis (UCmicroOME)” funded by Research Council of Lithuania (grant no. S-MIP-20-56); project leader: dr. Simonas Juzėnas)
- 09/2018–09/2020 **Project Specialist**
 “Development of novel methods for gut microbiome modification” funded by EU structural fund (grant no. 09.3.3-LMT-K-712-01-0130; project leader: prof. dr. Jurgita Skiecevičienė)

International experience:

- 10/2023 **Young Faculty Member**
 International congress “UEG Week 2023”, Copenhagen, Denmark (Co-chair at two abstract-based oral and one moderated poster sessions)

- 04/2023–07/2023 **Research Internship**
 Institute of Clinical Molecular Biology, Christian-Albrechts
 University of Kiel, Kiel, Germany (Systems Immunology group
 (head: prof. Philip Rosenstiel))
- 02/2022–03/2022 **Research Internship**
 Institute of Clinical Molecular Biology, Christian-Albrechts
 University of Kiel, Kiel, Germany (Systems Immunology group
 (head: prof. Philip Rosenstiel))

Scientific achievements, awards, scholarships:

- 03/2025 Selected to participate in the 74th Lindau Nobel Laureate Meeting
 dedicated to chemistry
- 12/2024 1st place winner in the contest “Best LSMU PhD Student 2024”
- 10/2023 Travel grant award for abstract in the Congress “UEG Week 2023”
- 11/2022 Best oral presentation in Bridging Meeting in Gastroenterology and
 EAGEN Postgraduate Course “Closing the knowledge gap in GI after
 COVID-19 pandemics“
- 10/2022 “UEG Week 2022“ Best presentation award in Abstract-based Session:
 Upper GI cancer: Basic Aspects
- 05/2022 Keystone Symposia Future of Science Fund Scholarship 2022
- 11/2021 2nd place in the section for oral presentation in the Conference
 “Bioateitis: gamtos ir gyvybės mokslų perspektyvos“
- 10/2021 UEG National Scholar Award for abstract in the Congress “UEG Week
 Virtual 2021“
- 11/2020 Best abstract in the session of the International Conference “Health for
 All 2020“
- 04/2019 Honorary Scholarship of Lithuanian Science Support Dr. Juozas and
 Birutė Skrinskai Fund

ACKNOWLEDGEMENTS

I am sincerely grateful to all who contributed to this research and supported me throughout this journey – this work would not have been possible without them.

I am especially grateful to my scientific supervisor, Prof. Dr. Jurgita Skiecevičienė, for her continuous support, trust, thoughtful guidance, and professional example. Her leadership, experience, and constructive feedback were invaluable for both this dissertation and my academic growth. I also thank my co-supervisor, Prof. Dr. Juozas Kupčinskas, Head of the Institute for Digestive Research, for his clinical insights, for facilitating essential collaboration between the Institute and the Department of Gastroenterology, and for entrusting me with challenging tasks. I am equally thankful to Prof. Habil. Dr. Limas Kupčinskas for his ongoing support and encouragement in academic initiatives.

I would like to thank the interdisciplinary team at the Clinical and Molecular Gastroenterology and Bioinformatics Laboratories, as well as the Department of Gastroenterology, for creating a professional, supportive, and motivating environment. I am proud to be part of this exceptional team. Special thanks go to Dr. Simonas Juzėnas for his significant contributions to our shared research goals, particularly in sequencing data analysis and manuscript preparation. I also thank Dr. Rūta Steponaitienė and Dr. Greta Gedgaudienė for their collaboration in molecular studies, Dr. Ugnė Kūlokienė and Deimantė Tilindė for their work on organoid-based research, and Dr. Rolandas Gedgaudas and Dr. Rokas Lukoševičius for their input in microbiome studies. My gratitude extends to gastroenterologists Prof. Dr. Gediminas Kiudelis, Prof. Dr. Laimas V. Jonaitis, Vytautas Kiudelis, and others involved in clinical material collection and scientific discussions.

I am grateful to Prof. Dr. Philip Rosenstiel, Head of the Institute of Clinical Molecular Biology at Kiel University, for the opportunity to conduct internships within the Systems Immunology Group. I thank Dr. Neha Mishra for her guidance in bioinformatics, Prof. Dr. Florian Tran for his expertise on intestinal organoids, and the entire group for their warm welcome and collaboration.

I also acknowledge the patients who kindly agreed to participate in this study, as well as the financial support from the Research Council of Lithuania (project no. S-MIP-20-56), the European Structural Funds (project no. 01.2.2-LMT-K-718-04-0003), the LSMU Science Fund, and the LSMU Open Fund.

Finally, my thanks go to my family and friends for their unwavering support, patience, and belief in me. Their presence and understanding were essential in maintaining balance between academic work and personal well-being.